Dissertation

submitted to the
Combined Faculties of the Natural Sciences and Mathematics
of the Ruperto-Carola University of Heidelberg, Germany
for the degree of
Doctor of Natural Sciences

Put forward by
Dipl.-Phys. Tobias Henz
born in Iserlohn, Germany

Oral examination: 10.05.2016

Physics on all Scales

Scalar-Tensor Theories of Quantum Gravity in
Particle Physics and Cosmology

Referees:
Prof. Dr. Jan M. Pawlowski
Prof. Dr. Tilman Plehn

Physics on all Scales: Scalar-Tensor Theories of Quantum Gravity in Particle Physics and Cosmology

Abstract

In this thesis, we investigate dilaton quantum gravity using a functional renormalization group approach. We derive and discuss flow equations both in the background field approximation and using a vertex expansion as well as solve the fixed point equations globally to show how realistic gravity, connecting ultraviolet and infrared physics, can be realized on a pure fixed point trajectory by virtue of spontaneous breaking of scale invariance.
The emerging physical system features a dynamically generated moving Planck scale resembling the Newton coupling as well as slow roll inflation with an exponentially decreasing effective cosmological constant that vanishes completely in the infrared. The moving Planck scale might make quantum gravity experimentally accessible at a different energy scale than previously believed. We therefore not only provide further evidence for the existence of a consistent quantum theory of gravity based on general relativity, but also offer potential solutions towards the hierarchy and cosmological constant problems, thereby opening up exciting opportunities for further research.

Physik über alle Skalen: Skala-Tensor Theorien der Quantengravitation in Teilchenphysik und Kosmologie

Kurzfassung

In dieser Arbeit widmen wir uns der Untersuchung der Dilaton-Quantengravitation unter Zuhilfenahme der funktionalen Renormierungsgruppe. Wir leiten Flussgleichungen sowohl im Hintergrundfeld-Formalismus als auch in einer verbesserten Vertexentwicklung in Vertizes her und diskutieren diese. Wir lösen die Fixpunktgleichungen global und demonstrieren, wie ein realistisches Modell der Gravitation auf einer reinen Fixpunktkurve Infrarot- mit Ultraviolettphysik verbindet. Die spontane Brechung von Skaleninvarianz ist dabei von zentraler Bedeutung.
Die so entstehende physikalische Theorie beinhaltet sowohl eine dynamisch generierte, nicht-konstante Planckskala, die die Newton-Kopplung realisiert, als auch Slow-Roll Inflation mit einer exponentiell abfallenden und im Infraroten verschwindenden kosmologischen Konstanten. Eine nicht-konstante Planckskala könnte dazu führen, dass Spuren von Quantengravitation bei einer anderen Energieskala experimentell sichtbar werden als bisher angenommen. Daher sammeln wir in dieser Arbeit nicht nur weitere Hinweise für die Existenz einer konsistenten Quantentheorie der Gravitation basierend auf der Allgemeinen Relativitätstheorie, sondern tragen auch zu möglichen Lösungen des Hierarchie- und kosmologischen Konstantenproblems bei. Dabei öffnen sich spannende Möglichkeiten für weitere Forschungsfragen.

Contents

Introduction

Without doubt, modern physics has experienced remarkable validation in its quest to describe the physical world in terms of only a few fundamental theories, culminating in the recent probable experimental discovery of gravitational waves [1] as well as the Higgs boson [2, 3]. However, the aforementioned spectacular verifications of longstanding physical theories happened in radically different arenas: While gravitational waves are a feature of general relativity, the underlying framework for our understanding of the gravitational force between masses, the Higgs boson is a cornerstone in the standard model of particle physics. The latter is based on quantum field theory and the basis of our current understanding of the other three fundamental forces of nature, namely the strong, weak and electromagnetic interactions.
To date however, a unified description of all of nature's fundamental interactions is still pending. At the root of this void is the lack of a quantum theory of gravity, describing the gravitational interaction at high energies. On a conceptual level, the difficulty in finding a quantum theory of gravity stems from the fact that with general relativity and quantum field theory, two drastically different frameworks are used to describe physical observations. While quantum field theory relies on a fixed and flat spacetime, the spacetime itself is dynamical and usually also curved in general relativity, adhering to its own set of field equations. A naive attempt to describe gravity as a quantum field theory looses its predictivity by means of infinitely many independent infinities arising in the process. This is equivalent to the statement that a quantum field theory of gravity is perturbatively not renormalizable [4, 5].
Even more profoundly, the two theories describe physics at very different scales with seemingly very little overlap. While gravity governs physical effects on large length scales, thereby successfully describing cosmological phenomena, it becomes mostly irrelevant at small length scales, where the standard model of particle physics describes the interaction between the fundamental building blocks of matter with

remarkable precision. The reason for this separation lies in basic properties of the forces involved: While strong and weak interactions are short-ranged and the combination of positive and negative electrical charges shields the electromagnetic interaction on large distances, gravity is not only long-ranged but also knows only one charge, amounting to the absence of shielding effects. Furthermore, the measured strength of gravity is approximately 10^{40} times smaller than the other forces, rendering it irrelevant on small distance scales.

This separation is a demonstration of the immensely different scales present in modern physics, which also manifests itself in the large Planck scale $M \sim 10^{19}$ GeV, where effects of quantum gravity are believed to become important, in comparison with the typical scale of the standard model of particle physics, which is determined by the masses of W, Z and H bosons to be approximately 10^2 GeV. This, however, also means that general relativity is a viable description of gravity as an effective field theory for energies considerably below the Planck scale, without any need to know the precise high energy limit [6,7]. With the formal development of renormalization group methods, a mathematical tool became available to track the evolvement of a given physical theory when the energy scale is varied. It is in this context that Weinberg's idea of asymptotic safety [8] was born, holding that the high energy behavior of general relativity may be governed by a non-Gaussian fixed point inaccessible by perturbation theory, rendering gravity non-perturbatively renormalizable and thus "asymptotically safe".

Sparked by the development of the functional renormalization group [9, 10], multi-faceted evidence has been collected for the so called asymptotic safety scenario in recent years [11–17] following the initial computations [18], thereby circumventing the need to introduce radically new concepts for the description of the short range effects of gravity.

Nevertheless, various important open questions still await a solution, such as the dependency of the various results obtained on technical and mathematical tools employed, as well as the stability under the inclusion of other theories, resembling predominantly the standard model of particle physics. Finding a trajectory that smoothly connects the ultraviolet fixed point with infrared physics is of paramount importance, even though considerable progress has been made in recent times [19]. On top of that, the hierarchy and the cosmological constant problem play a crucial role. The former refers to the very question of why there are so vastly different scales emerging in physical theories, while the latter addresses the vast mismatch of the value of the cosmological constant as predicted by quantum vacuum fluctuation computations with what can be measured today.

In this thesis, we contribute to the current debate by considering asymptotic safety in the context of dilaton gravity, at the core of which lies the idea to encode the renormalization group scale in a scalar field. With that, it is possible on the one hand to construct a theory that is scale invariant and thus does not contain a physical

scale, and on the other hand to connect ultraviolet with infrared physics by means of varying the value of the scalar field. In contrast to Einstein gravity approaches to asymptotic safety, there is no need to deviate from the fixed point. If scale invariance is spontaneously broken, a physical scale arises naturally in the theory.
The idea of introducing scalar fields into general relativity was first pursued as early as 1961 by Brans and Dicke [20, 21] with the aim of allowing for a spacetime dependent Newton coupling. Some authors even argue that the notion of dynamical "constants" lies at the very heart of general relativity [22] and quantum gravity [23]. Combining the ideas of dilaton gravity and dynamical couplings, hope is kindled that dilaton gravity may be vital towards resolving the hierarchy and cosmological constant problem [24, 25].
It becomes evident that there are also multifaceted applications of such a system to both particle physics and cosmology. In this work, we focus on the latter.
Specifically, we derive flow equations for dilaton gravity both with standard as well as with improved functional renormalization group techniques and invest ourselves in finding a globally defined fixed point solution. Once established, it turns out to have remarkable physical features: Not only does it smoothly connect the infrared with the ultraviolet limit in an intuitive manner, but we also find an explicit breaking of scale invariance which leads to a naturally arising physical scale. The theory allows for inflation with a moving Planck scale and a vanishing cosmological constant in the deep infrared, as was already suspected in [26]. Moreover, we suggest a possibility to connect the quantum field theory prediction for the value of the cosmological constant with its measured infrared value, and show how a moving Planck scale might make quantum gravity effects experimentally accessible at a different scale than previously expected. This offers insights into possible solutions to both the hierarchy and the cosmological constant problem.
Thus, dilaton gravity truly corresponds to physics on all scales: Not only do we smoothly connect ultraviolet with infrared physics, but we also gain insights into the origin of physical scales as such with applications from both fundamental physical theories: General relativity with physics on large length scales and cosmology as well as quantum field theory with the standard model of particle physics for small length scales.
To cover these topics, this thesis is structured as follows: In part I, we set the stage for the investigations to follow by introducing both functional renormalization group as the formal framework in chapter 1 as well as the physical environment and scenario of asymptotic safety in chapter 2 and connect it with scalar fields and dilaton gravity in chapter 3. Moving forward, chapter 4 is devoted to discussing gauge theories in the context of functional renormalization in general and to develop suitable methods to deal with the challenges arising from overcounting and consecutive gauge fixing which are then applied to dilaton gravity in the form of background field methods and vertex expansions.

Part II is devoted to the first analysis of this work, namely the global fixed point structure of dilaton gravity derived from background flow equations. We sketch the derivation of these equations in chapter 6, while results are presented and discussed in chapter 7 and summarized in chapter 8.
In part III, we discuss flow equations for an enlarged truncation that are derived using vertex expansions and a flat background spacetime. We explain the procedure in chapter 10, after which we present prestudies leading to the final setup in chapter 11. In chapter 12, an approximated system of flow equations for the final system is solved to gain insights into its features, before chapter 13 presents the final results of this work, which are summarized in chapter 14.
After a summary of the overall findings, the appendix provides notes on mathematical and technical details.

Part I

Setting the Stage: Quantum Gravity, Asymptotic Safety, Scale Invariance, and Scalar Fields

CHAPTER 1

The Functional Renormalization Group

The functional renormalization group (FRG) offers a framework for a formal implementation of the Wilsonian idea of integration over momentum shells [27]. In order to do so, an effective average action Γ_k, which can depend on a certain momentum scale k, is introduced and a corresponding differential equation for its change with said scale k is derived.
As a starting point, we recall several fundamental concepts from standard quantum field theory, before we proceed to the derivation of the functional renormalization group equation. At the end of this chapter, we discuss applications of the functional renormalization group, with a special focus on a suitable formulation for gauge theories.
We aim for an introduction that focuses on our later applications to scalar-tensor theories of quantum gravity. For broader reviews in the context of asymptotic safety, we suggest to consider [11–17] or [28–41] for general reviews and other applications including QCD and cold atoms.
The presentation in this chapter merely serves to recapitulate the main points of the tools used in this thesis. For a more comprehensive treatment, we point to [42], which this chapter parallels in parts.

1.1 A Quantum Field Theory Primer

Our starting point for the description of a quantum field theory (QFT) is the generating functional $Z[J]$, defined as[1]

$$Z[J] = \int \mathcal{D}\psi \exp\left[iS[\psi] + i\int \mathrm{d}^d x J^a \psi_a\right]. \tag{1.1}$$

We work in natural units setting $\hbar = c = 1$. $\psi \equiv \{\psi_1, \psi_2, \ldots, \psi_N\}$ represents the entire field content of the quantum field theory. This indicates in particular that the path integral measure $\mathcal{D}\psi$ is to be taken as a product over all fields, $\mathcal{D}\psi = \prod_i \mathcal{D}\psi_i$. In contrast, $\mathcal{D}\psi_i$ itself is a formal Lebesgue measure at every space time point, that is $\mathcal{D}\psi_i = \prod_{x\in\mathbb{R}^n} \mathcal{D}\psi_i(x)$. Moreover, the order in which the fields evaluated at different points of spacetime enter is of importance. We will assume them to be time-ordered. For simplicity, let us resort to a single bosonic scalar field ψ for the remainder of this section, thus dropping the index at the field variable ψ and the sources J.
The generating functional $Z[J]$ plays a role that is comparable to the partition function's role in statistical physics: It allows for the extraction of all n point correlation functions in the form of

$$\begin{aligned}\langle\psi(x_1)\ldots\psi(x_n)\rangle &\equiv \mathcal{N}\int \mathcal{D}\psi\, \psi(x_1)\ldots\psi(x_n)\exp\left[iS[\psi]\right] \\ &= \frac{1}{Z[0]}(-i)^n \frac{\delta^n Z[J]}{\delta J(x_1)\ldots\delta J(x_n)}\Big|_{J=0},\end{aligned} \tag{1.2}$$

and thus for a complete description of the theory in question. The normalization arises from the requirement that $\langle 1\rangle = 1$.
The measure $\mathcal{D}\psi$ can and usually will contain both infrared (IR) and ultraviolet (UV) divergences, triggered by both infinitely many field configurations and over-counting in gauge field theories. In this text, we will always assume that we are working with a measure that has already been regularized to remove the divergences, $\mathcal{D}\psi \equiv \mathcal{D}\psi_{[\mathrm{reg}]}$.
In our applications to the exact renormalization group, the factor of i in the exponential in equation 1.1 will cause some issues connected to the convergence properties of the path integral. To at least partially cure these, we will henceforth work in Euclidean, rather than in Minkowski spacetime. This is achieved by performing a Wick rotation of the physical time t, $t \mapsto it$, changing the signature of the metric from $(-1, 1, \ldots, 1)$ to $(1, 1, \ldots, 1)$ and leaving us with a Riemannian rather than a Lorentzian spacetime manifold. As this transformation also renders the exponent in equation 1.1 real.
In general, one would expect physics to be invariant under Wick rotations, i.e. after performing our computations, we should be able to apply an inverse mapping $t \mapsto -it$

[1] See [43], for a more formal treatment also see [44].

to recover the original theory. However, this is only true provided the Osterwalder-Schrader axioms hold, for a thorough discussion see [45]. Furthermore, a discussion of the implications for asymptotic safety, a concept which will be introduced in section 2.2, can be found in [46].
The correlation functions calculated with (1.2) contain both connected and unconnected portions. Considering $n = 2$, we have

$$\langle\psi(x_1)\,\psi(x_2)\rangle = \langle\psi(x_1)\,\psi(x_2)\rangle_c + \langle\psi(x_1)\rangle\,\langle\psi(x_2)\rangle, \tag{1.3}$$

where the subscript c denotes the connected part of the correlation function. The second term is a product of the two field expectation values, which arises already for $n = 1$.
Since the physically relevant information is stored in the connected part, we further introduce the generator of connected correlation functions $W[J] = \log Z[J]$, also called the Schwinger functional, and its Legendre transform in the source J via

$$\Gamma[\varphi] = \sup_J \left(\int \mathrm{d}^d x J(x)\varphi(x) - W[J] \right), \tag{1.4}$$

which is a convex function. From it, the one particle irreducible (1PI) Green functions are generated through functional derivation with respect the field φ at $\varphi = 0$. Due to $\Gamma[\varphi]$ and $W[J]$ being related through a Legendre transform, we conclude

$$\varphi(x) = \frac{\delta W[J]}{\delta J(x)} = \langle\psi(x)\rangle \quad \text{and} \quad J(x) = \frac{\delta\Gamma[\varphi]}{\delta\varphi(x)}, \tag{1.5}$$

where we always assume J to take the value needed to satisfy the supremum condition from equation (1.4), $J = J_{\mathrm{sup}}$. Here we discovered the full quantum equation of motion in which the effective action $\Gamma[\varphi]$ governs the evolution of the field expectation value, taking all quantum effects into account.
At this point it is of paramount importance to understand that there are two equivalent ways of defining a Quantum Field Theory: The more familiar way is to define an action S leading to a generating functional $Z[J]$ which in turn gives rise to the correlation functions (1.2). However, it is completely equivalent to start with a complete set of correlation functions $\langle\psi(x_1)\dots\psi(x_n)\rangle$ and use these to define a theory. This is of course also true when we consider connected one particle irreducible representations. Though it is naturally always possible to derive correlation functions from an action, finding an algebraically closed expression for an action for a given set of correlation functions may not be possible. This will become important when introducing the vertex construction in section 4.4.2.
Having understood the role that $\Gamma[\varphi]$ plays in a generic quantum field theory, we can take the definition of the generating functional to derive an equation obeyed by

the effective action, reading

$$\exp\left(-\Gamma[\varphi]\right) = \int \mathcal{D}\psi \exp\left(-S[\psi+\varphi] + \int \mathrm{d}^d x \frac{\delta\Gamma[\varphi]}{\delta\varphi}\psi\right). \tag{1.6}$$

Solving this functional integro-differential equation is rarely possible and solutions are only known for special cases. That is why, when setting up the effective average action for our theory in section 3.1, we will need to make an ansatz well suited for the desired investigations. It is usually determined by demanding invariance with respect to a certain symmetry group, it needs to tend to the full and quantum action for large and small k, respectively.
Nevertheless, we can give a one-loop approximation to $\Gamma[\varphi]$ reading

$$\Gamma[\varphi] = S[\psi]\,|_{\psi=\varphi} + \frac{1}{2}\,\mathrm{Tr}\left(\log S^{(2)}[\varphi]\right) + \mathcal{O}(\text{two loop}), \tag{1.7}$$

where $S^{(2)}[\varphi] = \frac{\delta^2 S}{\delta\psi\delta\psi}\,|_{\psi=\varphi}$ is the second functional derivative with respect to the fields.
Having introduced some basic concepts of quantum field theory, we can now move on to the derivation of the Wetterich equation, which governs the evolution of a scale dependent effective average action Γ_k.

1.2 The Wetterich Equation

In this section, we will first introduce the effective average action Γ_k which depends on a variable mass or momentum scale k, and then proceed to derive a differential equation satisfied by Γ_k. This procedure should be thought of as a continuum realization of the Wilsonian renormalization group in the sense that we do not, as in equation (1.6), integrate over all quantum fluctuations (i.e. the field ψ) at once, but use the mass scale k to divide the Fourier modes of the quantum field ψ into two classes:

$$\text{modes with } p^2 \begin{cases} < k^2 & \text{contribute with a reduced weight.} \\ > k^2 & \text{contribute without any supression.} \end{cases} \tag{1.8}$$

This is achieved by adding a cutoff term to the bare equation S, transforming

$$S[\psi] \to S_k[\psi] = S[\psi] + \Delta S_k[\psi], \tag{1.9}$$

where $\Delta S_k[\psi]$ is assumed to be of second order in the fields and therefore acts like a

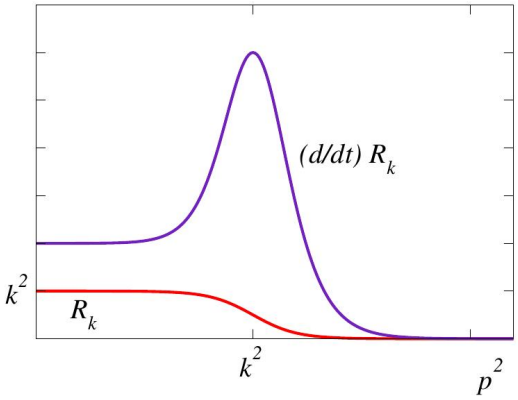

Figure 1.1: Sketch of a typical regulator function $\mathcal{R}_k(p^2)$ and its derivative $\partial_t \mathcal{R}_k(p^2)$, taken from [33]. The regulator itself provides an infrared regularization, whereas its derivative implements the integration over small momentum shells.

dynamical mass. In momentum space we write

$$\Delta S_k[\psi] = \frac{1}{2} \int \frac{\mathrm{d}^d p}{(2\pi)^d} \, \psi(-p) \, \mathcal{R}_k(p^2) \, \psi(p), \tag{1.10}$$

where $\mathcal{R}_k(p^2)$ is a regulator function. For later reference, we will also need the Fourier transformed version in position space, which takes the form

$$\Delta S_k[\psi] = \frac{1}{2} \int \mathrm{d}^d x \, \mathrm{d}^d y \, \psi(x) \, \mathcal{R}_k(x, y) \, \psi(y). \tag{1.11}$$

In order to achieve the suppression (1.8), we require $\mathcal{R}_k(p^2)$ to scale like

$$\mathcal{R}_k(p^2) \propto \begin{cases} k^2 & \text{for } p^2 \ll k^2. \\ 0 & \text{for } p^2 \gg k^2. \end{cases} \tag{1.12}$$

A sketch of a typical regulator function is depicted in figure 1.1.
We further introduce W_k as $W_k = \log Z_k$, where $Z_k = Z_{S \to S_k}$. Γ_k then is the modified Legendre transform of W_k (compare (1.4)), reading

$$\Gamma_k[\varphi] = \sup_J \left(\int \mathrm{d}^d x J(x) \varphi(x) - W_k[J] \right) - \Delta S_k[\varphi], \tag{1.13}$$

where we henceforth set $J = J_{\text{sup}}$ as in (1.4).
There are two crucial points to notice: Firstly, the reason for the subtraction of $\Delta S_k[\varphi]$ is not obvious from the arguments presented so far. However, it allows for a

cancellation when deriving the flow equation.[2] Secondly, Γ_k is not guaranteed to be convex anymore, in contrast to Γ from equation (1.4).
The quantum equations of motion receive regulator corrections and are transformed to

$$\varphi(x) = \frac{\delta W_k[J]}{\delta J(x)} = \langle \psi(x) \rangle \quad \text{and} \quad J(x) = \frac{\delta \Gamma_k[\varphi]}{\delta \varphi(x)} - (\mathcal{R}_k \varphi)(x), \tag{1.14}$$

from which we deduce

$$\frac{\delta J(x)}{\delta \varphi(y)} = \Gamma_k^{(2)}[\varphi](x,y) + \mathcal{R}_k(x,y). \tag{1.15}$$

With this step, we introduced the n-th functional derivative of the effective average action Γ_k with respect to the field ϕ as

$$\Gamma_k^{(n)}[\varphi](x_1, \ldots, x_n) = \frac{\delta^n \Gamma_k}{\delta\varphi(x_1) \ldots \delta\varphi(x_n)}. \tag{1.16}$$

The spacetime as well as the field dependence will be dropped, whenever there is no potential for confusion.
Let us discuss some implications of the scaling (1.12) of $\mathcal{R}_k$ in connection with the definition of Γ_k, equation (1.13). First and most prominently, we recover the full effective action Γ in the limit of $p^2 \gg k^2$,

$$\lim_{p^2/k^2 \to \infty} \Gamma_k = \lim_{k^2 \to 0} \Gamma_k = \Gamma \tag{1.17}$$

for any finite momentum p.
Accordingly, in the other limiting case $k^2 \to \infty$, the regulator $\mathcal{R}_k$ diverges. Thus, the saddle point approximation (1.7) to the path integral (1.6) becomes exact when appropriately renormalized and we recover the bare action S,

$$\lim_{k^2 \to \Lambda \to \infty} \Gamma_k = S, \tag{1.18}$$

where Λ is an ultraviolet cutoff that is much larger than the physical scale of relevance. Note that this also implements an infrared regularization, as infrared modes are screened by the mass like regulator $\mathcal{R}_k \propto k^2 \psi^2$.
Thus, Γ_k interpolates between the bare action S with no quantum fluctuations integrated out for large k, and the effective average action Γ, where all quantum fluctuations have been integrated out already for small k, therefore implementing the Wilsonian idea of sequential integration over momentum shells.

[2] We will use the names FRGE as well as Wetterich and flow equation interchangeably.

Having established the limiting cases, we can now compute the intermediate trajectory of Γ_k, that is the dimensionless logarithmic derivative $k\frac{\mathrm{d}}{\mathrm{d}k}\Gamma_k = \partial_t\Gamma_k$ with $t = \log\frac{k}{k_0}$.[3] We assume that the field $\varphi = \langle\psi\rangle$ does not depend on the scale k, which renders the introduction of dimensionless quantities mandatory. A step by step derivation is presented for instance in [42, 47]. We only give the final result, called the Wetterich [9, 10], functional renormalization group equation (FRGE) or simply flow equation, which reads

$$\partial_t\Gamma_k = \frac{1}{2}\,\mathrm{STr}\left[\frac{1}{\Gamma_k^{(2)} + \mathcal{R}_k}\partial_t\mathcal{R}_k\right]. \tag{1.19}$$

As this equation will be the starting point for our further investigations, let us review its basic properties as far as they are apparent at this stage already.

Supertrace. In equation (1.19), STr denotes the supertrace, which entails the usual Trace operator, tracing all discrete indices alongside with a spacetime or momentum integration, and a factor of -1 for fermionic contributions as well as an additional factor 2 for ghosts, such that they would enter with a prefactor of -1 in total.

Trajectory. According to equations (1.18) and (1.17), we are now equipped with a differential equation for the intermediate trajectory in the space of all effective actions, the theory spaces (c.f. 1.2). Opposed to (1.6), no functional integral has to be solved to reveal the full structure.
However, the intermediate trajectory will depend on the exact choice of the regulator $\mathcal{R}_k$. Only the endpoints S and Γ are fixed.

Finiteness. The flow equation ensure both infrared and ultraviolet finiteness. In the infrared, the famous propagator singularity at $1/p^2$ is shifted to

$$\frac{1}{p^2 + \mathcal{R}_k} \to \frac{1}{k^2} \text{ for } p^2 \to 0$$

due to equation (1.12). The occurrence of $\partial_t\mathcal{R}_k$ on the RHS further implements UV regularization, since the predominant support of $\partial_t\mathcal{R}_k$ lies within a small momentum shell around $p^2 \sim k^2$ and $\lim_{p^2\gg k^2}\mathcal{R}_k = 0$, see figure 1.1.

Quantization. Our starting point for deriving the flow equation was the standard generating functional for a QFT (1.1). However, in the light of the previous two remarks, an inverse perspective is also admissible: We can define a QFT based on the flow equation, thus achieving a new kind of quantization procedure.

[3] The choice $k_0 = \Lambda$, where Λ is the ultraviolet cutoff is most frequently made, especially when ultraviolet poles make it impossible to consider the limit $\Lambda \to \infty$.

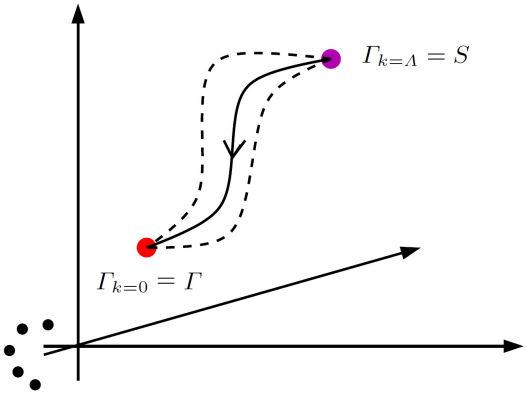

Figure 1.2: Sketch of a trajectory in theory space, taken from [33]. The endpoints are fixed to be S and Γ, but the intermediate trajectory depends on the exact choice of $\mathcal{R}_k$ (dashed lines).

Moreover, it is instructive to understand the link to standard perturbative quantisation and renormalization in this process on a deeper level, see for instance [35]. While in the latter one performs a loop expansion and adds counterterms at a scale μ to subtract divergent quantities and realize experimental results. In the context of FRG, the occurrence of divergent quantities is avoided altogether. However, of course the same experimental input is still necessary, but is now used to fix initial conditions at $\Gamma_{k=0} = \Gamma$, since this is where the cutoff is removed and thus pure physical observations can be made.[4] Both constructions are explicitly compared in [49].

one-loop structure. Even though the flow equation has one-loop structure, it is an exact equation, as the fully dressed propagator $\Gamma_k^{(2)}$ (or equivalently $W_k^{(2)}$) entered the equation by virtue of having chosen ΔS_k to be of second order in the fields only. To derive a true one-loop approximation, we expand $\Gamma_k = S + \Gamma_k^{\text{one-loop}} + \mathcal{O}(\text{two loop})$ (equation (1.7)) and obtain

$$\partial_t \Gamma_k^{\text{one-loop}} = \frac{1}{2}\,\text{STr}\left[\frac{1}{S^{(2)} + \mathcal{R}_k}\partial_t \mathcal{R}_k\right]. \tag{1.20}$$

Note how only the free propagator enters. The one-loop structure of the flow equation becomes visible when seeking a diagrammatic representation, see figure 1.3.

[4] We mention that at $k = 0$, the physical momentum plays its traditional role again, calling for full momentum dependent flows. This is, however, a delicate task we will not tackle in this thesis. We point to [48] for a thorough discussion.

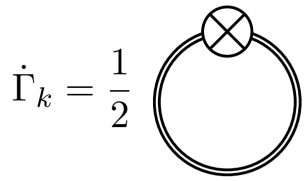

Figure 1.3: Diagrammatic representation of the flow equation (1.19). Due to all indices being contracted, it is simply given by a full 1 PI loop (double line) with an insertion of $\partial_t \mathcal{R}_k$ (crossed circle).

1.3 Theory Space and Truncations

The flow equation (1.19) describes the change of arbitrary theories with the scale k. A theory is specified by an effective average action, which a priori comprises an infinite number of fields and couplings between theses fields. Thus, in order to allow for feasible calculations in practice, we need to find a way to formally define a certain theory as well as an approximation scheme.
To obtain such an approximation on a formal level, let us give some breadth to the concept of a theory space. Assume that a set of basis functionals $\{\mathcal{P}_\alpha[\varphi]\}_{1\leq\alpha\leq\infty}$ exists, such that every element $\mathcal{A}[\varphi]$ entering our considerations can be written as

$$\mathcal{A}[\varphi] = \sum_{\alpha=1}^{\infty} \tilde{u}_\alpha \mathcal{P}_\alpha[\varphi]. \tag{1.21}$$

Of course the set $\{\mathcal{P}_\alpha[\varphi]\}_{1\leq\alpha\leq\infty}$ will be adapted to the problem considered. For instance in a gauge theory, the elements $\mathcal{P}_\alpha[\varphi]$ should be invariant under gauge transformations.
In particular, we can expand the effective average action to read

$$\Gamma_k[\varphi] = \sum_{\alpha=1}^{\infty} \tilde{u}_\alpha(k) \mathcal{P}_\alpha[\varphi], \tag{1.22}$$

where the sum still runs over infinitely many elements. Substituting the expansion

into both the left hand side (LHS) and the RHS of the flow equation, we obtain

$$\begin{aligned} \text{LHS} = \partial_t \Gamma_k[\varphi] &= \sum_{\alpha=1}^{\infty} (\partial_t \, \tilde{u}_\alpha) \mathcal{P}_\alpha[\varphi] \\ \text{RHS} = \frac{1}{2} \, \text{STr} \left[\frac{1}{\Gamma_k^{(2)}[\varphi] + \mathcal{R}_k} \partial_t \mathcal{R}_k \right] &= \frac{1}{2} \, \text{STr} \left[\frac{1}{\sum_{\alpha=1}^{\infty} (\partial_t \, \tilde{u}_\alpha) \mathcal{P}_\alpha^{(2)}[\varphi] + \mathcal{R}_k} \partial_t \mathcal{R}_k \right] \\ &= \sum_{\alpha=1}^{\infty} \tilde{\beta}_\alpha(\tilde{u}_i, 1 \leq i \leq \infty; k) \mathcal{P}_\alpha[\varphi], \end{aligned} \tag{1.23}$$

and with that

$$\partial_t \tilde{u}_\alpha = \tilde{\beta}_\alpha(\tilde{u}_i, 1 \leq i \leq \infty; k), \quad 1 \leq \alpha \leq \infty, \tag{1.24}$$

which is a system of infinitely many coupled differential equations for the generalized couplings $\tilde{u}_\alpha$. The function $\tilde{\beta}_\alpha$ is called the β-function of $\tilde{u}_\alpha$ and describes, how the generalized coupling changes with the scale k. If the RHS of the functional renormalization group equation contains derivatives of the generalized couplings with respect to the scale t, the β-functions cannot be obtained from equation (1.23) directly. Instead, a set of algebraic equation for the derivatives $\partial_t \tilde{u}_\alpha$ needs to be solved.
The twiddle signals that we are still working with dimensionful couplings. Introducing their dimensionless counterparts as $u_\alpha = k^{-n_\alpha} \tilde{u}_\alpha$, we can rewrite equation (1.24) to

$$\partial_t u_\alpha = \beta_\alpha(u_i, 1 \leq i \leq \infty), \quad 1 \leq \alpha \leq \infty. \tag{1.25}$$

Note that the explicit dependence on the scale k is no longer present within the β-functions, leading to considerable simplifications. We will therefore almost exclusively deal with dimensionless quantities and equations from now on.
Nevertheless, solving the system (1.25) is still impossible, which is why we need to resort to an approximation scheme, namely truncating the theory space to be spanned by only finitely many base elements. Thus we transform

$$\{\mathcal{P}_\alpha[\varphi]\}_{1 \leq \alpha \leq \infty} \to \{\mathcal{P}_\alpha[\varphi]\}_{1 \leq \alpha \leq N}, \tag{1.26}$$

where we assume that the base functionals have been reordered beforehand to produce the desired truncation.
Recalculating the resulting β-functions in dimensionless units (equation (1.23)), we

arrive at

$$\begin{aligned} \text{LHS} = \partial_t \Gamma_k[\varphi] &= \sum_{\alpha=1}^{N} (\partial_t u_\alpha) \mathcal{P}_\alpha[\varphi] \\ \text{RHS} = \frac{1}{2}\,\text{STr}\left[\frac{1}{\Gamma_k^{(2)}[\varphi] + \mathcal{R}_k}\partial_t \mathcal{R}_k\right] &= \frac{1}{2}\,\text{STr}\left[\frac{1}{\sum_{\alpha=1}^{N}(\partial_t u_\alpha)\mathcal{P}_\alpha^{(2)}[\varphi] + \mathcal{R}_k}\partial_t \mathcal{R}_k\right] \\ &\cong \sum_{\alpha=1}^{N} \beta_\alpha(u_i, 1 \le i \le N; k)\mathcal{P}_\alpha[\varphi]. \end{aligned} \tag{1.27}$$

It is crucial to note that a second approximation has just been made: In general, inverting $\sum_{\alpha=1}^{N}(\partial_t u_\alpha)\mathcal{P}_\alpha^{(2)}[\varphi] + \mathcal{R}_k$ and computing the trace will produce terms that are not represented in the span of $\{\mathcal{P}_\alpha[\varphi]\}_{1\le\alpha\le N}$. However, using a truncation as an approximation to the full theory, we will neglect these terms and write

$$\partial_t u_\alpha = \beta_\alpha(u_i, 1 \le i \le N), \quad 1 \le \alpha \le N, \tag{1.28}$$

which is now a system of finitely many coupled differential equations and can, in principle, be solved.
In this context, a good or stable truncation is one in which the couplings neglected in equation (1.27) are not essential to the physics one seeks to describe. A given truncation might be improved by either including more base functionals,

$$\{\mathcal{P}_\alpha[\varphi]\}_{1\le\alpha\le N} \to \{\mathcal{P}_\alpha[\varphi]\}_{1\le\alpha\le N+n},$$

or by changing the base system altogether,

$$\{\mathcal{P}_\alpha[\varphi]\}_{1\le\alpha\le N} \to \{\bar{\mathcal{P}}_\alpha[\varphi]\}_{1\le\alpha\le \bar{N}}.$$

This somewhat weak definition of a stable truncation reveals one of the major drawbacks of the non-perturbative equation (1.19): Once we utilize approximations, we usually loose all means of estimating the error we are making. Thus, in practice one would try to enlarge the truncation slightly by, for instance, looking at $N \to N+1$ and study the effect of the enlarged theory.

1.4 Fixed Points and Linearizations

A fixed point is a point in theory space characterized by a set of generalized couplings $\{u_\alpha^*\}$ at which the renormalization group (RG) flow stops. That means that all

β-functions need to vanish simultaneously, put in writing

$$0 = \beta_\alpha(u_i^*, 1 \leq i \leq N) \qquad \forall \quad \alpha \in \{1, \ldots, N\}. \tag{1.29}$$

Fixed points can be assumed for either $t \to -\infty$ (IR fixed point) or $t \to \infty$ (UV fixed point). The case of greater interest depends majorly on the problem under consideration.
To study the flow near a fixed point, we introduce $\delta u_i = u_i - u_i^*$ and linearize the β-functions, reading

$$\beta_\alpha(\delta u_i) = \beta_\alpha(u_i) \mid_{u_i = u_i^*} + \frac{\partial \beta_\alpha(u_i)}{\partial u_\gamma} \mid_{u_i = u_i^*} \delta u_\gamma + \mathcal{O}(\delta u^2), \tag{1.30}$$

where the first term on the RHS vanishes at a fixed point. Let us define

$$B_{\alpha\gamma} = \frac{\partial \beta_\alpha(u_i)}{\partial u_\gamma} \mid_{u_i = u_i^*} = \frac{\partial^2 u_\alpha}{\partial t \, \partial u_\gamma} \mid_{u_i = u_i^*} . \tag{1.31}$$

Then $B_{\alpha\gamma}$ can be diagonalized with a complete set of eigenvectors e_i and the corresponding eigenvalues Θ_i,

$$B_{ab} e_b = \Theta_b (e_b)_a, \quad \text{no sum over b on RHS.} \tag{1.32}$$

Since the e_i form a basis, we can understand u_α and δu_α as vectors and expand them[5] to be $u = \sum u_i e_i \quad \text{and} \quad \delta u = \sum \delta u_i e_i$, which allows us to rewrite equation (1.30) as

$$\partial_t \delta u_i = \Theta_i \delta u_i, \quad \text{no sum over i on RHS.} \tag{1.33}$$

This is a set of N uncoupled differential equations and can therefore be solved directly to

$$\delta u_i = C \exp(\Theta_i t), \tag{1.34}$$

where the constant of integration C can be fixed through the value of the couplings at the fixed points. From this solution, it is obvious that the fixed point in the new basis is (UV) attractive if all $\mathrm{Re}\,\Theta_i < 0$ and (UV) repulsive if all $\mathrm{Re}\,\Theta_i > 0$. In the context of the functional renormalization group, we will seldom encounter a purely attractive or repulsive fixed point. That is why we distinguish certain directions in theory space and call them relevant if $\mathrm{Re}\,\Theta_i > 0$ and irrelevant if $\mathrm{Re}\,\Theta_i < 0$. The notion of a relevant direction stems from the observation that the value of the corresponding coupling constant needs to be chosen carefully in order to arrive at

[5] On a more formal level, we perform a change of basis in the theory space.

the fixed point. A theory is predictive if there is only a finite number of relevant couplings.
The UV-critical surface is the subspace of theory space consisting of all theories that will hit the fixed point for $k \to \infty$. Therefore, its dimension is fixed by the numbers of irrelevant coupling parameters.
For our later applications we also define a fixed point to be a Gaussian fixed point if $u^*_\alpha = 0 \; \forall \, \alpha$. Perturbation theory is always an expansion around Gaussian fixed points.

CHAPTER 2

The Asymptotic Safety Scenario

In this chapter, we introduce the asymptotic safety conjecture first proposed by Weinberg [8], starting from general relativity as a classical field theory and the arising challenges for a direct perturbative quantisation. The chapter culminates in an account of current research in the area, including the role of this thesis.

2.1 General Relativity as a Classical Field Theory and Challenges for a Direct Quantisation

When aiming to study a quantum theory of gravity with functional renormalization group methods, which in turn have been derived from the standard effective action in quantum field theory, we first need to introduce general relativity as a classical field theory before we can adapt it to the cases of special interest in this thesis.
Moreover, we will take prerequisites for our later quantization procedure by considering general relativity as a gauge theory with the group of general diffeomorphisms as its gauge group. A detailed treatment of diffeomorphisms and their appearance in general relativity is given in appendix F. In this spirit, we need to construct an action S that is invariant under diffeomorphisms and produces field equations for the metric $g_{\mu\nu}$. Working in Wick rotated space time (section 1.1), the Einstein-Hilbert action [50] with a metric $g_{\mu\nu}$ of Riemanian signature reads

$$S_{\mathrm{EH}}[g_{\mu\nu}] = \frac{1}{16\pi\, G_N} \int \mathrm{d}^d x \sqrt{g}\,(2\,\Lambda - R)\,, \tag{2.1}$$

denoting by G_N and Λ the (dimensionful) Newton and cosmological constants, respectively, and dropping the explicit spacetime dependence of the dynamical field $g_{\mu\nu} = g_{\mu\nu}(x)$. We identify $\sqrt{g} = \sqrt{\det(g_{\mu\nu})}$, and therefore $\mathrm{d}^d x\sqrt{g}$ is a shorthand for the covariantly invariant measure.[1] For later use, we also define $g_N = k^{d-2}G_N$ and $\lambda = k^{-2}\Lambda$ as the dimensionless counterparts to G_N and Λ.
The Ricci scalar R is the fully contracted representative of the spacetime curvature and is defined as usual.
The field equations for the metric $g_{\mu\nu}$ are obtained by varying (2.1) with respect to the only dynamical field appearing at this stage, which is $g_{\mu\nu}$ itself. The equations are usually expressed as

$$R_{\mu\nu} - \frac{1}{2}R\, g_{\mu\nu} + \Lambda\, g_{\mu\nu} = 0. \tag{2.2}$$

An important concept in the context of general relativity as a gauge theory is the Lie derivative [51], as it generates the gauge transformations, namely general coordinate diffeomorphisms, on the metric $g_{\mu\nu}$. Consider an infinitesimal change in the coordinates generated by $\epsilon_\nu(x)\partial^\nu$. The coordinates x_μ change according to

$$x_\mu \to x_\mu + \epsilon_\mu(x), \tag{2.3}$$

suggesting that the metric should transform as

$$g_{\mu\nu} \to g_{\mu\nu} + \mathcal{L}_\epsilon g_{\mu\nu}. \tag{2.4}$$

It appendix F it is shown that $\mathcal{L}_\epsilon$ is the Lie derivative assigned to the vector field $\epsilon_\nu(x)\partial^\nu$, which has a local coordinate representation of the form

$$\begin{aligned}\mathcal{L}_\epsilon g_{\mu\nu} &= \epsilon^\sigma \partial_\sigma g_{\mu\nu} + \partial_\mu \epsilon^\sigma g_{\sigma\nu} + \partial_\nu \epsilon^\sigma g_{\sigma\mu} \\ &= \nabla_\mu \epsilon^\sigma g_{\sigma\nu} + \nabla_\nu \epsilon^\sigma g_{\sigma\mu},\end{aligned} \tag{2.5}$$

where the last equality holds if we use the covariant derivative operator ∇_μ instead of the ordinary partial derivative ∂_μ to define the vector fields on our spacetime manifold.
Returning to the Einstein-Hilbert formulation of general relativity (2.1), we find the Newton constant G_N to have mass dimension $[G_N] = 2 - d$. Thus, for $d > 2$ we have $[G_N] < 0$, which renders standard general relativity asymptotically non-renormalizable as a quantum field theory [4, 5]. This is rooted deeply in diffeomorphisms as the gauge group of gravity: Forgetting about a cosmological constant for a moment, the Ricci scalar R scales like p^2, which has mass dimension +2. But then

[1] At this stage, we have explicitly excluded a matter Lagrangian $\mathcal{L}_{\text{matter}}$ in equation (2.1), which would lead to an energy momentum tensor on the RHS of the field equations (2.2).

the coupling necessarily needs to have mass dimension -2, and there are infinitely many diagrams at tree level already, since the action is of infinite order in the metric due to the canonical volume form. As perturbation theory is essentially a power series in the coupling constant, there will be new divergences occurring in every order. Thus, one needs to rely on new constants to counter these divergences at every order, leaving us with an infinite number of constants to be fixed. Thereby, the theory looses all its predictive power and a direct perturbative quantization fails.

2.2 Quantum Gravity and Asymptotic Safety

There have been innumerous attempts to provide alternative theories of quantum gravity, usually also aiming for a unified description of particle physics and gravitational effects, including but not limited to string theory and loop quantum gravity. These solutions usually rely on the inclusion of completely new physics which are not or just barely justifiable by current experiments.
However, Einstein's theory of general relativity has been proved to provide an accurate description of physics, ranging from cosmological scales down to one-tenth of a millimeter, kindling the ambition to understand general relativity as an effective low energy field theory rather than giving it up altogether [6, 7], possibly including higher curvature derivative terms [52] or requiring BRST symmetry [53] or combining both [54].
Given the functional renormalization group methods developed in chapter 1, which allow to study the evolution of a given theory over energy scales, we are equipped with means to proceed in this direction.
A major development is the rise of the idea of asymptotic safety, which can be traced back to a 1979 text by Weinberg [8], stating:

> *A theory is said to be asymptotically safe if the essential coupling parameters approach a fixed point as the momentum scale of their renormalization point goes to infinity.*

Translating this into the language of the FRG developed in chapter 1, the following equivalence holds:

> *Quantum gravity is considered asymptotically safe if the UV-critical surface is finite dimensional and the dimensionless coupling constants*[2] *cease to increase if the momentum scale k goes to infinity, but approach a set of ultraviolet fixed points instead.*

[2] To be more precise, we should speak of the essential couplings here - couplings that cannot be absorbed into field redefinitions and are thus independent.

The requirement of the UV-critical surface being finite dimensional stems from the fact that all parameters on the critical surface need to be determined experimentally. Thus, the theory is only predictive if a finite number of parameters remains to be fixed.
To date, there is much evidence for gravity's asymptotic safety, starting with the 1998 paper by Reuter [18] and subsequent works, which are for instance summarized in the review [11]. In [55], a discussion of possible underlying physical principles is provided and for a comprehensive overview of papers on quantum gravity and asymptotic safety we suggest [56]. However, since the RG flow depends on a variety of input parameters, a rigid proof has not been given.
Even though numerical results differ slightly depending on the chosen method and approximation, all authors find a Gaussian fixed point at $g_n^* = 0$, $\lambda^* = 0$ as well as a second fixed point at $g_n^* > 0$, $\lambda^* > 0$ referred to as the Wilson-Fisher fixed point. As perturbation theory is always an expansion around vanishing couplings, studying a non-Gaussian fixed point inherently requires the utilization of non-perturbative methods.[3] That is the reason why in this thesis, we will use the non-perturbative functional renormalization group to study the properties of dilatation symmetric scalar-tensor theories of quantum gravity.

2.3 Advances in Asymptotic Safety

After the first hint towards asymptotic safety [18] to which numerical results where added in [58] and the first diagram of the flow in the theory space provided by the Einstein-Hilbert truncation was published in [59], which we show in figure 2.1, a lot of progress has been made in terms of substantiating the non-perturbative fixed point, realizing technical advances, enlarging the truncation and coupling to other fundamental theories as well as applications. For reviews we point to [11–17].
To mention only a few important works, bootstrapping methods and $f(R)$ truncations also including higher derivative terms have been put forward in [60–63], in some cases up to $\mathcal{O}(R^{34})$. Even then, only three relevant directions remain. [64–66] put even more emphasis on higher derivative terms, while [12] considers higher asymptotic safety in higher dimensions.
Unimodular gravity is studied [67, 68], the ghost sector was made dynamical [69–71] and the background approximation was partially lifted in bi-metric studies [72–74], see also section 4.3. Matter interactions are studied in [75–88], while [84, 86, 89, 90, 90–92] focus on scalar interaction.
Potential signatures at collider experiments such as the LHC are studied in [93–96], usually in the context of extra dimensions that would lower the fundamental Planck

[3] We mention that limited evidence for the existence of a non-Gaussian expansion point was already obtained in $2 + \epsilon$-gravity [8, 57].

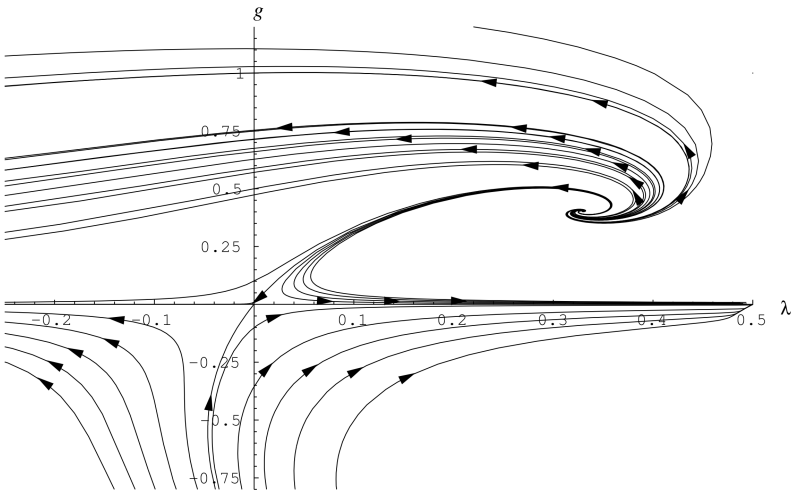

Figure 2.1: Original flow diagram of the flow of the Einstein-Hilbert truncation in theory space, taken from [59].

scale. Asymptotic safety is used to predict the Higgs mass in [97], while the context of black holes [98–100] and cosmology, more specifically inflation [101, 102] is also studied.

On a more conceptual note, vertex expansions allow for a well defined expansion around a flat background [19, 103, 104], see also section 4.4.2, and recently the attention was brought to locality [105], which boils down to the very of when a separation of momentum modes, as necessary for the FRG, is actually possible.

There is also a considerable amount of work put into connecting asymptotically safe quantum gravity with other fundamental theories of physics. Whenever scalar fields are involved, we refer to the more detailed treatment of sections 3.3 (cosmology) and 3.2 (particle physics).

In this cornucopia of research the current thesis connects at various junctions. Not only do we extend the study of scalars coupled to asymptotically safe gravity, we also use the emerging theory to establish a full theory of dilaton Gravity for the first time, smoothly connecting infrared with ultraviolet physics on a pure fixed point trajectory. While doing so, a dynamical generation of the Planck scale is explicitly shown and cosmological scenarios are discussed.

CHAPTER 3

Scalar Fields in Quantum Gravity

This chapter serves as an introduction to scalar fields in quantum gravity. Focusing on pure gravity first, we will give a brief historical outline pointing out the different roles scalar fields can play, before we move to applications in the areas of both cosmology and particle physics.

3.1 Pure Gravity and the Idea of Dilaton Quantum Gravity

In the context of pure gravity, there are two main motivations for including scalar fields into the theory. On the one hand, replacing couplings by scalar fields is a way of making said couplings spacetime dependent and with that, dynamical. On the other hand, scalar fields can be used to encode the physical scale, thus accessing questions of scale invariance and how physical scales are generated in a theory. While both motivations have important applications, the latter one will be more relevant to this thesis. The main result of this chapter will be the definition of the general class of theories to be considered in this thesis.

Dynamical Couplings

The idea of introducing a scalar field into the pure theory of gravity was originally presented by Brans and Dicke in 1961 [20] as an extension of Einstein's theory of general relativity [106], manifestly respecting Mach's principle [107].

When neglecting the cosmological constant, the action proposed reads

$$S_{\mathrm{BD}} = \int \mathrm{d}^4x\sqrt{g}\left(\frac{\omega}{\phi}\,\partial_\mu\phi\,\partial^\mu\phi - \phi\,R\right), \tag{3.1}$$

where the field ϕ is associated with G_N^{-1} and the factor $\frac{\omega}{\phi}$ in front of the kinetic term was introduced to account for correct dimensions. The field equations (2.2) are altered to

$$R_{\mu\nu} - \frac{1}{2}R\,g_{\mu\nu} = \frac{\omega}{\phi^2}(\partial_\mu\phi\,\partial_\nu\phi - \frac{1}{2}g_{\mu\nu}\partial_\rho\phi\,\partial^\rho\phi) + \frac{1}{\phi}(\partial_\mu\,\partial_\nu\phi - g_{\mu\nu}\partial_\rho\,\partial^\rho\phi) \tag{3.2}$$

as well as appended by a wave equation for the scalar field which remains sourceless if no energy momentum tensor is introduced and reads

$$\partial_\mu\partial^\mu\phi = 0. \tag{3.3}$$

Thus, the most striking change was the replacement of the static Newton constant with a scalar field that depends on spacetime and was equipped with its own evolution equation.
Brans-Dicke gravity was considered an extremely intriguing alternative to Einstein's pure general relativity at the time. As a member of Kip Thorne's working group allegedly once put it [108]:

> *We believed in Einstein's general relativity on Mondays, Wedensdays, and Fridays, and in Brans-Dicke gravity on Tuesdays, Thursdays, and Saturdays.*
> *On Sundays, we went to the beach.*

With regard to the constant ω, which can be utilized to scale the modification made to general relativity, it was shown that one recovers the pure Einstein theory in the limit $\omega \to \infty$ [109], provided certain conditions hold [110].
Experiments can be used to put constraints on ω which currently suggest $\omega \gtrsim 40,000$, meaning that experimental data suggests the convergence of Brans-Dicke theory to classical general relativity. Despite this discouraging perspective for the traditional Brans-Dicke theory, a more general class of scalar-tensor theories is still of great importance for both cosmology and particle physics.

Scale Invariance and the Dilaton

As derived in appendix G, a theory is scale invariant if and only if all couplings g_j have scaling dimension 0. It is evident that this is not usually the case for an arbitrarily given theory. For instance, looking at standard Einstein gravity as defined

by the effective Einstein-Hilbert action

$$\Gamma_{\mathrm{EH}}\left[g_{\mu\nu}\right] = \frac{1}{16\pi G_N}\int \mathrm{d}^4x\sqrt{g}\left(2\Lambda - R\right), \tag{3.4}$$

where G_N is the Newton coupling and Λ the cosmological constant, that are allowed to depend on the renormalization group scale. We find

$$[G_N] = -2 \text{ and } \left[\frac{\Lambda}{G_N}\right] = 4.$$

However, introducing a scalar field χ with $[\chi] = 1$, there is a way to make any theory scale invariant: Simply replace any dimensionful coupling g_i with $[g_i] = d_i$ with $\chi^{d_i}\hat{g}_i$ it is clear that now $[\hat{g}_i] = 0$: The theory is scale or dilatation invariant. That is why we will call χ the dilaton henceforth.[1]
Turning back to Einstein gravity, it is straightforward from the scaling dimensions given abovehand to find a Dilatation symmetric version, reading

$$\tilde{\Gamma}\left[g_{\mu\nu},\chi\right] = \int \mathrm{d}^4x\sqrt{g}\left(\lambda\chi^4 - \frac{1}{2}\xi\chi^2 R\right).$$

Note that λ and ξ, are both dimensionless and the coupling λ should not be confused with the scaling parameter from appendix G. So far, $\tilde{\Gamma}$ has little physical significance, as the scalar field will not be able to propagate. That is why in dilaton gravity, we promote the mathematical field χ to a true physical scalar by virtue of a kinetic term $\frac{1}{2}Zg_{\mu\nu}\partial^\mu\chi\partial^\nu\chi$, where Z is a wave function renormalization rescaling the scalar field and obeying $[Z] = 0$. Thus, we do not have to include additional powers of χ and hence define dilaton gravity through the action

$$\Gamma_{\mathrm{dilaton}}\left[g_{\mu\nu},\chi\right] = \int \mathrm{d}^4x\sqrt{g}\left(\lambda\chi^4 - \frac{1}{2}\xi\chi^2 R + \frac{1}{2}Zg_{\mu\nu}\partial^\mu\chi\partial^\nu\chi\right). \tag{3.5}$$

Given $[\xi] = [\lambda] = [Z] = 0$, the physical scale is only encoded in the scalar field χ and its expectation value $\langle\chi\rangle$, as we will show more explicitly in section 3.1.4. Equivalently speaking, all scales are measured in units of the dilaton χ. Thus, defining the dimensionless combination

$$y = \frac{\chi^2}{k^2}$$

fulfills two purposes: It is not only the dimensionless version of the field χ^2, but also

[1] Sometimes, the dilaton is also defined as the Goldstone boson emerging when Dilatation symmetry is spontaneously broken. As we will not deal with that boson in this thesis explicitly, we will drop the distinction.

a bookkeeping device for the RG scale k. This may also be a step towards a physical interpretation of the RG scale k.
In fact only two of the three couplings in this theory are independent, we can for instance understand Z as a mere rescaling of the scalar field. We will revisit this point in great detail in section 12.2.2.
For our later analysis it will be important to not only study theories in the dilatation symmetric phase where scale symmetry is intact, but also emerge into the broken phase. Furthermore, it will become evident in section 3.1.2 that in dilaton gravity, it is important to understand the full dependency of a class of theories on the scalar field χ. Hence, we need to enlarge the truncation (3.5). The truncation employed throughout this thesis is therefore

$$\Gamma\left[g_{\mu\nu},\chi\right]=\int d^4x\sqrt{g}\left(V(\chi^2)-\frac{1}{2}F(\chi^2)\,R+\frac{1}{2}K(\chi^2)g^{\mu\nu}\partial_\mu\chi\partial_\nu\chi\right). \tag{3.6}$$

Classical field equations for the action (3.6) are presented in appendix E. As soon as the form of the functions V, F and K admits a nonzero expectation value $\langle\chi\rangle$, the theory as a distinct scale and scale invariance is broken. In the appendix, we also clarify the notion of an effective cosmological constant.
Before moving on, we want to comment on two more points. Firstly, so far we only considered scale invariance. However, if one actually enhances the global scale to a local conformal symmetry, thereby allowing for the scaling parameter Ω to depend on spacetime, $\Omega=\Omega(x)$ (see appendix G) and thus defines $\hat{g}_i=\Omega(x)^{d_i}g_i$ the introduction of the dilaton is mandatory on even more fundamental level: to realize the induced spacetime dependency of couplings. This is precisely where our two original motivations overlap.
Secondly, we want to point out the fact that there are two fundamentally different interpretations of the field χ in the literature. If one is aiming for a manifestly Dilatation invariant RG flow, as for instance [111, 112], one needs to gauge fix χ, introduce position-dependent cut-off functions and modify geometrical quantities. However, then χ is not a real propagating physical scalar anymore, thus we would be unable to realise things like a spontaneous breaking of scale invariance and will not be able to dynamically generate physical scales, as we describe in the next sections.
For an action of the type (3.5), global scale invariance is enhanced to local conformal invariance at $\xi=-\frac{1}{6}$ [113–115]. This is also visible in the flow [111, 112], for a detailed treatment see [42], section 5.3 and section 7.8 of this thesis. This may be related to the classical conformal symmetry being broken on quantum level, which is called the Weyl anomaly [116, 117].

3.1.1 Frame Freedom and Physical Scales

When considering scalar-tensor theories of gravity, there are two classically equivalent frames available, the so called Jordan frame, in which the Ricci scalar R multiplies the scalar field χ, and the Einstein frame, where it does not. Our considerations in the last section clearly employed the Jordan frame, but can easily be transformed into the Einstein frame by means of a conformal or Weyl-scaling of the metric.
Rescaling the metric according to

$$g_{\mu\nu} = \Omega(\chi)^2 \tilde{g}_{\mu\nu}, \tag{3.7}$$

where we encoded the spacetime dependency through the scalar field, leads to a rescaled Ricci scalar, more explicitly

$$R = \Omega^{-2}\left[\tilde{R} - 6\tilde{g}^{\mu\nu}\left(\nabla_\mu\nabla_\nu \ln\Omega + \partial_\mu \ln\Omega\, \partial_\nu \ln\Omega\right)\right].$$

Considering the action (3.5) with $\lambda = 0,\ Z = 1$ and $\xi = 1$ for simplicity, we find that $\Omega = M\chi^{-1}$ produces the desired result, namely

$$\tilde{\Gamma}_{\text{dilaton}}\left[g_{\mu\nu}, \chi\right] = \int d^4x\sqrt{\tilde{g}}\left(-\frac{1}{2}M^2\tilde{R} + \frac{1}{2}g_{\mu\nu}\partial^\mu\varphi\,\partial^\nu\varphi\right),\ \text{where } \varphi = M\ln\frac{\chi}{M}.$$

Here, M is a scale which we will give meaning to in section 3.1.4.
Given that we have two equivalent frames at our disposal related by a conformal transformation, it is natural to seek for a formulation invariant under (3.7). The full truncation (3.6) maintains its form when setting

$$\tilde{F} = \Omega^2 F,\ \tilde{V} = \Omega^4 V \text{ and } \tilde{K} = \Omega^2\left[K - 6F\partial_\chi \ln\Omega\left(\partial_\chi \ln\Omega + \partial_\chi \ln F\right)\right].$$

Therefore, the combinations

$$\hat{V} = \frac{V}{F^2} \text{ and } \hat{K} = \frac{K}{F} + \frac{3}{2F^2}\left(\partial_\chi F\right)^2 \tag{3.8}$$

are invariant under (3.7) and thus contain the physical content of a given model [118]. To specify a certain frame, one needs to specify a form of the function $F(\chi^2)$
Thus, transforming to the Einstein frame (where $F(\chi^2) = M^2$) and absorbing $\hat{K}$ in an appropriately redefined field ϕ, it is always possible to cast a theory (3.6) into its standard form

$$\mathit{\Gamma} = \int \mathrm{d}^4x\left(\hat{V}_{\text{norm}}(\phi) - \frac{1}{2}M^2R + \frac{1}{2}g_{\mu\nu}\partial^\mu\phi\partial^\nu\phi\right). \tag{3.9}$$

In this form, the physical scale is encoded in the mass M, while the dynamics are

those of a scalar field minimally coupled to gravity. This form is especially convenient when discussing cosmic inflation, see section 3.3 and 13.4. Further note that since $\hat{V}_{\text{norm}}$ is the only dynamical function in this formulation, we can directly read off the effective cosmological constant as a function of ϕ,

$$\Lambda_{\text{eff}} = 8\pi G_N \hat{V}_{\text{norm}}(\phi).$$

A small value of the potential in the infrared thus opens up intriguing possibilities for explaining why the measured value of the cosmological constant is about 10^{-120} times smaller than the value that can be estimated from quantum vacuum fluctuations [119, 120].

3.1.2 Fixed Points in Einstein and Dilaton Gravity

Let us step back for a moment and put some thought into the notion of a fixed point. The traditional condition given in section 1.4 is rooted in sets of algebraic or differential equations for the dimensionless couplings, reading

$$\partial_t g_i = \beta_i(\{g_j\}) = 0 \ \forall i, \tag{3.10}$$

where g_i is the i-th coupling of the system, and $\{g_j\}$ denotes a potential dependence on all couplings present in the system. The physical meaning of this condition is more readily put as follows: On the fixed point, the scale becomes irrelevant, the theory exhibits a dilatation or scale symmetry.[2]
Having shown in the previous section that we can always make a theory dilatation invariant by multiplying couplings with appropriate powers of a scalar field χ, and also allowing for additional, not dilatation invariant terms to emerge, we can now work with a different condition for a fixed point, applicable to dilaton gravity: On the fixed point, Dilatation symmetry of the action Γ is exact, while away from the fixed point, Dilatation symmetry is broken, leading to a nonzero Planck mass and with that to an explicit scale in the theory as explained in section 3.1.4.
Hence, y parametrises a trajectory from the infrared to the ultraviolet regime of gravity, and with that from classical general relativity to quantum gravity, which we will map to different epochs of existence of the universe in several cosmological applications. We emphasize that there is no need to deviate from the fixed point as defined by 3.10 to evolve from the infrared to the ultraviolet in contrast to the situation in standard Einstein gravity. We will make extensive use of this fact when determining the fundamental scale of our theory, the Planck mass, in section 3.1.4. In this spirit, we will use ultraviolet interchangeably with $y \to 0$ and infrared

[2] There is ongoing debate in the community whether this scale symmetry is always enhanced to a conformal symmetry, see for instance [112, 121–124].

interchangeably with $y \to \infty$ in this thesis. As it turns out, there are even more profound reasons to do so: The system under considerations exhibits classical scaling relations and vanishing quantum contributions to the flows for $y \to \infty$, while this is not true for $y \to 0$.
In particular that means that flow diagrams in theory space customary to treatments of Einstein quantum gravity such as figures 1.2 and 2.1 are replaced with ordinary plots of y dependent coupling functions, see for instance figure 12.4, in dilaton quantum gravity. Thereby, different trajectories in Einstein quantum gravity may correspond to different sets of initial conditions for functions potentially viable in dilaton gravity. This is discussed in detail in sections 13.4 and 13.5.
Note that there is one more fundamental difference between a fixed point in Einstein and dilaton gravity: A fixed point is always defined for the dimensionless couplings. To determine the effective physical couplings, appropriate powers of the scale k need to be added. However, this makes it impossible to write down a fixed point action, the only thing we can give are fixed point values for the dimensionless couplings. In contrast to that, for a dilatation symmetric theory no powers of k need to be added, and we can write down the full fixed point action. This is precisely the reason why the aforementioned scale invariance exhibited once a fixed point is approached cannot manifestly be seen in any action in Einstein gravity. What may seem like a pedagogical distinction will become very important in a bit.

3.1.3 An infrared fixed point for Dilaton Gravity

Without having to calculate any flow equations, we can already learn a lot about possible infrared fixed points from simple physical arguments. The main ingredient is the simple observation that if

$$F \sim \xi\chi^2 \text{ for } y \to \infty \tag{3.11}$$

the strength of the gravitational interaction is given by $\xi^{-1}\chi^{-2}$. The limit 3.11 is inspired by Dilatation symmetry. For the gravity induced flow of the dimensionless quantities only the dimensionless combination $\xi^{-1}y^{-1}$ can be of relevance. However, this quantity vanishes for $y \to \infty$ and the gravitational interactions are absent in this limit. For $y \to \infty$ and $V(y \to \infty) \to const.$ one is then left with a scalar field that is only minimally coupled to gravity. In turn, for a free scalar field the flow cannot induce a nontrivial χ-dependent effective potential, such that only a constant term can flow in V. For large y, the leading term in v_k is then proportional to y^{-2} and vanishes for $y \to \infty$, such that at the fixed point

$$\lim_{y\to\infty} V = const. \tag{3.12}$$

remains true. For a vanishing strength of the gravitational interaction the leading term in the gravitational sector of the effective action does not flow either. Thus ξ does not depend on k, establishing an asymptotic behavior

$$F \sim \xi\chi^2,\ V \sim const. \text{ for } y \to \infty.$$

Since the constant part of the potential would need to be multiplied by k^4 to obtain physical dimensionful quantities, infrared physics is solely driven by F.

3.1.4 The Planck scale in Einstein and Dilaton Quantum Gravity

The Planck mass as the fundamental scale of quantum gravity is of special importance to our considerations. That is why we want to take a moment to comment on how it emerges in the different approaches to quantum gravity.
Let us first consider the case of conventional Einstein Gravity, defined by the Euclidian Einstein Hilbert action (3.4). Assuming the asymptotic safety scenario to hold, both dimensionless couplings $g = k^2 G_N$ and $\lambda = k^{-2}\Lambda$ have to approach fixed points g^* and λ^* of the RG flow when the scale is increased. This is believed to happen around the scale set by the Planck mass M. Furthermore, in the classical regime of small $\frac{k}{M}$ all quantum effects should vanish leading to a vanishing anomalous dimensions, and the couplings should thus only run according to their canonical mass dimensions. For G_N we have $[G_N] = 2$ and would thus expect a straight line with slope $+2$ in the infrared. This is schematically illustrated in figure 3.1.
Having established

$$g = Ak^2 \text{ for } \frac{k}{M} \ll 1,$$

where A is the slope of the curce and keeping in mind that $g = G_N k^2$, we can immediately write

$$A = G_N.$$

The constant that has mass dimension 1 derived from G_N is called Planck mass. We thus have

$$M^2 = \frac{1}{8\pi G_N},$$

and can read off the Planck mass from the slope of the curve in the infrared,

$$M = \sqrt{\frac{2}{A}}.$$

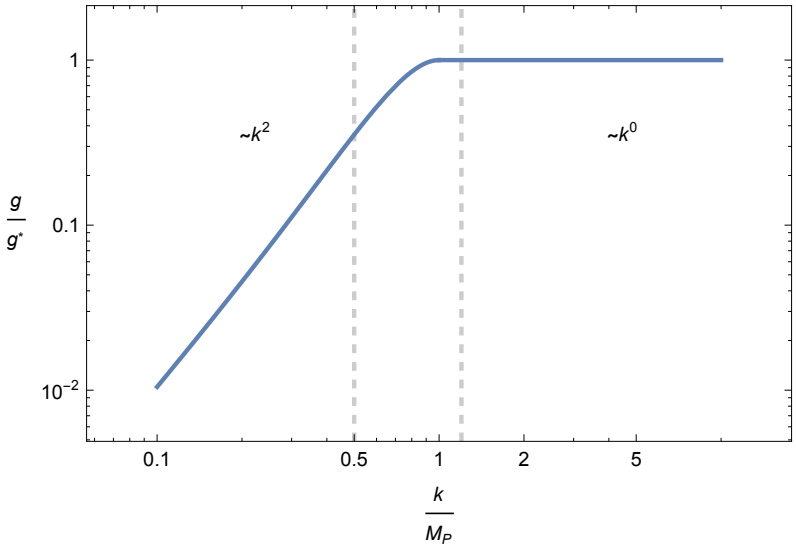

Figure 3.1: Schematic plot of the scale dependence of the dimensionless Newton coupling g. A physically realistic version of this can be found for instance in [48], figure 5.13.

Rewriting the Einstein-Hilbert action in terms of the Planck mass we have

$$\Gamma_{\mathrm{EH}} = \frac{1}{2} Z_h M^2 \int \mathrm{d}^4x \, (2\Lambda - R) \,,$$

where we also absorbed all RG runnings into a prefactor Z_h. In this notation, M is the constant fundamental scale of the physical system, and Z_h acts as the wave function renormalization for the graviton. Normalizing $Z(k = 0) = 1$, the RG flow should yield

$$\eta_h = -\frac{\dot{Z}_h}{Z_h} = 0 \text{ for } \frac{k}{M} \ll 1,$$

in accordance with our previous analysis. This behavior has been established for instance in [19].
Note that this way of defining the Planck mass crucially depends on the flow of a relevant parameter away from the fixed point.
Let us now turn to dilaton Gravity. We have already established in section 3.1.2 that dilaton Gravity offers a novel characterization of the fixed point by means of using the scalar field χ to rescale all couplings in a way that makes them dimensionless and thus the theory invariant under global rescalings, also see appendix G. When this so called Dilatation symmetry is broken, the theory is no longer scale invariant and we have therefore departed from the fixed point. This is encoded in a nonzero

expectation value for the scalar field $\langle\chi\rangle$. We give some details on how to determine said expectation value in appendix E. The RG scale k is encoded in the field via $y = \frac{\chi^2}{k^2}$. Taking the form of the proposed Dilatation symmetric fixed point for large y (or small k) from section 3.1.3 reading

$$\Gamma(k \to 0) = \int d^4x\sqrt{g}\left(\frac{1}{2}g^{\mu\nu}\partial_\mu\chi\,\partial_\nu\chi - \frac{1}{2}\xi\chi^2\,R\right), \tag{3.13}$$

we can perform a Weyl rescaling to the Einstein frame (see section 3.1.1) to arrive at

$$\Gamma(k \to 0) = \int d^4x\sqrt{g}\left(\frac{1}{2}g^{\mu\nu}\partial_\mu\phi\,\partial_\nu\phi - \frac{1}{2}M^2\,R\right).$$

Including a constant potential only makes the calculations more cumbersome but does not change any physical aspects at this stage. This is the familiar Einstein-Hilbert action with an additional massless scalar field. From here it becomes clear that in dilaton gravity, the Planck mass emerges through the scalar field, namely

$$M = \sqrt{\xi}\,\langle\chi\rangle.$$

We emphasize that the possibility to write down a full fixed point action and not just fixed values for dimensionless couplings is a result of the construction of dilaton gravity.
Note that there is no need to deviate from the fixed point to set the Planck scale. It is set by the scalar field acquiring a nonzero expectation value $\langle\chi\rangle$, signaling the breaking of scale or dilatation invariance. Thus, the equivalent of classical infrared scaling of Einstein Gravity in dilaton Gravity is the breaking of the dilatation symmetric infrared fixed point [125, 126]. This is the main reason why we are interested in the full form of the functions V and F for all values of the scalar field χ, and do not simply consider a finite subset of couplings.

3.2 Applications I: Particle Physics

Concerning applications to particle physics, the most immediate application could be the coupling of the Standard Model Higgs Sector, which essentially consists of a scalar ϕ^4-theory, to gravity [127], also in relation with the scale of new physics [96]. In recent works [97], the authors have been able to forecast the mass of the Higgs boson with great numerical accuracy to $m_H \sim 126$ GeV from the assumption that gravity is asymptotically safe, which is in complete accordance with original data from the Large Hadron Collider [2, 3].
On a more conceptual level, scalar fields can be used to generate arbitrary constants dynamically. Thus, the study of scalar-tensor theories is a first step towards resolving

the hierarchy problem, addressing the question why gravity is so much weaker than the other three fundamental forces described by the standard model. Another facet of the hierarchy problem is the small numerical value for the cosmological constant, predicted by experiments. Explicit studies of a dilaton at the LHC are presented in [128, 129].
Furthermore, scalar matter is discussed in [86] and as a dark matter candidate in [130, 131].

3.3 Applications II: Cosmology

Shifting our focus to cosmology, scalar fields are known to appear at a variety of stages, including but by far not limited to inflation [132] and dark matter, see [101, 133, 134] for FRG studies. Moreover, virtually every constant can be promoted to a dynamical variable by virtue of identifying it with a scalar field. For example, the implications of a variable Newton constant were studied in [135], the investigation of a dynamical cosmological constant was put forward in [136], while [118, 137–142] combine the aforementioned ideas.
In this thesis, we will mainly be concerned with theories that possess a dilatation symmetry, which were found to exhibit interesting properties as early as in the 1960s. The author of [143] showed that classical electrodynamics with charged particles possessing finite mass is invariant under a group of mass dilatations and a corresponding conservation law was derived.
As explained in greater detail in appendix G, the requirement of dilatation symmetry takes the dynamical generation of constants to a new level, as in a dilatation symmetric theory the only notion of scale itself is introduced through the expectation value of the scalar field when the symmetry is spontaneously broken. The massless Goldstone boson arising in this process is usually referred to as the dilaton [125, 144].
In the framework of particle cosmology, a dilaton frequently arises. In cosmological scenarios one usually needs to add a potential $V(\phi)$ for the scalar field ϕ to the action (3.1). The dilaton arises naturally in the process of compactifying dimensions in Kaluza-Klein theory (for a review see [145]) and with that in string theory. Furthermore, it has a wide range of cosmologically relevant consequences, such as within the context of inflation and emerging dark energy and matter [25, 146–148] and moreover due to the connection of its potential with the cosmological constant and the hierarchy problem [149–151].
Using the Friedmann equations, on can show that accelerated expansion is possible for sufficiently negative pressure, which can be translated into the kinetic term of a scalar field needing to be sufficiently small with respect to its potential [152–154]. This is known as slow roll inflation. Exponentially decaying potentials are of special interest [155–158]. They make slow roll expansion possible and they vanish for large

fields, offering a potential explanation for the small value of the cosmological constant today.
We mention that the classical equivalence of $f(R)$ type theories and scalar-tensor theories may also offer interesting prospects [159], and the relation between conformal and nonconformal regimes are discussed [160, 161].

CHAPTER 4

Background Field Methods and Vertex Expansions

In this chapter, we introduce the basic notion of background fields in section 4.1, derive the formalism of background field approximations for quantum gravity and discuss its shortcomings in section 4.2. Lastly, we consider replacing the background approximation traditionally done in functional renormalization group quantum gravity computations by a vertex construction, facilitated by expanding around a flat background. This construction has both computational and conceptual advantages that we will discuss in section 4.4.2.
This chapter therefore defines the technical environment in which the two major computations presented in this thesis are carried out: In part II, we derive, solve and discuss flow equations in a symmetric background field approximation, while III deals with an expansion around a flat background, employing a partial vertex construction.

4.1 Gauge Theories and Background Field Formalism

Gauge theories are clearly a fundamental theoretical building block of modern physics. The formulation of the Standard Model of Particle Physics in terms of a quantum field theory processing a local gauge invariance is beyond doubt one of the very successful examples thereof. In order to formulate a quantum theory of gravity, this thesis relies on the machinery of quantum field theory together with the functional renormalization group, and with that on a formulation of classical general relativity as a gauge theory (section 2.1).
However, the formal treatment of gauge theories is far from simple. That is why we

will take some time here to develop technical means necessary, especially regarding the formulation of a quantum field theory in terms of the effective average action.
Consider a quantum field theory defined by an action S that is invariant under a certain global transformation with infinitesimal generator $\mathcal{G}$, i.e. $\mathcal{G}S = 0$. The effective action Γ defined in (1.4) will be invariant if in addition to S also the measure $\mathcal{D}\psi$ is invariant, in which case $\mathcal{G}\Gamma = 0$ holds. At this point, $\mathcal{G}S = \mathcal{G}\Gamma = 0$ signals that both the action as well as the average action are manifestly invariant under the transformation $\mathcal{G}$.
However, if $\mathcal{G}$ is promoted to a local gauge symmetry, the statement is not as straightforward anymore: The definition of Γ involves a functional integral over all field configurations. In the case of gauge theories, this is ill-defined a priori, as one has to make sure that gauge equivalent field configurations only contribute once. This is done by means of gauge fixing, usually through the standard Faddeev-Popov prescription [162, 163]. Therefore, in an effective action for a gauge theory, manifest gauge invariance is always lost, and the symmetry is now encoded in Ward identities [33].
Moreover, for the effective average action Γ_k introduced in (1.13) to be invariant, the transformation properties of the cutoff action ΔS_k need to be considered separately. Nonetheless, given the special form we chose for ΔS_k in equation (1.10), the regulator will rarely be invariant under the gauge symmetry: mass terms for gauge bosons are usually excluded. Even for $k = 0$, where $\Gamma_k = \Gamma$, the symmetry is only restored if a set of modified Ward identities, to be understood as Ward identities in the presence of a regulator, are fulfilled,[1] making keeping track of the fundamental symmetries a cumbersome task.

4.1.1 Background Fields and Background Transformations

Therefore, wouldn't it be nice to restore manifest gauge invariance in the effective average action Γ_k by means of a special construction? That is exactly the aim of the background field method widely used in functional renormalization group studies of gauge theories. It was first introduced in [164], see [28, 35, 165, 166] for applications to QCD and [33, 167] for reviews. Consider a generic quantum field theory defined by an effective action $\Gamma[\varphi]$. Here, φ is an arbitrary (super-)field, not necessarily a scalar, and not necessarily related to gravity at this stage. One possibility to overcome the aforementioned problem is provided by the background field formalism, which splits the field φ into a fixed background $\bar{\varphi}$ as well as a fluctuating part $\delta\varphi$, $\varphi = \bar{\varphi} + \delta\varphi$. We emphasize that this split is quite different from what is done in standard perturbation theory, as $\delta\varphi$ is not required to be small. Since we want $\delta\varphi$ to carry the dynamics of the theory, all functional integrals will be w.r.t ϕ, and thus

[1] Luckily it can be shown that the modified scale depended ward identity for a specific symmetry if satisfied at some scale $k = k_0$, $\mathcal{W}_{k_0} = 0$ is a fixed point under the RG flow, $\partial_t \mathcal{W}_k = 0$.

the gauge transformation $\mathcal{G}$ also acts on φ, leaving $\bar{\varphi}$ invariant. This allows for the introduction of an independent gauge transformation $\bar{\mathcal{G}}$ for the auxiliary field $\bar{\varphi}$. We can then construct a gauge fixed theory that is not manifestly invariant under $\mathcal{G}$ but can be made manifestly invariant under the combination $\bar{\mathcal{G}} + \mathcal{G}$ by choosing $\bar{\mathcal{G}}$ appropriately,

$$0 = (\bar{\mathcal{G}} + \mathcal{G})\Gamma_k[\bar{\varphi}, \delta\varphi], \tag{4.1}$$

thus saving us the trouble of having to deal with Ward identities. Note that the switch from Γ to Γ_k means that we always have to also take care of $(\mathcal{G} + \bar{\mathcal{G}})\Delta S_k = 0$. In order to let Γ_k inherit the full symmetry properties at the end, we will identify $\varphi = \bar{\varphi}$ at the end of our gauge fixed calculations,

$$0 = (\bar{\mathcal{G}} + \mathcal{G})\Gamma_k[\bar{\varphi}, \delta\varphi] \,\big|_{\varphi=\bar{\varphi}} = \mathcal{G}\Gamma_k[\bar{\varphi}, \bar{\varphi}]. \tag{4.2}$$

Then, physics is encoded in $\bar{\varphi}$, and the physically measurable couplings are the couplings of $\bar{\varphi}$.

4.1.2 Background Field Formalism and the Functional Renormalization Group

However, there are two major drawbacks of this formalism. The first concerns the dependence of the results on the specific background and gauge fixing chosen: Even though one could argue that the introduction of a separate background field is only an intermediate step, and thus the results should not depend on the background chosen, this is evidently not true for truncated FRG computations, and an open line of research.
Furthermore, one has to take care of the dependence of the results on the specific gauge fixing conditions used. This can be done by means of geometrical flows as briefly outlined in section 4.3.
The second drawback is related to the flow equation itself. After the background field split, the flow equation (1.19) is a function of both $\bar{\varphi}$ and $\delta\varphi$ separately and not just of the sum $\varphi = \bar{\varphi} + \delta\varphi$.
The LHS of the flow equation is a function of $\bar{\varphi}$ and $\delta\varphi$ at $\bar{\varphi} = \varphi$,

$$\partial_t \Gamma_k = \partial_t \Gamma_k[\bar{\varphi}, \delta\varphi] \,\big|_{\bar{\varphi}=\varphi} .$$

In contradistinction, the RHS depends on $\Gamma_k^{(2)}$ as

$$\frac{\delta^2 \Gamma_k[\bar{\varphi}, \delta\varphi]}{\delta\varphi\, \delta\varphi} \,\big|_{\bar{\varphi}=\varphi}, \tag{4.3}$$

which cannot be obtained from the LHS, as it is already evaluated at $\bar{\varphi} = \varphi$. That means that all we can feed back into the RHS is the background approximation

$$\frac{\delta^2 \Gamma_k[\varphi,\varphi]}{\delta\varphi\,\delta\varphi} = \frac{\delta^2 \Gamma_k[\bar{\varphi},\bar{\varphi}]}{\delta\bar{\varphi}\,\delta\bar{\varphi}}, \tag{4.4}$$

producing an inaccuracy triggered by

$$\frac{\delta^2 \Gamma_k[\varphi,\varphi]}{\delta\varphi\,\delta\varphi} = \frac{\delta^2 \Gamma_k[\bar{\varphi},\varphi]}{\delta\varphi\,\delta\varphi}\,\Big|_{\bar{\varphi}=\varphi} + \frac{\delta^2 \Gamma_k[\bar{\varphi},\varphi]}{\delta\bar{\varphi}\,\delta\bar{\varphi}}\,\Big|_{\bar{\varphi}=\varphi} + 2\frac{\delta}{\delta\varphi}\frac{\delta}{\delta\bar{\varphi}}\Gamma_k[\bar{\varphi},\varphi]\,\Big|_{\bar{\varphi}=\varphi}. \tag{4.5}$$

Thus, the flow only closes and, with that, identification is only possible on an exact level if

$$\frac{\delta^2 \Gamma_k[\bar{\varphi},\varphi]}{\delta\bar{\varphi}\,\delta\bar{\varphi}}\,\Big|_{\bar{\varphi}=\varphi} + 2\frac{\delta}{\delta\varphi}\frac{\delta}{\delta\bar{\varphi}}\Gamma_k[\bar{\varphi},\varphi]\,\Big|_{\bar{\varphi}=\varphi} = 0. \tag{4.6}$$

In quantum gravity, the situation is even worse: Any combination of metrics invariant under diffeomorphisms is automatically of infinite order in the field due to the factor $\sqrt{g}$ in the canonical volume element, thus spoiling the one loop structure of the flow equation. The only way out is to ensure that the regulator for the gravitational part of the theory is a function of the background metric only to make the full theory, including the inserted regulator part, invariant under $\mathcal{G} + \bar{\mathcal{G}}$, in the process furthering the individual dependence on background and fluctuating field. This is deeply routed in the structure of the flow equations for quantum gravity, even without any gauge fixing present.

In [168], a consistency criterion was derived based on the so called split identities [73, 74, 169–171] which control the inaccuracy. It reads

$$\begin{aligned} &\mathrm{Tr}\left[\frac{1}{\Gamma_k^{(2)}[\bar{\varphi},\varphi] + \mathcal{R}_k[\bar{\varphi}]}\Gamma_k^{(3)}[\bar{\varphi},\varphi,\varphi]\frac{1}{\Gamma_k^{(2)}[\bar{\varphi},\varphi] + \mathcal{R}_k[\bar{\varphi}]}\,\partial_t\mathcal{R}_k[\bar{\varphi}]\right] \\ &= \mathrm{Tr}\left[\frac{1}{\Gamma_k^{(2)}[\bar{\varphi},\varphi] + \mathcal{R}_k[\bar{\varphi}]}\left(\partial_t\Gamma_k^{(2)}[\varphi,\varphi]\right)\frac{1}{\Gamma_k^{(2)}[\bar{\varphi},\varphi] + \mathcal{R}_k[\bar{\varphi}]}\frac{\delta\mathcal{R}_k}{\delta\bar{\varphi}}\right] \end{aligned} \tag{4.7}$$

and can be used to measure the inaccuracy produced by the background approximation. More loosely speaking, the effect of the background approximation is that the flow picks up unphysical regulator contributions. It was shown that these can gain physical relevance in [172, 173], as the authors were able to flip the sign of the one-loop β-functions for QCD, which destroys the essential feature of confinement. For a further discussion of stability issues related to the background formalism in QCD coupled to quantum gravity we refer to [174, 175].

Even though for a general flow equation (4.6) certainly does not hold, we will

henceforth assume it as an approximation, the so called background approximation. Hence, the background approximation enables us to perform the field identification and close the flow equation.
Despite those difficulties, we will employ the background field formalism when deriving a first flow equation for scalar-tensor theories of quantum gravity in part II. In part III we will take a slightly different approach that will be explained in section 4.4.2.

4.2 Background Field Formalism for Quantum Gravity

This section is devoted to crafting the building blocks needed to investigate the coupling of scalar theories to general relativity in the context of gauge field theory. In order to do so, we resort to the ideas of section 4.1 applied to classical general relativity as defined in section 2.1 and modify them to fit quantum gravity.
Our derivation needs to focus on the graviton degrees of freedom, as they transform non-trivially under the gauge group of gravity, namely the group of diffeomorphisms on the spacetime manifold M usually denoted by $\mathrm{Diff}(M)$. This statement is further explained in appendix F. Thus, in order to not over-count, we need to restrain all path integrals to precisely one gauge orbit (i.e. a subspace of field configuration space that contains exactly one representative per gauge equivalent class). In mathematical terms, we need to find the factor-manifold $M(g_{\mu\nu})/\mathrm{Diff}(M)$. This is a delicate task, which is actually not carried out very well by standard quantum field theory gauge fixing procedures [176]. However, it can be shown [33] that if suitable initial conditions are picked for the FRG flow it automatically stays within one Gribov region, thus ensuring a well defined functional measure.
Having fixed the factor-manifold, we can then apply the standard Faddeev-Popov gauge fixing and quantization prescription, breaking the physical symmetry and collecting ghost and anti-ghost degrees of freedom C_μ and $\bar{C}_\mu$ in the process.
Let us now proceed to substantiate the construction of a background split presented in section 4.1 to quantum gravity, coupled to a scalar theory. We write

$$g_{\mu\nu} = \bar{g}_{\mu\nu} + h_{\mu\nu} \tag{4.8}$$

for the graviton degrees of freedom and split the scalar field according to

$$\chi = \bar{\chi} + \delta\chi. \tag{4.9}$$

The group $\mathrm{Diff}(M)$ acts on the dynamical metric $h_{\mu\nu}$, leading to the necessity of performing the factorization as $M(h_{\mu\nu})/\mathrm{Diff}(M)$. In a local chart, the action of a diffeomorphism is expressed through the Lie derivative and leaves the background

metric $\bar{g}_{\mu\nu}$ unaltered,

$$\mathcal{G}: \quad \left| \begin{array}{lcl} h_{\mu\nu} & \to & h_{\mu\nu} + \mathcal{L}_\epsilon h_{\mu\nu}, \\ \bar{g}_{\mu\nu} & \to & \bar{g}_{\mu\nu}, \end{array} \right. \tag{4.10}$$

in complete accordance with the statements made in section 2.1. The additional auxiliary gauge transformation $\bar{\mathcal{G}}$, rendering the theory invariant under $\mathcal{G} + \bar{\mathcal{G}}$, can now be readily written as

$$\bar{\mathcal{G}}: \quad \left| \begin{array}{lcl} h_{\mu\nu} & \to & h_{\mu\nu} - \mathcal{L}_\epsilon h_{\mu\nu}, \\ \bar{g}_{\mu\nu} & \to & \bar{g}_{\mu\nu} + \mathcal{L}_\epsilon \bar{g}_{\mu\nu}. \end{array} \right. \tag{4.11}$$

By definition, this construction remains valid if scalar fields are introduced.
Two more steps are to be completed: Extracting an action for the ghosts on the level of the effective action Γ from the elected gauge fixing condition and proving that the procedure still yields the desired results when carrying over to the effective average action Γ_k for our further renormalization group analysis.
Concerning the first, we select a gauge fixing action of the form

$$S_{\text{gauge fixing}} = \frac{1}{2\alpha} \int \mathrm{d}^d x \sqrt{\bar{g}} F(\bar{\chi}^2) \bar{g}^{\mu\nu} \bar{\mathcal{F}}_\mu \bar{\mathcal{F}}_\nu, \tag{4.12}$$

where $F(\chi^2)$ accounts for a later coupling of the scalar field to gravity via the Ricci scalar R and $\bar{\mathcal{F}}_\mu(h_{\rho\sigma})$ is a function of the dynamical metric and the background covariant derivative. The choice

$$\bar{\mathcal{F}}^\mu = \left(\bar{\nabla}_\nu h^{\nu\mu} - \frac{\beta+1}{d} \bar{\nabla}^\mu h \right) \tag{4.13}$$

is linear in the fluctuation field and thus only introduces linear interactions between gravitons and ghosts. Furthermore, this choice is invariant under $\mathcal{G} + \bar{\mathcal{G}}$ as introduced before.
Throughout this thesis, we will employ the limit $\alpha \to 0$, which ensures an exact implementation of the gauge fixing condition and is a fixed point of the renormalization group flow of both α and β for arbitrary β [177]. That is why we will always work with $\alpha = 0$, while will set β in a way to simplify computations where possible.
Exponentiating the Faddeev-Popov determinant, we arrive at a corresponding ghost action that reads

$$S_{\text{ghost}} = -\int \mathrm{d}^d x \sqrt{\bar{g}} C^\mu \left[\delta^\rho_\mu \bar{\Box} + \left(1 - \frac{2(1+\beta)}{d} \right) \bar{\nabla}_\mu \bar{\nabla}^\rho + \bar{R}^\rho_\mu \right] C_\rho. \tag{4.14}$$

Note that it is not necessary to introduce a background split for C_μ, and we regard the full C_μ as a fluctuating quantum field.

From a standard quantum field theory perspective no second step would be necessary. However, in the context of the functional renormalization group we still need to consider the transformation $\Gamma \to \Gamma_k$, which is carried out by adding a regulator action ΔS_k (see section 4.1). In appendix C.4 we address this issue by electing a regulator $\mathcal{R}_k$ that depends on the background fields only and scales like $\Gamma_k^{(2)}$, thereby respecting the requirement of invariance under $\mathcal{G} + \bar{\mathcal{G}}$ by construction. Even though we derive the properties of the regulator in the context of the calculation done in part III of this thesis, they also hold for the background calculation in part II with the exception of the insertion of anomalous dimensions. These can simply be set to 0 to arrive at the background results.

4.3 Extensions of the Background Field Method

Geometrical Flow Equations

We briefly mention a more enhanced approach for the construction of a diffeomorphism invariant[2] renormalization group flow for quantum gravity, utilizing geometrical flow equations through Vilkovisky connections. It was first introduced in [178] and subsequently put forward in [179] as well as more recently in [47, 180] and applied in [19, 48]. In contrast to the background field formalism, the split in the fields is not necessarily linear, allowing for the introduction of a nontrivial metric γ on the field space, which would be the space of all Riemannian metrics in the application to quantum gravity. Having introduced γ, the path integral measure $\mathcal{D}g_{\mu\nu}$ can be made invariant under reparameterizations by the inclusion of a factor $\sqrt{\det \gamma}$ with a suitable definition of the determinant function det. This leads to the effective average action depending on two independent dynamical fields, $\Gamma = \Gamma[\tilde{g}_{\mu\nu}; g_{\mu\nu}]$, and being invariant under gauge transformations with respect to either of them. The standard background field formalism as used in this thesis is recovered when performing a linear approximation. The geometrical approach provides further support for the asymptotic safety scenario as well as prospects for an infrared fixed point structure.

Nonlinear splits

There is no fundamental reason for the split (4.8) to be linear. In principle, one could construct an arbitrary background split with some function $\mathcal{Z}$,

$$g_{\mu\nu} = \mathcal{Z}(\bar{g}_{\mu\nu}, h_{\mu\nu}).$$

[2] When talking about gravity as a gauge theory, its gauge group is the group of coordinate diffeomorphisms. Thus, we use gauge invariant and diffeomorphism invariant interchangeably.

Originally introduced in a $2+\epsilon$ dimensions study [181], it was used in [91], where an exponential split

$$g_{\mu\nu} = \bar{g}_{\mu\rho}\left(e^{h}\right)^{\rho}_{\nu}$$

was used to circumvent some of the problems of the scalar-tensor system that we will also encounter in part II of this thesis. However, we will use a different approach to circumvent these shortcomings in part III.

Bimetric Approximations

A detailed account of the background dependence in quantum gravity is further given in [72]. Therein, the field identification is not performed and quantum gravity is considered as a bimetric theory. Conceptual issues are discussed in detail and some evidence pointing towards asymptotic safety is presented, but only in a conformally reduced toy model. Recent results are presented in [73, 74], where it was shown that it is possible to restore split symmetries in asymptotically safe gravity.

4.4 Approximation Schemes

In equation (1.22), we introduced an expansion of the effective action in terms of some basis functions $\{\mathcal{P}_\alpha\}$, and how the normally infinite basis needs to be reduced to a finite subset for practical calculations. Here we introduce two commonly used systematic expansion schemes that will also be employed in part II and III of this thesis, respectively: The derivative and the vertex expansion.

4.4.1 Derivative Expansion

Within a derivative expansion one sets a maximum number of spacetime derivatives of fields to appear in the effective action. In gravity, operators of $\mathcal{O}(R^n)$ contain $2n$ spacetime derivatives, such that the Einstein-Hilbert action is a derivative expansion of order 2. Since also the kinetic term for a generic scalar field $\sim g_{\mu\nu}\partial^\mu\chi\partial^\nu\chi$ effectively contains two spacetime derivatives, a derivative expansion of order 2 is commonly employed in quantum gravity calculations with and without scalar fields. This sets our truncation in consistency with equation (3.6). The approximation is again made if in equation (1.27) also the RHS is expanded in the exact same basis, allowing only for operators with up to two spacetime derivatives. The implications of this approximation are not easily assessed. Furthermore, since in momentum space a derivative is replaced by the momentum p, one might argue that the derivative expansion is an expansion in small momenta, the consequences of which are not clear to date. This is mainly due to the fact that it only recently became possible to

capture the momentum dependence of flowing quantities, using the vertex expansion discussed below [105].
Throughout part II of this thesis, we employ a derivative expansion. Additionally, to treat the functions V, F and K, an expansion in powers or inverse powers of χ^2 is used, which can be interpreted as an additional operator expansion, including operators up to a certain mass dimension.

4.4.2 Vertex Expansion

The vertex expansion as employed in part III of this thesis is a systematic expansion of the effective action in powers of the field φ according to

$$\Gamma_k[\varphi] = \sum_{n=0}^{\infty} \frac{1}{n!} \int \mathrm{d}^4x_1 \dots \mathrm{d}^4x_n \Gamma_k^{(n)}(x_1, \dots, x_n) \mid_{\varphi=0} \varphi(x_1) \dots \varphi(x_n), \tag{4.15}$$

meaning that the basis functionals are now expressed through the n-th correlation function,

$$\tilde{u}_n \mathcal{P}_n = \frac{1}{n!} \int \mathrm{d}^4x_1 \dots \mathrm{d}^4x_n \Gamma_k^{(n)}(x_1, \dots, x_n) \mid_{\varphi=0} \varphi(x_1) \dots \varphi(x_n). \tag{4.16}$$

A truncation thus amounts to cutting the series at a finite $n = N$, and the ansatz is not made for the effective action, but for $\Gamma_k^{(n)}$, $n \leq N$. $\Gamma^{(n)}$ is a fully dressed vertex in the language of standard quantum field theory and will therefore also ne referred to the RG improved object $\Gamma_k^{(n)}$ as a vertex or n-point function. The generalization to more than one field (or to superfield space) is straightforward and we have suppressed all indices for to unclutter notation. For instance, a vertex with m_1 gravitons and m_2 scalars has $2m_1$ spacetime indices.
In equation (4.16), $\tilde{u}_n$ is a (dimensionful) coupling. We can then project on the coupling by using an appropriate projector Π_n,

$$\tilde{u}_n = \Pi_n \left(\frac{1}{n!} \int \mathrm{d}^4x_1 \dots \mathrm{d}^4x_n \Gamma_k^{(n)}(x_1, \dots, x_n) \mid_{\varphi=0} \varphi(x_1) \dots \varphi(x_n) \right).$$

Finding suitable projectors is closely related with finding a suitable ansatz for the n-point functions and by no means trivial [48, 175].

Hierarchy of Flow Equations for Vertex Functions

One of the advantages of a vertex expansion [182] is that flow equations for n-point functions can readily be obtained by taking functional derivatives on both sides of the functional renormalization group equation (1.19). Note that the flow of the n-point function $\partial_t \Gamma_k^{(n)}$ will be a function of the $n+1$- and $n+2$-point functions.

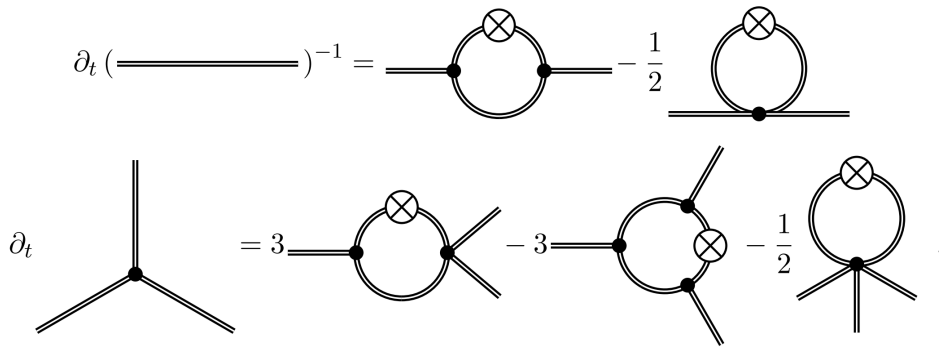

Figure 4.1: Structure of the flow of the 2- and 3-point functions.

While these calculations are technically involved and will only be presented in the cases needed for the theories considered in this thesis in chapter 10 and appendix C, a simple diagramatic representation is readily available and shown for the 2- and 3-point functions in figure 4.1.
The projection on the flow of a specific coupling is then carried out via

$$\partial_t \tilde{u}_n = \Pi_n \left(\frac{1}{n!} \int \mathrm{d}^4 x_1 \dots \mathrm{d}^4 x_n \, (\partial_t \Gamma_k)^{(n)} (x_1, \dots, x_n) \mid_{\varphi=0} \varphi(x_1) \dots \varphi(x_n) \right).$$

Here, $(\partial_t \Gamma_k)^{(n)}$ symbolizes the n-th functional derivative of equation (1.19), which itself is an expansion in the $n+1$ and $n+2$ point functions. The flow of the dimensionless functions can then be computed through standard methods. We also use the notation $\mathrm{Flow}^{(n)}$ as a shorthand for the RHS of the Wetterich equation of an n-point function.
The fact that the flow $\mathrm{Flow}^{(n)}$ depends on the $n+1$- and $n+2$-point functions also means that it depends on the corresponding couplings. Therefore, to close the flow, we have to set $\tilde{u}_{n+1} = \tilde{u}_{n+2} = \tilde{u}_n$ at $n = N$. Note how this is different from simply setting these couplings to zero.

Flat Backgrounds

So far, we did not have to worry about gauge symmetries or background fields. However, at some point we will have to deal with these issues. In the context of gauge symmetries, the vertex expansion (4.15) is carried out in the fluctuating field, so we replace $\varphi \to \delta\varphi$, which also yields $\varphi = 0 \to \delta\varphi = 0 \Leftrightarrow \varphi = \bar{\varphi}$. Thus, the vertex expansion systematically disentangles background and fluctuating fields. In this thesis, φ contains the fluctuating graviton and scalar fields as well as ghost and antighost.

A priori, the choice of background spacetime $\bar{g}_{\mu\nu}$ is arbitrary. However, working with a flat background $\bar{g}_{\mu\nu} = \eta_{\mu\nu}$ or, since all calculations are carried out in Euclidian spacetime, $\bar{g}_{\mu\nu} = \delta_{\mu\nu}$ has conceptual advantageous on top of the obvious computational simplifications.
Firstly, it restricts the higher derivative operators that can enter the vertices, as after taking n derivatives with respect to the metric, operators with more than n derivatives vanish on a flat background. Thus, the highest order operator entering the two point function is R^2.
Moreover, since $\bar{R} = 0$ we do not need to resort to heat-kernel techniques to capture the spectrum of the Laplace operator, allowing us to extract the flow of the kinetial K for the first time.
Note however, that $\bar{R} = 0$ also forces us to consider flows of higher correlation functions, as it is impossible to extract the running of the couplings of the Einstein-Hilbert action already from the original flow equation (1.19). Vice versa the latter also means that computations with a flat background are not possible without performing a vertex expansion.

Physical Scaling of the Vertices and Ansatz for the n-point functions

The last piece of ingredient is an ansatz for the n-point function $\Gamma_k^{(n)}$, consisting of a tensor structure as well as some couplings. Taking the standpoint of traditional Einstein gravity for a moment, the requirement of constructing a consistent quantum field theory and recovering classical general relativity in the infrared is the main guiding principle. Therefore, it seems natural to derive the tensor structure of the graviton n-point function (a vertex with n graviton legs) from the n-th functional derivative of the classical Einstein-Hilbert action S_{EH} with respect to the metric. Note how our starting point here is the action S and not some ansatz for the effective average action Γ_k. However, it turns out that if one also defines the couplings by just using the ones already present in the Einstein-Hilbert action, one ends up with an ill-defined infrared limit [19, 48]. Similar observations are already known from Yang-Mills theories [166].
That is why more general vertex functions are considered, first constructed for Yang-Mills theories [182] and also suggested in the context of quantum gravity [104]. Those vertex functions not only yield a physically well defined infrared limit in the form of classical general relativity, but also ensure the correct scaling of quantum fields via wave function renormalizations and disentangle the momentum dependent and momentum independent part of the vertex functions. They read

$$\Gamma_k^{(m_1,\dots,m_n)}(p_1,\dots,p_n) = \prod_{i=1}^{n} \left(\sqrt{Z_i(p_i)} \left(G_k^{(n)} \right)^{\frac{n}{2}-1} \right) \mathcal{T}_k^{m_1,\dots,m_n} \left(p_1,\dots,p_n; \Lambda_k^{(n)} \right)$$

(4.17)

with the tensor structure

$$\mathcal{T}_k^{m_1,\ldots,m_n}\left(p_1,\ldots,p_n;\Lambda_k^{(n)}\right)=S_{\mathrm{EH}}^{(m_1,\ldots,m_n)}\left(p_1,\ldots,p_n;G_N=k^2,\Lambda\to\Lambda_k^{(n)}\right). \quad (4.18)$$

Here, we have generalized our notation to m distinct fields and explicitly written all momentum dependencies. $Z_i(p_i)$ is the wave function renormalization for the i-th field, and $G_k^{(n)}$ and $\Lambda_k^{(n)}$ parametrize the momentum dependent and independent part of the n-point function, respectively. What looks like a technically involved construction has actually a very simple physical interpretation: As suggested by the vertex construction, we introduce different couplings at each order. We then proceed to disentangle the wave function renormlizations which rescale quantum fields and should be obtained from propagators, IE (inverse) 2-point functions from couplings that cannot occur for any n-point function with $n<3$. That is the reason for the different exponents. To take full advantage of the wave function renormalization, we will later on pick a regulator which ensures that all explicit dependencies on Z_i cancel out, and only the anomalous dimensions

$$\eta_i=-\frac{\dot{Z}_i}{Z_i}$$

remain [35].
Results have been obtained up to $N=3$, for the first time separately computing wave function renormalizations and flows of dynamical couplings [19, 105], also partially resolving the momentum dependence of the flows. Computations for $N=4$ are still pending to date.
When transforming Einstein gravity into dilaton gravity along the derivation of section 3.1, we introduce arbitrary functions of a scalar field χ^2, and with that couplings on infinite order in the dialaton-graviton system. That is why when applying the ideas presented in this section to dilaton gravity in the next chapters, we will adapt the ansatz 4.17 in the sense that we cut the expansion at $N=2$, and will thus introduce an independent wave-function renormalization for the scalar field only, while the full function $F(\chi^2)$ serves as a coupling, and is not replaced in the classical action.

Part II

Symmetric Background Configuration

CHAPTER 5

Introduction

This part is devoted to presenting one of the two main analyses of this thesis: The flow and fixed point structure of dilaton gravity as a scalar-tensor theory, introduced in chapter 3, in the background field approximation as defined in section 4.2 and, more specifically, 4.4.1. Our background spacetime here is a four dimensional sphere and thus maximally symmetric.
In this context, we gain considerable insight into the structure of the fixed point equations and their solutions, and with that a first glimpse at a globally defined fixed point solution, connecting ultraviolet with infrared physics on a pure fixed point trajectory.
Specifically, we show that for large ratios of $y = \chi^2/k^2$, which corresponds to the infrared regime, the fixed point equations are closed with respect to an expansion in inverse powers of y. Moreover, there exists a physically intriguing limiting case action of the form

$$\Gamma(k \to 0) = \int \mathrm{d}^4x\sqrt{g}\left(-\frac{1}{2}MR + \frac{1}{2}g^{\mu\nu}\partial_\mu\phi\partial_\nu\phi\right)$$

in the Einstein frame, which features a Planck mass as well as a vanishing cosmological constant.
Nevertheless, the exact global solution and with that, the theory approaching the aforementioned physical infrared limit remain indeterminably in the current framework. It becomes clear that we need to upgrade the kinetic configuration of the scalar χ to capture the physical features. This is done in part III.
However, even without the full theory it is possible to gain considerable insight

into the role of the scalar kinetic term and its influence on the flows, and to draw conclusions from the connection with the kinetic term of the graviton. The latter stems from the coupling to the Ricci scalar.
We furthermore explicitly demonstrate that the infrared limit is independent of ultraviolet couplings in our approach, while the ultraviolet limit is influenced by operators dominating infrared physics. With that insight, we refine our strategy for the search of global solutions.
This part is organized as follows: In chapter 6, we state our truncation and recap the most important steps of the derivation of the flow equations that will be used throughout this part. In chapter 7, we use the flow equations to pave the path towards a global solution by studying different special and limiting cases as well as expansions and improvements (sections 7.1 - 7.6) and finally presenting our current best approximation to a global solution in section 7.7. In section 7.8 we introduce a rescaled kinetic term for the scalar and study its implication with respect to field rescalings as well as regulator singularities, before we close the analysis of the background approximated flow equations in section 7.9 by utilizing simple truncation not aimed at solving the system to any accuracy, but rather at providing physical insights into the couplings of limiting cases to be used as guiding principled for part III. We summarize our findings in chapter 8.

CHAPTER 6

Setup and Derivation of the Background Flow Equations

To keep this introduction compact, we focus on the main points necessary to understand the procedure. A more comprehensive derivation can be found in [42].

6.1 Action and Inverse Propagators

In the spirit of chapter 3 and section 4.2 we define

$$\begin{aligned}\Gamma_k[g_{\mu\nu},\chi] = \int \mathrm{d}^d x\sqrt{g}\left(V_k(\chi^2) - \frac{1}{2}F_k(\chi^2)\,R[g_{\mu\nu}] + \frac{1}{2}g^{\mu\nu}\partial_\mu\chi\partial_\nu\chi\right) \\ + S_{\text{gauge fixing}}[\bar{g}_{\mu\nu},\, h_{\mu\nu},\bar{\chi}] + S_{\text{ghosts}}[\bar{g}_{\mu\nu},\, C_\mu,\, \bar{C}_\mu],\end{aligned} \tag{6.1}$$

thus supplementing the physical ansatz with a gauge fixing and ghost term.
We work in the background field formalism performing linear splits $g_{\mu\nu} = \bar{g}_{\mu\nu} + h_{\mu\nu}$ and $\chi = \bar{\chi} + \delta\chi$. The gauge group of our theory is the group of diffeomoprhisms on the spacetime manifold, with which we carry out the procedure discussed in section 4.2, and set $\alpha = 0$, $\beta = 1$ in the following analysis.
Note that in this part of the thesis, the kinetic term and the ghost action are k-independent, whereas $S_{\text{gauge fixing}}$ depends on the scale through the function $F_k(\chi^2)$. Nevertheless, the gauge fixing action will not contribute to the flow after we identify $\bar{g}_{\mu\nu} = g_{\mu\nu}$.
We compute $\Gamma^{(2)}_{\phi\phi}$ by expanding (6.1) up to second order in the fluctuating field $\delta\varphi$, where at this stage $\delta\varphi = (h_{\mu\nu},\ \delta\chi,\ C_\mu)$.
To allow for partial decomposition of the kinetic operators and with that, inversion,

we perform a transverse-traceless or York decomposition according to [183–185]

$$h_{\mu\nu} = h^{TT}_{\mu\nu} + \bar{\nabla}_\mu \xi_\nu + \bar{\nabla}_\nu \xi_\mu + \bar{\nabla}_\mu \bar{\nabla}_\nu \sigma - \frac{1}{d} g_{\mu\nu} \Box \sigma + \frac{1}{d} g_{\mu\nu} h \tag{6.2}$$

as well as

$$\bar{C}^\mu = \bar{C}^{\mu T} + \bar{\nabla}^\mu \bar{C} \ , \qquad C_\mu = C^T_\mu + \bar{\nabla}_\mu C \, , \tag{6.3}$$

where the transverse part satisfies the following differential constraints:

$$\bar{\nabla}_\mu \bar{C}^{\mu T} = 0 \ , \qquad \bar{\nabla}^\mu C^T_\mu = 0. \tag{6.4}$$

These decompositions are orthogonal for a maximally symmetric background. With that in mind, we will restrict ourselves to work on a d-dimensional sphere from now on. Arising Jacobians are cancelled by appropriate redefinitions of the fields, such that there are no further determinants to be exponentiated similar to the Faddeev-Popov determinant.
While at this stage, the transverse traceless decomposition was merely a technical tool to facilitate inversion of the kinetic operators, it will gain greater physical significance when working on a flat background in chapter 10. Details on the algebraic background are given in appendix C.3.
Collecting terms quadratic in $\delta\varphi$ we arrive at an inverse propagator that can be rewritten in superfield space with now decomposed fields $\delta\varphi = \left(h^{TT}_{\mu\nu},\ \xi_\mu,\ \sigma,\ h,\ \chi,\ C^T_\mu,\ C\right)$. Since we will not have to distinguish $\bar{\chi}$ from $\delta\chi$ again, we will just use χ from here on to simplify the notation.
This leads to

$$\Gamma^{(2)}_k = \begin{pmatrix} \Gamma^{(2)}_{h^T_{\mu\nu}} & 0 & 0_{1\times 3} & 0_{2\times 2} & \\ 0 & \Gamma^{(2)}_{\xi} & 0_{1\times 3} & & \\ 0_{3\times 1} & 0_{3\times 1} & \Gamma^{(2)}_{\text{scalar}} & 0_{3\times 1} & 0_{3\times 1} \\ & 0_{2\times 2} & 0_{1\times 3} & \Gamma^{(2)}_{C^T_\mu} & 0 \\ & & 0_{1\times 3} & 0 & \Gamma^{(2)}_{C} \end{pmatrix}, \tag{6.5}$$

where

$$\Gamma^{(2)}_{\text{scalar}} = \begin{pmatrix} \Gamma^{(2)}_{\sigma\sigma} & \Gamma^{(2)}_{\sigma h} & \Gamma^{(2)}_{\sigma\phi} \\ \Gamma^{(2)}_{h\sigma} & \Gamma^{(2)}_{hh} & \Gamma^{(2)}_{h\phi} \\ \Gamma^{(2)}_{\phi\sigma} & \Gamma^{(2)}_{\phi h} & \Gamma^{(2)}_{\phi\phi} \end{pmatrix} \tag{6.6}$$

is a 3×3 matrix coupling the three scalar modes of our theory. The detailed

expressions can be found in [42]. We will only give them here whenever needed at a later stage.

6.2 Flow Equations

In order to implement the momentum shell integration we choose an optimized cut-off [186, 187] and require the regulator function to scale like the second variation of the effective average action, thus introducing

$$\begin{aligned} \Gamma_k^{(2)}\left(p^2\right) + \mathcal{R}_k(p^2) &= \Gamma_k^{(2)}\left(p^2 + r_k(p^2)\right), \\ r_k(p^2) &= (k^2 - p^2) \times \Theta(k^2 - p^2). \end{aligned} \tag{6.7}$$

Therein, p^2 stands for the covariant Laplacian, $p^2 \hat{=} -\Box$ with $\Box = \nabla_\mu \nabla^\mu$. This cut-off corresponds to the one also used in part III of this thesis.
We can now solve for $\mathcal{R}_k$ and obtain

$$\mathcal{R}_k(p^2) = \left(\Gamma_k^{(2)}(k^2) - \Gamma_k^{(2)}(p^2)\right) \times \Theta(k^2 - p^2), \tag{6.8}$$

and derive an expression for $\partial_t \mathcal{R}_k$, reading

$$\begin{aligned} \partial_t \mathcal{R}_k(p^2) = &\left(\partial_t \Gamma_k^{(2)}(k^2) - \partial_t \Gamma_k^{(2)}(p^2)\right) \times \Theta(k^2 - p^2) \\ &+ \left(\Gamma_k^{(2)}(k^2) - \Gamma_k^{(2)}(p^2)\right) \times 2k\,\delta(k^2 - p^2), \end{aligned} \tag{6.9}$$

where we use a simplified notation and did not explicitly write out all integrals. Recognizing that the latter part assumes a zero at $k^2 = p^2$, it will not contribute to any integrals performed and will thus not explicitly be written out anymore. Furthermore, the Θ-function in the first part acts as a cutoff to the momentum integrals at $p^2 = k^2$, also allowing us to deal with the Θ-function in equation (6.7) in an easy and intuitive manner. This procedure applies to both the graviton and scalar field comprising the bosonic degrees of freedom and to the ghosts. A more detailed analysis can be found for instance in [188].
With the flow equation (1.19) we arrive at

$$\begin{aligned} \partial_t \Gamma_k &= \sum_{a \in \{h^T_{\mu\nu}, \xi, \text{scalar}, C^T_\mu, C\}} \partial_t \Gamma_k^a \\ &= \frac{1}{2} \sum_{a \in \{h^T_{\mu\nu}, \xi, \text{scalar}\}} \int_0^{k^2} dp^2\, \mathrm{Tr}\left[\frac{\partial_t \Gamma_a^{(2)}(k^2) - \partial_t \Gamma_a^{(2)}(p^2)}{\Gamma_a^{(2)}(k^2)}\right] \end{aligned}$$

$$- \sum_{a\in\{C_\mu^T,C\}} \int_0^{k^2} dp^2 \,\mathrm{Tr}\left[\frac{\partial_t \Gamma_a^{(2)}(k^2) - \partial_t \Gamma_a^{(2)}(p^2)}{\Gamma_a^{(2)}(k^2)}\right]. \tag{6.10}$$

We use heat kernel expansions as introduced in appendix B to compute the functional trace occurring on the RHS of equation (6.10) and keep only terms up to first order in the Ricci scalar. The expressions in square brackets are at most of order $p^2 = z$ and R^1, so we can define

$$W^a(z) \equiv \frac{\partial_t \Gamma_a^{(2)}(k^2) - \partial_t \Gamma_a^{(2)}(z)}{\Gamma_a^{(2)}(k^2)} = p_0^a + p_2^a\, z \tag{6.11}$$

with $p_0^a = W^a(0)$ and $p_2^a = \partial_z W^a(0)$. Using

$$\begin{aligned} Q_n(W) &= \frac{1}{\Gamma(n)} \int_0^\infty dz z^{n-1} W(z) \\ &= \frac{1}{\Gamma(n)} \int_0^{k^2} dz z^{n-1} (p_0 + p_2\, z) \\ &= \frac{k^{2n}}{\Gamma(n)} \left(\frac{p_0}{n} + \frac{p_2}{n+1} k^2\right), \end{aligned} \tag{6.12}$$

in the language of the aforementioned appendix, we are now able to compute the remaining functional trace. For instance, for the spin 2 graviton contributions, this leads to

$$\begin{aligned} \partial_t \Gamma_k^{h_{\mu\nu}^{TT}} \;=\; & \frac{1}{2\ (4\pi)^{d/2}} \int \mathrm{d}^d x \sqrt{g} \left\{ \frac{(d+1)(d-2)}{2} Q_{\frac{d}{2}}(W^{h_{\mu\nu}^{TT}}) \right. \\ & \left. + R \frac{(d+1)(d+2)(d-5)}{12(d-1)} Q_{\frac{d}{2}-1}(W^{h_{\mu\nu}^{TT}}) + \mathcal{O}(R^2) \right\}, \end{aligned}$$

the other contributions are constructed accordingly.
Computing all terms in equation (6.10) we project on flow equations for V and F by considering the terms of order R^0 and R^1, respectively. This is the heat kernel analogon to disentangling momentum dependent and momentum independent parts in the language of vertex expansions.
So far, we derived flow equations for dimensionful functions of a dimensionful field. However, we want to be able to distinguish the canonical running, induced by the canonical mass dimension, from the RG running introduced by quantum fluctuations. A generic β-function for a field independent coupling g with mass dimension d will then be of the form

$$\beta = -dg + k^{-d}\tilde{\beta},$$

where $-dg$ is the canonical running, and $k^{-d}\tilde{\beta}$ stems from quantum fluctuations. If g is field dependent, an additional canonical running from the mass dimension of the field enters, in our case $[\chi^2] = 2$.
We thus transform to a dimensionless field and dimensionless functions

$$y = \frac{\chi^2}{k^2},\ \tilde{V}(y) = \frac{V(\chi^2)}{k^4},\ \tilde{F}(y) = \frac{F(\chi^2)}{k^2}$$

as well as to the dimensionless RG time

$$t = \log\left(\frac{k}{k_0}\right).$$

Since we will only work with dimensionless functions for the remainder of this thesis, we drop the tilde. Furthermore, given the association of background and fluctuating field discussed in chapter 4, we write $h_{\mu\nu}$ for the metric and χ or y for the scalar field and arrive at flow equations

$$\begin{aligned} \partial_t V &= 2yV' - 4V + \zeta_V, \\ \partial_t F &= 2yF' - 2F + \zeta_F, \end{aligned} \tag{6.13}$$

where the flow generators ζ_V and ζ_F are given in appendix A for $d = 4$ and $\beta = 1$, $\alpha = 0$. A more detailed derivation and analysis of these equations for general dimensions d and gauge parameters α and β is presented in [42].

CHAPTER 7

Towards a Global Solution

Results presented in this chapter have partially been published in [26], and we are extending results from [42]. To unclutter notation, we drop the explicit k subscript for scale dependent quantities.

7.1 Einstein-Hilbert Solution

The most readily available global fixed-point solution to the flow equations (6.13) is given by setting both $V(y)$ and $F(y)$ equal to constants V and F, respectively. This corresponds to Einstein-Hilbert gravity with an additional scalar field χ, which couples to gravity only through the metric $g_{\mu\nu}$. This solution obeys equation (6.13) exactly for all y and is numerically given by

$$V = 0.008620 \quad \text{and} \quad F = 0.04751. \tag{7.1}$$

As presented in appendix B to [42], there are no more real fixed point solutions, and both eigenvalues have negative real parts. Note that the definition of F differs by a factor of 2.

The fixed points (7.1) stem from the equations

$$\begin{aligned}\partial_t V =& -4V + \frac{19F+5V}{96\pi^2(F-V)} + \frac{(5F-2V)}{96\pi^2(F-V)}\frac{\partial_t F}{F},\\ \partial_t F =& -2F + \frac{265F^2-138FV+4608\pi^2F^2V+33V^2}{1152\pi^2(F-V)^2}\\ &+ \frac{17F^2+18FV-15V^2}{1152\pi^2(F-V)^2}\frac{\partial_t F}{F}.\end{aligned} \tag{7.2}$$

For comparisons with results to be derived later, we also solved the reduced flow equations, which are obtained by setting $\delta_V = \delta_F = 0$. This amounts to neglecting RG-time derivatives in the regulator, and yields

$$V = 0.004089 \quad \text{and} \quad F = 0.03084. \tag{7.3}$$

It is intuitive that the numerical values differ, but physical features do not change. Even though we will not explicitly report results for reduced flows in this chapter, we have checked all features reported for their stability under reducing the flow equations.
Since in the spirit of section 3.1 we will be more interested in solving the fixed point equations for a general value of the scalar field than to consider the flow into the fixed point an RG trajectory in this thesis, we point to [42] for a more detailed classical RG treatment of the flow in theory space.

7.2 The Large Field Limit

We first investigate the generators ζ_V and ζ_F in the limit $y \to \infty$. In this limit we expand the dimensionless functions V and F in inverse powers of y

$$V = \lambda y^2 + m^2 y + \sum_{i=0}^{a} \frac{v_i}{y^i i!},\ F = \xi y + \sum_{i=0}^{b} \frac{f_i}{y^i i!}, \tag{7.4}$$

additionally allowing for dilatation symmetric contributions in both functions. Note that if $k \to 0$ the physical mass $m^2 k^2$ also vanishes and thus does not spoil dilatation symmetry in this limit.
Equations (A.2) yield

$$\lim_{y\to\infty} \zeta_V = \bar{\zeta}_V\ ,\ \lim_{y\to\infty} \zeta_F = \bar{\zeta}_F, \tag{7.5}$$

where the limits depend on ξ and λ. For reasons given in section 7.3, we concentrate

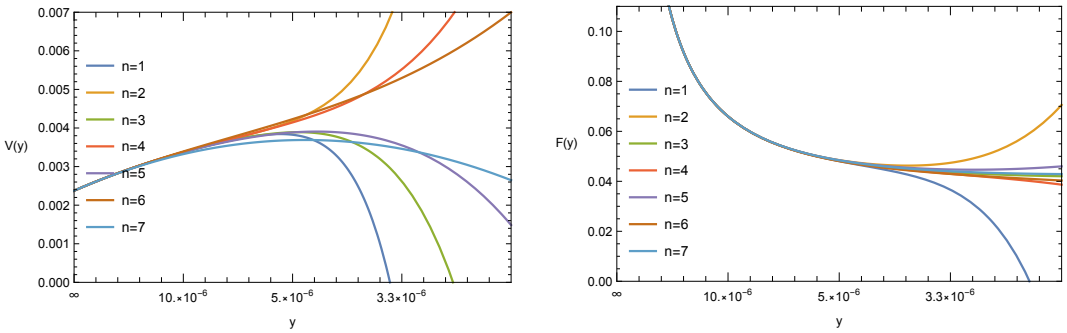

Figure 7.1: Taylor expansions around $y = \infty$ for $\xi = 4000$ up to order $a = b = n$ with $1 \leq n \leq 7$.

on $\lambda = m^2 = 0$,[1] where

$$\begin{aligned}\bar{\zeta}_V =& \frac{3}{32\pi^2} + \frac{5+33\xi}{96\pi^2(1+6\xi)}\frac{\partial_t \xi}{\xi},\\ \bar{\zeta}_F =& \frac{77+534\xi}{192\pi^2(1+6\xi)} + \frac{17+186\xi+720\xi^2}{576\pi^2(1+6\xi)^2}\frac{\partial_t \xi}{\xi}.\end{aligned} \tag{7.6}$$

We are interested in fixed-point solutions $F(y), V(y)$ for which $\partial_t F(y) = \partial_t V(y) = 0$. The contributions $\sim \partial_t \xi$ vanish in this case. This can also already be inferred from the fact that the limits of the flow generators remain finite for $y \to \infty$, and thus not running of the ξy term is induced. This also means that ξ is a free parameter at this stage. For $y \to \infty$ limit the equations (6.13) are then easily solved by

$$\lim_{y\to\infty} F(y) = \xi y + \frac{\bar{\zeta}_F}{2} \ , \ \lim_{y\to\infty} V(y) = \frac{\bar{\zeta}_V}{4}. \tag{7.7}$$

This coincides with the expectations (3.11) and (3.12).
In order to gain insight into other classes of solutions, we have performed an expansion of $F(y)$ and $V(y)$ in powers of y^{-1} including the order $a = b = 7$. We confirm that the fixed point equation for v_i and f_i only depend on v_j and f_k with $j, k \leq i$, thus allowing us to solve order by order. As is depicted in figure 7.1, the series show excellent convergence up to a distinct point, where the approximation breaks down. It is curious to notice that we apparently found the radius of convergence around $y_0 = \infty$, as the series cannot be improved by pushing the order of the expansions higher and higher. This signals a breakdown of perturbation theory as such as we

[1] On a physical level, the potential V is related to an effective cosmological constant. This will be discussed in detail in section 13.5.

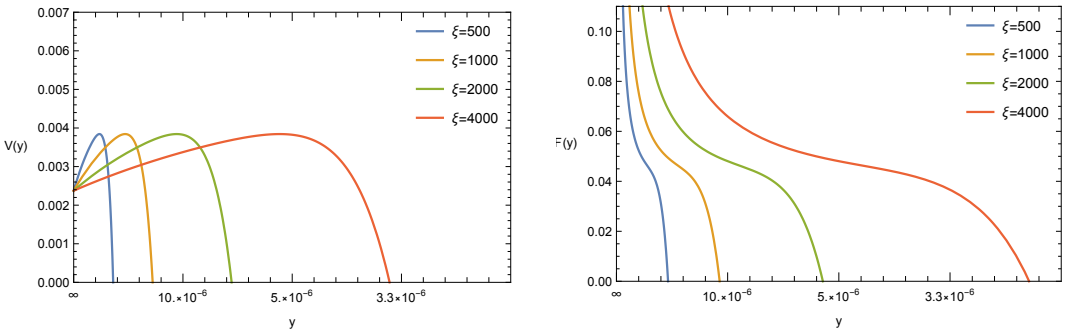

Figure 7.2: Taylor expansions around $y = \infty$ for $a = b = 7$ and for different values of ξ.

are leaving the infrared and move towards the ultraviolet regime of dilaton gravity and with that towards dilaton quantum gravity.
The result depends on the value ξ which is not fixed at present. In figure 7.2, we show the solutions gained via the Taylor expansion for different values of the parameter The series shows excellent apparent convergence for $y \geq y_0 \approx 1/|\xi|$. The dependence of the breakdown of convergence on ξ is already a hint towards the fact that the true physical variable of our system is $y\xi$ rather than y, the formal version whereof would be the introduction of a wave function renormalization. We will explore this observation further in part II.

7.3 Positivity of Propagators and the Limit of V

We emphasize that the flow equations (6.13) are meaningful only if the relevant inverse propagators Σ_0 and Δ in the spin 2 and spin 0 sector (see also appendix A for analytic expressions) remain positive for all y. These quantities correspond to the inverse graviton and scalar propagators in the presence of the cutoff k. For $y \to \infty$ one has $\Sigma_0 = \frac{1}{2}\xi y, \Sigma_1 = 1, \Delta = \frac{1}{2}\xi(1+6\xi)y$ such that Σ_0 and Δ are positive provided $\xi > 0$. This is true for the value of ξ shown in figure 7.1, which is the value we will use later in this chapter to obtain a globally defined approximate solution.
The positivity requirement for the propagators singles out asymptotic solutions for $y \to \infty$ for which $\lambda \leq 0$. In fact, the asymptotic fixed-point solutions of equations (6.13) also can be solved with $\lambda \neq 0$, with

$$\begin{aligned} \bar{\zeta}_V &= -\frac{1}{48\pi^2}\left(6 - \frac{\partial_t \xi}{\xi}\right), \\ \bar{\zeta}_F &= \frac{1}{1728\pi^2}\left(249 - 41\frac{\partial_t \xi}{\xi}\right), \end{aligned} \tag{7.8}$$

and corresponding values for the lowest order coefficients $v_0 = -0.00317$ and $f_0 =$

0.0073. For $\lambda \neq 0$ the asymptotic form $V = \lambda y^2$, $F = \xi y$ implies a negative Σ_0 if $\lambda > 0$, rendering the propagation of the graviton unstable. With $\Sigma_0 = -\lambda y^2, \Sigma_1 = 12\lambda y$, one has $\Delta = 36\lambda^2 y^3$ which remains positive for arbitrary $y \neq 0$.
Furthermore, we require that the potential V in our ansatz (6.1) is bounded from below in order to describe a stable theory. This holds for an asymptotic behavior with $\lambda \geq 0$. Combining the two requirements of a positive inverse propagator and a bounded potential only the asymptotic behavior $\lambda = 0$ is left. This absence of a term $\sim v_0 y^2$ is the crucial ingredient for the absence of a cosmological constant after Weyl scaling in (3.6), see section 13.5 for a detailed discussion in the case of flat backgrounds, where equivalent results were obtained.
Further arguments for $\lambda = 0$ were discussed in [42], section 5.1.2, where, though formally in the context of a weak field limit, a theory with $F \sim \xi\chi^2$ and $V \sim \lambda\chi^4$ was investigated. The main result was that the line of fixed points has a repulsive direction which can effectively be mapped onto λ, thus requiring $\lambda = 0$.
We will therefore consider theories with $\lim_{y\to\infty} V(y) = const.$ from hereon out.

7.4 The Small Field Limit

The region of small y is more difficult to access. One may investigate a Taylor expansion around $y = 0$ for the functions F and V,

$$V = \sum_{j=0}^{a} \frac{V_j}{j!} y^j, \quad F = \sum_{j=0}^{b} \frac{F_j}{j!} y^j. \tag{7.9}$$

The fixed-point equations

$$\begin{aligned} \zeta_F - 2F + 2yF' &= 0, \\ \zeta_V - 4V + 2yV' &= 0, \end{aligned} \tag{7.10}$$

involve F_0, F_1 and V_0, V_1 to $\mathcal{O}(y^0)$ already. The system is not closed, and this property extends to higher orders in the Taylor expansion. For given F_0 and V_0 the Taylor expansion shows apparent convergence, where we have expanded up to y^5.
Note that the method of truncating is different from what was done in [42], as we interpret the fact that the hierarchy of equations is not closed to yield two free parameters V_0 and F_0, whereas in [42] the system was solved by adding an additional power in y, but setting the corresponding coupling to 0, thus closing the system as a whole.
We show Taylor expansions around $y = 0$ in figure 7.3, where we set $V_0 = 0.01$ and $F_0 = 0.05$. In figure 7.4 we also present the small field expansions for different values of V_0 and F_0.

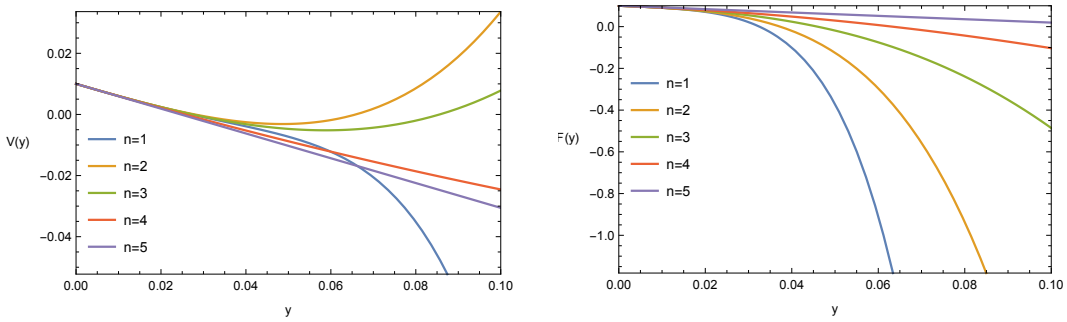

Figure 7.3: Taylor expansions around $y = 0$ for $V_0 = 0.01$ and $F_0 = 0.05$ up to order $a = b = n$ with $1 \leq n \leq 5$.

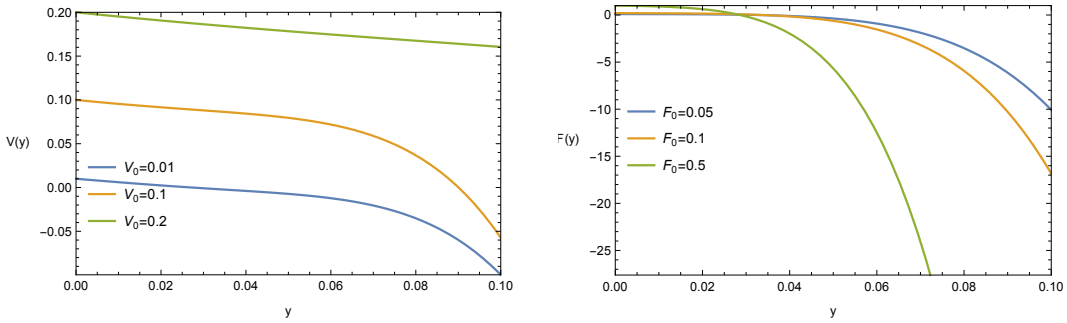

Figure 7.4: Taylor expansions around $y = 0$ to order y^5 for different values of V_0 and F_0.

7.5 Padé Improvement

It is of course no surprise that an expansion in negative powers of y does not approach a finite limit as y approaches 0. One simple way to circumvent this obvious shortfall is to use Padé approximations, where a function $\mathcal{H}(y)$ is expanded in a rational function according to

$$\mathcal{H}_P(y) = \frac{\sum_{k=0}^{m} \mathcal{H}_{num,k} y^k}{1 + \sum_{j=1}^{n} \mathcal{H}_{den,j} y^j} \tag{7.11}$$

with

$$\lim_{y\to 0} \mathcal{H}_P(y) = \mathcal{H}_{num,0} \text{ and } \lim_{y\to\infty} H_P = \begin{cases} 0, n > m, \\ \infty, m > n, \\ \dfrac{\mathcal{H}_{num,m}}{\mathcal{H}_{den,n}}, n = m. \end{cases}$$

The convergence for smaller y can be improved in this way, we call the corresponding Padé approximations $\tilde{V}_{\text{Padé}}$ and $\tilde{F}_{\text{Padé}}$, respectively. We show the result in figure 7.5, where numerator and denominator are expanded up to order y^{-4} and Padé and Taylor approximations agree at $y = \infty$.
While the Padé improvement provides a smooth function interpolating from $y = \infty$ to $y = 0$, it is evident that this cannot be the desired global fixed point solution yet. On the one hand, we would expect the limit of y approaching 0 to converge in the vicinity of the Einstein-Hilbert solution (7.1). This is clearly not the case for the Padé Improvement considered here, and we infer from section 7.4 that corrections to that Einstein-Hilbert value will not be large enough to account for this difference. Moreover, drawing from the error analysis presented later on, specifically in figure 7.7, we also conclude that the Padé Improvement does not yet capture the features of the solution well enough in an intermediate region.
We will work our way towards a global solution by first addressing the first shortcoming mentioned and seek an improved $y \to 0$ limit.

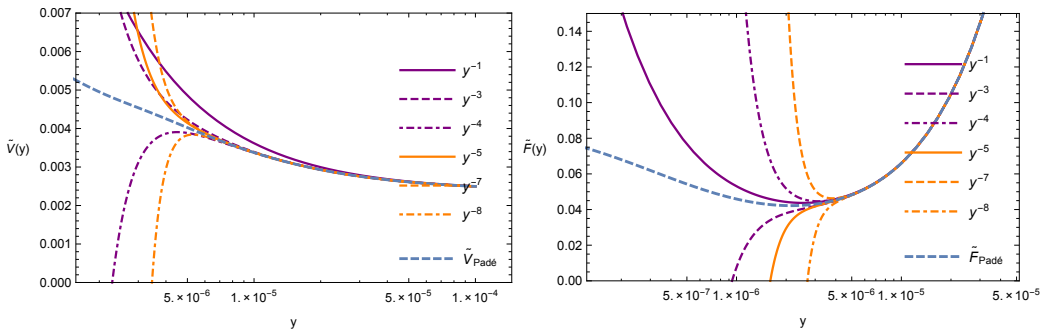

Figure 7.5: Taylor expansions for $\tilde{V}(y)$ and $\tilde{F}(y)$ at $y_0 = \infty$ with $\xi = 1000$, truncated at y^0 to y^{-8} and Padé improvement including powers of y^{-4} in both numerator and denominator, also carried out at $y_0 = \infty$. The splitting up of the Taylor series at the radius of convergence points to a breakdown of perturbation theory.

7.6 Exponential Improvements

In order to do so, we match the Taylor expansion to the Padé expansion by the ansatz

$$\begin{aligned} F_{\text{exp}}(y) &= F_{\text{Taylor}}(y) + e^{-c/y} F_e(y), \\ V_{\text{exp}}(y) &= V_{\text{Taylor}}(y) + e^{-c/y} V_e(y), \end{aligned} \tag{7.12}$$

where F_{Taylor}, V_{Taylor} are the Taylor expansions around 0 to order y^5 and F_e, V_e are polynomial functions of y to order y^n:

$$V_e = V_{e0} + V_{e1}(y-y_0) + \frac{1}{2} V_{e2}(y-y_0)^2 + \ldots, \; F_e = F_{e0} + F_{e1}(y-y_0) + \frac{1}{2} F_{e2}(y-y_0)^2 + \ldots.$$

The form of the expansion (7.12) is motivated by similar exponential contributions occurring in massless gauge theories with a singularity for the coupling g approaching zero [189], keeping in mind that y triggers couplings in dilaton quantum gravity.

Matching algorithm

As a measure of the quality of the approximate solution, we have solved equations (6.13) to read

$$\begin{aligned} V''(y) &= \mathcal{G}_V(y, F, F', V, V'), \\ F''(y) &= \mathcal{G}_F(y, F, F', V, V') \end{aligned}$$

and defined

$$\varepsilon = \frac{1}{2}\frac{(\mathcal{G}_V - V'')^2}{\mathcal{G}_V^2 + V''^2} + \frac{1}{2}\frac{(\mathcal{G}_F - F'')^2}{\mathcal{G}_F^2 + F''^2}, \tag{7.13}$$

where ε is evaluated on the proposed approximate solution. On an exact solution, ε vanishes for all y. We also define the integrated error

$$\mathcal{E} = y_0^{-1} \int_0^{y_0} \varepsilon(y)\,\mathrm{d}y. \tag{7.14}$$

The expansion (7.12) has a total of $3 + 2n$ free parameters: The lowest order Taylor coefficients V_0 and F_0, the exponential coupling c, as well as the $2n$ expansion coefficients for V_e and F_e.
They are determined as follows: For $y \to 0$, we have $\exp(-c/y) \to 0$, and thus only the Taylor part of (7.12) remains relevant. However, once we depart from $y = 0$, the exponential part quickly prevails. That is why we use the parameters $\{V_{e0}, V_{e1}, V_{e2}, \ldots, F_{e0}, F_{e1}, F_{e2}, \ldots\}$ to ensure a smooth[2] matching between the exponential improvement and the Padé solution at some $y = y_0$, which we set to $y_0 = 5 \cdot 10^{-6}$. This yields a system of $2n$ conditions in total.
Additionally, we vary V_0, F_0 around the Einstein Hilbert values (7.1) as well as c around $c_0 = 10^{-7}$, which is the right order of magnitude to achieve the transition from the Taylor to the exponential parts between $y = 0$ and $y = y_0 = 5 \cdot 10^{-6}$, thereby optimising the value of the integrated error (7.14) for the functions (7.12).

7.7 Approximate Global Solution

The best match

$$\begin{aligned} V_0 &= 0.0062, & F_0 &= 0.0226, & c &= 2.1 \cdot 10^{-6}, \\ V_{e0} &= -0.003300, & V_{e1} &= -33.7745, & V_{e2} &= -1.4250 \cdot 10^{7}, \\ F_{e0} &= 0.002358, & F_{e1} &= 2176.8945, & F_{e2} &= -5.4727 \cdot 10^{7} \end{aligned} \tag{7.15}$$

is shown in figure 7.6 and was obtained including powers up to y^6 in the polynomial and up to y^2 in the exponential part.
It yields an integrated error of $\mathcal{E} \approx 0.3$, which is a significant improvement over the results obtained with expansions around ∞ and could be further improved by extending the ansatz (7.12) and optimising the matching procedure. The detailed error is depicted in figure 7.7.
Even though the solution depicted in figure 7.6 is defined globally and our current

[2] More strictly speaking, of course we can only match up to two derivatives.

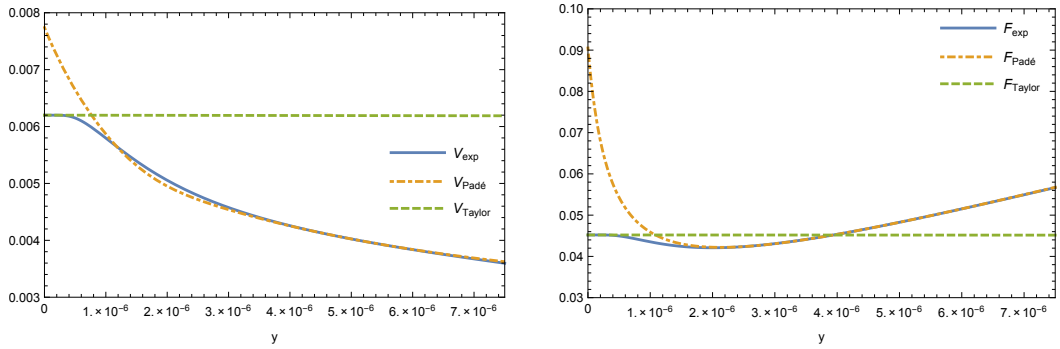

Figure 7.6: Taylor expansion at $y = 0$ with $V_0 = 6.2 \times 10^{-3}$ and $F_0 = 2.3 \times 10^{-2}$, Padé approximation at $y = \infty$ with $\xi = 4000$ and the exponential ansatz (7.12) matched at $y = 5 \times 10^{-6}$ for the fixed functions $V(y)$ and $F(y)$.

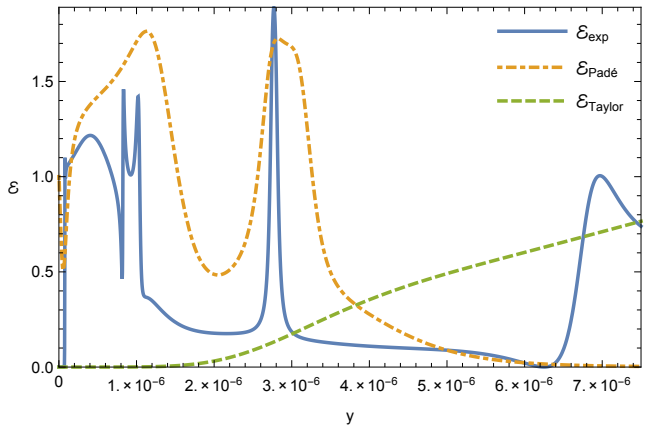

Figure 7.7: Relative error ε defined in (7.13) for the functions in Figure 7.6.

best approximation to an exact global solution, the error plot 7.7 alongside with the large highest order coefficients in equation (7.15) and the fact that we glued together a variety of approximations, makes it without any doubt necessary to employ different methods for finding a solution.
In the next two sections we will, building on the same flow equations, aim at gaining more physical insights by employing simple truncations, before we head out to derive a new set of flow equations in part III that not only employs a different truncation scheme and background, but also contains a completely new function alongside V and F.

7.8 Enhancing the Scalar Kinetic Term by a Constant Factor K

Even though our analysis with Taylor and Padé expansions complemented by an exponential improvement enabled us to gain considerable insight into the form of a global solution of the fixed point equations, we did not yet succeed in finding an actual solution. Of course there is a variety of possible reasons for that beyond technical insufficiency. In fact, advanced methods, specifically pseudo-scalar methods were successfully employed in [190] to solve a variety of challenging equations originating from functional renormalization group computations, but still failed to produce a global solution to the system considered here in $d = 4$ dimensions.
Assuming that there exists a global solution, which is not clear from the outset, it is very well conceivable that our current truncation is not able to capture its features, which would make it unlikely for to even find a satisfactory approximation at this point. In particular, there are solid reasons to consider a dynamical function $K(\chi^2)$ multiplying the scalar kinetic term, thus ultimately enlarging our truncation to

$$\Gamma = \int d^4x\sqrt{g}\left(V(\chi^2) - \frac{1}{2}F(\chi^2)\,R + \frac{K(\chi^2)}{2}g^{\mu\nu}\partial_\mu\chi\partial_\nu\chi\right). \tag{7.16}$$

The logic behind considering the enlarged truncation (7.16) goes as follows. First, consider the following consistency argument: While we did multiply the Ricci Scalar R with an arbitrary function $F(\chi^2)$, thus allowing for a generic coupling of gravity to the scalar theory, and included a generic potential $V(\chi^2)$, which is equivalent to coupling the cosmological constant from the familiar Einstein-Hilbert action to a scalar theory in a general manner, we only included the simplest form of the scalar kinetic term. However, as much as gravity relies on derivatives of the metric tensor, as much may the true coupling of the graviton rely on derivative couplings. To be consistent with gravity, we should at least include two derivatives of the scalar field, which exactly amounts to multiplying the scalar kinetic term by $K(\chi^2)$.

Moreover, it is well known for theories of a scalar coupled to gravity already in the classical regime that the scalar propagator shifts its momentum dependence from

$$\propto \frac{1}{Zp^2}$$

for small field values to scaling like

$$\propto \frac{1}{(Z+6)p^2}$$

for large field values, where Z is the familiar wave function renormalization for the scalar field. A trace of this behavior in our system is visible for instance through the $(\xi + 1/6)$ denominator in equation (7.6). The relation between ξ and a rescaling of the scalar field is of great importance for the system, as will become clear in a bit. Not only does this mean that stability bound for the propagator for the latter case is not at $Z = 0$ like one would naively expect, but at

$$Z = -6.$$

In particular that means that negative factors multiplying the scalar kinetic term may be physically stable and should be included in our considerations, which amounts to $K(\chi^2) < 0$ in (7.16). Moreover, when seeking for a global solution connecting $y \to \infty$ and $y \to 0$, we should allow for $K(\chi^2)$ to be a generic function of the scalar field, including the possibility of a change of signs.
However, deriving a flow equation for $K(\chi^2)$ is infeasible with the method employed in this part of the thesis, as it would require the use of off-shell heat kernel techniques, as the scalar kinetic term to which $K(\chi^2)$ vanishes on a constant background scalar field, and thus deviations from the background, scaling like p^2 in momentum space, would need to be considered. That is why we postpone the analysis of the full enlarged system to part III of this thesis, where expansions around a flat background will put us in a position to derive the desired flow equation.
However, it is possible with the current techniques to include a factor K independent of the scale k as well as the scalar field χ multiplying the scalar kinetic term and thus exploring the influence of such a factor on the current system. That is what this section is devoted to. More specifically, we will first understand the origin of the stability bound at $K = -6$ in our current system, before we move on to understand the interplay of K and ξ, leading us to some insights about the scalar propagator singularity which occurs at $\frac{K}{\xi} = -6$. This is the first hint towards a deeper connection between K and ξ, which will raise to its full glory in sections 12.2.2 and 13.1.
In section 7.9 we will further this analysis by including K in some simple, globally

defined expansions putting us into the position to gain more physical insight into the dilaton-graviton system.
In order to do so, we rederive the flow equations 6.13, and give the explicit expressions for the flow generators in appendix A.2. Unless explicitly noted otherwise, we set $\xi = 1$ in the following analysis

7.8.1 Origin of the $K + 6$ Denominator

As a first step we will spend some time to understand the mixed scalar propagator

$$\Gamma^{(2)}_{\text{scalar}} = \begin{pmatrix} \Gamma^{(2)}_{\sigma\sigma} & \Gamma^{(2)}_{\sigma h} & \Gamma^{(2)}_{\sigma\chi} \\ \Gamma^{(2)}_{h\sigma} & \Gamma^{(2)}_{hh} & \Gamma^{(2)}_{h\chi} \\ \Gamma^{(2)}_{\chi\sigma} & \Gamma^{(2)}_{\chi h} & \Gamma^{(2)}_{\chi\chi} \end{pmatrix}$$

introduced in equation (6.6) a bit better, in particular the role of K for large values of the field. Here, h is the trace of the graviton fluctuation $h_{\mu\nu}$ and σ is the longitudinal part of the vector degree of freedom in the York decomposition of the graviton.
In de Donder gauge and $d = 4$ we find for the limit $\chi \to \infty$ to $\mathcal{O}(R)$

$$\lim_{\chi\to\infty} \Gamma^{(2)}(p^2)^{-1} = \begin{pmatrix} 0 & 0 & 0 \\ 0 & 0 & 0 \\ 0 & 0 & \frac{1}{(K+6)p^2} - \frac{6R}{(K+6)^2p^4} \end{pmatrix},$$

meaning the scalar modes of the graviton do not propagate at all in this limit. This is in accordance with the simple analysis leading to the proposed fixed point presented in section 3.1.3.
Moving forward, we want to understand how the $(K + 6)$ denominator came to be in the first place. For this purpose is suffices to consider $\mathcal{O}(R^0)$. Formally inverting the scalar inverse propagator matrix, we find for its $(3, 3)$ component

$$\left(\Gamma^{(2)^{-1}}\right)_{33} = \frac{\Gamma_{hh}\Gamma_{\sigma\sigma} - \Gamma^2_{\sigma h}}{\Gamma_{hh}\Gamma_{\sigma\sigma}\Gamma_{\chi\chi} + 2\Gamma_{\sigma h}\Gamma_{\sigma\chi}\Gamma_{\chi h} - \Gamma^2_{\sigma h}\Gamma_{\chi\chi} - \Gamma_{hh}\Gamma^2_{\sigma\chi} - \Gamma_{\sigma\sigma}\Gamma^2_{\chi h}},$$

as well as

$$\lim_{\chi\to\infty} \left(\Gamma^{(2)^{-1}}\right)_{33} = \lim_{\chi\to\infty} \frac{\Gamma_{hh}\Gamma_{\sigma\sigma}}{\Gamma_{hh}\Gamma_{\sigma\sigma}\Gamma_{\chi\chi} - \Gamma_{hh}\Gamma^2_{\sigma\chi} - \Gamma_{\sigma\sigma}\Gamma^2_{\chi h}},$$

meaning that the σh component does not contribute in this limit.
Even though the inversion and the limit $\chi \to \infty$ do not commute as operations, we

can still gain some insights from varying their order. In particular, we have

$$\lim_{\chi\to\infty}\frac{\Gamma_{hh}\Gamma_{\sigma\sigma}-\Gamma_{\sigma h}^2}{\Gamma_{hh}\Gamma_{\sigma\sigma}\Gamma_{\chi\chi}-\Gamma_{\sigma h}^2\Gamma_{\chi\chi}}=\lim_{\chi\to\infty}\frac{\Gamma_{hh}\Gamma_{\sigma\sigma}}{\Gamma_{hh}\Gamma_{\sigma\sigma}\Gamma_{\chi\chi}}=\frac{R}{K^2p^2}+\frac{1}{Kp}$$

and

$$\lim_{\chi\to\infty}\frac{\Gamma_{hh}\Gamma_{\sigma\sigma}-\Gamma_{\sigma h}^2}{+2\Gamma_{\sigma h}\Gamma_{\sigma\chi}\Gamma_{\chi h}-\Gamma_{hh}\Gamma_{\sigma\chi}^2-\Gamma_{\sigma\sigma}\Gamma_{\chi h}^2}=\lim_{\chi\to\infty}\frac{\Gamma_{hh}\Gamma_{\sigma\sigma}}{-\Gamma_{hh}\Gamma_{\sigma\chi}^2-\Gamma_{\sigma\sigma}\Gamma_{\chi h}^2}=\frac{1}{6p}-\frac{7R}{36p^2},$$

as well as to $\mathcal{O}(R)$

$$\Gamma^{(2)}\to\begin{pmatrix}\frac{3}{16}\left(\chi^2p^2+F_\infty p^2-2V_\infty\right) & 0 & -\frac{1}{4}\left(3p^2\chi\right)\\ 0 & \frac{1}{16}\left(-F_\infty p^2-p^2\chi^2+2V_\infty\right) & -\frac{1}{4}\left(3p^2\chi\right)\\ -\frac{1}{4}\left(3p^2\chi\right) & -\frac{1}{4}\left(3p^2\chi\right) & Kp^2\end{pmatrix},$$

where $V_\infty=\lim_{\chi\to\infty}V$, $F_\infty=\lim_{\chi\to\infty}F$.
Thus, the number 6 in the factor $K+6$ is a combination of $\Gamma_{\chi h}$ and $\Gamma_{\chi\sigma}$, which have the form

$$\begin{aligned}\Gamma_{\sigma\chi}^{(2)}=\Gamma_{\chi\sigma}^{(2)}&=-2\,\chi\,\frac{3}{4}\,F'(\chi^2)\sqrt{-\Box\left(-\Box-\frac{R}{3}\right)},\\ \Gamma_{h\chi}^{(2)}=\Gamma_{\chi h}^{(2)}&=\left[-2\frac{3}{4}\,\chi\,F'(\chi^2)\,(-\Box)+\chi\,V'(\chi^2)-\frac{1}{2}\,\chi\,F'(\chi^2)\,R\right],\end{aligned}$$

and thus a genuine feature of a scalar-tensor theory.

7.8.2 Treatment of the Singularity K

Moreover, we might be tempted to set $K=-6$ already before inverting $\Gamma^{(2)}$, thus avoiding the emerging singularity. When doing so, the first observation is that a term proportional to the inverse Ricci scalar R^{-1} arises. Even though in our current regularization scheme this term is canceled by the regulator, it should be kept in mind for general considerations. More severely, fixing both K and ξ leads to

$$\partial_t F\propto\chi^2$$

for large values of χ^2, in disagreement with fixing ξ to 1. This divergence in the β-function of F can be cured by ensuring that V grows faster than F, meaning $\frac{V}{F}\to\infty$, for $\chi\to\infty$, amounting to introducing the by now familiar $\lambda\chi^4$ term in the potential V, spoiling the favored limit with a vanishing effective cosmological constant as well as rendering the system unstable as explained in section 7.3, and additionally leading to a vanishing scalar propagator for $\chi\to\infty$, rendering the

scalar sector of the theory completely trivial. This is due to the fact that in the infrared limit, the flow is governed by canonical contributions which vanish for the dimensionless couplings ξ and λ.
The singularity of $\frac{1}{K+6}$ at $K = -6$ and the singularity in $\frac{F}{V}$ at $\chi = \infty$ are both characteristic to coupling a scalar field to gravity in the infrared regime. Indeed, the line separating singular from non-singular behavior at $K = -6$ is a singularity of the spin 0 scalar propagator, while $\frac{F}{V} = 2$ is a singularity of the spin 2 graviton propagator. We speculate that there is a deeper physical meaning, even though we will not focus on this anymore in this thesis.
Allowing for both K and ξ in the system, the scalar propagator is shifted to

$$\propto \frac{1}{(K + 6\xi)p^2 + \ldots},$$

shifting the singularity to

$$\frac{K}{\xi} = -6.$$

This is in accordance with the observation that at $\chi = \infty$ both K and ξ rescale the scalar field, and thus only their ratio has physical significance. We will formalize this notion in section 12.2.2.
Lastly, we mention that $\frac{K}{\xi} = -6$ is exactly the point at which the global scale variance is enhanced to a conformal symmetry [191] (see also [111,112] in the context of functional renormalization). Further research should also focus on understanding the implications of the singularity encountered on the symmetry group of the system as $\frac{K}{\xi}$ is varied.

7.9 Physical Insights from Globally Defined Expansions

Clearly, connecting the limits $y \to 0$ and $y \to \infty$ is a formidable task still remaining to be accomplished. In order to take a further step towards a global solution, we thus devote this section to understanding the connection of the two limiting cases by investigating very simple truncations that have clear-cut features and are well defined in both limits. We emphasize that the aim is not to find a precise global solution, but to merely understand the connection and the coupling of the two limiting cases. To that end, we first disentangle the limits in the potential V (Truncation I), before we move on to also disentangle them in F (Truncation II).

7.9.1 Truncation I

We start by setting

$$\begin{aligned} V &= \frac{V_\infty y + V_0}{1+y}, \\ F &= F_\infty + \xi y, \end{aligned}$$

satisfying

$$\lim_{y\to 0} V = V_0, \ \lim_{y\to\infty} V = V_\infty.$$

Note that the limit in F is ambiguous, as F_∞ is of course also the limit of the function when y approaches 0. We will take care of that in the next section.
Plugging the truncation into our flow equations and projecting on the fixed point equations for V_0, V_∞ and F_∞ (note that $\partial_t \xi = 0$ is trivially satisfied) we find

$$\begin{aligned} 0 &= -4V_0 - \frac{1}{8\pi^2} - \frac{3F_\infty}{16\pi^2\,(2V_0 - F_\infty)} + \frac{K}{32\pi^2\,(K + 2V_\infty - 2V_0)}, \\ 0 &= -4V_\infty + \frac{3}{32\pi^2}, \\ 0 &= -2F_\infty + \frac{77K + 534\xi}{192\pi^2(K + 6\xi)}. \end{aligned}$$

There are two observations that we want to draw the reader's attention to: While it is unclear whether or not the apparent coupling of the limiting cases through the term $2V_0 - F_\infty$, stemming from the graviton propagator, is spurious and due to the ambiguous limits of F, the combination $K + 2V_\infty - 2V_0$, stemming from the propagator of the physical scalar χ, is a true feature of the theory, coupling $y \to 0$ to $y \to \infty$. Moreover, the two latter equations, stemming from the limit $y \to \infty$ are closed in the sense that there are no traces of the limit $y \to 0$, while this is not true vice versa.

7.9.2 Truncation II

Aiming at disentangling the limit in F as well, we set

$$\begin{aligned} V &= \frac{V_\infty y + V_0}{1+y}, \\ F &= \frac{F_\infty y + F_0}{1+y} + \xi y, \end{aligned}$$

satisfying

$$\lim_{y\to 0} V = V_0,\ \lim_{y\to\infty} V = V_\infty,\ \lim_{y\to 0} F = F_0,\ \lim_{y\to\infty} F = F_\infty + \xi y.$$

Plugging the truncation into our flow equations and projecting on the fixed point equations for $V_0,\ V_\infty$ and F_0, F_∞ we find

$$\begin{aligned}
0 &= -4V_0 - \frac{1}{8\pi^2} - \frac{3F_0}{16\pi^2\left(2V_0 - F_0\right)} + \frac{K}{32\pi^2\left(K + 2V_\infty - 2V_0\right)},\\
0 &= -4V_\infty + \frac{3}{32\pi^2},\\
0 &= -2F_0 + \frac{25}{192\pi^2} + \frac{5{F_0}^2}{24\pi^2\left(2V_0 - F_0\right)^2} - \frac{F_0}{12\pi^2\left(2V_0 - F_0\right)}\\
&\quad + \frac{K\left(F_0 - F_\infty - \xi\right)}{16\pi^2\left(K + 2V_\infty - 2V_0\right)^2} - \frac{K}{48\pi^2\left(K + 2V_\infty - 2V_0\right)},\\
0 &= -2F_\infty + \frac{77K + 534\xi}{192\pi^2(K + 6\xi)}.
\end{aligned}$$

In accordance with our suspicion from earlier, the inverse graviton propagator only enters as $2V_0 - F_0$ and is therefore not responsible for the coupling of the limits. Furthermore, $F_0 - F_\infty$ does not stem from a pure propagator, and is thus merely an algebraic collection of originally separate terms. Thus, the nontrivial coupling of $y \to 0$ and $y \to \infty$ is solely due to the propagator of the physical scalar containing $2V_\infty - 2V_0$, and thus solely through the limits of the potential V.
Even more importantly, we manifest our earlier statement that solving the fixed point equations close to $y = \infty$ first, and then moving towards lower values of y is the appropriate path to take, as those equations do not contain any contributions from $y = 0$.

CHAPTER 8

Conclusions and Extensions

Let us pause for a moment to collect our findings from this part's analysis. We derived field equations on a spherical background using heat kernel techniques for the functions V and F. In the simplest case of field independent V and F, one recovers a fixed point solution which resembles Einstein-Hilbert gravity, with only a minimally coupled massless scalar field. This solution is globally defined, but not well suited for dilaton gravity.
When expanding the functions in inverse powers of $y = \chi^2/k^2$, we found that an additional term proportional to $\xi\chi^2$ coupling to the Ricci scalar R is necessary to deviate from the Einstein-Hilbert solution. This term represents the strength of the gravitational coupling for large y, which corresponds to an infrared limit. It thus makes sense that ξ remains undetermined, as it has mass dimension 0, and all quantum contributions vanishing in the infrared, rendering its flow trivial. Furthermore, a finite rescaling of an infinite field is meaningless.
We provided arguments for V becoming constant in the infrared, amounting to a vanishing cosmological constant in the Einstein frame as represented by the infrared action

$$\Gamma(k \to 0) = \int \mathrm{d}^4x\sqrt{g}\left(-\frac{1}{2}MR + \frac{1}{2}g^{\mu\nu}\partial_\mu\phi\partial_\nu\phi\right).$$

This action not only features a nonvanishing Planck mass, thus making the scale of gravity naturally arise within the theory, but also a vanishing cosmological constant, which may be vital to resolving the cosmological constant problem.
Aiming at connecting infrared with ultraviolet physics, we investigated the limit of

small y, which allows for a natural generalization of the constant Einstein-Hilbert type solution. To connect these limits, we optimized an exponentially improved expansion, and presented our current best solution in figure 7.6.
Nevertheless, the quality of the global solution of the fixed point equations is not satisfactory at this point, and will be improved with the analysis presented in part III. In particular, it is not clear from the background field approximations how exactly scale invariance is broken and the Planck mass is generated, and therefore we lack a way of determining the relative strength of gravity. What is more is that a vanishing cosmological constant for $k \to 0$ is a desirable outcome from a cosmological perspective, but since we were unable to determine how the potential approaches its asymptotic value, we are unable to reconstruct the cosmology leading to it.
Furthermore, we understood that the inclusion of a field and RG scale dependent function K is a mandatory next step on the path towards establishing a global solution, both for reasons of consistency as well as to allow for the correct scaling of the scalar field, with emerging limiting cases for ultraviolet and infrared physics.
That is why part III of this thesis is devoted to address the shortcomings encountered.
Last but not least, we established that starting from the limit of large fields is the appropriate approach, given that the flow equations are not only closed in each order of a Taylor expansion, but also do not receive any small field contributions. Moving from large towards lower fields, the potential V will play a crucial role.
Given the results we obtained, it seems like there are two distinct possibilities to carry on. On the one hand, we could set out to improve calculations in the background field formalism. To this end, different implementations of the background split or the background field method in general as described in section 4.3 alongside with the inclusion of terms proportional to R^2, which have scale invariant couplings even without any powers of the scalar, come to mind. Furthermore, when continuing down this path, studies of background, regulator and gauge dependence are inevitable.
However, none of the aforementioned extensions or modifications offer a practicable possibility to include a field dependent function $K(\chi^2)$, multiplying the scalar kinetic term, or a wave function renormalization for any of the fields involved. In this spirit, we set out to include K, rederiving flow equations for V and F, supplemented by an equation for K using expansions around flat backgrounds and a vertex construction (section 4.4.2), thereby not only circumventing problems rooted in the background approximation, but also deriving flow equations for the enlarged truncation, with or without explicit anomalous dimensions for the scalar field. This will be the content of part III of this thesis.

Part III

Vertex Expansions and Flat Backgrounds

CHAPTER 9

Introduction

Inspired by both the result and the shortcomings of part II, we set out to substantiate and extend the results as well as to address the shortcomings.
To that end, we commit ourselves to implement the vertex construction on flat backgrounds as introduced in section 4.4.2 in our dilaton-graviton system, and derive flow equations for not only the functions V and F, but additionally for the function K and thereby for the full action

$$\Gamma\left[g_{\mu\nu},\chi\right]=\int d^4x\sqrt{g}\left(V(\chi^2)-\frac{1}{2}F(\chi^2)\,R+\frac{1}{2}K(\chi^2)g^{\mu\nu}\partial_\mu\chi\partial_\nu\chi\right).$$

This enables us to derive the central result of this thesis, namely a global solution to the dilaton gravity system as depicted in figure 9.1.
As argued in section 7.8, upgrading the system with a field dependent function K is crucial not only for reasons of consistency, but more importantly because it is believed that the scalar field scales differently in the infrared and ultraviolet regime, rendering the inclusion of $K(\chi^2)$ vital to finding a global solution. Moreover, we will disentangle the two roles played by K, namely mediating derivative couplings as well as rescaling the scalar field. We will therefore replace $\chi\to\bar{\chi}=Z\chi^2$ to make the rescaling explicit. Moreover, we will investigate the relationship between rescalings of the graviton and scalar kinetic term at large fields to eliminate redundancies in our description.
In the process, we will gain considerable insight in the physical features of the system, which can be written down in a compact form with only one remaining potential $\hat{V}_{\text{norm}}$, driving the generation of the Planck scale as well as inflation.

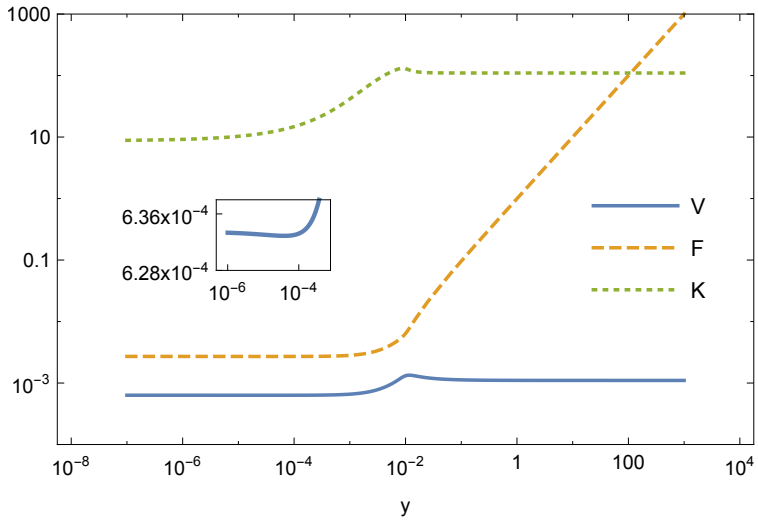

Figure 9.1: Global scaling solution for dilaton gravity.

In the process, we confirm the results presented in part II, most importantly the features of infrared physics, in the context of a vertex expansion with a flat background spacetime, taking advantage not only in terms of having a practicable way of deriving a flow equation for the function K, but also in terms of having a systematic expansion that disentangles background and fluctuating metric at our disposal. Moreover, this setup allows for multiple extensions.

This part is organized as follows. In chapter 10, we sketch the derivation of the desired flow equations using a vertex expansion and a flat background spacetime. In chapter 11, we discuss various prestudies to fix our final setup, where we study K mediated derivative couplings and field rescalings via wave function renormalizations and anomalous dimensions independently. In chapter 12 we derive a global solution using the final physical setup, but with an approximated set of flow equations, which will serve to both gain insights into general features as well as into physical ranges for the so far undetermined parameter ξ characterizing the strength of gravity in the infrared, while chapter 13 uses the full flow equations alongside the insights gathered to derive the final result of this thesis: A globally defined fixed point solution for the dilaton-graviton system, smoothly connecting infrared with ultraviolet physics. Physical implication with emphasis on cosmology, more specifically a moving Planck scale and a cosmology with slow roll inflation and a cosmological constant that decreases with scale are discussed in section 13.5, and we summarize our findings in chapter 14.

CHAPTER 10

Setup and Derivation of the Vertex Expanded Flow Equations

In this chapter, we outline the derivation of the flow equations for the functions V, F and K for a flat background and using an adapted version of the vertex expansion. Some notes on notation can be found in appendix C.1.

10.1 General Strategy

The crucial ingredient to being able to calculate the flow of the function $K(\chi^2)$, of course alongside with the flows of $V(\chi^2)$ and $F(\chi^2)$ is that in the context of the vertex construction introduced in section 4.4.2, we can resort to flows of correlation functions $\Gamma_k^{(n)}$ with $n \neq 0$. In particular, starting from the action (3.6) let us consider $\Gamma^{(\chi\chi)}$ first. We have

$$\begin{aligned}\Gamma^{(\chi\chi)} &= \frac{\delta^2 \Gamma_k^{(2)}}{\delta\chi\delta\chi} \\ &= \int \mathrm{d}^4x\sqrt{g}\left(\frac{\delta^2 V(\chi^2)}{\delta\chi\delta\chi} - \frac{1}{2}R\frac{\delta^2 F(\chi^2)}{\delta\chi\delta\chi} + \frac{1}{2}\frac{\delta^2}{\delta\chi\delta\chi}\left(K(\chi^2)g^{\mu\nu}\partial_\mu\chi\partial_\nu\chi\right)\right).\end{aligned} \tag{10.1}$$

Now, to safe us the trouble of actually computing each term, let us keep in mind that ultimately, we will evaluate all expressions on a flat background spacetime and with a constant background scalar field. While this does not help us with the derivative of the potential, the second term clearly vanishes, as in flat space $R = 0$. For the third term, formally carrying out a partial integration as customary to

shift both spacetime derivatives on one scalar field, we find that at $\chi = \bar{\chi}$ the only nonvanishing contribution is the one where no derivative hits the function $K(\chi^2)$. Due to combinatorics (or a second power in the scalar if you prefer), this term exists exactly twice, canceling the prefactor $\frac{1}{2}$. Now, carrying over to momentum space, this contribution goes with p^2, while the first term in equation (10.1) is momentum independent. Applying an RG time derivative on both sides, we learn that we can extract the flow of $K(\chi^2)$ through the flow of the momentum dependent part of $\Gamma^{\chi\chi}$,

$$\partial_t K(\chi^2) = \partial_{p^2} \mathrm{Flow}^{(2)}_{\chi\chi}(V, F, K) \mid_{p=0} . \tag{10.2}$$

Extracting flow equations for $V(\chi^2)$ and $F(\chi^2)$ works completely analogous to what was done in [103, 192] when replacing the cosmological constant times the inverse Newton coupling with the potential V and the inverse Newton coupling with F, as the dependency on the scalar field does not change the derivation of the graviton correlators, and we will not recast the derivation here. It yields

$$\begin{aligned} \partial_t V(\chi^2) &= - \mathrm{Flow}^{(2)}_{h_{TT}h_{TT}}(V, F, K) \mid_{p=0}, \\ \partial_t F(\chi^2) &= \partial_{p^2} \mathrm{Flow}^{(2)}_{h_{TT}h_{TT}}(V, F, K) \mid_{p=0} . \end{aligned} \tag{10.3}$$

Note that at this point, all functions and fields still carry their canonical mass dimension, and Flow thus is a flow of dimensionful quantities.

A few comments are in order. Our derivation is equivalent to a vertex expansion with $N = 2$, which is the lowest nontrivial order. Thus, at this point, we do not distinguish between a graviton wave function renormalization and a Newton coupling, like introduced in [19] and therefore do not to formally rescale any fields through the vertex construction. The reason for this is threefold. Firstly, already at $N = 2$, correlation functions up to $n = 4$ enter the flow. Given the arbitrary scalar functions introduced, this computation already is a formidable task on a computational level. We will give details in the next section. We mention that we did indeed attempt to also compute flows of the three point functions, but were not able to obtain analytic results with the computer soft- and hardware at our disposal.

What is more, one of the fundamental motivations to disentangle graviton wave function renormalization, entering the propagator, and the Newton coupling, stemming from the three graviton vertex, in the first place is the ill defined infrared limit in earlier pure gravity studies. However, we already found a well defined infrared limit within the framework of background field methods in part II, such that carrying over to the three point function might not even be necessary physically.

Thirdly, in the context of dilaton gravity we are more interested in higher correlations involving the scalar χ, which are automatically included in the functions V, F and K, than in graviton correlators. That is why, rather than focusing on a wave function

renormalization Z_h for the graviton and the emerging anomalous dimension η_h, we will introduce a simple case of the vertex constructions focusing on the scalar χ and its anomalous dimension $Z_\chi = Z$ and corresponding $\eta_\chi = \eta$.
Moreover, in equation (10.3), we use the transverse traceless mode of the graviton. There are two main reasons for this. On the one hand, numerically computing contributions from all modes, it turns out that the TT mode gives the dominant contribution, as one might expect given that classically, the graviton is believed to have spin 2 [193]. On the other hand, we show in appendix C.2 that this mode can be made gauge independent.
In addition to that, when deriving equation (10.2), we might have been tempted to also extract a flow for the potential V from the flow of the scalar-scalar two point function, as one would need to do in a scalar theory without gravity present. However, as we show in appendix E, the potential V is closely related to the effective cosmological constant, and so we prefer extracting the flow from the graviton contributions, as is done for a cosmological constant in quantum gravity.
Now, what is left is to compute the quantities $\text{Flow}^{(2)}_{h_{TT}h_{TT}}$ and $\text{Flow}^{(2)}_{\chi\chi}$.

10.2 Deriving the Flows

Throughout the derivation of the flow equations, we use an early version of the unpublished software package `TARDIS` (figure 10.1), which uses the proprietary software `mathematica` as a wrapper and was developed in Heidelberg mainly by Andreas Rodigast, with the help and support of various members of the institute, including myself.
In general, analytic expressions are lengthy and offer only very limited insights. That is why we refrain from writing them out explicitly in most places, and instead refer to `mathematica` files that can be made available upon request.
At various points of this section we refer to techniques first used in part II. We emphasize that this is solely due to the fact that we present the background derivations first and thus had to introduce certain general concepts also applicable to the current derivation in the context of background fields.

10.2.1 Propagators and Vertices

Starting from the action (3.6) with added gauge fixing (4.12) we derive expressions for $\Gamma^{(2)}$, $\Gamma^{(3)}$ and $\Gamma^{(4)}$, which are the quantities that enter the flow of a 2-point function. Here, we neglect ghost contributions for technical reasons. We perform a York decomposition (6.2), and gauge with $\alpha = \beta = 0$, which simplifies calculations considerably as derived in appendix C.2. For the derivation of vertices we rely heavily on `xTensor` [194].

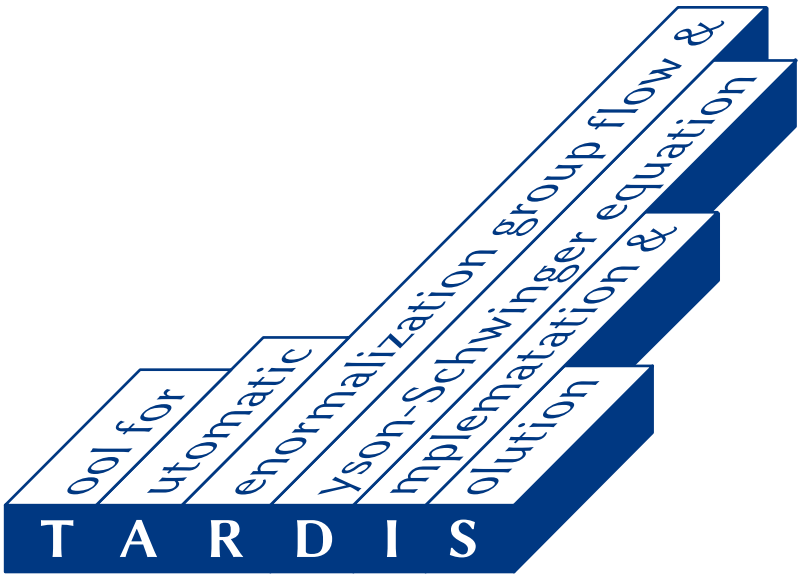

Figure 10.1: Logo of the main software package used in the derivation of the flat flow equations.

The inversion of the scalar 2-point function, which mixed scalar degrees of freedom of the graviton and the physical scalar χ, to derive the scalar propagator is an ordinary matrix inversion and thus straightforward. The inversion of the spin 2 component, which carries 4 spacetime indices is a bit more involved and depends on inverting the transverse traceless projector. We give details in appendix C.3.
To prepare for the later insertion of regulator, we already now replace all combinations of momenta $p_{\phi_1} \cdot p_{\phi_2}$ where $\phi_i \in \{h^{\mu\nu}_{TT}, h, \chi\}$ and we simply use χ to denote the scalar fluctuations, by

$$p_{\phi_1} \cdot p_{\phi_2} \left(1 + r\left(p_{\phi_1} \cdot p_{\phi_2}\right)\right),$$

where the function r will be determined later. Note that in this construction, V does not enter the regulator as it is does not couple to momentum directly.
To accommodate $\partial_t \mathcal{R}_k$, we also construct the corresponding combination where $p_{\phi_1} \cdot p_{\phi_2}$ is replaced by

$$\dot{r}_{\phi_1\phi_2}\left(p_{\phi_1} \cdot p_{\phi_2}\right) p_{\phi_1} \cdot p_{\phi_2},$$

where V needs to be set to zero manually. Note that $\dot{r}_{\phi_1\phi_2}$ is a distinct function and not any direct derivative of r, as will become evident later.

10.2.2 Diagrammatic Expansion

Having derived $\Gamma^{(3)}$, $\Gamma^{(4)}$ and $\left(\Gamma^{(2)}+\mathcal{R}_k\right)^{-1}$, we are now able to compute the flows $\text{Flow}^{(2)}_{h_{TT}h_{TT}}$ and $\text{Flow}^{(2)}_{\chi\chi}$ by applying the diagrammatic expressions given in the top panel of figure 4.1 to our scalar-tensor system with a York decomposed graviton.
We use `DoFUN` [195] do carry out the contractions of fully dressed propagators and 3- and 4-point vertices as well as to keep track of symmetry factors. The quantity $\text{Flow}^{(2)}_{\chi\chi}$ is a scalar expression already, while we need to employ the transverse traceless projector to arrive at the scalar quantity $\text{Flow}^{(2)}_{h_{TT}h_{TT}}$, which is part of the Supertrace operator in the functional renormalization group equation (1.19). These traces are computed in `FORM` [196], and details are given in appendix C.3.
There is a total of 28 diagrams to be treated, and for computational reasons we apply the projector to each one individually and add them up as scalar expressions.
The next step now it to replace the functions $r(p_{\phi_1}\cdot p_{\phi_2})$ and $\dot{r}_{\phi_1\phi_2}(p_{\phi_1}\cdot p_{\phi_2})$ by their specific expressions.

10.2.3 Regulator Insertions

We us the Litim [186,187] shape function

$$r(x) \;=\; \frac{1-x}{x}\Theta\left(1-x\right).$$

With $\phi_i \in \{h^{\mu\nu}_{TT}, h, \chi\}$, we have 3 distinct RG derivatives appearing in the regulator. They are given by

$$\begin{aligned}
\dot{r}_{\chi\chi}(x) &= \frac{2}{x}\Theta(1-x) - \eta\frac{1-x}{x}\Theta(1-x),\\
\dot{r}_{\hat{h}\chi}(x) &= \frac{2}{x}\Theta(1-x) - \frac{1}{2}\eta\frac{1-x}{x}\Theta(1-x),\\
\dot{r}_{\hat{h}\hat{h}}(x) &= \frac{2}{x}\Theta(1-x),
\end{aligned} \tag{10.4}$$

where $\hat{h}$ is shorthand for an arbitrary graviton fluctuation. However, only the trace mode mixes with the scalar χ.
Note that the distribution of η is due to the fact that in this work, $\eta=\eta_\chi$, and we do not introduce a wave function renormalization for the graviton. Furthermore, setting the functions $\dot{r}_{\phi_1\phi_2}$ in the way specified abovehand is exactly where the vertex construction enters, ensuring that $\Gamma^{(n\chi)(m\phi)} \propto Z^{\frac{n}{2}}$, where Z is the wave function renormalization for the scalar χ. When we work without an anomalous dimension, setting $\eta=0$ recovers the expression without the correct scaling for the scalar propagator. When we work with a field dependent anomalous dimension, we set

$\eta = \eta(y)$, $y = \frac{\chi^2}{k^2}$. Note that there are no derivatives of $\eta(y)$ entering the flows. r does not depend on the choice of fields, as all Z factors drop out by virtue of the correct scaling of propagators. Details can be found in appendix C.4.
Whenever we consider $\eta \neq 0$, we have to think of the field χ as ppearing in combination with an explicit wave function renormalization Z, and thus replace χ with $\bar{\chi} = Z^{1/2}\chi$ in all functions.

10.2.4 Momentum Dependencies

Given momentum integration, there are two distinct four-momenta present in our expressions, the external momentum p and one loop momentum q, entering as $p \cdot p = p^2$, $q \cdot q = q^2$ and $q \cdot p = p \cdot q$. We deal with the mixed scalar product in the standard way by setting $q \cdot p = p \cdot q = \sqrt{p^2}\sqrt{q^2}x$, where $x = \cos(\theta)$ and θ is the angle between p and q in four-space.
For the flows of $F(\bar{\chi}^2)$ and $K(\bar{\chi}^2)$ we compute derivatives with respect to the external momentum and evaluate all expressions at vanishing external momentum p^2. The lingering integration over the loop momenta is then carried out in spherical coordinates by integrating over q^2, which is constrained by the Θ functions in the expressions, and the angular distribution separately. For the latter, we do not attempt a direct integration due to the size of the analytic expressions, but rather use systematics of products of sines and cosines in a fully expanded version of the expressions as given in appendix C.6 to solve the integrals.
We circumvent difficulties with the delta distribution [188] by carefully setting the momentum projections in the derivatives of the Θ-function by hand.

10.2.5 Dimensionless Functions

After integrating over the loop momentum and thus arriving at $\text{Flow}^{(2)}_{h_{TT}h_{TT}}$ and $\text{Flow}^{(2)}_{\chi\chi}$, we are almost done. The last step to complete is to transform the flow of the dimensionful fields of dimensionful functions to a flow of dimensionless functions of a dimensionless field, thus disentangling canonical running and quantum contributions. This goes through in parallel to what we introduced at the end of section 6.2 given that $[Z] = 0$. There are two additions: First, we need to deal with $K(\bar{\chi}^2)$. Given that $[K(\bar{\chi}^2)] = 0$ already, the dimensionless $K(y)$ only receives a contribution from the mass dimension of $\bar{\chi}^2$.
The second, more subtle point is that we need to take care of the scale derivative of the rescaled field properly. For a function $\mathcal{H}(\bar{\chi}^2)$ we have

$$\partial_t \left(\mathcal{H}\left(\bar{\chi}^2\right)\right) = \chi^2 \dot{Z} \frac{\partial \mathcal{H}}{\partial \bar{\chi}^2} + \left(\partial_t \mathcal{H}\right)\left(\bar{\chi}^2\right) = -\eta \bar{\chi}^2 \frac{\partial \mathcal{H}}{\partial \bar{\chi}^2} + \left(\partial_t \mathcal{H}\right)\left(\bar{\chi}^2\right),$$

and thus the flows receive an additional term proportional to $\eta y \mathcal{H}'$. Since we will

use different types of exact implementations of this procedure in the different studies carried out in chapters 11 to 13, we will introduce the explicit expressions for the flows in the respective sections.
Last but not least, note that global rescalings of fields are always allowed, since they only alter the path integral by a constant. We can thus carry on with $y = \frac{\chi^2}{k^2}$ as the dimensionless field supplemented by its wave function renormalization Z.

CHAPTER 11

Results I: Prestudies

In this chapter, we present a series of prestudies alongside with their results that serve to fix the final setup with which we will work in chapter 12 and 13 to find a global solution for the dilaton-graviton system and discuss its physical consequences. In particular, we independently explore the properties of $K(y)$ as a mediator of derivative couplings with arbitrary powers of the scalar field, as well as in the framework of a in general field dependent anomalous dimension $\eta(y)$.

11.1 K(y) as a Coupling

To compare the flat expansion with what was previously derived using a symmetrical background, we drop the distinction between χ and $\bar{\chi}$ for a first calculation, regarding $K(y)$ as a coupling, and thus not introducing an anomalous dimension η. We derive flow equations according to

$$\begin{aligned}
\partial_t V &= -4V(y) + 2yV'(y) - \mathrm{Flow}^{(2)}_{h_{TT}h_{TT}}(V,F,K)\,|_{p=0}, \\
\partial_t F &= -2F(y) + 2yF'(y) + \partial_{p^2}\mathrm{Flow}^{(2)}_{h_{TT}h_{TT}}(V,F,K)\,|_{p=0}, \\
\partial_t K &= 2yK'(y) + \partial_{p^2}\mathrm{Flow}^{(2)}_{\chi\chi}(V,F,K)\,|_{p=0},
\end{aligned}$$

and focus on solving the corresponding fixed point equations, which are derived from the flow equations by setting $\partial_t V = \partial_t F = \partial_t K = 0$.

11.1.1 Lowest Order Results

Setting all functions equal to a constant, namely

$$V = v_0,\ F = f_0,\ K = k_0, \tag{11.1}$$

we find fixed point equations given in appendix D.1, equations (D.1), (D.2) and (D.3). They yield three sets of real fixed points that are numerically given by

$$\begin{aligned}(v_0,\ f_0,\ k_0) =&(-4.655, && -9.990, && 0\ ),\\ &(5.721\cdot 10^{-4}, && -2.751\cdot 10^{-3}, && 0\ ),\\ &(6.346\cdot 10^{-4}, && 2.713\cdot 10^{-3}, && 0\ ).\end{aligned} \tag{11.2}$$

Out of these fixed points, only the last one hast $v_0 > 0$ and $f_0 > 0$ corresponding to positive Newton coupling and cosmological constant and is thus physically viable. The result $k_0 = 0$, which is common to all three real fixed points, already provides deep insights into the structure of the equations. Even though we had introduced K as a coupling in the current analysis, at $y = \infty$ and in the truncation (11.1) it is evident that $K = k_0$ rescales the scalar field $y \propto \chi^2$ and thus acts as a wave function renormalization for the scalar field, commonly denoted by Z. However, we can already see from the original Callan–Symanzik equation [197], carried over to the functional context in [198], that the proper way to handle a wave function renormalization is to introduce an anomalous dimension and introduce a corresponding equation, rather than demanding $\dot{k}_0 = \dot{Z} = 0$. We will present a proper treatment in chapters 12 and 13, where we completely disentangle the influence of wave function renormalization and couplings. For the time being, note that

$$\eta = -\frac{\dot{Z}}{Z} \approxeq -\frac{\dot{k}_0}{k_0}$$

leads to

$$Z(t) = Z(t_{\text{init}}) \exp\left(-\int_{t_{\text{init}}}^{t} \eta(t')\,\mathrm{d}t'\right),$$

where t is the dimensionless RG time and t_{init} denotes some initial scale of integration. At some t, η will approach its fixed point value and become scale independent, and the integral can be replaced by a multiplication with t over a still infinite range. But then, if $\eta > 0$, the negative overall sign of the argument of the exponential forces the exponential to tend to 0 for an ultraviolet fixed point $t \to \infty$ leading to $k_0 = 0$. We suspect that this is exactly what we are witnessing here, and this observation points to a finite $\eta \neq 0$, which cannot be accommodated in the current setup.

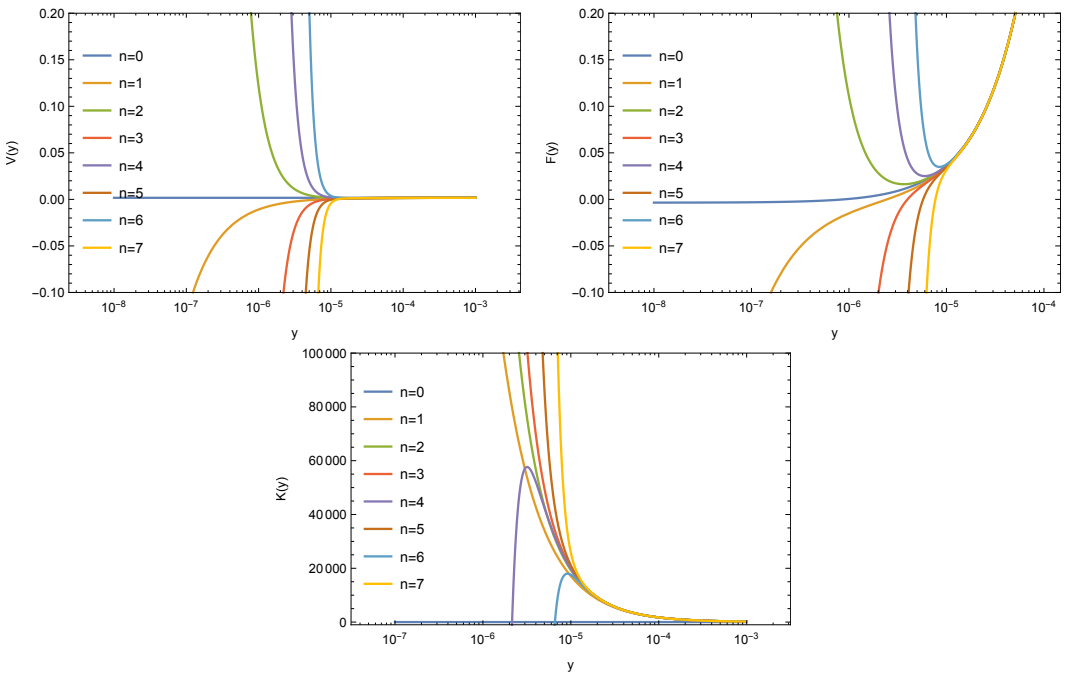

Figure 11.1: Functions $V(y)$, $F(y)$ and $K(y)$ Taylor expanded around $y = \infty$ to orders 0 to 7 and with $\xi = 4000$ and $k_0 = 1$. The breakdown of the expansion around $y \approx 1/\xi$ is clearly visible, in agreement with earlier calculations on symmetrical backgrounds.

11.1.2 Large Field Limit

Taylor expanding around $y = \infty$ according to

$$V = \sum_{i=0}^{a} \frac{v_i}{y^i i!}, \; F = \xi y + \sum_{i=0}^{b} \frac{f_i}{y^i i!}, \; K = \sum_{i=0}^{c} \frac{k_i}{y^i i!}, \tag{11.3}$$

we find that the inclusion of a term ξy in F is necessary to move beyond the Einstein-Hilbert solution, characterized by setting all couplings to a single, field independent value. Once a term ξy, resembling the original Brans-Dicke idea of including scalar fields into classical gravity, is included, we find non-constant solutions which have $\partial_t \xi = \partial_t k_0 = 0$ and therefore depend on ξ and $k_0 = \lim_{y\to\infty} K$ parametrically, consistently extending previous computations. The form of different orders of the Taylor expansions is shown in figure 11.1.
Once again we find excellent agreement between the different orders of the Taylor expansion, corresponding to only very small deviations from $V = v_0$, $F = \xi y + f_0$, $K = k_0$, up until the point where all orders in the expansion diverge at approximately the same value of y, signalling the breakdown of the expansion. This is in parallel to

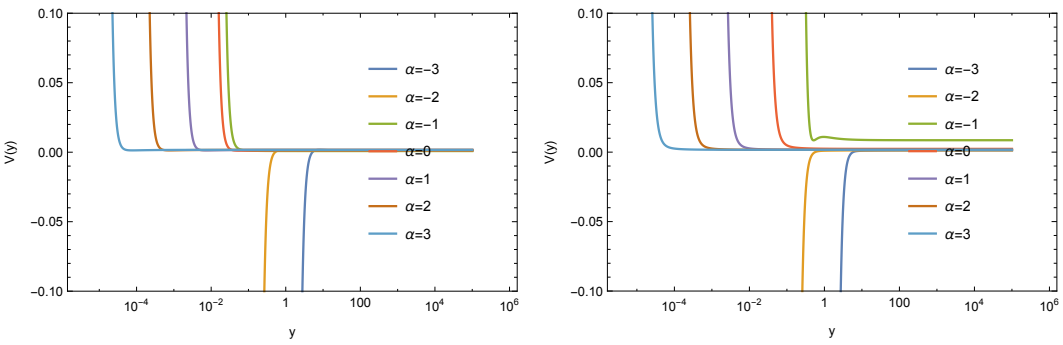

Figure 11.2: $V(y)$ plotted with $\xi = +10^{\alpha}$ (LHS) and $\xi = -10^{\alpha}$ (RHS) and $k_0 = 1$. Note, how the point where the expansion breaks down scales with ξ^{-1}, and how the influence of ξ is especially visible near the propagator singularity at $\xi = -\frac{1}{6}$.

the results obtained with the background field formalism in part II. Note however that K deviates from its asymptotic value before V and F diverge. We speculate that the so far insufficient treatment of a non-constant K triggers the breakdown. In figure 11.2 we study the point of divergence as a function of ξ for the potential V and find that it approximately scales with ξ^{-1}, already hinting towards the fact that the true physical field variable might need to be transformed in a similar manner.

11.1.3 Padé Improvements

We construct Padé improvements to the Taylor approximations by means of a smooth matching at some intermediate point y_0, much like in section 7.5. In figure 11.3, we show Padé improved approximations for $n = m = 5$ and different matching points y_0. We stress that we do not expect the Padé improvement to fully capture the solution for large y, as this is already sufficiently done by the Taylor approximations, and focus on the behavior for small y. It is evident that the Padé approximations are able to provide smooth continuations towards $y = 0$, but do not provide a unique limit, the value of the small field limit depends on the matching point.
Moreover, we observe that finding a Padé improvement for $K(y)$ seems to be numerically challenging. We interpret this as a further hint towards the fact that it is not consistent to simply treat $K(y)$ as a coupling, and progress to formally introducing a wave function renormalization η in the next section.
We conclude that the inclusion of $K(y)$ into the equations alone does not yet provide the desired improvement outlined in section 7, but that we are indeed able to reproduce the results gained therein.

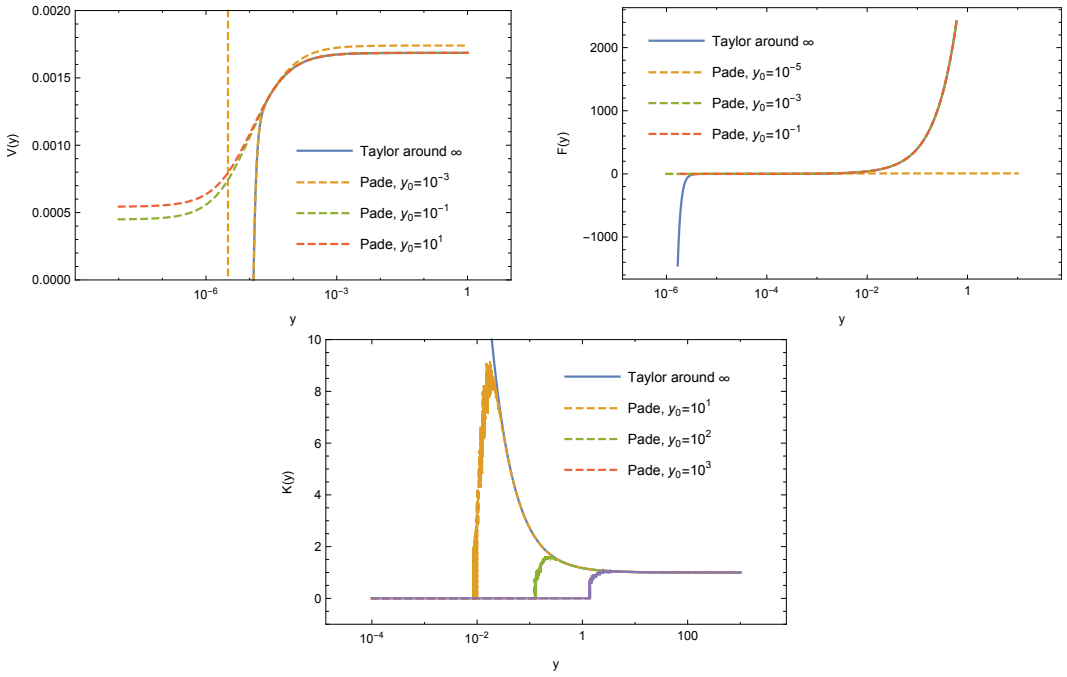

Figure 11.3: Taylor approximations to the solution of the fixed point equations obtained at $y_0 = \infty$ alongside with their Padé improved versions at different matching points y_0.

11.2 Introducing the Anomalous Dimension η

Having derived the need to introduce a wave function renormalization η in the last section, we will now prepare the formal means to do so. For that, we employ the vertex construction introduced in section 4.4.2 to ensure that

$$\Gamma_k^{(n\chi)(m\phi)} \propto Z_k^{\frac{n}{2}}, \tag{11.4}$$

where ϕ labels all other fields of the theory under consideration. Note that since we only introduce one wave function renormalization Z for the scalar field, we won't explicitly label it, $Z = Z_\chi$.
To that end, we consider the action

$$S = \int d^4x\sqrt{g}\left(V_k(\bar{\chi}^2) - \frac{1}{2}F_k(\bar{\chi}^2)\,R + \frac{1}{2}g^{\mu\nu}\partial_\mu\bar{\chi}\partial_\nu\bar{\chi}\right), \quad \bar{\chi} = \sqrt{Z_k(\chi^2)}\chi, \tag{11.5}$$

from which we derive vertices by taking functional derivatives and enforcing the scaling (11.4). Then,

$$\eta(\chi^2) := -\frac{\dot{Z}(\chi^2)}{Z(\chi^2)}$$

only enters through the regulators, in direct generalizations of the deviation presented in appendix C.4. We arrive at equations

$$\begin{aligned}
\partial_t V &= \eta y\partial_y V - 4V + 2yV' - \mathrm{Flow}^{(2)}_{h_{TT}h_{TT}}(V,F,\eta)\,|_{p=0}, \\
\partial_t F &= \eta y\partial_y F - 2F + 2yF' + \partial_{p^2}\mathrm{Flow}^{(2)}_{h_{TT}h_{TT}}(V,F,\eta)\,|_{p=0}, \\
\eta &= 2y\eta' - \partial_{p^2}\mathrm{Flow}^{(2)}_{\chi\chi}(V,F,\eta)\,|_{p=0},
\end{aligned}$$

where the dependence on the field $y = \frac{\chi^2}{k^2}$ is understood.
Note that the absence of a term proportional to $\eta y\partial_y\eta$ in the equation for η is due to the fact that we used $Z(\chi^2)$ instead of $Z(\bar{\chi}^2)$ to rescale fields and form η, which is consistent with neglecting derivative couplings of vertices with Z on the RHS of the flow equation. On the same grounds we also neglected a term $2y\eta'$, which arises due to the canonical running of the scalar field
Investigating the simplest case again, meaning setting

$$V = v_0,\ F = f_0,\ \eta = \eta_0$$

we find fixed point equations given in appendix D.2, equations (D.4), (D.5) and (D.6).

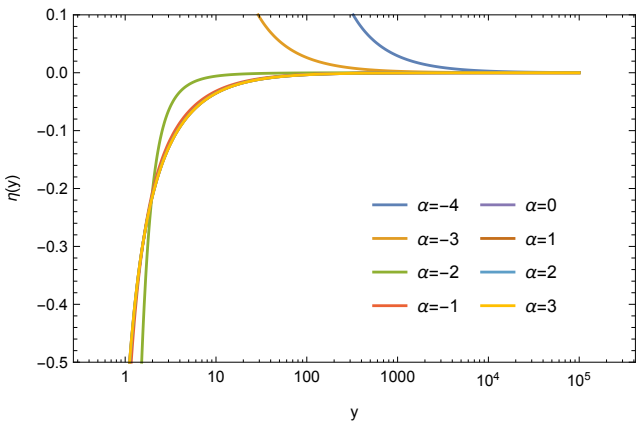

Figure 11.4: Field dependent anomalous dimension η as a function of y and for different $\xi = 10^{\alpha}$.

They lead to real fixed points

$$\begin{aligned}(v_0,\ f_0,\ \eta_0) =&(-4.6546, && -9.9903, && -1.354\cdot 10^{-3}\ )\\ &(5.675\cdot 10^{-4}, && -2.7624\cdot 10^{-3}, && -0.7514\ )\\ &(-1.932\cdot 10^{-4}, && -4.334\cdot 10^{-4}, && 78444.1639\ )\\ &(-5.882\cdot 10^{-5}, && -2.874\cdot 10^{-4}, && -101.1822\ )\\ &(6.365\cdot 10^{-4}, && 6.769\cdot 10^{-4}, && -1006.13\ )\\ &(1.444\cdot 10^{-3}, && 1.753\cdot 10^{-3}, && -4354.5049\ )\\ &(6.460\cdot 10^{-4}, && 2.757\cdot 10^{-3}, && 1.6669\ ).\end{aligned} \tag{11.6}$$

For comments on their physical viability we refer the reader to the discussion in section 12.4.1.
Moving past constant order by expanding V, F and η in negative powers of y and allowing for an additional term ξy in F, similar to equation (11.3), we find that η vanishes at $y \to \infty$, that is

$$\lim_{y\to\infty} \eta(y) = 0. \tag{11.7}$$

This is consistent with the physical expectation that the anomalous dimension should vanish in the infrared, signalling classical scaling.
Investigating η for finite y, we find that the deviations from $\eta = 0$ are only marginal for a wide range of large field values y, as depicted in figure 11.4.
There are two important conclusions to draw from this: Firstly, an almost vanishing η will not change the form of V and F considerably in comparison with what we

found in section 11.1, which is why we do not provide additional plots for V and F at this point.
Secondly, we stress that η is almost constant up until close to the point where we already know the Taylor approximations to break down. This means on the one hand that approximating η by a constant and neglecting derivative couplings is justified for large y, but once we approach an intermediate range of y, this approximation is no longer valid.
That is why in the next chapter we proceed to considering the constant anomalous dimension η and the field dependent coupling $K(y)$ in one truncation, but disentangling their influence. Partially neglecting derivative couplings for large y in a first attempt at solving the system will provide vital to understanding the influence of the currently free parameter ξ.

CHAPTER 12

Results II: Approximated Vertex Expanded Version

Having understood that we need a field dependency in the term multiplying the scalar kinetic term, and derivatives become important in the critical intermediate range. These cannot be captured by a field dependent anomalous dimension, therefore we now set out to disentangle a constant wave function renormalization for the scalar field and a dynamical function $K(y)$ accounting for derivative couplings in the flows. We call the wave function renormalization Z. It leads to a constant anomalous dimension η defined at a certain $y = y_0$.
In order to ultimately arrive at a global solution using numerical solvers for the flow equations, it will be crucial to find a suitable set of initial conditions. For that, understanding what values of the so far undetermined couplings ξ and k_0, or a combination thereof, might be suitable is crucial. To that end, we will first analyze an approximation to the full flow equations, partially incorporating derivatives of $K(y)$, before we use that knowledge to solve the complete system in chapter 13.

12.1 Generalities and Setup

In order to include an anomalous dimension η through a wave function renormalization Z we generalize our truncation to

$$S = \int d^4x\sqrt{g}\left(V(\bar{\chi}^2) - \frac{1}{2}F(\bar{\chi}^2)\,R + \frac{1}{2}K(\bar{\chi}^2)g^{\mu\nu}\partial_\mu\bar{\chi}\partial_\nu\bar{\chi}\right), \tag{12.1}$$

where $\bar{\chi} = Z^{1/2}\chi$, and this rescaled field should not be confused with the background field.

To compute quantum effective correlation functions, we take the tensor structures from S and construct Γ from S such that $\Gamma^{(n\chi)}$ scales with $Z^{n/2}$, and write $\eta = -\dot{Z}/Z$ where Z does not depend on χ, inspired by section 4.4.2.
We work at constant $y = \frac{\chi^2}{k^2}$ In order to distinguish between the field independent anomalous dimension η and the field dependent kinetial $K(y)$ we pick a reference field y_0 and set $k_0 = K(y_0) = \pm 1$, such that we can compute η at $y = y_0$.
This leads to flow equations

$$\begin{aligned}
\partial_t V &= \eta\ y\partial_y V - 4V + 2yV' - \mathrm{Flow}^{(2)}_{h_{TT}h_{TT}}(V,F,K,\eta)\ |_{p=0},\\
\partial_t F &= \eta\ y\partial_y F - 2F + 2yF' + \partial_{p^2}\mathrm{Flow}^{(2)}_{h_{TT}h_{TT}}(V,F,K,\eta)\ |_{p=0},\\
\partial_t K &= \eta\ y\partial_y K + 2yK' + \partial_{p^2}\mathrm{Flow}^{(2)}_{\chi\chi}(V,F,K,\eta)\ |_{p=0,\ k_0=\pm 1},\\
\eta &= -\partial_{p^2}\mathrm{Flow}^{(2)}_{\chi\chi}(V,F,K,\eta)\ |_{p=0,\ y=y_0}\ .
\end{aligned} \tag{12.2}$$

Note that η is not field dependent in this approach, but all field dependencies are encoded in $K = K(y)$. This allows for the inclusion of couplings that contain derivatives of $K(y)$ that were not included in the previous truncation.

12.1.1 Approximation

From the discussion of figure 11.4 we learned that $\partial_{p^2}\mathrm{Flow}^{(2)}_{\chi\chi}$, which enters the equations for η and K admits a solution that is constant for large y. Furthermore, as pointed out in chapter 7, understanding the influence and with that potential physical bounds of the so far undetermined parameter ξ may be integral to finding a global scaling solution. To that end, we approximate the β-function for K by neglecting the dimensional running $2yK'$ for the remainder of this chapter. The advantages of this approximation will become evident later. We again have $\eta = 0$ for $y_0 = \infty$, such that the flow equation for K reduces to

$$\partial_t K = \partial_{p^2}\mathrm{Flow}^{(2)}_{\chi\chi}(V,F,K,\eta)\ |_{p=0,\ k_0=\pm 1}\ . \tag{12.3}$$

12.2 Large Field Expansion

In this spirit we expand the functions V, F and K in negative powers of y according to

$$V = \lambda y^2 + m^2 y + \sum_{i=0}^{a} \frac{v_i}{y^i i!},\ F = \xi y + \sum_{i=0}^{b} \frac{f_i}{y^i i!},\ K = \sum_{i=0}^{c} \frac{k_i}{y^i i!}, \tag{12.4}$$

where we also accounted for the possibility of a Brans-Dicke like term ξy in F, as it is exactly scale invariant. We put k_0 in for pedagogical reasons, and will set it

to ± 1 later to not infer with the scaling via Z. Following this argument it would also be possible to include a term λy^2 to the potential V, and when doing so, a scalar mass term $m^2 y$ should also be included. However, the same arguments as in the background analysis in part II hold and unless otherwise noted, we will set $\lambda = m^2 = 0$.

Hierarchy of fixed point equations

The first important observation is that

$$\lim_{y\to\infty} \beta_K = 0,$$

yielding

$$\eta = 0$$

independently of the approximation.
In agreement with the results from the background calculations in section 7.2 we find a hierarchy of fixed point equations which is closed to each order in y, meaning that the β-function for the i-th order couplings, corresponding to y^{-i}, only contain j-th order couplings with $j \leq i$. In particular this property ensures $\eta = 0$ to all orders, and prevents new fixed points to arise when new orders of y are included.
More specifically, projecting on the β-function to lowest order y^1 we have

$$\partial_t \xi = 0 \quad \Rightarrow \quad \xi\eta = 0, \tag{12.5}$$

which is trivially true for $\eta = 0$.
To order y^0 we find

$$\begin{aligned}
\partial_t v_0 = 0 \Rightarrow v_0(\xi) &= \frac{\eta(-1104\xi^3 - 20\xi^2 + 32\xi + 1)}{7680\pi^2(6\xi+1)^3} \\
&\quad + \frac{2760\xi^3 + 612\xi^2 + 82\xi + 9}{768\pi^2(6\xi+1)^3}, \\
\partial_t f_0 = 0 \Rightarrow f_0(\xi) &= -\frac{\xi\eta\,(756\xi^2 + 1884\xi + 293)}{27648\pi^2(6\xi+1)^3} \\
&\quad - \frac{51840\xi^3 + 36240\xi^2 + 6094\xi + 253}{6912\pi^2(6\xi+1)^3},
\end{aligned}$$

while $\partial_t k_0 = 0$ is trivially satisfied, in agreement with $\eta = 0$.
To order y^{-1} we find conditions

$$\partial_t v_1 = 0 \qquad \Rightarrow \qquad v_1(v_0, f_0, k_1, \xi),$$

$$\partial_t f_1 = 0 \qquad \Rightarrow \qquad f_1(v_0, f_0, k_1, \xi),$$

and exploiting the equation $\partial_t k_1 = 0$ we find

$$\begin{aligned} 0 = &- k_1\eta + \frac{\eta\left(-1296\xi^4 + 108\xi^2 + 12\xi + 1\right)}{576\pi\xi(1+6\xi)^3} \\ &+ \frac{\left(26244\xi^4 + 12636\xi^3 + 2079\xi^2 + 90\xi - 1\right)}{36\pi^2\xi(6\xi+1)^3}, \end{aligned} \tag{12.6}$$

which for $\eta = 0$ does not yield a condition for k_1 but rather for ξ, and is for finite k_1 and $\xi \neq 0,\ -1/6$ only solved by

$$26244\xi^4 + 12636\xi^3 + 2079\xi^2 + 90\xi - 1 = 0, \tag{12.7}$$

thus yielding a condition to compute ξ. Note that this equation is due to the approximation (12.3), in the full version it would receive an additional term $-2k_1$. However, for the time being we assume this equation to be true in order to understand the influence of and physical bounds on ξ a bit better.
This is an important difference to the background calculations in section 7.2, where ξ was the free parameter of the theory, as being able to determine ξ allows to set precise initial conditions for numerical routines, which will ultimately enable us to globally understand the scalar-tensor system.
At this point, the free parameter of the system is k_1. Writing down the next order of equations, k_1 is determined by $\partial_t k_2 = 0$, while k_2 remains free, and using the equation $\partial_t k_c = 0$ we are able to determine all $k_i,\ i < c$, making k_c the free parameter. As the influence of k_c is suppressed by a factor of y^{-c}, it does not play a role for $y \gg 1$.

Classifying the Solutions

Solving equation 12.7 for ξ we find two real solutions for $k_0 = +1$ and two real solutions for $k_0 = -1$.
For $k_0 = +1$ we find two classes of solutions with

$$\xi = 0.00909 \text{ or } \xi = -0.0854,\ k_0 = +1.$$

Since ξ is connected to the strength of the gravitational interaction, we focus on solutions with $\xi > 0$. At the outset of this paragraph, we argued that fixing $K(y_0) = 1$ allows for an unambiguous calculation of $\partial_t K$ and η. Of course this argument goes through exactly as stated, if we fix $K(y_0) = -1$. When doing so we get two additional classes of solutions, connected to the first two classes by all even powers in K and all odd powers in F and V flipping sign. In particular, $K(y_0) = -1$ thus yields

$$\xi = -0.00909 \text{ or } \xi = 0.0854,\ k_0 = -1,$$

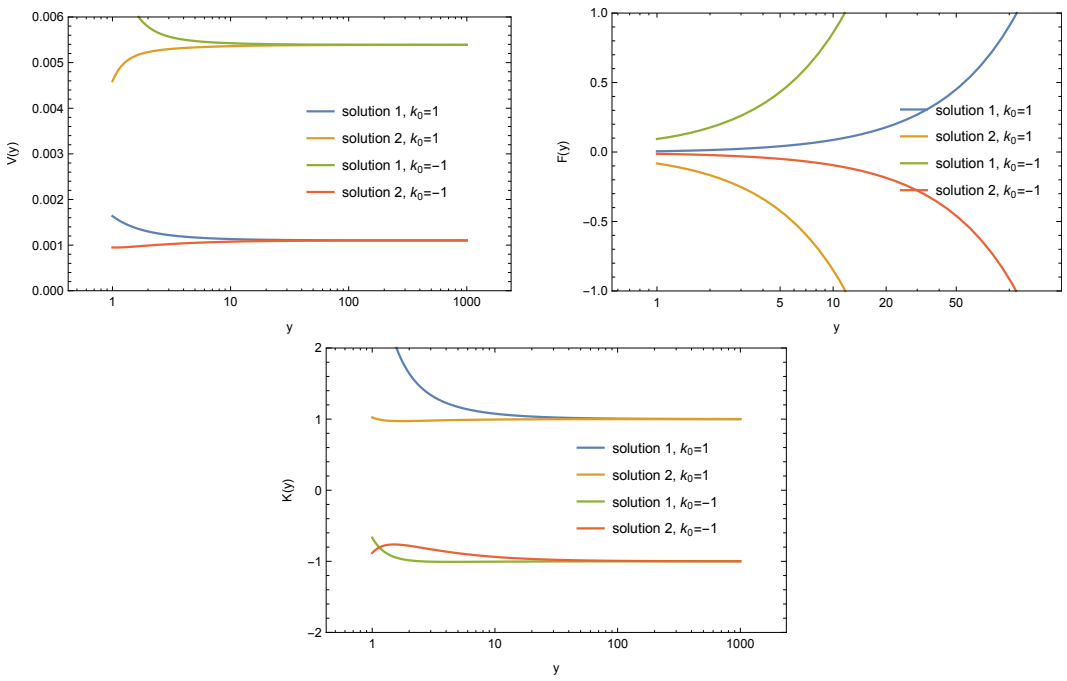

Figure 12.1: Plots of the different classes of solutions for the three functions V, F and K.

in agreement with the observation that for $y \to \infty$ only the ratio $\epsilon = \frac{k_0}{\xi}$ has physical relevance. Given that for large y the leading term in V and K is an even power and an odd power in F, at $y = \infty$ the transformation $K(y_0 = \infty) = 1 \to K(y_0 = \infty) = -1$ thus provides us with two solutions for K and V, distinguished by a flip in overall sign, while there are four distinct solutions for F, two with negative and two with positive ξ. All deviations are of subleading order and become more and more visible when y becomes smaller and smaller, as depicted in figure 12.1.
Solutions with $k_0 > 0$ are automatically stable, and we only need to ensure $\xi > 0$ to warrant for a positive effective gravitational coupling. To meet stability bounds known from earlier work on scalar-tensor theories of gravity (see section 7.8) also for $k_0 < 0$ we require $k_0/\xi > -6$, which translates to $\xi > 1/6$. We are thus left with a unique, physical solution at

$$k_0 = 1 \text{ and } \xi = 0.00909. \tag{12.8}$$

Our flow equations have vanishing denominators as ξ approaches $-1/6$, as one would expect from an infrared limit of a scalar-tensor theory of gravity. We point out that there is no consistent fixed point solution to lowest order already when approaching $\xi = -1/6$. The same is true when approaching $\xi = 0$.

$\xi = 9.0934 \times 10^{-3},\ \eta = 0$

i	v_i	f_i	k_i
0	1.1022×10^{-3}	-3.8929×10^{-3}	1
1	2.8936×10^{-4}	-2.5218×10^{-4}	0.6860
2	3.2830×10^{-4}	-5.8109×10^{-5}	1.3777
3	5.0355×10^{-4}	5.2381×10^{-4}	4.1194
4	6.1776×10^{-4}	3.8452×10^{-3}	15.6006
5	-2.2771×10^{-3}	2.4944×10^{-2}	68.0385
6	$1.8779 \times 10^{-5} \times (k_6 - 2363.26)$	$2.3542 \times 10^{-5} \times (k_6 + 6926.28)$	k_6

Table 12.1: Expansion coefficients in the for the large field expansion 12.4 on the fixed point up to order y^{-6}.

12.2.1 The Parameter k_c

Plotting the Taylor expansions with $a = b = c = 5$ and for different positive values of $k_c = k_5$ we can investigate the dependence on k_5. As expected, the dependence is only visible once y is approximately unity. Furthermore, as can be seen from figure 12.2, the value of k_5 changes the characteristics of the divergence of the Taylor expansion for small values of y. This is also true for negative values of k_5. Additionally, figure 12.2 suggests a convergence of the expansions for $k_5 \to 0,\ k_5 > 0$. A similar observation can be made for $k_5 \to 0,\ k_5 < 0$, such that a small absolute value of k_5 brings the different solutions closer and closer together. We also point out that the influence of the parameter k_c only becomes relevant shortly before the expansions break down, and thus only controls the exact form of divergence. The solutions are thus nearly unambiguous up until that point.
The picture is similar for the other classes of solutions. Note that even though we are able to flip the direction of divergence by virtue of varying k_c, we cannot avoid the divergence altogether. Furthermore, the influence of the parameter can be restricted to K by setting $a = b = c - 1$.

12.2.2 Scaling Relations

It may seem slightly odd that after putting a considerable effort into defining a scalar η we wind up with $\eta = 0$ to all orders for $y_0 = \infty$. This section aims at shedding some light onto the role of η, especially for large values of y. Furthermore we point out that for small y there are solutions with $\eta \neq 0$. They are discussed in section 12.4.1.
For large y, we effectively approach a free scalar theory. The argument goes as follows:

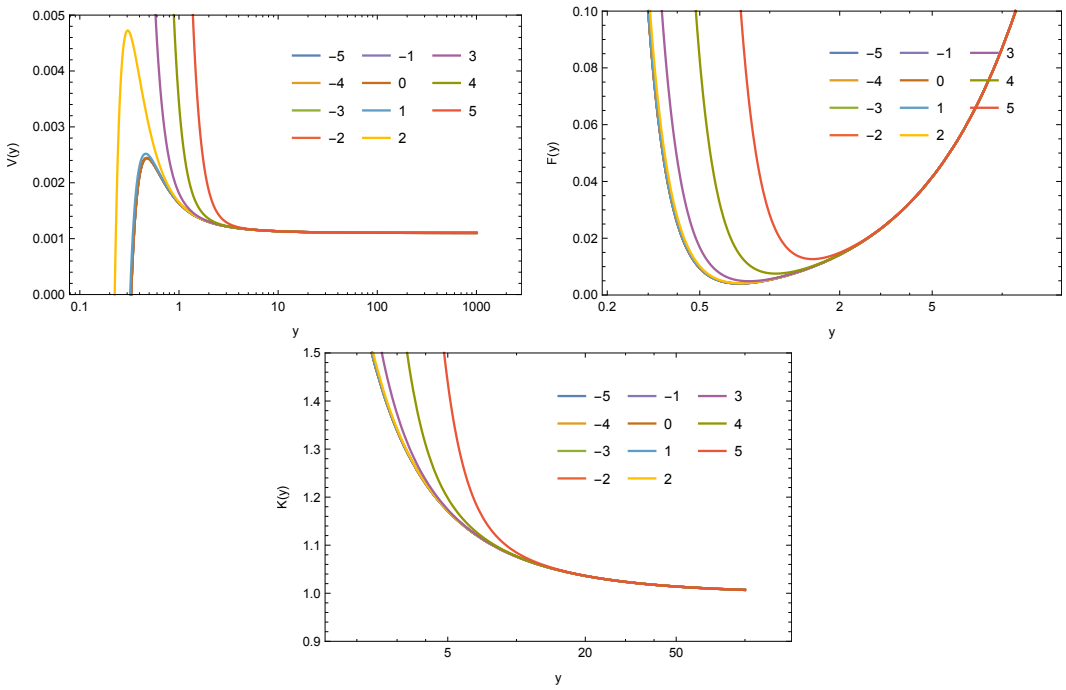

Figure 12.2: Taylor expansions for the functions $V(y)$, $F(y)$ and $K(y)$ to order 5 and different values of $k_5 = 10^{\alpha}$, $\alpha \in [-5, 5]$. We see a convergence of the solutions towards the solution with $k_5 \to 0$, $k_5 > 0$.

The effective strength of gravity, as given by the Newton constant, is determined by $\xi^{-1}y^{-1}$, which approaches 0 for $y \to \infty$. This is the only dimensionless combination that can possibly enter the other flows, and thus gravity ceases to drive the flow. Therefore one would expect both ξ and $k_0 = K(y_0)$ to globally rescale the scalar field strength. Indeed, for $K = k_0$ and $F = \xi y + f_0$, $V = v_0$ only the ratio

$$\epsilon := \frac{k_0}{\xi}$$

enters the equations.
More specifically, projecting on the β-function to order y^1 we have

$$\partial_t \xi = 0, \tag{12.9}$$

while the order y^0 yields

$$\begin{aligned} \partial_t v_0 &= \frac{9\epsilon^3 + 82\epsilon^2 + 612\epsilon + 2760}{192\pi^2(\epsilon+6)^3} - 4v_0, \\ \partial_t f_0 &= \frac{-253\epsilon^3 - 6094\epsilon^2 - 36240\epsilon - 51840}{3456\pi^2(\epsilon+6)^3} - 2f_0, \\ \partial_t k_0 &= 0. \end{aligned} \tag{12.10}$$

So far, we lack any conditions on the function K. Thus, we supplement these equations with $\partial_t k_1$ reading

$$\partial_t k_1 = \frac{-\epsilon^4 + 90\epsilon^3 + 2079\epsilon^2 + 12636\epsilon + 26244}{36\pi^2(\epsilon+6)^3}. \tag{12.11}$$

Note how all quantum contributions stem from ϵ and v_0 and f_0 exclusively enter canonically. Of course, $\partial_t \xi = \partial_t k_0 = 0$ yields $\partial_t \epsilon = 0$. Then the three remaining β-functions yield fixed point values for v_0, f_0 and ϵ, which are numerically given by

$$v_0 = 0.00110, \ f_0 = -0.00389, \ \epsilon = 109.97,$$

where we have excluded complex solutions as well as one real solution in the unstable region of $\epsilon \leq -6$. Note how this made the slightly complicated argument used earlier to determine the physical solutions much more concise.
The β-functions just discussed alongside $\partial_t v_1$ and $\partial_t f_1$ are depicted in figure 12.3 as functions of ϵ, showing the simultaneous zero at $\epsilon = 109.97$ as well as the pole at $\epsilon = -6$. We point out that there is no consistent fixed point solution emerging when approaching this pole.

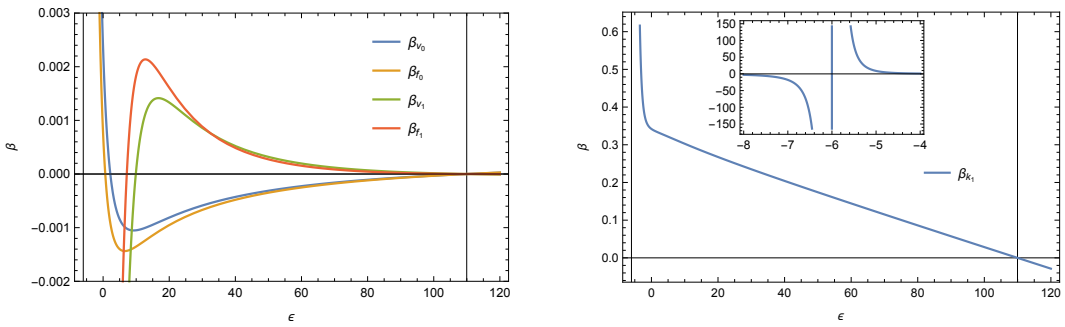

Figure 12.3: β-functions in next to leading order as functions of ϵ and on the fixed point values of the other couplings, showing the simultaneous zero at $\epsilon = 109.97$ as well as the pole at $\epsilon = -6$.

Turning to explicitly investigating the β-functions to order y^{-1}, we find for $\partial_t v_1$

$$\begin{aligned}\xi\partial_t v_1 =& \frac{1}{2592\pi^2(\epsilon+6)^4}(1080 f_0\epsilon^3 - 3240 f_0\epsilon^2 - 62208 f_0\epsilon \\ &+ 1080 k_1\epsilon^2 - 3240 k_1\epsilon - 62208 k_1 + 383 v_0\epsilon^4 \\ &+ 5004 v_0\epsilon^3 + 51120 v_0\epsilon^2 + 278208 v_0\epsilon \\ &+ 382320 v_0) - 6\xi v_1.\end{aligned} \tag{12.12}$$

Note how ξ explicitly enters the flow again, always in combination with v_1. This is also true for f_1 in $\partial_t f_1$. More generally, every factor of v_i or f_i appears with an explicit ξ^i, while every factor of k_i comes with a factor of ξ^{i-1}, apparently rendering the introduction of ϵ pointless. However, this can easily be circumvented by noting that v_i and f_i always multiply y^i, while k_i multiplies y^{i-1}, due to the additional fields in the scalar kinetic term. We conclude that in order to keep the scaling relation intact, every power of y needs to be rescaled by a power of k_0 or, equivalently, ξ. This is, however, exactly what a wave function renormalization does. This is why henceforth we work with the physical solution

$$\eta = 0,\ k_0 = 1 \text{ and } \xi = \frac{k_0}{\epsilon} = 0.00909, \tag{12.13}$$

circumventing the need to rescale fields by hand.

12.2.3 The Role of ξ

We argued earlier that a term ξy should be allowed in our large field expansion 12.4, because it is the scale invariant combination determining the effective strength of

gravity. While this is of course true, there is another reason why only the inclusion of a term of that variety allows for non-trivial solutions: Assume we set $\xi = 0$, and solve the lowest order equations for v_0, f_0 and η.[1] As a next step, we would include corrections of $\mathcal{O}(y^{-1})$, which however, following our earlier discussion, cannot alter the fixed point values at $\mathcal{O}(y^0)$. That is why all corrections are trivial, and the only solution we can obtain with $\xi = 0$ is one completely independent of y. We conclude that the inclusion of ξy in F is necessary to obtain non-trivial solutions.

12.2.4 Remarks on a $\lambda\chi^4$ Term in V

In our large field expansion 12.4 we did not include a term λy^2 in the potential, even though λ has scaling dimension 0 and this term would be allowed by dilatation symmetry. The reason for this is that if one allows for such a term, as well as an additional term $m^2 y$ for reasons of consistency, the flow is governed by the contributions from λy^2, drawing all quantum corrections to 0 in first order, such that the flow is solely driven by the canonical running induced by the scaling dimensions of the couplings. Thus, all β-functions for dilatation symmetric couplings λ, ξ, k_1 are trivially satisfied and yield no conditions, while $m^2 = v_0 = \xi = f_0 = 0$, $v_1, f_1 \propto 1/\lambda$ and K remains completely undetermined. If we do not include $m^2 y$, we find a similar result.
This is in addition to arguments presented in part II already based on positivity of propagators, which are of course still valid.
We conclude that the inclusion of such a term does not yield more physically interesting solutions.

12.3 Global Scaling Solution

In this section, we present our global solution in the context of the current approximation, which is obtained by numerical methods, and discuss its accuracy.

12.3.1 Numerical Solutions

To extend our solution for large y further towards small values of y, we solve the fixed point equations numerically, setting the initial conditions on the Taylor expansion 12.4 with $a = b = c = 5$ in a regime where they are still well behaved.
In figure 12.4 we show the numerical solutions, which resemble global solutions to our fixed point equations. The value of ξ from equation 12.13 is a crucial ingredient, as it allows us to set precise initial conditions.

[1] Note that in this case, the absence of the ξy term in $\partial_t K$ gives a non-vanishing anomalous dimension η.

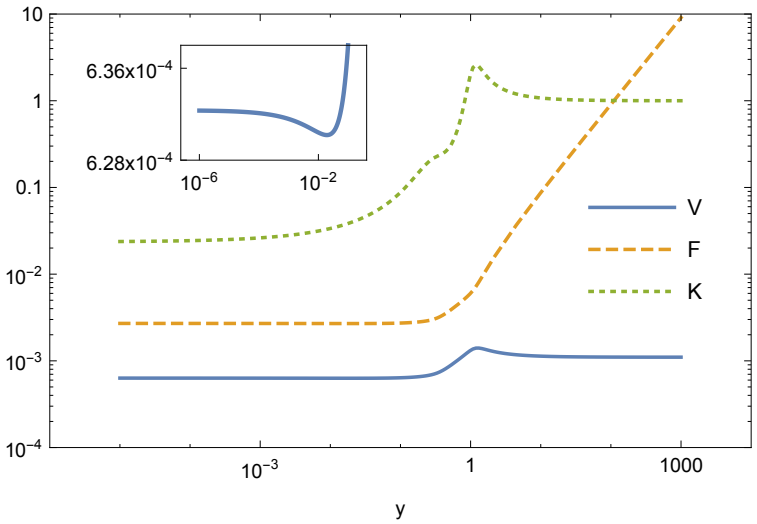

Figure 12.4: Global solutions for the functions $V(y)$, $F(y)$ and $K(y)$ in a double-log plot. The matching with the Taylor expansion was carried out at $y = 10^5$.

Note how there is no point at which $\frac{1}{2}F - V \approx 0$, meaning that the previously bothersome singularity discussed in [91] is not reached by the global scaling solution.

12.3.2 Error Estimates

We also attempt to integrate from a finite y towards ∞ to test agreement with the Taylor approximations. We find excellent agreement for F, while K quickly starts to oscillate around the Taylor approximation and V diverges to either $+\infty$ or $-\infty$, depending on where we define our initial conditions. We suspect numerical instability when integrating towards larger y.
However, when we choose initial conditions at an arbitrary $y = y_0$ and integrate up or down, read off new initial conditions and integrate back down or up, we are able to recover the scaling solution, as long as the interval does not become too large. We thus furthermore speculate that the manifold of solutions is larger locally, but only the scaling solution exists globally. This behavior is demonstrated in figure 12.5 for the potential V and the case when one integrates up first.
Note that in the light of the approximation made in this chapter this means that even though our initial conditions are probably slightly off, we can still be confident that the solution found resembles the main features of the physical solution.
Since it is infeasible to solve the fixed point equations into an explicit form for an error estimate, we instead use the value of the exact β-function normalized by the internal accuracy of the implicit numerical differential equation solver employed, provided by `mathematica`, as an estimate for the error. More precisely, we define the

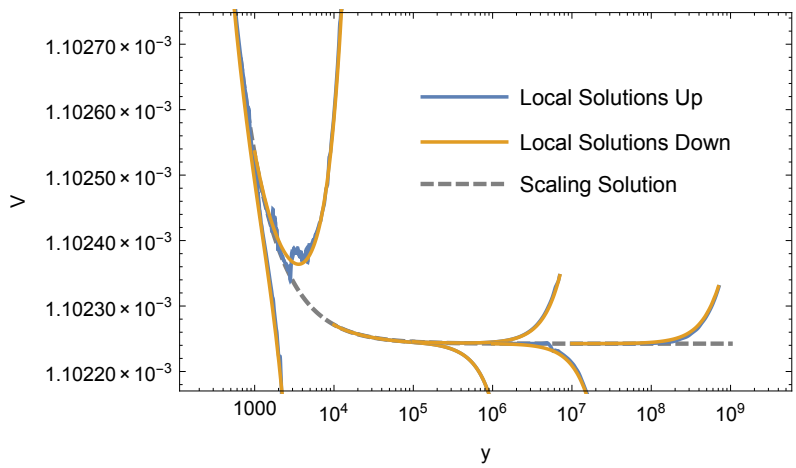

Figure 12.5: Exploration of the manifold of local solutions around $y_0 = 10^2, \ldots, 10^7$.

error for a function $\mathcal{H}(y)$ understood to be an approximate solution to the equation

$$\mathcal{G}(\mathcal{H}, \mathcal{H}', \ldots, y) = 0$$

to be

$$\epsilon_{\mathcal{H}}(y) = \frac{\mathcal{G}(\mathcal{H}, \mathcal{H}', \ldots, y)}{10^{-p}}, \tag{12.14}$$

where p is the number of decimal digits guaranteed to be correct by the numerical routine. In our application, $\mathcal{H} = V, F, K$, and $\mathcal{G} = \beta_{V,F,K}$.
As long as the relative error is of order 1, we can assume the solution to be reliable. As can be understood from figure 12.6, this is the case for most parts of the interval under consideration. The deviations are due to interpolation errors between the grid points of the numerical solution, which are inevitable when plotting and taking derivatives.

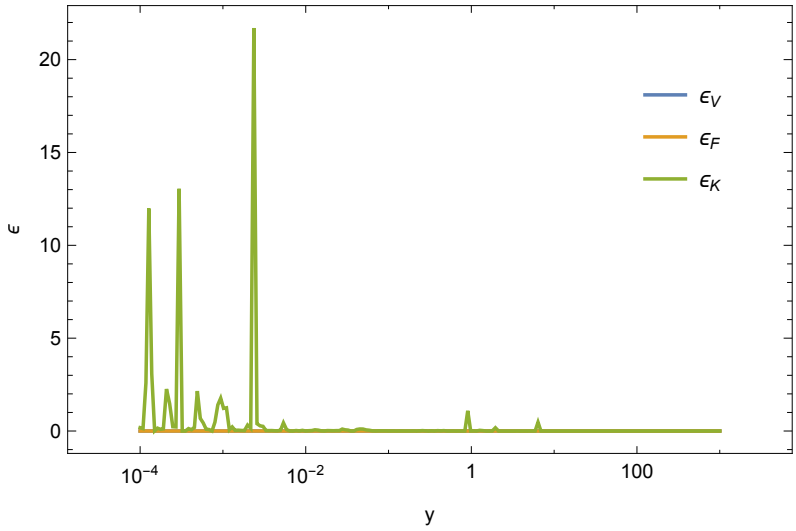

Figure 12.6: Value of the exact β-functions normalized to the accuracy of the numerical solver.

12.4 Small Field Limit

It is impossible to continue the numerical solution all the way until $y = 0$. Therefore, in this section we will present two different approaches to understanding the small field limit of our theory, which, when taken together, complete the global solution presented in section 12.3.

12.4.1 Small Field Expansions

In the spirit of what is presented in section 7.4 for the background field calculations, we attempt to expand the functions V, F and K in positive powers of y, again taking $K(y = 0) = 1$ to allow for the introduction of a scalar anomalous dimension η.

Leading order contributions

Keeping only the lowest order contributions, that is setting V and F equal to a field independent value and also retaining the anomalous dimension η, we find the fixed points reported in table 12.2. In order to keep our presentation concise we have excluded complex solutions already.
Physical fixed points have $V > 0,\ F > 0$, excluding fixed points 1 through 4. Fixed point 3 is also excluded for a different reason: The large positive anomalous dimension is likely to turn off the regulator, as well as to flip the sign of the β-function (appendix

FP	V	F	η
1	-4.6546	-9.9903	$-1.3537 \cdot 10^{-3}$
2	$5.6751 \cdot 10^{-4}$	$-2.7624 \cdot 10^{-3}$	-0.75136
3	$-1.9319 \cdot 10^{-4}$	$-4.3343 \cdot 10^{-4}$	78444.2
4	$-5.8818 \cdot 10^{-5}$	$-2.8737 \cdot 10^{-4}$	-101.18
5	$6.3653 \cdot 10^{-4}$	$6.7691 \cdot 10^{-4}$	-1006.13
6	$1.4444 \cdot 10^{-3}$	$1.7529 \cdot 10^{-3}$	-4354.50
7	$6.4603 \cdot 10^{-4}$	$2.7575 \cdot 10^{-3}$	1.6669

Table 12.2: Fixed point values for the small y expansion to lowest order in y.

C.4 and [87]), such that it is at least doubtful if a physical trajectory could arise from it.
Moreover, even though the large negative anomalous dimenisions of fixed points 5 and 6 are not excluded by any bounds a priori, they would hint to extremely large quantum corrections, which would point to both a fast residual running of Z on the fixed point and a drastic variation of η as y goes from ∞ to 0. The latter argument, being the requirement for a smooth connection of the IR and UV physics, will be substantiated in section 12.4.1.
For there reasons, we call the fixed point at

$$V = 0.0006460,\ F = 0.002757,\ \eta = 1.6669 \tag{12.15}$$

the Einstein-Hilbert limit of our theory. Note that this limit is independent of the approximation made to determine ξ earlier on.
When deriving the flat flow equations, we had neglected RG-time derivatives on the RHS of the flow equation. Comparing to numerical values derived in the symmetric background configuration (7.3), we find qualitative agreement, even though the solutions obtained with the flat expansion are approximately one order of magnitude smaller. Furthermore it is remarkable that the inclusion of an anomalous dimension leads to a significantly larger number of potential fixed points, but only one physical solution prevails.

Past leading order

As discussed in section 7.4 the hierarchy of fixed point equations is not closed order by order when expanding around $y = 0$. That is why solving the coupled system past leading order is extremely challenging, given the size of the algebraic expressions that enter in the flat background calculations.

FP	k_1	k_2	k_3
7.1	-39.5175	2502.6	-135823.0
7.2	-6.9321	77.009	1581.35
7.3	$3.3708 \cdot 10^{-15}$	0	0
7.4	0	0	0

Table 12.3: Splitting up of the fixed point 7 for $c \neq 0$. Note that the vanishing values for k_2 and k_3 in fixed point 7.3 are likely due to numerical effects.

That is why when expanding the functions according to

$$V = \sum_{i=0}^{a} \frac{v_i y^i}{i!},\ F = \sum_{i=0}^{b} \frac{f_i y^i}{i!},\ K = 1 + \sum_{i=1}^{c} \frac{k_i y^i}{i!}, \tag{12.16}$$

and projecting on the respective β-functions for the coefficients by means of expanding the full β-functions, we are to date only able to find solutions for $a = b = 0$, but including powers up to y^3 in K, meaning $c \leq 3$. We find that each fixed point reportet in table 12.2 splits up into $c+1$ fixed points, one of which has $k_i = 0,\ i \geq 1$, confirming the stability of the Einstein-Hilbert solution 12.15. The numerical values for fixed point 7 are reported in table 12.3.

12.4.2 Fits

From section 12.3 we infer that when y approaches zero, the functions become essentially flat. Therefore, it seems possible to fit their form with a simple ansatz, understanding the small y behavior even better. We emphasize that no input from section 12.4.1 is used unless explicitly state otherwise. We employ optimized fit routines provided by `mathematica`.

Fixing the ansatz

In order to derive an appropriate ansatz, we investigate all three functions and, more specifically, their derivatives for small values of y more closely. In figure 12.7 we show the three coupling functions alongside their first two derivatives, showcasing the divergence of the derivatives for $y \to 0$. In contrast to that, the functions themselves stay finite. This is exactly the behavior exhibited by a monomial

$$\sim y^\alpha \text{ with } 0 < \alpha < 1.$$

We also allow for another constant to be added. Indeed, the first derivative of all three functions diverge linearly in the double logarithmic plots, meaning their divergence is likely to be governed by a simple monomial. The dashed lines in the plots represent

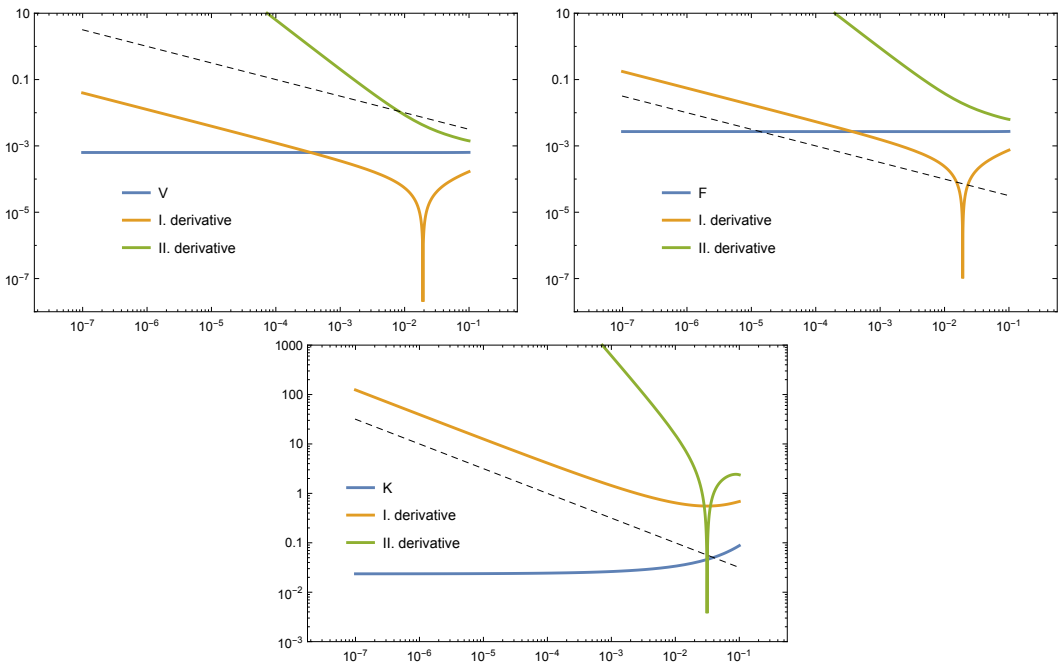

Figure 12.7: Functions V, F and K as well as their first two derivatives for $10^{-7} \leq y \leq 10^{-1}$ in double logarithmic plot, showcasing the divergence of the derivatives for $y \to 0$. The dashed lines are proportional to $y^{-\frac{1}{2}}$.

monomials $y^{-\frac{1}{2}}$, and we conclude from the fact that those lines seem to be almost parallel to the first derivatives of the functions that $\alpha = -\frac{1}{2}$ is a good ansatz for the exponent, leaving us to fix the exact form through fit routines.
Since we are ultimately interested in the functions themselves rather than in their derivatives, we point out that for $\mathcal{H}' \sim y^{-1/2} + const.$ we have $\mathcal{H} \sim y + y^{1/2} + const$, leading to the general ansatz

$$V = v_0 + v_{1/2} y^{1/2} + v_1 y, \quad F = f_0 + f_{1/2} y^{1/2} + f_1 y, \quad K = k_0 + k_{1/2} y^{1/2} + k_1 y. \tag{12.17}$$

We take approximately $n \sim 10^6$ data points in the range $10^{-7} \leq y \leq 10^{-5}$ to generate input for the fit routines in the form or pairs $(y, V(y))$, $(y, F(y))$, $(y, K(y))$, where the values are taken on the numerical solutions derived in the previous chapter. The range is chosen in such a way that y is small enough so we can expect only a few leading order contributions to contribute, yet large enough so the numerical solutions are still accurate.
Starting from the ansatz 12.17, we also present various extensions. Similar to the error definition in section 12.3.2 we use the values of the exact β-functions as error estimates for our solution. However, unlike previously we do not normalize them to

	$y^{-1/2}$	1	$y^{1/2}$	y	$y^{3/2}$
			V		
a	–	$6.3233 \cdot 10^{-4}$	$-2.5068 \cdot 10^{-5}$	$3.4680 \cdot 10^{-5}$	–
b	–	$6.4604 \cdot 10^{-4}$	$-1.4361 \cdot 10^{-2}$	3.3859	–
c	–	$6.3234 \cdot 10^{-4}$	$-2.5066 \cdot 10^{-5}$	$3.3543 \cdot 10^{-5}$	$2.0266 \cdot 10^{-4}$
d	$-6.2068 \cdot 10^{-16}$	$6.3234 \cdot 10^{-4}$	$-2.5069 \cdot 10^{-5}$	$3.4876 \cdot 10^{-5}$	–
			F		
a	–	$2.7026 \cdot 10^{-3}$	$-1.1056 \cdot 10^{-4}$	$1.5034 \cdot 10^{-4}$	–
b	–	$2.7575 \cdot 10^{-3}$	$-5.7426 \cdot 10^{-2}$	13.537	–
c	–	$2.7027 \cdot 10^{-3}$	$-1.1054 \cdot 10^{-4}$	$1.4529 \cdot 10^{-4}$	$9.0227 \cdot 10^{-4}$
d	$2.7634 \cdot 10^{-15}$	$2.7026 \cdot 10^{-3}$	$-1.1055 \cdot 10^{-4}$	$1.5122 \cdot 10^{-4}$	–
			K		
a	–	$2.3540 \cdot 10^{-2}$	$7.8323 \cdot 10^{-2}$	0.1854	–
b	–	$2.3540 \cdot 10^{-2}$	$7.8323 \cdot 10^{-2}$	0.1854	–
c	–	$2.3540 \cdot 10^{-2}$	$7.8323 \cdot 10^{-2}$	0.1858	0.3602
d	$-1.1035 \cdot 10^{-12}$	$2.3540 \cdot 10^{-2}$	$7.8323 \cdot 10^{-2}$	0.1858	–

Table 12.4: Fit parameters for the small y fits.

the precision of the routines used, as at this point both the precision of the numerical solver as well as the precision of the plot functions enter, limiting the amount of information to be gathered from such a normalization.

Results

Numerical results for four different variants are listed in table 12.4. These are:

a Three parameter fits

b Three parameter fits with v_0 and f_0 taken from the Einstein-Hilbert solution 12.15

c Four parameter fits, including $y^{3/2}$

d Four parameter fits, including $y^{-1/2}$

In addition to the values presented, we enlarged the working precision of the numerical input as well as the fit routines, upgraded our calculation to $n \sim 10^8$ data points and varied the interval that data is generated from. However, we could not see significant improvements in the quality of the fits.
The error estimates for the four variants are shown in figure 12.8, where the tail on the right hand side stems from the numerical solution. While we find the fits to

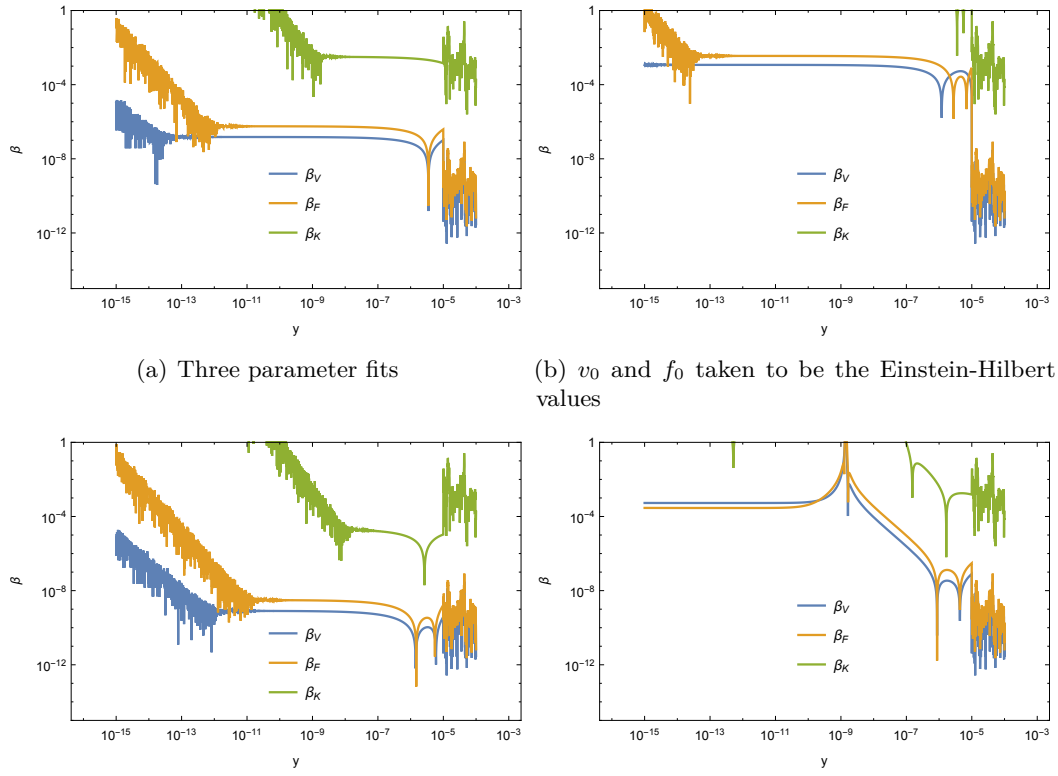

(a) Three parameter fits

(b) v_0 and f_0 taken to be the Einstein-Hilbert values

(c) Four parameter fits, including $y^{\frac{3}{2}}$

(d) Four parameter fits, including $y^{-\frac{1}{2}}$

Figure 12.8: Plots of the error estimates for the fits for small y in variations a-d.

be a reasonable solution up until some y_0, which depends on the specific setup, we also point out that for very small y our routines are not able to properly calculate values for the β-functions anymore, such that numerical noise becomes visible again. Furthermore, the slope of these functions suggest that for even smaller values of y, there may be additional terms proportional to y^α, $\alpha < \frac{1}{2}$ present. However, since it seems far fetched to generate data from ranges of even smaller y for such a fit, we do not investigate this possibility any further here.

Discussion

Starting with variant a, we find excellent numerical agreement with the small y expansion solution that we favoured for physical reasons already in section 12.4.1. This agreement is another reason why we call the solution 12.15 the Einstein-Hilbert solution and assume it to be the ultraviolet limit of dilaton quantum gravity.
In this spirit we attempt to improve the fits by setting the lowest order parameters v_0

and f_0 to their exact respective Einstein-Hilbert values, which constitutes variant b. From figure 12.8 we infer that this does lead to numerical noise taking over somewhat later, however, the overall quality of the solution is not improved. This is due to the fact that for small y, the Taylor expanded system is not closed order by order, thus higher order corrections will slightly alter the values of the Einstein-Hilbert limit.
Note how the fitted k_0 is not equal to 1 in any of the cases considered. This is due to the scalar wave function renormalization Z, which is not trivial in the ultraviolet limit, in agreement with $\eta \neq 0$, and in contrast to the infrared limit discussed in section 12.2, as well as due to the approximation made in this section. We will revisit this point in the next chapter.
From the numerical values for variant c we conclude that there does not seem to be a term proportional to a negative power of y present in any of the functions, meaning that the Einstein-Hilbert solution indeed is the limit we are aiming to find. We expect terms proportional to $y^{\frac{3}{2}}$ to be present as confirmed by variant d. However, they only become relevant once our numerical solutions are an accurate solution to the fixed point equations again, and are thus not relevant for us here.
These results suggest that if one attempts to do a Taylor expansion around $y = 0$ discussed in section, it should be carried out in $\sqrt{y}$ rather than in y as discussed in section 12.4.1. However, the technical difficulties discussed above still remain, such that we will not pursue this path any further in this chapter.
We point out that even though the Einstein-Hilbert limit is independent of the approximation made in this chapter, the numerically determined solutions for V and F show excellent agreement with this limit, furthering our statement that the approximation produces physically meaningful results. Due to the anomalous dimensions, such a statement cannot be made for K, as we simply cannot infer the correct limit at this point. We will comment more on that later, when we present the corresponding analysis for the full set of equations.

CHAPTER 13

Results III: Full Vertex Expanded Version

In this chapter, we present and discuss the final result of this thesis: A global scaling solution to the full set of flow equations (12.2) stemming from the action (12.1), without the approximation (12.3), as well as its physical consequences.
As discussed in the previous chapter, many physical features will remain the same. The most disruptive change in the process of determining the scaling solution will be that ξ, determined by equation (12.7) in our previous treatment, will become a free parameter again. However, it turns out that realistic physical solutions can best be found in the close vicinity of the value of ξ singled out by equation (12.7). We will call this value ξ_0, and the corresponding value of ϵ will be denoted by ϵ_0.
Deriving a solution for large y again first, we will refine and substantiate the analysis presented in section 12.2.2, in the process eliminating one redundant parameter from the system to all orders by means of a redefined field and set of couplings.
After that, we will present our global scaling solution obtained by numerical procedures as before, and lay emphasis on comparing it with the old solution as well as on physical consequences for the spontaneous generation of the Planck scale as well as cosmological models in sections 13.4 and 13.5.
Throughout this chapter, we will focus on what substantially changes when abandoning the approximation and will thus not rederive all results or restate all equations.

13.1 Large Field Scalings

Not neglecting the term $2yK'$ in $\partial_t K$ and redoing the analysis from section 12.2, equation (12.6) picks up an extra term $-2k_1$, now reading

$$\begin{aligned} 0 = &- k_1\eta - 2k_1 + 2y\frac{\eta\left(-1296\xi^4 + 108\xi^2 + 12\xi + 1\right)}{576\pi\xi(1+6\xi)^3} \\ &+ \frac{\left(26244\xi^4 + 12636\xi^3 + 2079\xi^2 + 90\xi - 1\right)}{36\pi^2\xi(6\xi+1)^3}. \end{aligned} \tag{13.1}$$

Even though $\eta = 0$ remains true for $y_0 = \infty$, the extra term spoils our equation (12.7) to determine ξ, such that now ξ is a free parameter in the system, much like in part II. However, in part II, we had no approximation that told us which values of ξ might be suitable for finding a global scaling solution, which will be of paramount importance throughout the rest of this chapter.
Given that ξ will now explicitly enter all equations, extracting the physical scaling like we already started to do in section 12.2.2 when classifying the solutions becomes even more important. The previous treatment ended with the result that past leading order, one needs to put a bit more effort into redefining variables and couplings to make the all equations depend on

$$\epsilon = \frac{k_0}{\xi}$$

only. This is exactly what we will do here.
Of course we have the wave function renormalization for the scalar at our disposal and could thus use it to implicitly carry out the rescalings. However, as argued in the introductory remarks to section 7.8, negative values for K are physically viable, and we are thus seeking a formulation where this becomes manifest.
To that end, we modify the large field expansion (12.4), already setting $\lambda = m^2 = 0$ by redefining the couplings to now read

$$V = \sum_{i=0}^{a} \frac{v_i}{\xi^i i!} y^{-i},\ F = \xi y + \sum_{i=0}^{b} \frac{f_i}{\xi^i i!} y^{-i},\ K = k_0 + \sum_{i=1}^{c} \frac{k_i}{\xi^{i-1} i!} y^{-i}. \tag{13.2}$$

After plugging these expansions into the flow equation we replace $k_0 = \xi\epsilon$, after which every power of y is accompanied by the respective power of ξ. Thus, redefining $y \to \xi y$ makes our system completely independent of ξ and k_0 to all orders, and the free parameter is henceforth ϵ. Translated to the context of explicit wave function remormalization, this amounts to dividing the lingering $Z \sim \epsilon$ dependence from the variable y, to be able to study the scaling separately and consistently. Note that

global rescalings of fields only later the path integral by a constant and are thus allowed.
Henceforth, unless explicitly stated otherwise, y will denote the rescaled field. Note that since $\xi_0 \approx 10^{-2}$, the old and rescaled fields differ approximately by a factor of 10^2 if we evaluate our equations at $\xi = \xi_0$. This of course corresponds to $\epsilon_0 \approx 10^2$.
There is one more subtlety when using ξ instead of Z to rescale fields: since $K(y)$ enters the action together with two powers of the scalar field χ, we need to put in the additional rescalings by hand. This is done in equation (13.2) by means of rescaling the couplings differently, as well as by at the end dividing $\partial_t K$ by a factor of ξ to account for the additional scaling stemming from the scalar kinetic term. We then obtain $K(y \to \infty) = \epsilon$, contrary to $K(y \to \infty) = 1$ if using the wave function renormalization Z.
Exactly like before, we derive β-functions for the redefined couplings and solve them, to obtain an expansion for large y.

13.2 Global Scaling Solution

We are now ready to present the scaling solution obtained by the exact same numerical procedure as in chapter 12 and at $\epsilon = \epsilon_0$, picking initial conditions on the large field expansions. It is depicted in figure 13.1, and is the starting point for all future investigations in this chapter. Note how due to the rescaling, the intermediate range is shifted to $y \sim 10^{-2}$.

13.2.1 Comparison to the Approximated Scaling Solution

Our first step in the analysis is to compare the newly obtained solutions to the ones obtained in chapter 12. We show both in figure 13.2, where we voided the rescaling procedure presented in the previous section to allow for easier comparison.
It is evident that V and F change only slightly in the intermediate region, where also derivatives of K enter the flow equations, while K remains the same for large y thus a posteriori justifying the application made, but assumes a numerically different limit for $y \to 0$. Note that we could not have possibly have seen that when comparing to the Einstein-Hilbert limit in section 12.4, as the anomalous dimension η is nontrivial in this limit.
We emphasize that the physically relevant minimum in the potential V is still present (see inset of figure 13.1), and the singularity in the graviton propagator at $\frac{1}{2}F - V = 0$ that caused much trouble in earlier investigations [91] is not hit.

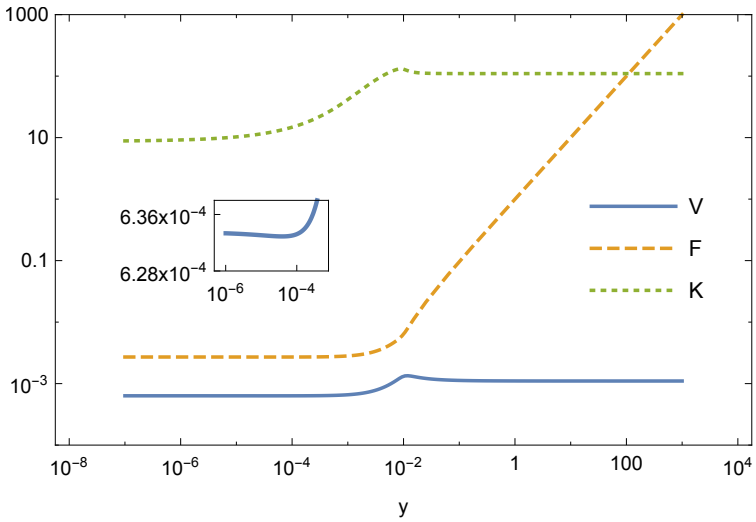

Figure 13.1: Full solutions to the fixed point equations when starting at the initial conditions defined by the large field expansions and $\epsilon = \epsilon_0$ as determined in chapter 12 at $y = 10^3$.

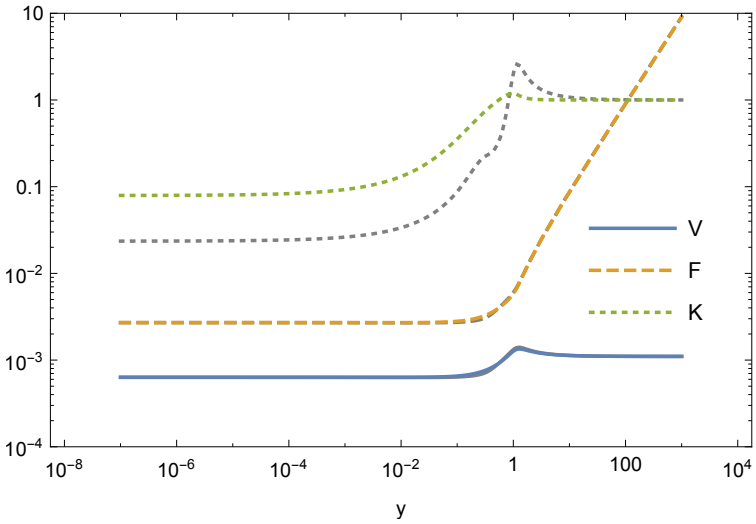

Figure 13.2: Approximated (gray) and full (colored) solutions to the fixed point equations, when starting at the equivalent initial conditions defined by ϵ_0.

13.2.2 ϵ Dependence

We study the scaling solutions for different values of ϵ. It turns out that it is not possible to obtain a solution numerically for arbitrary values of ϵ. This was tested by attempting to solve the system for a large number of different numerical values $-6 < \epsilon \leq 10^5$. In fact, solutions could only be obtained in the vicinity of ϵ_0, more specifically for

$$\epsilon \in \{79.43,\ 100,\ 125.89,\ 158.49,\ 199.53,\ 316.23\}\,. \tag{13.3}$$

We emphasize that there are most likely more solutions in the vicinity of ϵ_0 and that we are of course unable to exclude the possibility of more solutions in a different regime by means of this procedure, for there might always be a different way to solve the system numerically, or of course even some kind of analytic procedure. Despite that, we observe that the numerical routine systematically breaks down earlier and earlier when deviating from ϵ_0, until we are not able to initiate it at all in the vicinity of $\epsilon = -6$.
The aforementioned observation is curious. Note that due to equation (13.1), $\epsilon = \epsilon_0 \Leftrightarrow \xi = \xi_0$ yields $k_1 = 0$, making K field independent to leading order for large y. This seems to be favored by the system, and we will investigate it in greater detail later.
In figure 13.3, we depict the solutions for the 6 values of ϵ given in equation (13.3) in the original and a rescaled version $K \to \epsilon^{-1}K$. Note that the location of the intermediate regime does not change visibly, and V and F are independent of ϵ to good accuracy. Regarding K, while ϵ rescales the large field limit, it seems to become less and less relevant for smaller fields. However, with the current methods we do not find ϵ to become completely irrelevant in K for $y \to 0$. At this point, we cannot decide if this is rooted in technical inaccuracies or physically relevant. As argued in section 3.1.1, at this stage the system still has a physical redundancy. That is why we defer any further discussion of the dependency on the parameter ϵ until after section, 13.4 where we will present conformal invariants as well as the normal form of the theory on the scaling solution.

13.2.3 Error Estimates

We use the error definition from equation (12.14) and find what is shown in figure 13.4. Note that in comparison to previous studies, the current error plot was obtained using a much larger working precision due to the current system being numerically more challenging, and thus shows much more noise. Despite that, we again find that β_K is the most sensitive β-function, but still remains well behaved even after the intermediate region around $y = 10^{-2}$. The fact that the error becomes smaller again

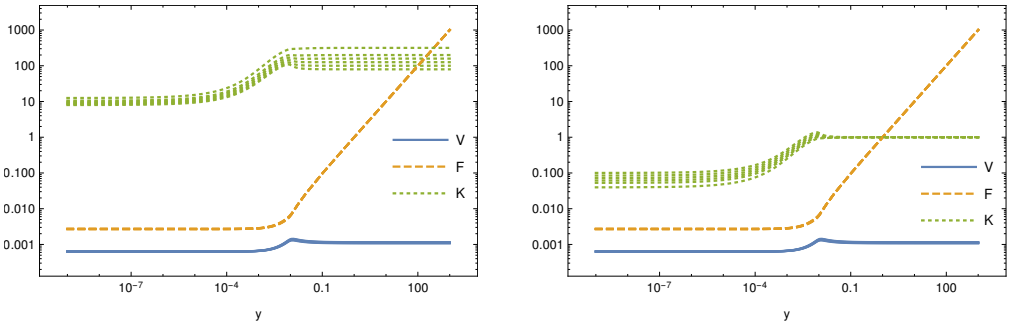

Figure 13.3: Functions V, F and K for $\epsilon \in \{79.43, 100, 125.89, 158, 49, 199.53, 316.228\}$ (LHS), alongside with a version where $K \to \epsilon^{-1}K$ (RHS).

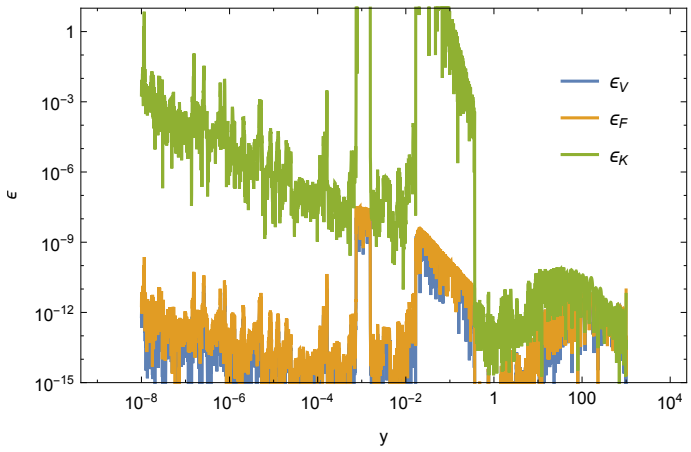

Figure 13.4: Value of the exact β-functions normalized to the accuracy of the numerical solver.

after it spiked suggests that the solver is able to stabilize the system, and we can thus trust the solutions obtained.

Now that we have the full β-functions at our disposal, it is also insightful to study the approximated solution from chapter 12 on the full β-functions. Results are depicted in figure 13.5, where the left panel shows the regime of large y, where a Taylor expansion was performed, while the right panel uses the numerical solution in the intermediate range and the fits for small y.

Just like one would expect, the error ϵ_K is the first one to become large, signalling the breakdown of our approximation. Since β_F dominates the system for $y \to \infty$ due to the divergent $2yF'$ term and ξ is inaccurate in approximation, ϵ_F ultimately diverges. Just like V and F change very little when lifting the approximation, ϵ_V and ϵ_F are also well behaved, while ϵ_K grows large.

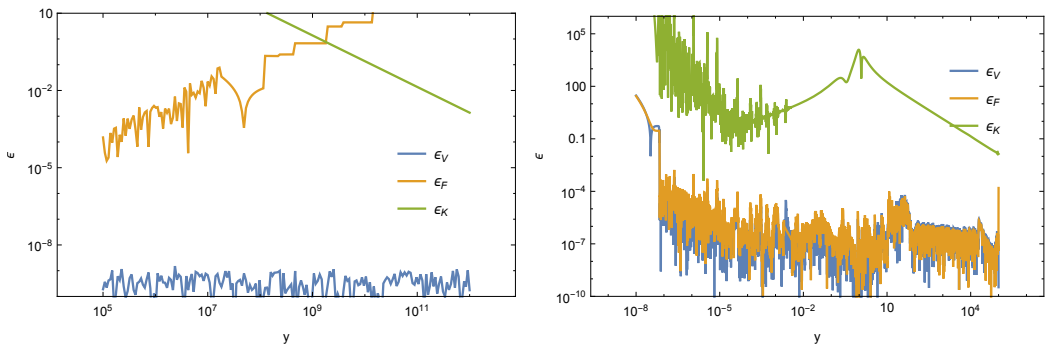

Figure 13.5: Value of the full β-functions on the approximated solutions for large field Taylor (LHS) and fitted approximations (RHS).

13.3 Extending to $y \to 0$

While we have carried out the calculations presented here for all values of ϵ for which solutions were found, we only present the results for $\epsilon = \epsilon_0$, since ϵ seems to become less and less relevant for small fields. To substantiate this statement, we report that while the difference between the smallest and largest possible value for ϵ from equation (13.3) is of the order of 300%, the limits of K for small fields differ by only about 50%.
We present two ways of continuing our numerical solutions towards smaller values of y: Fits as well as numerical searches in expansion in $\sqrt{y}$.

13.3.1 Fits

Drawing from our insights presented in section 12.4.2, we first attempt to continue our solution further towards $y = 0$ by means of fits, sparked by the discovery that all first derivatives diverge with $y^{-1/2}$. The procedure goes through exactly as beforehand, but we find that the inclusion of a term proportional to $y^{3/2}$ is crucial to obtain satisfactory results. This is due to the fact that the variable transformation presented in section 13.1 trigger higher order terms to become important earlier.
We find as the best fits

$$\begin{aligned} V(y) &= 6.3350 \cdot 10^{-4} - 1.7137 \cdot 10^{-4}\, y^{1/2} + 8.3172 \cdot 10^{-3}\, y + 0.5626\, y^{3/2}, \\ F(y) &= 2.7077 \cdot 10^{-3} - 3.7688 \cdot 10^{-4}\, y^{1/2} + 3.6550 \cdot 10^{-3}\, y + 2.4944\, y^{3/2}, \\ K(y) &= 8.7018 + 455.269\, y^{1/2} + 12940.3\, y + 223285\, y^{3/2}. \end{aligned} \tag{13.4}$$

The values of the β functions on the best fit are depicted in figure 13.6. It is well conceivable that the errors could be improved by adding more powers of $y^{1/2}$. However, since we are only interested in the general behavior of our solution for

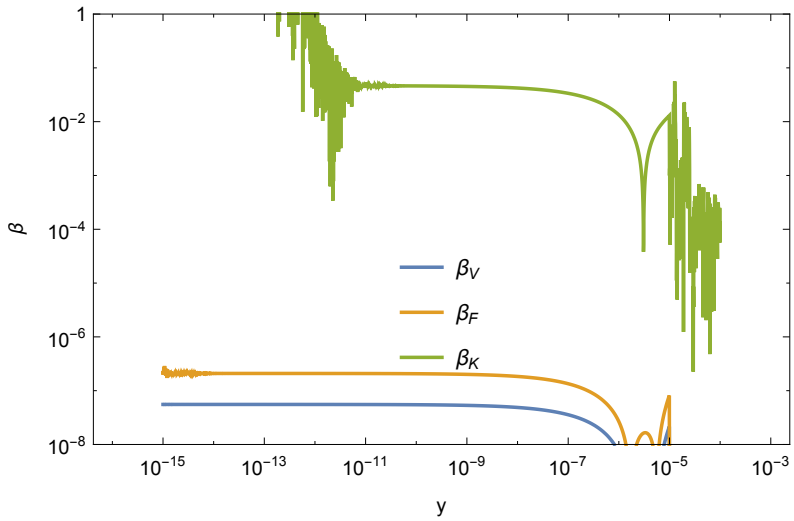

Figure 13.6: Value of the β-function on the small y fits.

small y, and since we see numerics break down at some point anyway, we will not pursue this path any further.
We emphasize again that the values obtained for the Einstein-Hilbert limit, equation (12.15) remain accurate even after the approximation is lifted. Comparing the limits of $y \to 0$ with the Einstein-Hilbert limit, we again find excellent agreement. Also note however that the slight differences between the limits of the fits and the numerical values of the Einstein-Hilbert limit only decreased marginally by considering the full β functions.
What is more, the $y^{3/2}$ contributions are comparatively large, especially in K. We take that as a hint that our definition of a wave function renormalization at one scale set by y_0 is not sufficient to capture all physical features.

13.3.2 Numerical Searches

To further understand the aforementioned difference, we move on to seeking a small y expansion by means of numerically converging to solutions from given initial guesses. This was done for a large number of initial values. To order $\sqrt{y}$,

$$V = v_0 + v_{1/2}\sqrt{y},\ F = f_0 + f_{1/2}\sqrt{y},\ K = 1 + k_{1/2}\sqrt{y}$$

we find 4 distinct solutions which are presented in table 13.1.
The first crucial observation is that pure Einstein-Hilbert, where all nontrivial orders in y are simply zero, is a viable, yet hardly intriguing possibility even for finite y (FP 1). Furthermore, it is consistent to only allow for nontrivial y dependencies in

FP	v_0	$v_{1/2}$	η
1	$6.4604 \cdot 10^{-4}$	0	1.6669
2	$6.4604 \cdot 10^{-4}$	0	1.6669
3	$6.7120 \cdot 10^{-4}$	$-3.2918 \cdot 10^{-3}$	5.3724
4	$6.7476 \cdot 10^{-7}$	$1.2541 \cdot 10^{-4}$	−72.590
	f_0	$f_{1/2}$	$k_{1/2}$
1	$2.7575 \cdot 10^{-3}$	0	0
2	$2.7575 \cdot 10^{-3}$	0	−3.0926
3	$2.8576 \cdot 10^{-3}$	$-3.0269 \cdot 10^{-3}$	−6672.85
4	$3.4630 \cdot 10^{-6}$	$6.2473 \cdot 10^{-4}$	111.06

Table 13.1: Numerical expansion parameters around $y = 0$ in powers of $\sqrt{y}$.

K, while V and F remain constant (FP 2). This changes the scaling of the fields, and we will comment more on the role of K and possible rescalings and anomalous dimensions for finite y in section 13.5.

While especially fixed point 3 appears interesting, as it allows for field dependencies in all functions while still having a small field limit close to the Einstein-Hilbert values, $\eta > 2$ is beyond the bond for an anomalous dimension that we can resolve with our current regulator setup (see appendix C.4.2), and fixed point 4 suggests a scaling of the scalar that can hardly be considered physically viable.

Despite these pessimistic results, it is both possible that there are fixed point solutions that we did not capture with our current procedure, or that for instance the anomalous dimension of FP 3 is pushed back below the bound by the next order in $\sqrt{y}$, and that also the values of the limit for $y \to 0$ are changed, potentially alongside the value for $k_{1/2}$, which strongly disagrees with our fitted results. This may be due to the fact that we are not yet resolving the anomalous dimension for $y \neq y_0$ and thus are potentially requiring fixed points where in fact physically there is a residual running of the wave function renormalization. We refer to section 13.5 for a more detailed account.

Moreover, we explicitly checked that the β-functions depend on the expansion parameters of the function to order $\sqrt{y}$ to order y^0 already, thus making it likely for the Einstein-Hilbert limit to be slightly changed in the presence of nontrivial $\sqrt{y}$ terms. This would mean that there is no smooth connection between the global field independent and the field dependent solutions.

We thus conclude that the small field limit remains challenging to resolve, but we are confident that our global scaling solution has a limit closely related to the Einstein-Hilbert solution for small fields.

We also point out that drawing from insights gained in section 12.4.1 it seems reasonable to believe that more classes of solutions indeed do exist.

13.4 Physical Models

Inspired by the discussion in section 3.1.1 we compute and present both the conformal invariants $\hat{V}$ and $\hat{K}$, equation (3.8), as well as the potential for the standard form (3.9) $\hat{V}_{\text{norm}}$. This section serves to state the results, while they are discussed in section 13.5.

13.4.1 Conformal Invariants

The physical content of a model is specified by the two invariants $\hat{V}$ and $\hat{K}$. In figure 13.7 we show these invariants for different values of ϵ. The numerical invariants obey

$$\lim_{y\to\infty} \hat{V} = 0, \ \lim_{y\to\infty} \hat{K} = 0, \tag{13.5}$$

as can be easily inferred from their definition and the form of the functions V, F and K for large y: As both V and K go to a constant for $y \to \infty$, while F grows with ξy, we can immediately understand that the ratios V/F^2 and K/F vanish in this limit. Furthermore, we have $y(F')^2/F^2 = 1/y$, such that the claim becomes clear. The maximum in the function $\hat{V}$ is located at

$$y_{\max} = 3.8362 \cdot 10^{-5}, \ \hat{V}(y_{\max}) = 86.494, \tag{13.6}$$

whereas $\hat{K}$ has its maximum at

$$y_{\max} = 4.9878 \cdot 10^{-3}, \ \hat{K}(y_{\max}) = 27854.8.$$

We find that $\hat{V}$ is essentially independent of ϵ as is clear from its definition, while ϵ rescales K but leaves the position of the maximum unaltered. Further note that while the limit $y \to 0$ may very well remain ϵ dependent, the limit for $y \to \infty$ must be independent of ϵ. This is encouraging, as $y \to \infty$ corresponds to infrared physics observable today.

13.4.2 Einstein Frame and Standard Form

We are interested in transforming the physical model defined by the conformal invariants $\hat{V}$ and $\hat{F}$ into its standard form in the Einstein frame (3.9). In order to do so, two steps are necessary: We first need to define $F(\chi^2)$, thereby picking a physical reference frame, and then will rescale our scalar field in such a way that the kinetic term also assumes its standard form. The first step is simple - for the Einstein frame we have $F(\chi^2) = M^2$, and we now deal with a field φ as described in section 3.1.1. The second steps needs a bit more careful work.

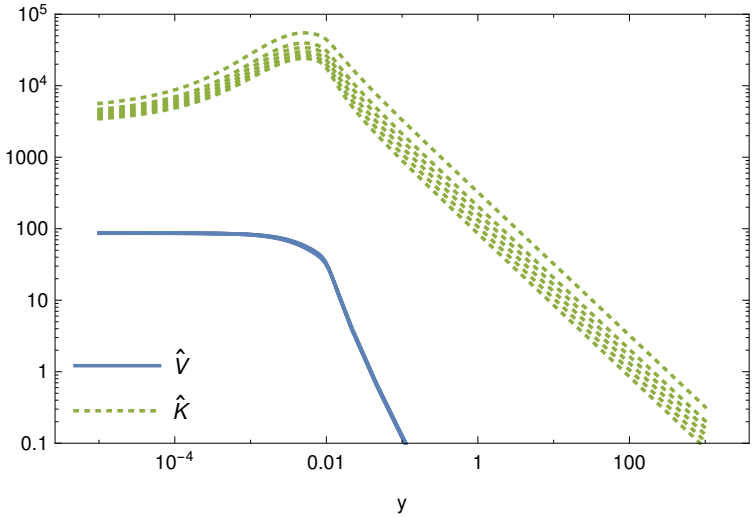

Figure 13.7: Invariants $\hat{V}$ and $\hat{K}$ for different values of ϵ around ϵ_0.

Coming from a kinetic term $\frac{1}{2}\hat{K}(\varphi^2)\partial_\mu\varphi\partial^\mu\varphi$, we need to define a field ϕ, such that

$$\frac{1}{2}\hat{K}(\varphi^2)\partial_\mu\varphi\partial^\nu\varphi = \partial_\mu\phi\partial^\nu\phi, \tag{13.7}$$

meaning we need to loosely speaking wrap $\int\sqrt{\hat{K}(\varphi^2)}\,\mathrm{d}\varphi$ into the new field. More precisely, we can rewrite the LHS of the condition (13.7) to read

$$\frac{1}{2}\hat{K}(\varphi^2)\partial_\mu\varphi\partial^\nu\varphi = \frac{1}{2}\hat{K}(\varphi^2)\left(\frac{\mathrm{d}\varphi}{\mathrm{d}\phi}\right)^2\partial_\mu\phi\partial^\nu\phi \Rightarrow \hat{K}(\varphi^2)\left(\frac{\mathrm{d}\varphi}{\mathrm{d}\phi}\right)^2 = 1.$$

To compute the field transformation, we then define $x = \sqrt{y}$, where here $y = \varphi^2/k^2$, and transform the dimensionless function $\hat{K}(y)$ to $\hat{K}(x)$, after which we compute

$$\tilde{x}(x) = \tilde{x}(x_0) + \int_{x_0}^{x}\sqrt{\hat{K}(\bar{x})}\,\mathrm{d}\bar{x}.$$

However, since the function $\hat{K}(x)$ is only known numerically, there is no direct way to computer this expression. Therefore, we pick an x_0 low enough to capture all interesting features and large enough to be able to still rely on the accuracy of the function $\hat{K}(x)$ in the vicinity of x_0. The results presented here were obtained with $x_0^2 = y_0 = 10^{-6}$. After that, we pick 10^3 logarithmically spread points in the y-interval $\left[10^{-6}, 10^2\right]$, numerically compute the integral for each one, and obtain $\tilde{x}(x)$ by means of interpolating.

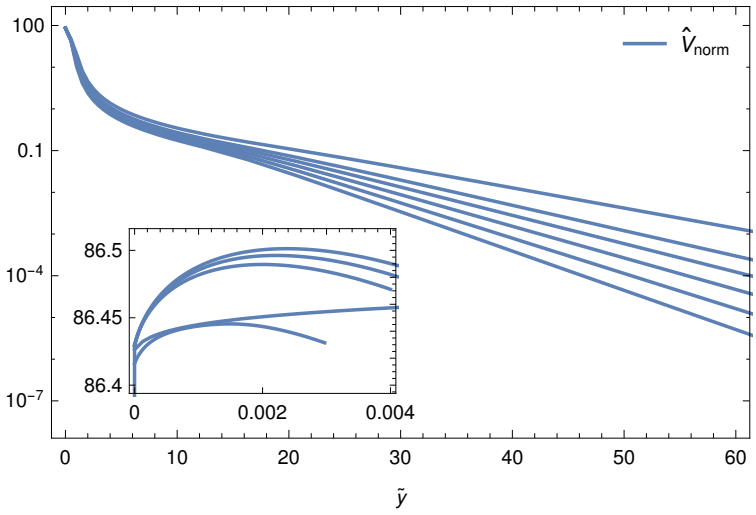

Figure 13.8: Potential for the standard form for inflation $\hat{V}_{\text{norm}}$ for different values of ϵ around ϵ_0. Note the maximum for small $\tilde{y}$ as well as the exponential tail for large $\tilde{y}$.

The last step left to complete is to evaluate $\hat{V}$ on the new field variable, for which we have to invert $\tilde{x}(x)$ to $x(\tilde{x})$. The result, to be interpreted as $\hat{V}_{\text{norm}}(\tilde{y})$ in the Einstein frame with $\tilde{y} = \tilde{x}^2 = \frac{\phi^2}{k^2}$ is shown in figure 13.8 for different values of ϵ. The subscript "norm" signals, that this is the potential that enters into the form (3.9).
$\hat{V}_{\text{norm}}$ assumes a maximum at

$$y_{\max} = 3.1628 \cdot 10^{-3}, \ \hat{V}_{\text{norm}}(y_{\max}) = 86.4937.$$

We once again study the ϵ dependency of the solution. Since $\hat{V}_{\text{norm}}$ now captures the whole system in just one function, the ϵ dependency becomes visible in the potential and cannot be absorbed any further. Since we lack an analytic expression for $\hat{V}_{\text{norm}}$, we are unable to comment on limiting cases, but assume that the potential approaches 0 for large fields $\tilde{y}$, which would then be ϵ independent again. The exponential form is visible for $y \gtrsim 10$.
It is instructive to study the position and the values of the maxima as a function of ϵ. We present them in table 13.2. Note that while the value of the standardized potential is rather stable, $y_{\max}$ changes considerably, and even becomes negative, signaling a breakdown of our numerical routine. Nevertheless, it appears that for $\epsilon \lesssim \epsilon_0 \sim 109$, the results agree much better. This can readily be interpreted by reconsidering equation (13.1) rewritten in terms of ϵ, which is equation (12.11) with an additional $-2k_1$ added. From there (also see the right panel of figure 12.3) it becomes clear that $\epsilon < \epsilon_0$ yields $k_1 > 0$, and since $K' \sim -k_1 y^{-2}$ to leading order, we

ϵ	$\hat{V}_{\text{norm}}(\tilde{y}_{\max})$	$\tilde{y}_{\max}$ $[10^{-3}]$
79.43	86.501	2.381
100.00	86.496	2.211
125.89	86.490	2.000
158.49	86.481	−84.22
199.53	86.471	12.69
316.23	86.445	1.485

Table 13.2: Position and value of the maxima of $\hat{V}_{\text{norm}}$ for different values of ϵ.

have for large y

$$\epsilon < \epsilon_0 \Rightarrow K' < 0.$$

It seems natural that this favored by the system, as $K' > 0$ would require an additional minimum in K, which may change physics. We thus conclude that the most reliable choices for ϵ are $\epsilon \lesssim \epsilon_0$.

13.5 Discussion and Conclusions

Based on the results of this chapter, we discuss physical consequences regarding the dependence on the parameter ϵ, Planck scale generation as well as cosmology and inflation.

13.5.1 ϵ Dependency

Up until now one may have hoped that the ϵ dependency observed was just owed to the fact that we used more functions than necessary to describe our system, and that the potential for the standard form $\hat{V}_{\text{norm}}$ would have turned out to be independent of the parameter. However, this is clearly not the case.
Nevertheless, in the context of dilaton gravity, we would ultimately expect a distinct solution given that there is only one physical Planck mass and scale of gravity.
However, after the results of the previous sections it is well conceivable that our formulation does not yet capture all physical features of the full theory, which leads to the unsettling dependence on the parameter ϵ. Looking back at figure 13.7 we see that the potential $\hat{V}$ is largely ϵ independent, and the ϵ dependence in $\hat{V}_{\text{norm}}$ thus stems from $\hat{K}$. The latter however corresponds to a field-dependent rescaling of the scalar field itself, as is evident from the derivation of the standard form in section 13.4.2.
From there it almost seems likely that our definition of the anomalous dimension at a fixed value of the field $y = y_0$ (equation (12.2)) overdetermines the system, as we

demand fixed points of the renormalization group flow in $K(y \neq y_0)$ where in fact a residual running of a wave function renormalization should be allowed.
What is more, our theory was originally defined in terms of three functions, then reduced to two conformal invariants, and then further reduced to one redefined field and one potential. It is also well conceivable that including these redundant functions from the onset on leads to the lingering dependence on ϵ and that it would be resolved if we were able to find a formulation that only included the physically relevant information from the beginning on and ensured the correct physical scaling of fields. This idea is somewhat parallel to the vertex construction as introduced in the process of the vertex expansion procedure, section 4.4.2, but of course technically much more involved and beyond the scope of this thesis.

13.5.2 Scale Generation

One of our main motivations when starting the quest to find a global scaling solution in dilaton gravity was the dynamical generation of a Planck mass via a nontrivial expectation value for the scalar field $\langle\chi\rangle$, see section 3.1. For that, the minimum in V in figure 13.1 at

$$y_{\min} = 3.8684 \cdot 10^{-5}$$

looked promising. However, given the field equations presented in appendix E, the situation is a little more involved, and an extremum of V only determines $\langle\chi\rangle$ if F and K are approximately independent of the scalar around that point. In our solution this is clearly not the case at least for K.
That is why even though scale invariance is manifestly broken for $y \neq \infty$, we need to work a bit more to extract the Planck scale.
Nonwithstanding that, we point out that F also exhibits a minimum at $y_{\min} = 3.8530 \cdot 10^{-5}$, which almost coincides with the minimum of V. That is why when carrying over to $\hat{V}$ and $\hat{K}$ (see figure 13.7), the potential now exhibits a maximum at the same position (equation (13.6)), again explicitly breaking scale invariance. Interpreted in the Einstein frame, we have $F' = 0$, simplifying analysis. This is however again accompanied by a nontrivial, field dependent $K \neq 1$, thus $\hat{V}'$ alone is not decisive for $\langle\chi\rangle$: We are still neglecting a field rescaling, highlighting the need to carry over to $\hat{V}_{\text{norm}}$ to capture the full physical picture, and already hinting towards a moving, nonconstant Planck scale as we will discuss in greater detail in the next section.
Note that once a Planck scale is established by means of the dimensionless field y, we still need one other reference scale to fix the ratio of the Planck scale to that reference scale.

13.5.3 Cosmology and Inflation

From figure 13.8 we know that the potential potential $\hat{V}_{\text{norm}}$ decays exponentially for sufficiently large values of $\tilde{y}$. This represents a realistic cosmology in the infrared with inflation of the slow roll type [152].
More explicitly, for slow roll inflation to be realized we need the two conditions

$$M\left(\frac{V'(\Phi)}{V(\Phi)}\right)^2 \ll 1,\ M\frac{V''(\Phi)}{V(\Phi)} \ll 1$$

to be satisfied [153, 154].
Let's safe ourselves the trouble of taking care of the fact that all our functinos dependent on the square of the scalar instead of the scalar itself. The derivation goes through similarly, just with additional terms stemming from chain rules. To make the argument of V dimensionless in the physical regime, where the cutoff can ultimately be removed, we need to write

$$V = V\left(\frac{\Phi}{M}\right) \sim \exp\left(C\frac{\phi}{M}\right),$$

where C is a dimensionless constant of order unity. But then, each derivative produces an additional factor of $\frac{1}{M}$, so that ultimately

$$M\left(\frac{V'(\Phi)}{V(\Phi)}\right)^2 \sim \frac{1}{M} \ll 1,\ M\frac{V''(\Phi)}{V(\Phi)} \sim \frac{1}{M} \ll 1$$

holds, and our exponential solution realizes slow roll inflation initialized at the maximum of $\hat{V}_{\text{norm}}$.
In this scenario, there is no stable vacuum configuration of the system, since the potential does not exhibit a minimum. However, there is still a maximum solving the field equations. In the context of dilaton gravity, this would amount to a moving Planck scale, initialized at the maximum and then moving towards larger y, offering exciting prospects to tune the Newton constant to today's measured value and thereby towards resolving the hierarchy problem.
Moreover, the solution for $\hat{V}_{\text{norm}}$ in figure 13.8 has a vanishing effective cosmological constant in the Einstein frame for large values of the field, offering a possibility to explain today's measured value which is very close to but yet non zero. Since this result is derived in the context of quantum gravity, a potential of this form explains why the cosmological constant indeed deviates from the value expected by simple estimates of the vacuum energy density. It becomes smaller as the energy scale is lowered, which is closely related to the fact that the that the potential $\hat{V}_{\text{norm}}$ does

not exhibit a minimum and thus allows for a moving Planck scale in combination with slow roll inflation.
We mention that a moving Planck scale that is smaller today than expected from dimensional analysis might make quantum gravity effects accessible much more easily [93–95].
Before proceeding, let us go back to the conformal invariants $\hat{V}$ and $\hat{K}$ depicted in figure 13.7 for a moment. By definition, we can interpret them in any frame, and more specifically, we want to interpret them in the Einstein frame for convenience. Though the details are a bit more complicated due the nontrivial field dependencies, we in principle need to rescale our scalar field χ as described in section 3.1.1, such that $\varphi \sim \ln(\chi)$ or $\chi \sim \exp(\varphi)$. Since $\hat{V} = V/F^2 \sim \chi^{-4}$ for large χ/k, this leads to $\hat{V} \sim \exp(-4\varphi)$ in this limit. This is precisely where the exponential form appears, even without transforming the potential into its standard form $\hat{V}_{\text{norm}}$. Note that this would not be true if V would scale like χ^4 for large fields.

Deviations from an exact scaling solution

To wrap up, let us demonstrate an application to cosmology where we assume the fixed point of dilaton gravity is only approximately realized. We are interested in the range of large y or small k, where the fixed point potential V is approximately constant with asymptotic value V_0 and the fixed point of F scales like $F_0 + \xi y$. In this scenario, we start out with a constant K that we have rescaled to 1. Let us then assume that V and F are perturbed by dimensionful values $\bar{V}$ and $\bar{F}$. For the dimensionful functions we can then write

$$\begin{aligned} V &= V_0 k^4 + \bar{V}, \\ F &= \xi\chi^2 + F_0 k^2 + \bar{F}. \end{aligned} \tag{13.8}$$

Plugging this ansatz into the fixed point equations, we see that the addition of $\bar{V}$ and $\bar{F}$ does not change the asymptotic values, as both perturbations only enter in $\mathcal{O}(y^{-1})$. Note that this is different for a χ dependent mass term in V.
Then, the effective action of dilaton quantum gravity for $k \to 0$ tends to

$$\Gamma = \int d^4x\sqrt{g}\left(\frac{1}{2}g^{\mu\nu}\partial_\mu\chi\,\partial_\nu\chi - \frac{1}{2}(\xi\chi^2 + \bar{F})\,R + \bar{V}\right), \tag{13.9}$$

generalizing the simple fixed point in equation (3.13). Here, $\bar{V}$ plays the role of an effective cosmological constant in the Jordan frame. Transforming to the Einstein frame via a Weyl scaling

$$\tilde{g}_{\mu\nu} = \frac{\xi\chi^2 + \bar{F}}{M^2}\,g_{\mu\nu},$$

combined with a rescaling of the scalar field

$$\varphi = M \ln\left(\frac{\xi\chi^2 + \bar{F}}{M^2}\right), \tag{13.10}$$

we arrive at an effective action of the form

$$\begin{aligned} \Gamma &= \int d^4x\sqrt{g}\left\{-\frac{M^2}{2}R + \frac{1}{2}K(\varphi)\partial^\mu\varphi\partial_\mu\varphi + V(\varphi)\right\}, \\ K(\varphi) &= \frac{1}{4\xi}\left[1 + 6\xi + \left(\frac{M^2}{\bar{F}}\exp\left(\frac{\varphi}{M}\right) - 1\right)^{-1}\right], \end{aligned} \tag{13.11}$$

with a potential

$$V(\varphi) = \bar{V}\exp\left(-\frac{2\varphi}{M}\right), \tag{13.12}$$

which decays exponentially for large φ/M. This is in line with what we found in earlier in this section, even though here the exponential potential was generated via small deviations from the fixed point solution, rather than by the fixed point solution itself.

Note how, even though we started out with $K = 1$ in the Jordan frame, the transformation to the Einstein frame generated a nontrivial, field dependent K as a function of the rescaled field φ, underlining the importance of considering such a function in the context of dilaton gravity.

CHAPTER 14

Conclusions and Extensions

14.1 Conclusions

In this part, we derived, investigated and globally solved the fixed point equations for the dilaton-graviton system (3.6), thus smoothly connecting infrared with ultraviolet physics on a pure fixed point trajectory.
In order to do so, we had to derive a set of flow equations for the functions V, F and K using a vertex expansion as well as a flat background spacetime, and carefully disentangle couplings from field rescalings.
The physical features of dilaton gravity turn out to be rich an can be described in a very concise manner, as discussed at length in section 13.5. Among those features, the explicit breaking of scale invariance through a finite expectation value $\langle\chi\rangle$ is of paramount importance, as it introduces an explicit scale into our theory. While the potential V exhibits a minimum, the conformally reduced potential $\hat{V}$ does not anymore, highlighting the need to eliminate physical redundancies. The same is true when we absorb the lingering prefactor of the scalar kinetic term $\hat{K}$ into a field redefinition to arrive at the final potential $\hat{V}_{\text{norm}}$, which captures the whole physical content of the model in just one function. This potential exhibits a maximum, which of course solves the field equations, but is not a stable configuration. This hints towards a moving Planck scale, which may be vital towards resolving the hierarchy problem. Furthermore, quantum gravity effects may arise at a different scale than expected. Our solution additionally naturally implements inflation.
When moving from the maximum further towards the infrared, we showed the potential to decay exponentially, and explicitly demonstrated the slow roll conditions

to be satisfied. Thus slow roll inflation takes place in the universe described by the fixed point trajectory of dilaton gravity. An exponentially decaying potential vanishes in the deep infrared, which corresponds to a vanishing effective cosmological constant. This explains why the cosmological constant measured today differs by many orders of magnitude from the value expected by pure quantum vacuum expectation value computations.
On a slightly more technical note, we find that the system shows a residual dependency on the ratio of kinetic terms of scalar and graviton in the infrared ϵ, which should ultimately be resolved to arrive at one definite model for our universe without explicitly given initial conditions in the form of initial scales. We argue that this residual dependency might be rooted in the way we describe the system and set up the flow equations. A possible resolution lies in a generalized vertex construction procedure, but the details are beyond the scope of the current work and material for future research.

14.2 Extensions

The research presented in this part opens up a cornucopia of possibilities for extensions, in addition to the upgraded setup mentioned at the end of the previous section.
As for technical aspects, the inclusion of terms of order $\mathcal{O}(R^2)$ is even more intriguing than it has already been in the background calculations, as these still appear in the flows of the two point functions, while terms of $\mathcal{O}(R^3)$ do not by virtue of the vertex expansion with a flat background. Furthermore, we learned that disentangling couplings from rescalings is important for the system, so it would be insightful to understand the role of a wave function renormalization for the graviton as well, ideally dependent on the scalar field and therefore on the scale, similar to the upgrades proposed for the scalar wave function renormalization. This, however, requires the flow of the three point function in order to disentangle kinematic quantities, entering the propagators, from couplings, entering the n-point functions with $n \geq 3$. Calculating flows for the three point functions for the dilaton-graviton system is a formidable task, but we report that considerable progress has already been made towards completion, and we are confident that improved and optimized programs currently being developed will help us overcome technical difficulties in the near future.
Moving on to connections to particle physics, the inclusion of fermions into the system would be a vital step towards modeling a more realistic standard model scalar sector, and with that understand scale generation in the context of particle physics, that can then ultimately be compared to the Planck scale generated in pure dilaton gravity. To that end, both mechanisms would need to be studied in a coupled system, requiring at least two scalar fields. Shifting our focus to cosmology, we would like to

further disentangle the role of the scalar in regards to scale generation and inflation, which also points to studying a similar theory like the one considered in this part with a second scalar field added.
On a more technical note, including the full ghost interactions as well as RG time derivatives on the RHS of the flow equations is a natrual next step and last but not least, the numerical results obtained need to be tested for stability with respect to all approximations made to ultimately extract solid numerical values for experimentally accessible quantities from an enlarged truncation.

Conclusions and Outlook

In this thesis, we set out to investigate dilaton gravity as a theory of quantum gravity using functional renormalization group methods. To that end, we introduced a formulation of dilaton gravity and the notion of scale invariance in the context of scalar-tensor theories and discussed the differences to traditional Einstein gravity. In dilaton gravity, the scalar field serves as a bookkeeping device for the renormalization group scale and a spontaneously broken scale symmetry leads to a natural notion of the Planck scale even without deviating from the fixed point. We then derived flow equations utilizing background field methods first, and an upgraded approach that more clearly disentangles background from fluctuation fields and allows for the correct implementation of physical scalings in a second step.
Conclusions emphasizing the individual part's contributions were already given at the end of the respective parts. We therefore only summarize the most important results at this point.
When investigating special and limiting cases we found that in the regime where the scale is much smaller than the scalar field, the system exhibits features of infrared physics, more specifically a classical scaling law for the scalar field as well as vanishing quantum contributions in the flow, while the contrary is true for the reverse limiting case. We find a direct generalization of the ultraviolet fixed point in the Einstein-Hilbert truncation, thereby collecting further evidence for the asymptotic safety scenario.
Intrigued by these observations we derived a global fixed point solution connecting the limiting cases, for which we find it to be vital to allow for derivative couplings in the scalar sector and to carefully disentangle these from rescalings of the scalar field. We therefore discuss at length the relations between different scaling parameters of the theory and reformulate our theory in terms of a reduced number of physically relevant parameters and functions.

Once achieved, this reformulation makes the rich physical content of dilaton gravity readily accessible. We demonstrate explicitly how infrared scale invariance is spontaneously broken and thereby the scale of quantum gravity is set. However, the corresponding solution is not stable, leading to a scenario with a moving Planck scale. Not only does this offer a possibility to understand the measured value of Newtons constant today, but also features naturally arising slow roll inflation on an exponentially decreasing potential, which leads to a cosmological constant that vanishes in the infrared limit. In this context, the unstable solution offers a natural opportunity to explain why the measured value of the cosmological constant today differs from predictions made by vacuum energy computations. Furthermore, a moving Planck scale might make quantum gravity effects experimentally accessible at a different scale than currently believed.
While these results are certainly encouraging, we also mention that work remains to be done to single out only one physical solution, that is to eliminate a lingering dependence on the ratio of scalar and graviton kinetic term in the infrared. We emphasize that this unsettling parametric dependence does not change any physical features, and is likely due to our system falling short at correctly implementing field rescalings at finite values of the scalar field, or due to the current infeasibility of formulating flow equations that only depend on the physically relevant functions from the outset on. Finding this formulation is certainly material for further research and pushes towards further disentangling the distinct roles of different parts of the system. An improved vertex expansion including flows for the three point functions would contribute towards this goal as well, as it would allow to distinguish wave function renormalizations from couplings also in the gravity sector. Furthermore, the inclusion of a term of order $\mathcal{O}(R^2)$ as well as ghost and RG time derivatives is suggested for reasons of consistency and closure of the truncation and stability under all approximations made is vital to extract solid numerical results. Adding a second scalar is suggested to disentangle the role a scalar field plays for inflation and the generation of the physical scale. Furthermore, a second scalar is also needed to ultimately compare the scale generated in pure gravity with another physical scale, ideally from the area of particle physics. This would bring us considerably closer to our ultimate goal of finding a unified and natural mathematical description of all of nature's features and further our understanding of physics on all scales.

Part IV

Appendices

APPENDIX A

Background flows in $d = 4, \alpha = 0, \beta = 1$

The full flow equation in arbitrary dimensions $d > 2$ and gauge parameters α and β can be found in [42]. However, since for most of the work in the following chapters, the structure of the equation can be very well inspected in $d = 4$ and deDonder gauge, we give those results explicitly at this point.

A.1 Original System

$$\Gamma_k = \int d^4x\sqrt{g}\left(V_k(\chi^2) - \frac{1}{2}F_k(\chi^2)\,R + \frac{1}{2}g^{\mu\nu}\partial_\mu\chi\partial_\nu\chi\right)$$

We use the same notations and shorthands as [26] and write

$$\begin{aligned}\partial_t V &= 2\chi^2 V' - 4V + \zeta_V,\\ \partial_t F &= 2\chi^2 F' - 2F + \zeta_F,\end{aligned} \tag{A.1}$$

where the flow generators ζ_V and ζ_F are given by

$$\begin{aligned}\zeta_V &= \frac{1}{192\pi^2}\left\{6 + \frac{30\,V}{\Sigma_0} + \frac{3(2\Sigma_0 + 24\,y\,F'\,\Sigma_0' + F\Sigma_1)}{\Delta} + \delta_V\right\},\\ \zeta_F &= \frac{1}{1152\pi^2}\left\{150 + \frac{30\,F\,(3\,F - 2V)}{\Sigma_0^2}\right.\end{aligned} \tag{A.2}$$

$$
\begin{aligned}
&-\frac{12}{\Delta}\left(24\,y\,F'\,\Sigma_0' + 2\Sigma_0 + F\Sigma_1\right) - 6y\left(3\,F'^2 + 2\Sigma_0'^2\right)\\
&-\frac{36}{\Delta^2}\Bigg[2y\,\Sigma_0\,\Sigma_0'\left(7\,F' - 2V'\right)\left(\Sigma_1 - 1\right) + 2\,\Sigma_0^2\,\Sigma_2\\
&+2\,y\Sigma_1\left(7\,F' - 2V'\right)\left(2\,\Sigma_0\,V' - V\,\Sigma_0'\right)\\
&+24\,y\,F'\,\Sigma_0\,\Sigma_0'\,\Sigma_2 - 12\,y\,F\,\Sigma_0'^2\,\Sigma_2\Bigg] + \delta_F\Bigg\}.
\end{aligned}
$$

Here we employ

$$
\begin{aligned}
\Sigma_0 = \frac{1}{2}F - V\ ,\ \Delta &= \left(12\,y\,\Sigma_0'^2 + \Sigma_0\,\Sigma_1\right),\\
\Sigma_1 = 1 + 2\,V' + 4\,y\,V''\ ,\ \Sigma_2 &= F' + 2\,y\,F''.
\end{aligned}
\tag{A.3}
$$

The contributions

$$
\begin{aligned}
\delta_V &= \left(\frac{4}{F} + \frac{5}{2\Sigma_0} + \frac{\Sigma_1}{2\Delta}\right)\left(\partial_t F + 2\,F - 2\,y\,F'\right)\\
&\quad + \frac{12\,y\,\Sigma_0'}{\Delta}\left(\partial_t F' - 2\,y\,F''\right),\\
\delta_F &= -\frac{\partial_t F + 2\,F - 2\,y\,F'}{F}\Bigg[30 - \frac{5F\left(7\,\Sigma_0 + 4\,V\right)}{\Sigma_0^2}\\
&\quad + \frac{3}{\Delta^2}\Bigg(F\,\Sigma_1\,\Delta + 8\,y\,V'\,\Sigma_0'\,\Delta - 24\,y\,F\,\Sigma_0'^2\,\Sigma_2\\
&\quad -2y\,F\,\Sigma_0'\,\Sigma_1(7\,F' - 2V')\Bigg)\Bigg]\\
&\quad + \frac{6\,y}{\Delta^2}\Bigg[\left(F' + 10\,V'\right)\Delta - 24\,\Sigma_0\,\Sigma_0'\,\Sigma_2\\
&\quad -2\left(7F' - 2V'\right)\Sigma_0\,\Sigma_1\Bigg]\left(\partial_t F' - 2\,y\,F''\right),
\end{aligned}
\tag{A.4}
$$

arise from the field dependence in the cutoff. They vanish for $y \to \infty$ and neglecting these contributions altogether does not change the structure of the results obtained.

A.2 System with a Scaled Kinetic Term

$$
\Gamma_k = \int d^4x\sqrt{g}\left(V_k(\chi^2) - \frac{1}{2}F_k(\chi^2)\,R + \frac{K}{2}g^{\mu\nu}\partial_\mu\chi\partial_\nu\chi\right)
$$

Introducing an RG-constant K to scale the kinetic term changes the flow generators ζ_V and ζ_F to

$$\zeta_V = \frac{1}{192\pi^2}\left\{6+\frac{30\,V}{\Sigma_0}+\frac{3(2K\Sigma_0+24\,y\,F'\,\Sigma_0'+\,F\Sigma_1)}{\Delta}+\delta_V\right\},$$

$$\begin{aligned}\zeta_F = \frac{1}{1152\pi^2}\Bigg\{&150+\frac{30\,F\,(3\,F-2V)}{\Sigma_0^2}\\ &-\frac{12}{\Delta}\,(24\,y\,F'\,\Sigma_0'+2K\Sigma_0+F\Sigma_1)-6y\,(3\,F'^2+2\Sigma_0'^2)\\ &-\frac{36}{\Delta^2}\Big[2y\,\Sigma_0\,\Sigma_0'\,(7\,F'-2V')\,(\Sigma_1-K)+2\,\Sigma_0^2\,\Sigma_2\\ &+2\,y\Sigma_1\,(7\,F'-2V')\,(2\,\Sigma_0\,V'-V\,\Sigma_0')\\ &+24\,y\,F'\,\Sigma_0\,\Sigma_0'\,\Sigma_2-12\,y\,F\,\Sigma_0'^2\,\Sigma_2\Big]+\delta_F\Bigg\}.\end{aligned} \tag{A.5}$$

The shorthands introduced originally remain unchanged with the exception of Σ_1, which no reads

$$\Sigma_1 = K + 2\,V' + 4\,y\,V'' \ .$$

Furthermore, whenever referring to this class of equations, we understand

$$\delta_V = \delta_F = 0.$$

Note that the alteration in Σ_1 is directly due to the propagator of the scalar field, while the additional factors of K explicitly entering the flow generators are due to inverting $\Gamma^{(2)}$ and multiplying with our field dependent $\partial_t\mathcal{R}_k$.

APPENDIX B

Heat Kernel Expansions

In this appendix, we will develop the tools necessary to evaluate the functional traces occurring on the RHS of the FRGE. Our presentation is footed on three distinct sets of sources: The mathematically rigorous part is inspired by [199, 200], whereas the practical computations are sparked by [201]. Lastly, [202, 203] provide a way of applying our findings to the setup of this thesis.
Throughout this appendix, M will denote a smooth and compact Riemannian manifold of dimension d, which is usually taken to not have a boundary.

B.1 Motivation

First of all, let us introduce a rewriting of our setup enabling us to use heat kernel techniques. To that end, let D be a second order differential operator of Laplace type on the vector bundle V on M. Then a unique connection and an endomorphism E on V exist such that locally

$$D = -(g^{\mu\nu}\nabla_\mu\nabla_\nu + E), \tag{B.1}$$

where ∇_μ is a covariant derivative, containing both curvature and gauge parts if applicable. Note that in this appendix we explicitly write out the covariant derivatives to emphasize their geometrical meaning.
Let $W(D)$ be a function of the operator D. Its trace over the space of square

integrable functions can then be written as

$$\mathrm{Tr}_{L^2} W(D) = \sum_i W(\lambda_i), \tag{B.2}$$

where λ_i are the eigenvalues of the the operator D. Note that usually, i will assume infinitely many values, so properly defining the trace is actually more subtle than it might seem. For a short introduction to calculus on spaces of infinite dimension, see [47].
With $\tilde{W}(s)$ being connected to $W(z)$ via a Laplace transformation,

$$W(z) = \int_0^\infty \mathrm{d}s e^{-zs} \tilde{W}(s),$$

we can now rewrite equation (B.2) as

$$\mathrm{Tr}_{L^2} W(D) = \int_0^\infty \mathrm{d}s K(s, f = \mathrm{id}, D) \tilde{W}(s), \tag{B.3}$$

where

$$K(s, f, D) = \mathrm{Tr}_{L^2} \left(f \exp(-sD)\right) = \sum_i f \exp(-s\lambda_i) \tag{B.4}$$

is the trace of the heat kernel[1] $f \exp(-sD)$ of D.
These somewhat tedious rewritings lead to the advantage of allowing for the ready application of a well established asymptotic expansion (see for instance [204]) for the trace in the limit $s \to 0^+$ reading

$$\mathrm{Tr}_{L^2} \left(f \exp(-sD)\right) = K(s, f, D) = \sum_{k \geq 0} s^{\frac{k-d}{2}} a_k(f, D), \tag{B.5}$$

where the objects $a_k(f, D)$ are the heat kernel coefficients of the differential operator D.
Further introducing $Q_n(W) = \int_0^\infty \mathrm{d}t\, t^{-n} \tilde{W}(t)$ and using

$$\Gamma(n) = \int_0^\infty \mathrm{d}t e^{-t} t^{n-1}$$

[1] The name heat kernel stems from the fact that it is a fundamental solution to the heat equation, used to study heat conduction as well as diffusion in solid state physics. It describes the evolution of temperature.

allows us to write

$$Q_n(W) = \frac{1}{\Gamma(n)} \int_0^\infty \mathrm{d}t\, t^{n-1} W(t) \tag{B.6}$$

for n a positive real number. Since we are only interested in the local behavior of the theory, that is on length scales much smaller than the typical curvature radius, we can plug (B.5) into (B.3) to obtain

$$\mathrm{Tr}_{L^2}\, W(D) = \sum_{k\geq 0} s^{\frac{k-d}{2}} a_k(f, D) Q_{\frac{d-k}{2}}(W). \tag{B.7}$$

This is our desired result, as it enables us to rewrite the functional trace in terms of the heat kernel coefficients $a_k(f, D)$.[2] Even though we will need the case $f = \mathrm{id}$ for our concrete calculations, we left the function f arbitrary to be able to obtain the form of $a_k(f, D)$ for the differential operators in consideration.
It should be mentioned that there is a close relationship between the function $Q_n(W)$ and the well known ζ function [205] of a Laplace type differential operator D, used to make rigor sense of the trace on the infinitesimally dimensional function space L^2. Defining, as usual in mathematical literature,

$$\zeta(u, f, D) = \mathrm{Tr}_{L^2}(fD^{-u}), \tag{B.8}$$

we can carry out the same steps as in (B.6) to arrive at

$$\zeta(u, f, D) = \frac{1}{\Gamma(u)} \int_0^\infty \mathrm{d}t\, t^{u-1} K(t, f, D). \tag{B.9}$$

Thus, $Q_n(W)$ is a version of $\zeta(u, f, D)$, adapted to our task of obtaining the spectrum of a function of the differential operator D.
In principle, equation (B.9) can be inverted directly to

$$K(t, f, D) = \frac{1}{2\pi i} \oint ds\, t^{-s} \Gamma(s) \zeta(s, f, D), \tag{B.10}$$

meaning that we would be able to obtain the coefficients $a_n(f, D)$ by applying the residue theorem,

$$a_k(f, D) = \mathrm{Res}_{s=\frac{d-k}{2}} \left(\Gamma(s)\zeta(s, f, D)\right), \tag{B.11}$$

and, in particular, $a_d(f, D) = \zeta(0, f, D)$. However, we will employ a different approach, emphasizing the geometrical aspects of the heat kernel expansion.

[2] For our discussion, we only need heat kernel coefficients for $d > 2$ and $k \leq 2$, thus $\frac{d-k}{2}$ is always greater than zero.

B.2 Obtaining the Coefficients $a_k(f, D)$

The most important property of the coefficients $a_k(f, D)$, which we will not proof in this thesis, is that they can locally be expressed in terms of geometrical invariants $\mathcal{A}_k^I$ of dimension k. Given the fact that for manifolds without a boundary all boundary integrals need to vanish, we conclude that no odd-dimensional invariant constructed from the metric $g_{\mu\nu}$ and its derivatives exists. Thus,

$$a_{2k+1}(f, D) = 0 \tag{B.12}$$

holds.
Furthermore, we are only interested in expansions that are at most linear in the curvature scalar R, hence we only need $a_0(f, D)$ and $a_2(f, D)$.
To obtain explicit expressions, we write

$$a_k(f, D) = \mathrm{Tr}_V \int \mathrm{d}^d x \sqrt{g} (f u_k^I \mathcal{A}_k^I), \tag{B.13}$$

where the u_k^I are constants and a summation over I is assumed. Note that the trace is now taken on the vector bundle V, a much more accessible space than the functional space L^2. For $k = 0$, there is only one invariant, namely the identity matrix $\mathbb{1}$, whereas for $k = 2$ we already have R as well as the endomorphism E. Thus we are now able to write, using rescaled constants α_k^I

$$\begin{aligned}
a_0(f, D) =& \frac{1}{(4\pi)^{d/2}} \int \mathrm{d}^d x \sqrt{g}\, \mathrm{Tr}_V(\alpha_0 f), \\
a_2(f, D) =& \frac{1}{(4\pi)^{d/2}} \frac{1}{6} \int \mathrm{d}^d x \sqrt{g}\, \mathrm{Tr}_V\, f(\alpha_2^1 E + \alpha_2^2 R), \\
a_4(f, D) =& \frac{1}{(4\pi)^{d/2}} \frac{1}{360} \int \mathrm{d}^d x \sqrt{g}\, \mathrm{Tr}_V\, f(\alpha_3^1 \Box E + \alpha_3^2 R E + \alpha_3^3 E^2 \\
&+ \alpha_3^4 \Box R + \alpha_3^5 R^2 + \alpha_3^6 R^{\mu\nu} R_{\mu\nu} + \alpha_3^7 R^{\mu\nu\rho\sigma} R_{\mu\nu\rho\sigma} + \alpha_3^8 \Omega^{\mu\nu} \Omega_{\mu\nu}),
\end{aligned} \tag{B.14}$$

with $\Box = \nabla^\mu \nabla_\mu$ and $\Omega_{\mu\nu} = [\nabla_\mu, \nabla_\nu]$ and expressions within the traces multiplied by the identity $\mathbb{1}$ on the space V where necessary.
Even though it will not be needed in this thesis, we briefly mention that for $k = 6$, there are already 37 invariants to be considered. Thus, the complexity of obtaining the coefficients increases rapidly.
Our goal for the remainder of this section is to determine the three constants α_k^I relevant for our $\mathcal{O}(R)$ considerations. Let us begin with a rather simple observation: Assume that M can be written as a direct sum of two manifolds M_1 and M_2, that is $M = M_1 \oplus M_2$. Then, the differential operator D can be decomposed into its actions on the manifolds M_1 and M_2, namely $D = D_1 \otimes \mathbb{1} + \mathbb{1} \otimes D_2$, also leading

to two independent sets of indices and coordinates on the vector bundles V_1 and V_2. Symbolically, we are then able to write $\exp(-tD) = \exp(-tD_1) \otimes \exp(-tD_2)$ or, after plugging the decompositions just obtained into the expressions for the heat kernel coefficients,

$$a_k(x, D) = \sum_{i+j=k} a_i(x_1, D_1)\, a_j(x_2, D_2), \tag{B.15}$$

where we have taken f to be just the coordinate function, canonically defined on the manifolds M as well as on M_1 and M_2.
Let us further specialize $M_1 = S_1$ and choose a simple Laplacian, $D_1 = -\partial^2_{x_1}$. This means that the geometric invariants are solely determined by D_2 on M_2 and by virtue of equation (B.13), therefore we can write

$$\begin{aligned} a_k(f(x_2), D) &= \int_{S^1 \times M_2} \mathrm{d}^d x \sqrt{g} \sum_i \mathrm{Tr}_V(f(x_2) u^I_{(d)} \mathcal{A}^I_k(D)) \\ &= 2\pi \int_{M_2} \mathrm{d}^{d-1} \sqrt{g} \sum_i \mathrm{Tr}_V(f(x_2) u^I_{(d)} \mathcal{A}^I_k(D_2)). \end{aligned} \tag{B.16}$$

As a second step, we can employ equation (B.15). Thee spectrum of the operator $-\partial_{x_1}$ on S^1 is just $\{l^2\}_{l \in \mathbb{Z}}$. Utilizing the Poisson summation formula, we can obtain the asymptotic behavior of the heat kernel explicitly, reading

$$\begin{aligned} K(t, D_1) &= \sum_{l \in \mathbb{Z}} \exp(-tl^2) \\ &= \sqrt{\frac{\pi}{t}} \sum_{l \in \mathbb{Z}} \exp(-\pi^2 l^2 / t) \\ &= \sqrt{\frac{\pi}{t}} + \mathcal{O}(\exp(-1/t)). \end{aligned} \tag{B.17}$$

Moreover, we can also rewrite equation (B.16) to read

$$a_k(f(x_2), D) = \sqrt{\pi} \int_{M_2} \mathrm{d}^{d-1} \sqrt{g} \sum_i \mathrm{Tr}_V(f(x_2) u^I_{(d-1)} \mathcal{A}^I_k(D_2)), \tag{B.18}$$

which yields upon comparison with equation (B.16)

$$u^I_{(d)} = \sqrt{4\pi} u^I_{(d+1)}. \tag{B.19}$$

These investigations reveal two conclusions: Firstly, we fixed the dependence of the constants u^I on the dimension d to be encoded in prefactors $(4\pi)^{-d/2}$ only. That is why we rescaled the prefactors in equation (B.14), transforming them into true

constants in the process. Secondly, we fixed the constant α_0 to equal unity, $\alpha_0 = 1$, when considering the free Laplacian on the sphere S^1.
Proceeding to calculate α_2^1 and α_2^2, we will need the function f introduced with the definition of the heat kernel expansion. So let f and F be smooth functions. The following relations can be checked by explicit calculations:

$$\frac{d}{d\epsilon} a_k(1, e^{-2\epsilon f} D) \mid_{\epsilon=0} = (d-k) a_k(f, D), \tag{B.20}$$

$$\frac{d}{d\epsilon} a_k(1, D - \epsilon F) \mid_{\epsilon=0} = a_{k-2}(F, D), \tag{B.21}$$

$$\frac{d}{d\epsilon} a_{d-2}(e^{-2\epsilon f} F, e^{-2\epsilon f} D) \mid_{\epsilon=0} = 0. \tag{B.22}$$

Equation (B.21) restricts the coefficients in the presence of an endomorphism E, whereas equations (B.20) and (B.22) yield properties for the behavior under local scale transformations.
Let us use equation (B.21) for $k = 2$ to see that

$$\frac{1}{6} \int \mathrm{d}^d x \sqrt{g}\, \mathrm{Tr}_V\, f \alpha_1^1 = \int \mathrm{d}^d x \sqrt{g}\, \mathrm{Tr}_V\, f, \tag{B.23}$$

or equivalently, $\alpha_1^1 = 6$. For $k = 4$ we obtain $\alpha_2^3 = 180$ as well as $\alpha_2^2 = 60\alpha_1^2$. To proceed further, we will need to examine how the quantities involved in equation (B.14) scale under the transformation $g_{\mu\nu} \to \exp(2\epsilon f) g_{\mu\nu}$. Again, the following equations can be checked via explicit calculations:

$$\begin{aligned}
\frac{d}{d\epsilon} \sqrt{g} \mid_{\epsilon=0} &= df \sqrt{g}\,, \\
\frac{d}{d\epsilon} R_{\mu\nu\rho\sigma} \mid_{\epsilon=0} &= -2f R_{\mu\nu\rho\sigma} \\
&\quad + g_{\nu\sigma} \nabla_\mu \nabla_\rho f + g_{\mu\rho} \nabla_\nu \nabla_\sigma f_{;\nu\sigma} - g_{\mu\sigma} \nabla_\nu \nabla_\rho f - g_{\nu\rho} \nabla_\mu \nabla_\sigma f\,, \\
\frac{d}{d\epsilon} E \mid_{\epsilon=0} &= -2fE + \frac{1}{2}(d-2) \Box f\,, \\
\frac{d}{d\epsilon} R \mid_{\epsilon=0} &= -2fR - 2(d-1) \Box f\,, \\
\frac{d}{d\epsilon} \Box E \mid_{\epsilon=0} &= -4f \Box E - 2 \Box f E + \frac{1}{2}(d-2) \Box^2 f + (d-6) \nabla^\mu f \nabla_\mu E\,, \\
\frac{d}{d\epsilon} RE \mid_{\epsilon=0} &= -4fRE + \frac{1}{2}(d-2) \Box f R - 2(d-1) \Box f E\,, \\
\frac{d}{d\epsilon} E^2 \mid_{\epsilon=0} &= -4fE^2 + (d-2) \Box f E\,,
\end{aligned}$$

$$
\begin{aligned}
\frac{d}{d\epsilon}\Box R\,|_{\epsilon=0} &= -4f\Box R - 2\Box fR - 2(d-1)\Box^2 f + (d-6)\nabla^\mu f\nabla_\mu R\,,\\
\frac{d}{d\epsilon}R^2\,|_{\epsilon=0} &= -4fR^2 - 4(d-1)\Box fR\,,\\
\frac{d}{d\epsilon}R^{\mu\nu}R_{\mu\nu}\,|_{\epsilon=0} &= -4fR^{\mu\nu}R_{\mu\nu} - 2\Box fR - 2(d-2)\nabla^\mu\nabla^\nu f\nabla_\mu\nabla_\nu R\,,\\
\frac{d}{d\epsilon}R^{\mu\nu\rho\sigma}R_{\mu\nu\rho\sigma}\,|_{\epsilon=0} &= -4fR^{\mu\nu\rho\sigma}R_{\mu\nu\rho\sigma} - 8\nabla^\mu\nabla^\nu f\nabla_\mu\nabla_\nu R\,,\\
\frac{d}{d\epsilon}\Omega^{\mu\nu}\Omega_{\mu\nu}\,|_{\epsilon=0} &= -4f\Omega^{\mu\nu}\Omega_{\mu\nu}\,.
\end{aligned}
\tag{B.24}
$$

We can now apply equation (B.22) to $d = 4$ to obtain $\alpha_1^1 = 6\alpha_1^2$ or $\alpha_1^2 = 1$ and $\alpha_2^2 = 60$. The other coefficients present in equation (B.14) can be obtained with similar techniques, with the exception of α_2^8, for which one can apply the Gauss-Bonnet theorem [200]. However, since in this thesis our considerations are restricted to α_0 and α_1^1, α_1^2, we only state the final version of equation (B.14), reading

$$
\begin{aligned}
a_0(f,D) =& \frac{1}{(4\pi)^{d/2}}\int \mathrm{d}^d x\sqrt{g}\,\mathrm{Tr}_V(f),\\
a_2(f,D) =& \frac{1}{(4\pi)^{d/2}}\frac{1}{6}\int \mathrm{d}^d x\sqrt{g}\,\mathrm{Tr}_V\, f(6E+R),\\
a_4(f,D) =& \frac{1}{(4\pi)^{d/2}}\frac{1}{360}\int \mathrm{d}^d x\sqrt{g}\,\mathrm{Tr}_V\, f(60\Box E + 60RE + 180E^2\\
&+ 12\Box R + 5R^2 - 2R^{\mu\nu}R_{\mu\nu} + 2R^{\mu\nu\rho\sigma}R_{\mu\nu\rho\sigma} + 30\Omega^{\mu\nu}\Omega_{\mu\nu}).
\end{aligned}
\tag{B.25}
$$

In order to obtain expressions for $a_4(f,D)$ that only depend on the fully contracted curvature scalar R as a geometrical quantity, we would need to explicitly work in a maximally symmetric background, allowing for construction of $R_{\mu\nu}$ from R.
We are now able to apply our findings to the fields carrying different spin and satisfying numerous differential constraints from our theory. For this, we will set $f = \mathrm{id}$. The main goal will be to determine the dimensionality of the respective vector bundles and with that $\mathrm{Tr}_V\,\mathbb{1}$.

B.3 Differentially Constrained Fields

Reconsidering equation (6.1), we see that the fields occurring in the FRGE for our theory are the scalar ϕ as well as a vector ghost C_μ, $\bar{C}_\mu$ and the symmetric tensor graviton $h_{\mu\nu}$. Obtaining the expressions for $\mathrm{Tr}_V\,\mathbb{1}$ for these unconstrained fields is a simple task in d dimension, as a scalar has only one, a vector d and a symmetric tensor $\frac{d(d+1)}{2}$ independent components. However, to allow for feasible inversion of the kinetic operators, we decomposed our fields in equations (6.2) and

(6.3), leaving us with the computation of $\mathrm{Tr}_V \mathbb{1}$ for scalars $(\phi, \sigma, h, C, \bar{C})$, transverse vectors $(C^T_\mu, \bar{C}^T_\mu, \xi_\mu)$ and transverse traceless symmetric tensors $(h^T_{\mu\nu})$ instead.
Let us proceed to calculating the trace of the heat kernel coefficients $K(s, f = \mathrm{id}, D)$, using equation (B.4). To unclutter the notation, we will drop the explicit dependence on s and f. Consider a vector field decomposed into its transverse and its longitudinal part first,

$$A_\mu = A^T_\mu + \nabla_\mu \Phi \tag{B.26}$$

where we require $\nabla^\mu A^T_\mu = 0$. Our task is to relate the spectrum of $\Box = \nabla^\mu \nabla_\mu$ when acting on the longitudinal part $\nabla_\mu \Phi$ to its spectrum when acting on scalars.
On a d-dimensional sphere, the following commutation relation holds:

$$\Box \left(\nabla_\mu \Phi\right) = \nabla_\mu \left(\Box + \frac{R}{d}\right) \Phi, \tag{B.27}$$

allowing us to write $K(-\Box)$ as

$$K\left(-\Box\right)|_{A_\mu} = K(-\Box)|_{A^T_\mu} + K\left(-\left(\Box + \frac{R}{d}\right)\right)|_{\Phi} - \exp\left(s\frac{R}{d}\right). \tag{B.28}$$

The first two terms arise directly from the commutation relation, whereas the last term needs to be subtracted to exclude the constant eigenfunction of $-\left(\Box + \frac{R}{d}\right)$, leading to a negative, unphysical eigenmode, which will be dealt with separately.
Similarly, the two commutation relations

$$\begin{aligned} \Box \left(\nabla_\mu \xi_\mu + \nabla_\nu \xi_\mu\right) =& \nabla_\mu \left(\Box + \frac{d+1}{d(d-1)} R\right) \xi_\nu + \nabla_\nu \left(\Box + \frac{d+1}{d(d-1)} R\right) \xi_\mu \quad \text{and} \\ \Box \left(\nabla_\mu \nabla_\nu - \frac{1}{d} g_{\mu\nu} \Box\right) \sigma =& \left(\nabla_\mu \nabla_\nu - \frac{1}{d} g_{\mu\nu} \Box\right) \left(\Box - \frac{2}{d-1} R\right) \sigma \end{aligned} \tag{B.29}$$

enable us to write for the fields appearing in the York decomposition (6.2)

$$\begin{aligned} K\left(-\Box\right)|_{h_{\mu\nu}} =& K\left(-\Box\right)|_{h^T_{\mu\nu}} + K\left(-\left(\Box + \frac{d+1}{d(d-1)} R\right)\right)|_{\xi_\mu} \\ &+ K\left(-\Box\right)|_{h} + K\left(-\left(\Box + \frac{2}{d-1} R\right)\right)|_{\sigma} \\ &- \exp\left(s\frac{2}{d-1} R\right) - (d+1) \exp\left(s\frac{1}{d-1} R\right) \\ &- \frac{d(d+1)}{2} \exp\left(s\frac{2}{d(d-1)} R\right). \end{aligned} \tag{B.30}$$

field	S	V	VT	T	TTT
$\mathrm{Tr}(\mathbb{1})$	1	d	$d-1$	$\frac{d(d+1)}{2}$	$\frac{(d+1)(d-2)}{2}$
$\mathrm{Tr}(\mathbb{1}\,R)$	R	$d\,R$	$\frac{d(d-1)-6}{d}\,R$	$\frac{d(d+1)}{2}\,R$	$\frac{(d+1)(d+2)(d-5)}{2(d-1)}\,R$

Table B.1: Traces for use in the heat kernel coefficients a_0 and a_2 in d-dimensions. We adopted the shorthands S (scalar), V (vector), VT (transverse vector), T (symmetric tensor) and TTT (symmetric transverse traceless tensor).

The subtractions appear as explained above. To see where the excluded modes enter, recall that $a_k(D) = \mathcal{O}\left(\int \mathrm{d}^d x\sqrt{g}R^{\frac{k}{2}}\right) = \mathcal{O}\left(R^{\frac{k-d}{2}}\right)$. Expanding the exponential subtractions in Taylor series of the form $\sum_i c_i R^i$, we see that the coefficient c_i enters into the heat kernel coefficient with $i = \frac{k-d}{2}$, or, put in another way, there is no contributions for $k < d$. For our $\mathcal{O}(R)$ analyses, this means that the only critical case is $d = 2$, which we will exclude from our further considerations.
We will demonstrate how to obtain explicit expressions for a_0 and a_1^i for the decomposition of a vector. The coefficients for the York decomposed symmetric rank two tensor are obtained in a completely equivalent manner. Reconsidering equation (B.5), we apply it to both the RHS and the LHS of equation (B.28), neglecting the constant subtractions. Comparing powers of s yields for a_0

$$\begin{aligned} &\mathrm{Tr}_{A_\mu}(\mathbb{1}) = \mathrm{Tr}_{A_\mu^T}(\mathbb{1}) + \mathrm{Tr}_\Phi(\mathbb{1}) \\ \Longrightarrow\quad &\mathrm{Tr}_{A_\mu^T}(\mathbb{1}) = d-1 \end{aligned} \tag{B.31}$$

and for a_2

$$\begin{aligned} &\mathrm{Tr}_{A_\mu}(R\mathbb{1}) = \mathrm{Tr}_{A_\mu^T}(R\mathbb{1}) + \mathrm{Tr}_\Phi\left(6\frac{R}{d} + R\mathbb{1}\right) \\ \Longrightarrow\quad &\mathrm{Tr}_{A_\mu^T}(R\mathbb{1}) = R\left(\frac{d(d-1)-6}{d}\right). \end{aligned} \tag{B.32}$$

We summarize the coefficients in table B.1.

APPENDIX C

Notes on the Derivation of the Flat Flow Equations

C.1 Notation

For n point functions involving n_i derivatives of the field ϕ_i and m distinct fields in total, we use different, equivalent notations, including

$$\Gamma^{(n)}_{n_1\phi_1\ldots n_m\phi_m},\ \Gamma^{(n)}_{\underbrace{\phi_1\ldots\phi_1}_{n_1\text{ times}},\ldots\underbrace{\phi_m\ldots\phi_m}_{n_m\text{ times}}},\ \Gamma^{(n_1\phi_1\ldots n_m\phi_m)},\ \Gamma^{(\overbrace{\phi_1\ldots\phi_1}^{n_1\text{ times}},\ldots\overbrace{\phi_m\ldots\phi_m}^{n_m\text{ times}})},$$

depending on what needs to be emphasized in a specific situation. When it is either obvious from the context or insignificant what the specific fields are, we abbreviate to $\Gamma^{(n)}$.
Furthermore, we denote the RHS of the flow equation for the function $\Gamma^{(n)}$ with $\mathrm{Flow}^{(n)}$, and use the same different notations as abovehand when multiple fields are involved.

C.2 Gauge Fixing

We consider the gauge fixing (4.12), and start out with simply decomposing the graviton into a tracefree part $h^{TF}_{\mu\nu}$ and the trace,

$$h_{\mu\nu} = h^{TF}_{\mu\nu} + \frac{1}{d}\bar{g}_{\mu\nu}h. \tag{C.1}$$

Thus, in comparison with the Yorck decomposition (6.2), we did not decompose the tracefree part further for the time being. Now consider the gauge function in the gauge fixing, reading

$$\begin{aligned}\bar{\mathcal{F}}^{\mu} &= \bar{\nabla}_{\nu} h^{\nu\mu} - \frac{\beta+1}{d}\bar{\nabla}^{\mu} h \\ &= \bar{\nabla}_{\nu} h^{\nu\mu\ TF} + \frac{1}{d}\bar{g}^{\mu\nu}\bar{\nabla}_{\nu} h - \frac{\beta+1}{d}\bar{\nabla}^{\mu} h \\ &= \bar{\nabla}_{\nu} h^{\nu\mu\ TF} + \left(\frac{1}{d} - \frac{\beta+1}{d}\right)\bar{\nabla}^{\mu} h.\end{aligned} \tag{C.2}$$

The bracketed prefactor of the second term vanished for $\beta = 0$ making the gauge fixing independent of the trace h. But then also, $\bar{\nabla}_{\nu} h^{\nu\mu\ TF}$ is exclusively longitudinal such that, when carrying over to the full Yorck decomposition (6.2), the transverse traceless mode $h^{TT}_{\mu\nu}$ does not enter the gauge fixing. That is why we think about this mode as the gauge independent and, since it is also numerically dominating, the physical mode.
Now, if we fix $\alpha = 0$ in the gauge fixing (4.12), we ensure an exact implementation of the gauge fixing in the sense that the integral kernel tends towards a δ distribution, and thus the gauge fixing condition gets reduced even further to the statement that only $h^{TT}_{\mu\nu}$ and h will be able to propagate. This can also be shown by explicitly computing all propagators [206]. We conclude that the gauge fixing $\alpha = 0$, $\beta = 0$ significantly simplifies our computations, which is why we use it throughout part III of this thesis, and leave the study of dependencies of the results of the choice of gauge parameters for later work.

C.3 Projectors

Any vector v_{μ} can be decomposed into its transverse and longitudinal components through the projectors

$$\begin{aligned}\Pi^{T}_{\mu\nu} &= \delta_{\mu\nu} - \frac{p_{\mu}p_{\nu}}{p^2}, \\ \Pi^{L}_{\mu\nu} &= \frac{p_{\mu}p_{\nu}}{p^2}.\end{aligned} \tag{C.3}$$

This decomposition is orthogonal and we can then write

$$v_{\mu} = v^{T}_{\mu} + v^{L}_{\mu} = \Pi^{T}_{\mu\nu} v^{\nu} + \Pi^{T}_{\mu\nu} v^{\nu}.$$

This is possible, because the projectors (C.3) form a basis of the space of symmetric rank two tensors. Similar systems can be found for tensors of higher rank, even

though they are usually much more difficult to access. For instance, for the York decomposition [183–185] as used in equation (6.2) or chapter 10, expressions for the projectors on the spin 0 modes are unknown. A potential way out is the Stelle decomposition [52], which differs from the Yorck decomposition in the spin 0 modes. However, in this thesis we only explicitly need the transverse traceless propagator. It is given by

$$\Pi^{TT}_{\mu\nu\rho\sigma} = \frac{1}{2}\left(\Pi^{T}_{\mu\rho}\Pi^{T}_{\nu\sigma} + \Pi^{T}_{\mu\sigma}\Pi^{T}_{\nu\rho}\right) - \frac{1}{3}\Pi^{T}_{\mu\nu}\Pi^{T}_{\rho\sigma}. \tag{C.4}$$

We use it at two points during the derivation of the flat flow equations: Firstly, we decompose the graviton into its York components. After having done so, inversion is straightforward: We can write the full propagator in matrix notation, see the explicit formula in the background derivation (6.5), invert the block diagonal matrix, and add the TT projector to the transverse traceless component, since it is the corresponding basis element.
Secondly, to extract $\mathrm{Flow}^{(2)}_{h_{TT}h_{TT}}$ from the diagrammatic expressions, which amounts to tracing over spacetime indices in the process of carrying out the Supertrace in equation (1.19), we also use the TT projector (C.4).

C.4 Vertex Construction and Regulator

We implement the regularization of our theory by replacing

$$p^2 \to p^2 + r_k(p^2),$$

to form the fully dressed propagator

$$G := \left(\Gamma_k^{(2)} + \mathcal{R}_k\right)^{-1},$$

where the k-dependent function $r_k(p^2)$ realizes an optimized Litim cutoff [186, 187],

$$r(x) = \frac{1-x}{x}\Theta\left(1-x\right). \tag{C.5}$$

Then, consider the flow equation (1.19) for the effective action, from which the flow equations for the n-point function are derived by means of functional derivation.

Schematically we can write

$$\begin{aligned}\partial_t \Gamma &\sim \frac{\dot{\mathcal{R}}_k}{\Gamma^{(2)} + \mathcal{R}_k} \\ &= \frac{\dot{\Gamma_k^{(2)}}(p^2) - \dot{\Gamma_k^{(2)}}\left(p^2 + r_k(p^2)\right)}{\Gamma_k^{(2)}\left(p^2 + r_k(p^2)\right).}\end{aligned} \tag{C.6}$$

At this point, we need an ansatz for the 2-point functions to carry out our vertex construction. Focusing on $\Gamma^{(2)}_{\chi\chi}$, we set

$$\Gamma^{(2)}_{\chi\chi} = Z\left(K(\bar{\chi}^2)p^2 + 2V'(\bar{\chi}^2) + 4\bar{\chi}^2 V''(\bar{\chi}^2)\right),$$

which is just the well known inverse propagator for a rescaled scalar field $\bar{\chi}^2 = Z\chi^2$, which should not be confused with the background field, with the additional function $K(\chi^2)$. It becomes visible at this stage already that we will need to set a relative scaling of Z and K to avoid double ambiguities. Note that on a flat background $\bar{R} = 0$, and thus no terms proportional to $F(\bar{\chi}^2)$ should enter. All other 2-point function will just be set to be their respective functional derivatives of Γ from equation (3.6).
Now, going back to equation (C.6), we can write

$$\begin{aligned}\partial_t \Gamma &\sim \frac{\partial_t\left(ZK(\bar{\chi}^2)r\right)}{Z} G\,|_{Z=1} \\ &\sim K(\bar{\chi}^2)\left(\dot{r} - \eta r\right) G\,|_{Z=1}\,.\end{aligned} \tag{C.7}$$

Note that in the second step we neglected RG time derivatives of the function K, which is consistent with neglecting all RG time derivatives on the RHS of the flow equation in the current analysis, and corresponds to neglecting $\dot{F}$ in the equivalent expressions with the graviton 2 point function.
Having understood the construction for a pure scalar two point function, the generalization to mixed two point functions as well as higher order correlation functions that enter, once we differentiate equation (1.19) twice with respect to χ or $h^{\mu\nu}_{TT}$ is straightforward. The crucial ingredient is to require any n-point function to scale according to

$$\Gamma^{(n\chi\, m\hat{h})} \propto Z^{\frac{n}{2}},$$

C.4.1 Z Factors from the Vertex Construction

More explicitly, we use equations (4.17) with

$$\Gamma^{(n\chi m\hat{h})}(p_1,\dots,p_{n+m}) = Z^{\frac{n}{2}}\frac{\delta^{n+m}}{\delta\bar{\chi}^n\delta\hat{h}^m}\Gamma(p_1,\dots,p_{n+m}). \tag{C.8}$$

Note how at this point also the generalization to more than one wave function renormalization is straightforward but would, however, require the flows of the 3-point functions to distinguish wave function renormalizations from couplings for the graviton modes.
The first point we want to make here is that for a mixed two point function, the above derivation goes through almost exactly alike, with the slight complication that now there is a term $\partial_t Z^{1/2}$, which, however, is of course simple to calculate, and the result is the one stated in equation (10.4).
The second point concerns higher correlation functions entering diagrammatic expansions like the ones we showed in figure 4.1. For simplicity, assume that we introduce wave function renormalization for all fields ϕ_i and call them Z_i. We can of course set an arbitrary number equal to 1 if desired. We further assume that there are n distinct fields at an n-point vertex to simplify combinatorics. Again, setting $\phi_i = \phi_j$ is straightforward. Then, an n-point vertex $\Gamma^{(n)}$ scales like $\sqrt{Z_1 Z_2 \dots Z_n}$, and has n propagators attached. If we assume there is no regulator insertion, then each regulator scales like $(Z_i)^{-1/2}$, so the contraction is Z independent like it should be. Adding the regulator, whenever the RG time derivative in $\partial_t\mathcal{R}_k$ hits a Z it gets combined to η, and whenever it hits anything else, the Z factors drop out again. That is why our schematic derivation also holds once higher correlation functions are involved.

C.4.2 Bounds the Anomalous Dimensions

In equation (C.7), we derived that

$$\partial_t\mathcal{R}_k \sim \dot{r} - \eta r.$$

This must not become negative, as otherwise the suppression of momentum modes would be turned around. This condition depends on the choice of shape function. Considering the limit $k \gg p$ for the shape function (C.5), which we only use in the bosonic case, we arrive at the bound

$$\eta < 2.$$

For details or the fermionic case, see [206].

C.5 Master Equation

We explain how to arrive at diagrammatic expansions like the ones shown in figure 4.1. For a complete, closed formula we refer to [48, 192].
Start from the flow equation (1.19). Then, the flow of the n-point function of an arbitrary field ϕ is derived by taking n functional derivatives with respect to ϕ. The field dependent quantity is the fully dressed propagator

$$G = \left(\Gamma^{(2)} + \mathcal{R}_k\right)^{-1}.$$

For a general invertable tensor $T(\phi)$ we have

$$\begin{aligned} 1 &= T(\phi)T^{-1}(\phi) \\ \Rightarrow 0 &= \left(\frac{\delta}{\delta\phi}T(\phi)\right)T^{-1}(\phi) + T(\phi)\left(\frac{\delta}{\delta\phi}T^{-1}(\phi)\right) \\ \Rightarrow \frac{\delta}{\delta\phi}T^{(-1)}(\phi) &= -T^{-1}(\phi)\frac{\delta T(\phi)}{\delta\phi}T(\phi)T^{-1}(\phi). \end{aligned} \tag{C.9}$$

Then G evolves to

$$\frac{\delta}{\delta\phi}G = -G\Gamma^{(3)}G,$$

and further to

$$\frac{\delta^2}{\delta\phi^2} = 2G\Gamma^{(3)}G\Gamma^{(3)}G - G\Gamma^{(4)}G,$$

where we have dropped all indices to unclutter notation.
After inserting the RG time derivative of the regulator $\partial_t\mathcal{R}_k$, carrying out the supertrace and adding the prefactor, this is exactly what is represented in the upper pane of figure 4.1. The specific expressions for scalar and transverse traceless graviton mode are derived exactly like this, only taking care of the different field combinations that can enter propagators and vertices.

C.6 Momentum Integrals

Having set $x = \cos(\theta)$, where θ is the angle between loop and external momentum, we necessarily pick up an additional factor of $\sqrt{1-x^2} = \sin(\theta)$ from the volume element. Directly solving these momentum integrals is impossible given the size of the expressions. But note that all combinations that can enter the flow are of the form $x^n\sqrt{1-x^2}$ with n an integer. Then, expanding all expressions in powers of x

we can solve the angular integrals by setting

$$x^n\sqrt{1-x^2} = \begin{cases} \frac{\pi}{2} & \text{if } n = 0, \\ 0 & \text{if } n = 1, \\ \frac{\sqrt{\pi}}{2}\frac{\Gamma\left(\frac{1+n}{2}\right)}{\Gamma\left(2+\frac{n}{2}\right)} & \text{if } n \text{ is even}, \\ 0 & \text{if } n \text{ is odd}, \end{cases} \tag{C.10}$$

in exchange for the angular integral $\int \mathrm{d}\Omega x^n\sqrt{1-x^2}$.

APPENDIX D

Flat Flow Equations

D.1 K(y) as a Coupling

$$\begin{aligned}0 =&\frac{355f_0^3}{5184\pi^2(2v_0-f_0)^3}+\frac{f_0^3}{64\pi^2(4v_0-3f_0)^3}+\frac{395f_0^2}{2592\pi^2(2v_0-f_0)^2}\\&+\frac{f_0^2}{12\pi^2(4v_0-3f_0)^2}+\frac{25f_0}{864\pi^2(2v_0-f_0)}+\frac{5f_0}{144\pi^2(4v_0-3f_0)}-4v_0-\frac{1}{192\pi^2}\end{aligned} \tag{D.1}$$

$$\begin{aligned}0 =&-\frac{5f_0^4}{384\pi^2(2v_0-f_0)^4}-\frac{3f_0^4}{128\pi^2(4v_0-3f_0)^4}-\frac{185f_0^3}{1296\pi^2(2v_0-f_0)^3}\\&-\frac{235f_0^2}{1152\pi^2(2v_0-f_0)^2}+\frac{233f_0^2}{576\pi^2(4v_0-3f_0)^2}+\frac{115f_0}{1152\pi^2(2v_0-f_0)}\\&-\frac{305f_0}{1728\pi^2(4v_0-3f_0)}-\frac{1}{384\pi^2}-2f_0\end{aligned} \tag{D.2}$$

$$0 =\frac{k_0}{24\pi^2(4v_0-3f_0)}-\frac{f_0k_0}{8\pi^2(4v_0-3f_0)^2} \tag{D.3}$$

D.2 Introducing the Anomalous Dimension η

$$
\begin{aligned}
0 = &- \frac{2048 v_0^7}{(3f_0 - 4v_0)^3 (f_0 - 2v_0)^3} + \frac{7680 f_0 v_0^6}{(3f_0 - 4v_0)^3 (f_0 - 2v_0)^3} \\
&- \frac{8 v_0^6}{3\pi^2 (3f_0 - 4v_0)^3 (f_0 - 2v_0)^3} - \frac{11904 f_0^2 v_0^5}{(3f_0 - 4v_0)^3 (f_0 - 2v_0)^3} \\
&+ \frac{590 f_0 v_0^5}{27\pi^2 (3f_0 - 4v_0)^3 (f_0 - 2v_0)^3} + \frac{9760 f_0^3 v_0^4}{(3f_0 - 4v_0)^3 (f_0 - 2v_0)^3} \\
&- \frac{4979 f_0^2 v_0^4}{162\pi^2 (3f_0 - 4v_0)^3 (f_0 - 2v_0)^3} - \frac{4464 f_0^4 v_0^3}{(3f_0 - 4v_0)^3 (f_0 - 2v_0)^3} \\
&+ \frac{239 f_0^3 v_0^3}{54\pi^2 (3f_0 - 4v_0)^3 (f_0 - 2v_0)^3} + \frac{1080 f_0^5 v_0^2}{(3f_0 - 4v_0)^3 (f_0 - 2v_0)^3} \\
&+ \frac{1073 f_0^4 v_0^2}{72\pi^2 (3f_0 - 4v_0)^3 (f_0 - 2v_0)^3} - \frac{108 f_0^6 v_0}{(3f_0 - 4v_0)^3 (f_0 - 2v_0)^3} \\
&- \frac{26 f_0^5 v_0}{3\pi^2 (3f_0 - 4v_0)^3 (f_0 - 2v_0)^3} + \frac{81 f_0^6}{64\pi^2 (3f_0 - 4v_0)^3 (f_0 - 2v_0)^3} \\
&+ \frac{\eta_0}{1920\pi^2}
\end{aligned}
\tag{D.4}
$$

$$
\begin{aligned}
0 = &- \frac{5 f_0^4}{384\pi^2 (2v_0 - f_0)^4} - \frac{3 f_0^4}{128\pi^2 (4v_0 - 3f_0)^4} \\
&- \frac{185 f_0^3}{1296\pi^2 (2v_0 - f_0)^3} - \frac{235 f_0^2}{1152\pi^2 (2v_0 - f_0)^2} \\
&+ \frac{233 f_0^2}{576\pi^2 (4v_0 - 3f_0)^2} + \frac{115 f_0}{1152\pi^2 (2v_0 - f_0)} \\
&- \frac{305 f_0}{1728\pi^2 (4v_0 - 3f_0)} - 2f_0 - \frac{1}{384\pi^2}
\end{aligned}
\tag{D.5}
$$

$$
\eta_0 = \frac{3f_0 - 2v_0}{12\pi^2 (3f_0 - 4v_0)^2} + \frac{\eta_0}{192\pi^2 (3f_0 - 4v_0)}
\tag{D.6}
$$

APPENDIX E

Notes on Classical Dilaton Gravity

Building on our discussion of scalar fields in gravity in section 3.1, we give the classical field equations for the action (3.6), where we replaced $\chi^2 \to \chi$ for convenience, obtained by varying w.r.t to the metric $g_{\mu\nu}$ as well as to the scalar field χ. We neglect possible energy momentum tensors.
Using standard tensor calculus, $\frac{\delta \Gamma}{\delta g^{\mu\nu}} = 0$ yields

$$\begin{aligned} 0 =& F\left(R_{\mu\nu} - \frac{1}{2}R\, g_{\mu\nu}\right) + \Box F g_{\mu\nu} - \nabla_\mu \nabla_\nu F \\ &+ V g_{\mu\nu} + \frac{1}{2}K\partial^\rho\chi\partial_\rho\chi g_{\mu\nu} - K\partial_\mu\chi\partial_\nu\chi. \end{aligned} \tag{E.1}$$

Here, $\Box = \nabla^\mu\nabla_\mu$, where ∇_μ is the covariant derivative. $\frac{\delta \Gamma}{\delta \chi} = 0$ on the other hand gives

$$\nabla_\mu\left(K\partial^\mu\chi\right) + \partial_\chi V = \frac{1}{2}\left[(\partial_\chi F)R - (\partial_\chi K)\partial_\mu\chi\partial^\mu\chi\right]. \tag{E.2}$$

Note that this only reduces to the curved generalization of the Klein-Gordan equation $K\Box\chi + \partial_\chi V = 0$ well known from scalar field theories if F and K are field independent.[1]
In reminiscence of the classical Einstein field equations

$$G_{\mu\nu} + \Lambda g_{\mu\nu} = T_{\mu\nu},$$

[1] Note that $\Box$ explicitly contains the spacetime connection, for a scalar field $\Box = \nabla_\mu\partial^\mu$.

where $G_{\mu\nu}$ is the Einstein and $T_{\mu\nu}$ the energy momentum tensor, we call the term multiplying the metric the effective cosmological constant throughout this thesis. In equation (E.1) there are contributions from all three functions V, F and K to the effective cosmological constant. Since we will regard scalar contributions as contributions to the effective cosmological constant rather than to the energy momentum tensor, the latter does not play a role in our treatment. However, it is exactly this equivalence that triggers the connection between the cosmological constant and the vacuum energy [119, 120].

APPENDIX F

Diffeomorphisms and Lie Derivatives

This appendix serves as a brief introduction to diffeomorphisms as the gauge group of general relativity and their action on the dynamical degrees of freedom. This can infinitesimally best be described with the help of Lie derivatives, as was done already in equation (2.5). We follow the treatment outlined in [207].

F.1 Coordinate Transformations and Diffeomorphisms

Let us begin with a brief discussion concerning the classification of diffeomorphisms as the gauge group of general relativity. Let

$$\begin{aligned} \Phi: \quad M &\to N \\ p &\mapsto \Phi(p), \end{aligned} \tag{F.1}$$

where M and N are manifolds with $\dim M = \dim N = n$ and $p \in M$. Φ is called a diffeomorphism if $\Phi \in C^\infty$ is one-to-one, onto and Φ^{-1} exists as well as $\Phi^{-1} \in C^\infty$ holds.
Two manifolds M and N are said to be diffeomorphic if a diffeomorphism Φ exists between them. Diffeomorphic manifolds have the same manifold structure and thus the spacetime structure will result in equivalent physics. To understand this statement in greater detail, let us find a definition of a diffeomorphism based on our knowledge of mappings on the vector space $\mathbb{R}^n$ rather than on the abstract manifolds M and N. Let $a \in M$ and $b \in N$ be points on the manifolds and Ψ_a and Ψ_b local

coordinate charts defined on neighborhoods U_a and U_b, i.e.

$$\begin{aligned} \Psi_a : \quad & U_a \subset M \quad \to \mathbb{R}^n, \\ \Psi_b : \quad & U_b \subset N \quad \to \mathbb{R}^n. \end{aligned} \tag{F.2}$$

We can then introduce the notion of a C^∞ map between manifolds resorting to ordinary functions on $\mathbb{R}^n$ via the identification

$$\Phi \in C^\infty \quad \Leftrightarrow \quad \Psi_b \circ \Phi \circ \Psi_a^{-1} \in C^\infty, \tag{F.3}$$

illustrating how M and N have identical manifold structure.
It is in this sense that diffeomorphisms are to be understood as the gauge group of general relativity. If two spacetime manifolds are diffeomorphic, the physics in the context of general relativity are equivalent, and therefore altering the spacetime by means of the action of a diffeomorphism is a gauge freedom.
To this end, it is useful to familiarize oneself with the two different viewpoints that can be taken when considering a diffeomorphism. The perspective taken so far is an active one, as a point $p \in M$ was carried over to a different point $\Phi(p) \in M$[1] and with that, all tensor quantities are now evaluated at $\Phi(p)$. On the other hand, we could also use local charts Ψ_p and $\Psi_{\Phi(p)}$ acting on $U_p \subset M$ and $U_{\Phi(p)} \subset M$, respectively, and defining local coordinate systems $\{x^\mu\}$ and $\{y^\mu\}$ to understand the action of Φ as defining a new local coordinate system $\{x'^\mu\}$ on $U'_p = \Phi^{-1}(U_{\Phi(p)})$ via the identification

$$x'^\mu(q) = y^\mu(\Phi(q)) \qquad \forall\, q \in U'_p. \tag{F.4}$$

This second, passive point of view demonstrates why invariance under general coordinate transformations is equivalent to requiring the action of diffeomorphisms to represent a gauge freedom.
For our later applications, we will need the notion of a one-parameter group of diffeomorphisms. Let

$$\begin{aligned} \Phi_t : \quad \mathbb{R} \times M \quad &\to \quad M, \\ (t, p) \quad &\mapsto \quad \Phi_t(p), \end{aligned} \tag{F.5}$$

and require the map Φ_t to be a diffeomorphism for fixed $t \in \mathbb{R}$. We call Φ_t a one-paramter group of diffeomorphisms, if for $s, t \in R$

$$\Phi_s \circ \Phi_t = \Phi_{s+t} \tag{F.6}$$

[1] Since M and N are assumed to be diffeomorphic and thus equivalent from a physical point of view, we will resort to diffeomorphisms $\Phi : M \to M$.

holds. We can now naturally associate a vector field v with Φ_t as follows. For fixed $p \in M$, $\Phi_t : \mathbb{R} \to M$ defines a curve on the manifold M. Define $v(p)$ to be the tangent to this curve at $t = 0$, i.e. at the point p. Then v is a vector field on M and generates the infinitesimal version of the transformation induced by Φ_t.

F.2 Maps of Manifolds

Let us go back one step and consider an arbitrary C^∞ map

$$\begin{aligned} \Phi: \quad & M \to N \\ & p \mapsto \Phi(p), \end{aligned} \tag{F.7}$$

where now M and N do not necessarily need to have the same dimension anymore. We can use Φ to define a pull-back of a function $f : N \to \mathbb{R}$ onto the manifold M by considering $f \circ \Phi : M \to \mathbb{R}$. In a similar manner, we can use Φ to identify tangent vectors at $p \in M$ with tangent vectors at $\Phi(p) \in N$ by virtue of the map Φ^*, defined as

$$\begin{aligned} \Phi^*: \quad T_pM &\to T_{\Phi(p)}M, \\ v &\mapsto \Phi^* v, \end{aligned} \tag{F.8}$$

where $\Phi^* v$ is defined with the help of the pull-back $f \circ \Phi$ to act on a smooth function f as

$$(\Phi^* v)(f) = v(f \circ \Phi). \tag{F.9}$$

An identical construction can be utilized to introduce a map Φ_* which identifies cotangent vectors $w \in T_{\Phi(p)}M^*$ with their canonical counterparts in T_pM^*, requiring

$$(\Phi_* w)v = w(\Phi^* v) \tag{F.10}$$

for any $v \in T_pM$. The action of Φ^* can be extended in a natural way to $(l, 0)$-tensor fields $T^{\mu_1 \dots \mu_l}$ and the action of $\Phi_*$to $(0, k)$-tensor fields $T_{\nu_1 \dots \nu_k}$ as

$$\begin{aligned} (\Phi^* T)^{\mu_1 \dots \mu_l}(w_1)_{\mu_1} \dots (w_l)_{\mu_l} &= T^{\mu_1 \dots \mu_l}(\Phi^* w_1)_{\mu_1} \dots (\Phi^* w_l)_{\mu_l} \\ (\Phi_* T)_{\nu_1 \dots \nu_k}(v_1)^{\nu_1} \dots (v_k)^{\nu_k} &= T_{\nu_1 \dots \nu_k}(\Phi_* v_1)^{\nu_1} \dots (\Phi_* v_k)^{\nu_k}, \end{aligned} \tag{F.11}$$

where we introduced the usual index notation for vectors and their duals and used equation (F.10) to rewrite our original condition (F.9). Note that Φ^* only acts on upper indices, whereas the action of Φ_* is limited to lower indices. Thus, so far we are unable to transform tensors of type (l, k) for both l and k being nonzero. However,

if Φ is both one-to-one, onto, and if in addition Φ^{-1} exists and is in C_∞ as well (i.e. if Φ is a diffeomorphism, equation (F.1)), we can extend the action of Φ^* to tensors of arbitrary type by using the fact that for a diffeomorphism, $\Phi^{-1} : N \to M$ and thus, identifying M with N as before,

$$\left(\Phi^{-1}\right)^* : \quad T_{\Phi(p)}M^* \to T_pM^*, \tag{F.12}$$

which leads to

$$\begin{aligned}&(\Phi^*T)^{\mu_1\dots\mu_l}{}_{\nu_1\dots\nu_k}\ (v_1)^{\nu_1}\dots(v_k)^{\nu_k}\ (w_1)_{\mu_1}\dots(w_l)_{\mu_l}\\ =&T^{\mu_1\dots\mu_l}{}_{\nu_1\dots\nu_k}\ ((\Phi^{-1})^*v_1)^{\nu_1}\dots((\Phi^{-1})^*v_k)^{\nu_k}\ (\Phi^*w_1)_{\mu_1}\dots(\Phi^*w_l)_{\mu_l}.\end{aligned} \tag{F.13}$$

It is of course also possible to perform the corresponding construction, using Φ_* instead of Φ^*.

F.3 The Lie Derivative

Let us now proceed to define the Lie derivative $\mathcal{L}_v$ along a vector field v. In order to do so, let Φ_t be a one-parameter group of diffeomorphisms that generates the vector field v. For a small t, we define $\mathcal{L}_v$ to be the change in a tensor field as $T^{\mu_1\dots\mu_l}{}_{\nu_1\dots\nu_k}$ is carried over to $\Phi^*_{-t}T^{\mu_1\dots\mu_l}{}_{\nu_1\dots\nu_k}$, more precisely

$$\mathcal{L}_v\, T^{\mu_1\dots\mu_l}{}_{\nu_1\dots\nu_k}\ \big|_p = \lim_{t\to 0}\left[\frac{\left(\Phi^*_{-t}T^{\mu_1\dots\mu_l}{}_{\nu_1\dots\nu_k}\right) - T^{\mu_1\dots\mu_l}{}_{\nu_1\dots\nu_k}}{t}\right]_p. \tag{F.14}$$

By virtue of defining v to be tangent to the curve Φ_t (equation (F.5)) this definition is reduced to

$$\mathcal{L}_v\, f = v(f) \tag{F.15}$$

for smooth functions $f : M \to \mathbb{R}$, for instance if taking f to be the scalar field considered in this thesis.
Note that (F.14) defines a linear map on the space of all (l,k)-tensor fields and satisfies the Leibniz rule.
We will now derive a local coordinate representation of the Lie derivative (F.14). Let us begin by assuming that we elect a local coordinate basis such that $v = \partial_1$. Then the action of Φ_{-t} from the passive point of view is simply a shift in the first coordinate with all others held fixed, namely $\Phi_{-t} : (x_1,\dots,x_n) \mapsto (x_1+t,\dots,x_n)$.

But that means that the Lie derivative has a local coordinate representation reading

$$\mathcal{L}_v\, T^{\mu_1\cdots\mu_l}{}_{\nu_1\ldots\nu_k}\ \big|_{p\leftrightarrow(x_1,\ldots,x_n)} = \frac{\partial T^{\mu_1\cdots\mu_l}{}_{\nu_1\ldots\nu_k}}{\partial x_1}\ \big|_{p\leftrightarrow(x_1,\ldots,x_n)}\ . \tag{F.16}$$

To obtain a more general expression, we expand v as well as an arbitrary vector w to

$$w = w^\mu \partial_\mu \quad \text{and} \quad v = v^\mu \partial_\mu,\ v^\mu = \delta^\mu{}_1. \tag{F.17}$$

Computing the commutator $[v, w]$ we find

$$\begin{aligned}[v,w] &= (v^\nu \partial_\nu)(w^\mu \partial_\mu) - (w^\nu \partial_\nu)(v^\mu \partial_\mu) \\ &= \partial_1 w^\mu \partial_\mu \\ &= \mathcal{L}_v(w^\mu \partial_\nu),\end{aligned} \tag{F.18}$$

and therefore, for an arbitrary vector field w we have

$$\mathcal{L}_v w = [v, w], \tag{F.19}$$

which is our desired local coordinate expression. Note that at this point we can resort to the covariant derivative ∇_μ, writing

$$\mathcal{L}_v w = [v, w] = (v^\nu \nabla_\nu)(w^\mu \nabla_\mu) - (w^\nu \nabla_\nu)(v^\mu \nabla_\mu). \tag{F.20}$$

Expressions for higher order tensors can be obtained by using (F.15), (F.19) as well as the Leibniz rule for the Lie derivative acting on the scalar function $v^\mu w_\mu$. By induction, the most general result reads

$$\begin{aligned}\mathcal{L}_v\, T^{\mu_1\cdots\mu_l}{}_{\nu_1\ldots\nu_k} =& v^\rho \nabla_\rho\, T^{\mu_1\cdots\mu_l}{}_{\nu_1\ldots\nu_k} \\ &- \sum_{i=1}^{l} T^{\mu_1\ldots\sigma\ldots\mu_l}{}_{\nu_1\ldots\nu_k}\, \nabla_\sigma v^{\mu_i} \\ &+ \sum_{i=1}^{k} T^{\mu_1\cdots\mu_l}{}_{\nu_1\ldots\sigma\ldots\nu_k}\, \nabla_{\nu_i} v^\sigma,\end{aligned} \tag{F.21}$$

where σ is substituted into the ith slot. Specializing to the metric $g_{\mu\nu}$, we use $\nabla_\rho\, g_{\mu\nu} = 0$ and obtain

$$\mathcal{L}_v g_{\mu\nu} = \nabla_\mu v^\sigma g_{\sigma\nu} + \nabla_\nu v^\sigma g_{\sigma\mu}, \tag{F.22}$$

which is the same as equation (2.5).

APPENDIX G

Dilatations and Conformal Transformations

This appendix serves both to give a more precise mathematical meaning to the notion of conformal and scale invariance as well as to discuss the physical implications of both concepts. Large portions of this section have been inspired by works on conformal field theory and string theory [208, 209], where conformal invariance on the two-dimensional worldsheet is a crucial property, but we also refer to less generalized physical literature such as [210] and works on canonical quantum gravity [211] for further discussion.

G.1 The Conformal Group

Let us begin with the discussion of the conformal group in d spacetime dimensions. As laid out in appendix F, a physical theory of general relativity is characterized by the structure of its spacetime manifold M, which in turn is identified with metric $g_{\mu\nu}$. We define a conformal transformation Φ as a scaling of the metric by a factor, namely

$$\Phi: \quad g_{\mu\nu}(x) \mapsto \Omega(x)\, g_{\mu\nu}(x), \tag{G.1}$$

where we emphasize the spacetime dependence of both the metric and the conformal factor $\Omega(x)$. To obtain infinitesimal counterparts of (G.1) on the level of local coordinates, we assume that one can write

$$\Phi_x: \quad x^\mu \mapsto x^\mu + \epsilon^\mu \tag{G.2}$$

for a suitable to choice of ϵ. In order to derive constraints on ϵ, we consider the line element $g_{\mu\nu}\,\mathrm{d}x^\mu\,\mathrm{d}x^\nu$, which transforms under (G.2) as

$$\begin{aligned}\Phi_x\left(g_{\mu\nu}\,\mathrm{d}x^\mu\,\mathrm{d}x^\nu\right) &= g_{\mu\nu}\,\mathrm{d}\left(x^\mu+\epsilon^\mu\right)\,\mathrm{d}\left(x^\nu+\epsilon^\nu\right)\\ &= g_{\mu\nu}\,\mathrm{d}x^\mu x^\nu + \left(\partial_{\,\mu}\epsilon_\nu + \partial_{\,\nu}\epsilon_\mu\right)\,\mathrm{d}x^\mu\,\mathrm{d}x^\nu.\end{aligned} \tag{G.3}$$

However, we may also write

$$\Phi\left(g_{\mu\nu}\,\mathrm{d}x^\mu\,\mathrm{d}x^\nu\right) = \Omega(x) g_{\mu\nu}\,\mathrm{d}x^\mu\,\mathrm{d}x^\nu, \tag{G.4}$$

leading to

$$\left(\Omega(x)-1\right) g_{\mu\nu} = \partial_{\,\mu}\epsilon_\nu + \partial_{\,\nu}\epsilon_\mu \quad \Rightarrow \quad \Omega(x) - 1 = \frac{2}{d}\left(\partial\cdot\epsilon\right), \tag{G.5}$$

or, combining the two previous equations,

$$\frac{2}{d}\left(\partial\cdot\epsilon\right) g_{\mu\nu} = \partial_{\,\mu}\epsilon_\nu + \partial_{\,\nu}\epsilon_\mu. \tag{G.6}$$

From here on it can be shown using standard tensor calculus that the constraint (G.6) leads to a fairly limited possible form of ϵ^μ provided $d > 2$, reading

$$\epsilon^\mu = a^\mu - \omega^{\mu\nu}x_\nu - \lambda x^\mu + \left(b^\mu\left(x\cdot x\right) - 2x^\mu\left(b\cdot x\right)\right), \tag{G.7}$$

where $\omega^{\mu\nu}$ is antisymmetric. Thus, the d-dimensional conformal group has $(d + d(d-1)/2+1+d)$ generators, corresponding to translations, Lorentz transformations, dilatations and proper conformal transformations, respectively. Hence, the conformal group consists of the Poincaré group appended by proper conformal transformations and their global counterparts, the dilatations. As will be apparent shortly, the latter are of paramount importance for the physical aim of this thesis.
The case $d = 2$ is special, as may already be seen from (G.6). As is revealed in the course of the derivation of equation (G.7), all constraints vanish for $d = 2$ and we obtain an infinite numbers of generators, rendering the study of 2-dimensional conformal field theories especially fascinating, because a wide class of theories is actually completely soluble just from the requirement of conformal invariance.

G.2 Physical Implications

Restricting ourselves to global rescalings that act on local coordinates via $x^\mu \mapsto \lambda x^\mu$, we may define the scaling dimension of a dynamical physical quantity z as the number s which enters the transformation law $z \mapsto \lambda^s z$. In the context of quantum gravity, it is customary to think of scale transformations as transformations acting on the fields

rather than on the coordinates, thereby using coordinates as labels for spacetime points only. That means for reasons of consistency that the metric $g_{\mu\nu}$ needs to scale as $g_{\mu\nu} \mapsto \lambda^2 \, g_{\mu\nu}$. To determine the scaling dimensions of all other fields ϕ_i and couplings g_j, we use the requirement that the (effective) action needs to be dimensionless, that is $\Gamma \mapsto \Gamma$, which is equivalent to

$$\Gamma \left[g_{\mu\nu}, \phi_i, g_j \right] = \Gamma \left[\lambda^2 g_{\mu\nu}, \lambda^{s_i} \phi_i, \lambda^{s_j} g_j \right]. \tag{G.8}$$

From (G.8) it follows that a rescaling of all dimensionful quantities is always an exact symmetry of the theory. However, the rescaling of the coupling coefficients is not included in the transformation law expressed in and (G.1) and (G.7), as the couplings are taken to be independent of spacetime.[1] But that means that true dilatations opposed to simple rescalings act on the action as

$$\Gamma \left[g_{\mu\nu}, \phi_i, g_j \right] \mapsto \Gamma \left[\lambda^2 g_{\mu\nu}, \lambda^{s_i} \phi_i, g_j \right], \tag{G.9}$$

leading to a condition for an action to be invariant under dilatations:

$$\begin{gathered} \Gamma \text{ is invariant under dilatations} \\ \Updownarrow \\ \text{all couplings } g_j \text{ have scaling dimension 0.} \end{gathered}$$

Up to now, we did not comment on the connection between the canonical length dimension and the scaling dimension. At the beginning of this section stood the statement that we will consider scalings and dilatations as transformations on the fields and coordinates as labels for spacetime points only. Thus, coordinates can not carry a physical dimension. It is due to this approach that the scaling dimension of $g_{\mu\nu}$ is 2, whereas its canonical length dimension is 0. Nevertheless, both viewpoints agree on the level of physical quantities, the simplest of which is the line element $\mathrm{d}s^2 = g_{\mu\nu} \, \mathrm{d}x^\mu \, \mathrm{d}x^\nu$. Here, we can treat either the metric or the differentials as dimensionless. The same is true for the volume form $\mathrm{d}^d x \sqrt{g}$ or the scalar kinetic term $g_{\mu\nu} \, \partial^\mu \phi \, \partial^\nu \phi$, where the latter example shows that both the canonical length and scaling dimension of a scalar field are equal to -1, corresponding to a mass dimension of $+1$. Thus, when it comes to singling out the terms allowed by the requirement of dilatation symmetry, we may adopt either strategy.

We emphasize that in a dilatation symmetric theory, the only nontrivial notion of dimension arises from a scalar field. Thus, the notion of dilatation symmetry takes the ideas that sparked the original idea of a scalar-tensor theory by Brans and Dicke [20, 21] to the next level and has been discussed vividly in literature ever since [212]. On a technical level, a scale is generated from a scalar field if dilatation

[1] If we aim to introduce a spacetime dependence of a coupling parameter, we would have to replace it by a scalar field. This is what was described in section 3.1.

symmetry is spontaneously broken and a nonzero expectation value of the scalar field arises. The associated massless Goldstone boson is usually referred to as the dilaton [144].

APPENDIX H

Lists

H.1 List of Figures

H.2 List of Tables

APPENDIX I

Bibliography

[1] **LIGO Scientific Collaboration and Virgo Collaboration** Collaboration, B. P. Abbott *et al.*, "Observation of Gravitational Waves from a Binary Black Hole Merger," *Phys. Rev. Lett.* **116** no. 6, (2016) 61102, arXiv:1602.03837. http://link.aps.org/doi/10.1103/PhysRevLett.116.061102.

[2] **ATLAS Collaboration** Collaboration, G. Aad *et al.*, "Observation of a new particle in the search for the Standard Model Higgs boson with the ATLAS detector at the LHC," *Phys.Lett.B* (2012) , arXiv:1207.7214 [hep-ex].

[3] **CMS Collaboration** Collaboration, S. Chatrchyan *et al.*, "Observation of a new boson at a mass of 125 GeV with the CMS experiment at the LHC," *Phys.Lett.B* (2012) , arXiv:1207.7235 [hep-ex].

[4] S. Deser and P. van Nieuwenhuizen, "One loop divergencies of quantized einstein-maxwell fields," *Phys. Rev. D* **10** (1974) 401.

[5] G. 't Hooft and M. J. G. Veltman, "One loop divergencies in the theory of gravitation," *Ann. Inst. Henri Poincare A* **20** (1974) 69–94.

[6] J. F. Donoghue, "Introduction to the effective field theory description of gravity," arXiv:gr-qc/9512024 [gr-qc].

[7] C. P. Burgess, "Quantum gravity in everyday life: General relativity as an effective field theory," *Living Reviews in Relativity* **7** no. 5, (2004) .

[8] S. Weinberg, "Ultraviolet divergences in quantum theories of gravitation," in *General Relativity: An Einstein Centenary Survey*, S. W. Hawking and W. Israel, eds. 1979.

[9] C. Wetterich, "Exact evolution equation for the effective potential," *Phys.Lett.* **B301** (1993) 90–94.

[10] M. Reuter and C. Wetterich, "Effective average action for gauge theories and exact evolution equations," *Nuclear Physics B* **417** no. 1–2, (1994) 181 – 214.

[11] M. Niedermaier and M. Reuter, "The asymptotic safety scenario in quantum gravity," *Living Reviews in Relativity* **9** no. 5, (2006) . `http://www.livingreviews.org/lrr-2006-5`.

[12] D. F. Litim, "Fixed points of quantum gravity," *Physical Review Letters* **92** no. 20, (2004) , `arXiv:0312114 [hep-th]`.

[13] R. Percacci, "Asymptotic Safety," `arXiv:0709.3851 [hep-th]`.

[14] A. Codello, R. Percacci, and C. Rahmede, "Investigating the ultraviolet properties of gravity with a Wilsonian renormalization group equation," *Annals of Physics* **324** no. 2, (2009) 414–469, `arXiv:0805.2909`.

[15] D. F. Litim, "Renormalization group and the Planck scale.," *Philosophical transactions. Series A, Mathematical, physical, and engineering sciences* **369** no. 1946, (2011) 2759–78, `arXiv:1102.4624`. `http://arxiv.org/abs/1102.4624`.

[16] M. Reuter and F. Saueressig, "Quantum Einstein gravity," *New Journal of Physics* **14** (2012) 1–87, `arXiv:1202.2274`.

[17] S. Nagy, "Lectures on renormalization and asymptotic safety," *Annals of Physics* **350** (2014) 310–346, `arXiv:1211.4151`.

[18] M. Reuter, "Nonperturbative evolution equation for quantum gravity," *Phys. Rev. D* **57** (Jan, 1998) 971–985.

[19] N. Christiansen, B. Knorr, J. M. Pawlowski, and A. Rodigast, "Global Flows in Quantum Gravity," *arXiv preprint arXiv: ...* (2014) 18, `arXiv:1403.1232`. `http://arxiv.org/abs/1403.1232`.

[20] C. Brans and R. H. Dicke, "Mach's principle and a relativistic theory of gravitation," *Phys. Rev.* **124** (Nov, 1961) 925–935.

[21] R. H. Dicke, "Mach's principle and invariance under transformation of units," *Phys. Rev.* **125** (Mar, 1962) 2163–2167.

[22] T. Damour, "Theoretical Aspects of the Equivalence Principle," arXiv:1202.6311 [gr-qc].

[23] A. Lahanas and D. V. Nanopoulos, "The Road to No Scale Supergravity," *Phys.Rept.* **145** (1987) 1.

[24] M. Shaposhnikov and D. Zenhausern, "Quantum scale invariance, cosmological constant and hierarchy problem," *Phys.Lett.* **B671** (2009) 162–166, arXiv:0809.3406 [hep-th].

[25] M. Shaposhnikov and D. Zenhausern, "Scale invariance, unimodular gravity and dark energy," *Phys.Lett.* **B671** (2009) 187–192, arXiv:0809.3395 [hep-th].

[26] T. Henz, J. M. Pawlowski, A. Rodigast, and C. Wetterich, "Dilaton quantum gravity," *Physics Letters, Section B: Nuclear, Elementary Particle and High-Energy Physics* **727** no. 1-3, (Nov, 2013) 298–302, arXiv:1304.7743. http://www.sciencedirect.com/science/article/pii/S0370269313008083.

[27] K. G. Wilson, "The Renormalization Group and Strong Interactions," *Phys.Rev.* **D3** (1971) 1818.

[28] D. F. Litim and J. M. Pawlowski, "On Gauge Invariant Wilsonian Flows," arXiv:9901063 [hep-th]. http://arxiv.org/abs/hep-th/9901063.

[29] J. Berges, N. Tetradis, and C. Wetterich, "Non-Perturbative Renormalization Flow in Quantum Field Theory and Statistical Physics," *Physics* (May, 2000) 178, arXiv:0005122 [hep-ph]. http://arxiv.org/abs/hep-ph/0005122.

[30] C. Bagnuls and C. Bervillier, "Exact Renormalization Group Equations. An Introductory Review," arXiv:0002034 [hep-th]. http://arxiv.org/abs/hep-th/0002034http://dx.doi.org/10.1016/S0370-1573(00)00137-X.

[31] K. I. Aoki, "Introduction to the non-perturbative renormalization group and its recent applications," *International Journal of Modern Physics B* **14** no. 12-13, (2000) 1249–1326. papers2://publication/doi/10.1142/S0217979200000923.

[32] J. Polonyi, "Lectures on the functional renormalization group method," *Central European Journal of Physics* **1** no. 1, (2003) 1, arXiv:0110026 [hep-th].

[33] H. Gies, "Introduction to the functional RG and applications to gauge theories," *Lecture Notes in Physics* **852** (2012) 287–348, arXiv:0611146 [hep-ph].

[34] B.-J. Schaefer and J. Wambach, "Renormalization Group Approach towards the QCD Phase Diagram," *Physics of Particles and Nuclei* **39** no. 7, (2006) 14, arXiv:0611191 [hep-ph]. http://arxiv.org/abs/hep-ph/0611191.

[35] J. M. Pawlowski, "Aspects of the functional renormalisation group," *Annals of Physics* **322** no. 12, (2007) 2831–2915, arXiv:0512261v2 [hep-th]. http://www.sciencedirect.com/science/article/pii/S0003491607000097papers2://publication/doi/10.1016/j.aop.2007.01.007.

[36] O. J. Rosten, "Fundamentals of the exact renormalization group," *Physics Reports* **511** no. 4, (2012) 177–272, arXiv:1003.1366.

[37] M. Scherer, S. Floerchinger, and H. Gies, "Functional renormalization for the BCS-BEC crossover," arXiv:1010.2890. http://arxiv.org/abs/1010.2890.

[38] J. M. Pawlowski, "The QCD phase diagram: Results and challenges," *AIP Conference Proceedings* **1343** (2011) 75–80, arXiv:1012.5075.

[39] W. Metzner, M. Salmhofer, C. Honerkamp, V. Meden, and K. Schönhammer, "Functional renormalization group approach to correlated fermion systems," *Reviews of Modern Physics* **84** no. 1, (2012) 299–352, arXiv:1105.5289.

[40] J. Braun, "Fermion Interactions and Universal Behavior in Strongly Interacting Theories," *Journal of Physics G: Nuclear and Particle Physics* **39** no. 3, (2011) 131, arXiv:1108.4449. http://arxiv.org/abs/1108.4449$\delimiter"026E30F$nhttp://iopscience.iop.org/0954-3899/39/3/033001$\delimiter"026E30F$nhttp://stacks.iop.org/0954-3899/39/i=3/a=033001?key=crossref.13f399810f8603e84934ac11b468ef99.

[41] I. Boettcher, J. M. Pawlowski, and S. Diehl, "Ultracold atoms and the Functional Renormalization Group," *Nuclear Physics B - Proceedings Supplements* **228** (2012) 63–135, arXiv:1204.4394.

[42] T. Henz, *Dilatation Symmetric Scalar-Tensor Theories of Quantum Gravity*. Diplom, Heidelberg U., 2012.

[43] M. E. Peskin and D. V. Schroeder, *An introduction to quantum field theory*. ABP - The advanced book program. Westview Press, Boulder, Colorado, reprint ed., 2007.

[44] V. P. Nair, *Quantum field theory*. Graduate texts in contemporary physics. Springer, New York, 2005.

[45] K. Osterwalder and R. Schrader, "Axioms for Euclidean Green's functions," *Comm. Math. Phys.* **31** (1973) 83–112.

[46] E. Manrique, S. Rechenberger, and F. Saueressig, "Asymptotically safe lorentzian gravity," *Phys. Rev. Lett.* **106** (Jun, 2011) 251302.

[47] I. Donkin, "The Geometrical Flow Equation for Quantum Gravity," Diploma Thesis, University of Heidelberg, 2008.

[48] N. Christiansen, *Non-Perturbative Aspects of Quantum Field Theory*. PhD thesis, Heidelberg University, 2015.

[49] U. Ellwanger, "The Running Gauge Coupling in the Exact Renormalization Group Approach," *Recherche* no. January 1997, (1997) 17, `arXiv:9702309 [hep-ph]`. `http://arxiv.org/abs/hep-ph/9702309`.

[50] D. Hilbert, "The foundations of physics (first communication)," in *The Genesis of General Relativity*, M. Janssen, J. D. Norton, J. Renn, T. Sauer, and J. Stachel, eds., vol. 250 of *Boston Studies in the Philosophy and History of Science*, pp. 1925–1938. Springer Netherlands, 2007. `http://dx.doi.org/10.1007/978-1-4020-4000-9_44`.

[51] M. Göckeler and T. Schücker, *Differential geometry, gauge theories, and gravity*. Cambridge monographs on mathematical physics. Cambridge Univ. Pr., Cambridge, repr. ed., 1999.

[52] K. S. Stelle, "Renormalization of higher-derivative quantum gravity," *Phys. Rev. D* **16** (Aug, 1977) 953–969.

[53] K.-j. Hamada, "BRST Analysis of Physical Fields and States for 4D Quantum Gravity on RxS^3," `arXiv:1202.4538 [hep-th]`.

[54] K.-j. Hamada, "Brst invariant higher derivative operators in 4d quantum gravity based on cft," *Phys. Rev. D* **85** (Jun, 2012) 124036.

[55] A. Nink and M. Reuter, "On the physical mechanism underlying Asymptotic Safety," `arXiv:1208.0031 [hep-th]`.

[56] R. Percacci, "A bibliography on asymptotic safety." http://www.percacci.it/roberto/physics/as/biblio.html.

[57] H. Kawai, Y. Kitazawa, and M. Ninomiya, "Renormalizability of quantum gravity near two-dimensions," *Nucl.Phys.* **B467** (1996) 313–331, arXiv:hep-th/9511217 [hep-th].

[58] W. Souma, "Non-Trivial Ultraviolet Fixed Point in Quantum Gravity," *Progress of Theoretical Physics* **102** no. 1, (1999) 181–195, arXiv:9907027 [hep-th]. http://arxiv.org/abs/hep-th/9907027.

[59] M. Reuter and F. Saueressig, "Renormalization group flow of quantum gravity in the Einstein-Hilbert truncation," *Phys. Rev. D* **65** (Feb, 2002) 065016.

[60] K. Falls, D. Litim, K. Nikolakopoulos, and C. Rahmede, "Further evidence for asymptotic safety of quantum gravity," arXiv:arXiv:1410.4815v1.

[61] J. A. Dietz and T. R. Morris, "Redundant operators in the exact renormalisation group and in the f (R) approximation to asymptotic safety," *Journal of High Energy Physics* **2013** no. 7, (2013) , arXiv:1306.1223.

[62] D. Benedetti, "On the number of relevant operators in asymptotically safe gravity," arXiv:arXiv:1301.4422v1. http://arxiv.org/abs/1301.4422.

[63] K. Falls and D. Litim, "A bootstrap towards asymptotic safety," arXiv:arXiv:1301.4191v1. http://arxiv.org/abs/1301.4191.

[64] M. Demmel, F. Saueressig, and O. Zanusso, "RG flows of Quantum Einstein Gravity in the linear-geometric approximation," *Annals of Physics* **359** (2015) 141–165, arXiv:1412.7207.

[65] N. Ohta and R. Percacci, "Higher derivative gravity and asymptotic safety in diverse dimensions," *Classical and Quantum Gravity* (2014) 32, arXiv:1308.3398. http://arxiv.org/abs/1308.3398$\delimiter"026E30F$nhttp://iopscience.iop.org/0264-9381/31/1/015024.

[66] D. Benedetti, P. F. Machado, and F. Saueressig, "Asymptotic Safety in Higher-Derivative Gravity," *Modern Physics Letters A* **24** no. 28, (2009) 2233–2241, arXiv:0901.2984. http://arxiv.org/abs/0901.2984.

[67] A. Eichhorn, "On unimodular quantum gravity," arXiv:1301.0879. http://arxiv.org/abs/1301.0879.

[68] A. Eichhorn, "The Renormalization Group flow of unimodular f(R) gravity," *Journal of High Energy Physics* **2015** no. 4, (2015) , arXiv:1501.0584.

[69] A. Eichhorn and H. Gies, "Ghost anomalous dimension in asymptotically safe quantum gravity," *Physical Review D - Particles, Fields, Gravitation and Cosmology* **81** no. 10, (2010) 1–12, arXiv:1001.5033.

[70] K. Groh and F. Saueressig, "Ghost wave-function renormalization in Asymptotically Safe Quantum Gravity," arXiv:1001.5032. http://arxiv.org/abs/1001.5032.

[71] A. Eichhorn, H. Gies, and M. M. Scherer, "Asymptotically free scalar curvature-ghost coupling in quantum Einstein gravity," *Physical Review D - Particles, Fields, Gravitation and Cosmology* **80** no. 10, (2009) 1–8, arXiv:0907.1828.

[72] E. Manrique and M. Reuter, "Bimetric Truncations for Quantum Einstein Gravity and Asymptotic Safety," *Annals Phys.* **325** (2010) 785–815, arXiv:0907.2617 [gr-qc].

[73] E. Manrique, M. Reuter, and F. Saueressig, "Bimetric renormalization group flows in quantum Einstein gravity," *Annals of Physics* **326** no. 2, (2011) 463–485, arXiv:1006.0099.

[74] D. Becker and M. Reuter, "En route to Background Independence: Broken split-symmetry, and how to restore it with bi-metric average actions," *Annals of Physics* **350** (2014) 225–301, arXiv:1404.4537.

[75] D. Dou and R. Percacci, "The running gravitational couplings," *Classical and Quantum Gravity* **15** no. 11, (1998) 3449–3468, arXiv:9707239 [hep-th]. http://arxiv.org/abs/hep-th/9707239.

[76] R. Percacci and D. Perini, "Constraints on matter from asymptotic safety," *Physical Review D* **67** no. 8, (2003) 081503, arXiv:0207033 [hep-th].

[77] J. E. Daum, U. Harst, and M. Reuter, "Non-perturbative QEG corrections to the Yang-Mills beta function," *General Relativity and Gravitation* **43** no. 9, (2011) 2393–2407, arXiv:1005.1488.

[78] U. Harst and M. Reuter, "QED coupled to QEG," *Journal of High Energy Physics* **2011** no. 5, (2011) , arXiv:1101.6007.

[79] A. Codello, "Large N quantum gravity," *New Journal of Physics* **14** (2012) 1–20, arXiv:arXiv:1108.1908v2.

[80] A. Eichhorn and H. Gies, "Light fermions in quantum gravity," 2011.

[81] A. Eichhorn, "Quantum-gravity-induced matter self-interactions in the asymptotic-safety scenario," *Physical Review D - Particles, Fields, Gravitation and Cosmology* **86** no. 10, (2012) 1–23, arXiv:arXiv:1204.0965v2.

[82] A. Eichhorn, "Experimentally testing asymptotically safe quantum gravity with photon-photon scattering," *arXiv preprint arXiv:1210.1528* (2012) 13–15, arXiv:arXiv:1210.1528v1.

[83] R. Percacci and D. Perini, "Asymptotic safety of gravity coupled to matter," *Physical Review D* **68** no. 4, (2003) , arXiv:0304222 [hep-th].

[84] P. Dona, A. Eichhorn, and R. Percacci, "Matter matters in asymptotically safe quantum gravity," *Physical Review D - Particles, Fields, Gravitation and Cosmology* **89** no. 8, (2014) 1–26, arXiv:1311.2898.

[85] P. Donà, A. Eichhorn, and R. Percacci, "Consistency of matter models with asymptotically safe quantum gravity," arXiv:1410.4411. http://arxiv.org/abs/1410.4411v1.

[86] P. Donà, A. Eichhorn, P. Labus, and R. Percacci, "Asymptotic safety in an interacting system of gravity and scalar matter," arXiv:1512.01589. http://arxiv.org/abs/1512.01589.

[87] J. Meibohm, J. M. Pawlowski, and M. Reichert, "Asymptotic safety of gravity-matter systems," arXiv:1510.07018. http://arxiv.org/abs/1510.07018.

[88] J. Meibohm and J. M. Pawlowski, "Chiral fermions in asymptotically safe quantum gravity," arXiv:arXiv:1601.04597v1. http://arxiv.org/abs/1601.04597.

[89] G. Narain and R. Percacci, "Renormalization Group Flow in Scalar-Tensor Theories. I," *Class. Quant. Grav.* **27** (2010) 75001, arXiv:0911.0386 [hep-th].

[90] G. Narain and C. Rahmede, "Renormalization Group Flow in Scalar-Tensor Theories. II," *Group* (Nov, 2009) 14, arXiv:0911.0394. http://arxiv.org/abs/0911.0394.

[91] R. Percacci and G. P. Vacca, "Search of scaling solutions in scalar-tensor gravity," *European Physical Journal C* **75** no. 5, (2015) , arXiv:1501.0088.

[92] P. Labus, R. Percacci, and G. P. Vacca, "Asymptotic safety in O(N) scalar models coupled to gravity," *Physics Letters, Section B: Nuclear, Elementary Particle and High-Energy Physics* **753** (2016) 274–281, arXiv:arXiv:1505.05393v1.

[93] D. F. Litim and T. Plehn, "Signatures of gravitational fixed points at the large hadron collider," *Physical Review Letters* **100** no. 13, (2008) 4, arXiv:0707.3983. http://arxiv.org/abs/0707.3983.

[94] E. Gerwick and T. Plehn, "Extra dimensions and their ultraviolet completion," *Proceedings of Science* (2008) , arXiv:0912.2653.

[95] E. Gerwick, D. Litim, and T. Plehn, "Asymptotic safety and Kaluza-Klein gravitons at the LHC," *Physical Review D - Particles, Fields, Gravitation and Cosmology* **83** no. 8, (2011) 1–25, arXiv:1101.5548.

[96] A. Eichhorn, H. Gies, J. Jaeckel, T. Plehn, M. M. Scherer, and R. Sondenheimer, "The Higgs mass and the scale of new physics," *Journal of High Energy Physics* **2015** no. 4, (2015) 1–27, arXiv:1501.02812.

[97] M. Shaposhnikov and C. Wetterich, "Asymptotic safety of gravity and the Higgs boson mass," *Phys.Lett.* **B683** (2010) 196–200, arXiv:0912.0208 [hep-th].

[98] K. Falls, D. F. Litim, and A. Raghuraman, "Black Holes and Asymptotically Safe Gravity," *International Journal of Modern Physics A* **27** no. 05, (2012) 1250019, arXiv:1002.0260.

[99] K. Falls and D. F. Litim, "Black hole thermodynamics under the microscope," *Physical Review D - Particles, Fields, Gravitation and Cosmology* **89** no. 8, (2014) 1–26, arXiv:1212.1821.

[100] B. Koch and F. Saueressig, "Black holes within Asymptotic Safety," arXiv:1401.4452. http://arxiv.org/abs/1401.4452.

[101] S. Weinberg, "Asymptotically safe inflation," *Physical Review D - Particles, Fields, Gravitation and Cosmology* **81** no. 8, (2010) 1–17, arXiv:0911.3165.

[102] E. J. Copeland, C. Rahmede, and I. D. Saltas, "Asymptotically Safe Starobinsky Inflation," arXiv:1311.0881. http://arxiv.org/abs/1311.0881.

[103] N. Christiansen, D. F. Litim, J. M. Pawlowski, and A. Rodigast, "Fixed points and infrared completion of quantum gravity," *Physics Letters, Section B: Nuclear, Elementary Particle and High-Energy Physics* **728** no. 1, (2014) 114–117, arXiv:arXiv:1209.4038v1.

[104] A. Codello, G. D'Odorico, and C. Pagani, "Consistent closure of renormalization group flow equations in quantum gravity," *Physical Review D - Particles, Fields, Gravitation and Cosmology* **89** no. 8, (2014) , arXiv:1304.4777.

[105] N. Christiansen, B. Knorr, J. Meibohm, J. M. Pawlowski, and M. Reichert, "Local quantum gravity," *Physical Review D - Particles, Fields, Gravitation and Cosmology* **92** no. 12, (2015) 1–5, arXiv:1506.07016.

[106] A. Einstein, "Über das Relativitätsprinzip und die aus demselben gezogene Folgerungen," *Jahrbuch der Radioaktivitaet und Elektronik* **4** (1907) 411.

[107] D. J. Raine, "Mach's Principle in general relativity," *Monthly Notices of the Royal Astronomical Society* **171** (June, 1975) 507–528.

[108] C. Will, *Was Einstein Right?: Putting General Relativity to the Test*. BasicBooks, 1993. https://books.google.de/books?id=9ZuP9JQzc00C.

[109] A. Miyazaki, "Physical Significance of the Difference between the Brans-Dicke Theory and General Relativity," *ArXiv General Relativity and Quantum Cosmology e-prints* (Dec., 2000) , arXiv:gr-qc/0012104.

[110] V. Faraoni, "Illusions of general relativity in Brans-Dicke gravity," *Phys. Rev. D* **59** no. 8, (3, 1999) 084021.

[111] R. Percacci, "RG flow of Weyl-invariant dilaton gravity," *arXiv preprint arXiv:1110.6758* (2011) 20, arXiv:1110.6758. http://arxiv.org/abs/1110.6758.

[112] A. Codello, C. Pagani, and R. Percacci, "The Renormalization Group and Weyl–invariance," *arXiv* (2012) 1–32, arXiv:arXiv:1210.3284v1.

[113] N. D. Birrell and P. C. W. Davies, *Quantum fields in curved space*. Cambridge monographs on mathematical physics. Cambridge Univ. Pr., Cambridge, repr. ed., 1994.

[114] A. A. Grib and W. A. Rodrigues, "On the problem of conformal coupling in field theory in curved spacetime," *Gravitation and Cosmology* **1** (Dec., 1995) 273–276.

[115] V. Faraoni, E. Gunzig, and P. Nardone, "Conformal transformations in classical gravitational theories and in cosmology," *Fund.Cosmic Phys.* **20** (1999) 121, arXiv:gr-qc/9811047 [gr-qc].

[116] M. J. Duff, "Twenty years of the weyl anomaly," *Classical and Quantum Gravity* **11** no. 6, (1994) 1387. http://stacks.iop.org/0264-9381/11/i=6/a=004.

[117] D. Capper and M. Duff, "Conformal anomalies and the renormalizability problem in quantum gravity," *Physics Letters A* **53** no. 5, (1975) 361–362.

[118] C. Wetterich, "Primordial cosmic fluctuations for variable gravity," arXiv:1511.03530. http://arxiv.org/abs/1511.03530.

[119] S. Weinberg, "The cosmological constant problem," *Rev. Mod. Phys.* **61** no. 1, (Jan, 1989) 1–23. http://link.aps.org/doi/10.1103/RevModPhys.61.1.

[120] J. Martin, "Everything You Always Wanted To Know About The Cosmological Constant Problem (But Were Afraid To Ask)," arXiv:1205.3365. http://arxiv.org/abs/1205.3365http://dx.doi.org/10.1016/j.crhy.2012.04.008.

[121] B. Delamotte, M. Tissier, and N. Wschebor, "Scale invariance implies conformal invariance for the three-dimensional Ising model," *arXiv* (2015) 1–7, arXiv:arXiv:1501.01776v2.

[122] A. Codello, G. D'Odorico, and C. Pagani, "A functional RG equation for the c-function," *Journal of High Energy Physics* **2014** no. 7, (2014) 1–41, arXiv:1312.7097.

[123] J. F. Fortin, B. Grinstein, and A. Stergiou, "Scale without conformal invariance: Theoretical foundations," *Journal of High Energy Physics* **2012** no. 7, (2012) , arXiv:1107.3840.

[124] J.-F. Fortin, B. Grinstein, and A. Stergiou, "Limit cycles and conformal invariance," *Journal of High Energy Physics* **2013** no. 1, (2013) 184, arXiv:1208.3674. http://arxiv.org/abs/1208.3674$\delimiter"026E30F$nhttp://link.springer.com/article/10.1007/JHEP01(2013)184$\delimiter"026E30F$nhttp://link.springer.com/10.1007/JHEP01(2013)184.

[125] C. Wetterich, "Cosmology and the fate of dilatation symmetry," *Nuclear Physics, Section B* **302** no. 4, (1988) 668–696.

[126] F. Bezrukov, G. K. Karananas, J. Rubio, and M. Shaposhnikov, "Higgs-dilaton cosmology: An effective field theory approach," *Physical Review D* **87** no. 9, (2013) 096001, arXiv:1212.4148. http://link.aps.org/doi/10.1103/PhysRevD.87.096001.

[127] K.-y. Oda and M. Yamada, "Non-minimal coupling in Higgs-Yukawa model with asymptotically safe gravity," arXiv:1510.03734. http://arxiv.org/abs/1510.03734.

[128] V. Barger, M. Ishida, and W.-Y. Keung, "Dilaton at the LHC," *Phys.Rev.* **D85** (2012) 015024, arXiv:1111.2580 [hep-ph].

[129] V. Barger, M. Ishida, and W. Y. Keung, "Dilaton at the LHC," *Physical Review D - Particles, Fields, Gravitation and Cosmology* **85** no. 1, (2012) 1–9, arXiv:1111.2580 [hep-ph].

[130] A. Eichhorn and M. M. Scherer, "Planck scale, Higgs mass, and scalar dark matter," *Physical Review D - Particles, Fields, Gravitation and Cosmology* **90** no. 2, (2014) 1–11, arXiv:1404.5962.

[131] O. Antipin, J. Krog, M. Mojaza, and F. Sannino, "Stable Extensions with(out) Gravity," arXiv:1311.1092. http://arxiv.org/abs/1311.1092http://dx.doi.org/10.1016/j.nuclphysb.2014.06.023.

[132] D. Gorbunov and A. Tokareva, "Scale-invariance as the origin of dark radiation?," *Physics Letters, Section B: Nuclear, Elementary Particle and High-Energy Physics* **739** (2014) 50–55, arXiv:1307.5298.

[133] A. Bonanno, A. Contillo, and R. Percacci, "Inflationary solutions in asymptotically safe f(R) theories," *Class.Quant.Grav.* **28** (2011) 145026, arXiv:1006.0192 [gr-qc].

[134] A. Bonanno, A. Contillo, and R. Percacci, "Inflationary solutions in asymptotically safe f (R) theories," *Classical and Quantum Gravity* **28** no. 14, (2011) 145026, arXiv:1006.0192. http://arxiv.org/abs/1006.0192$\delimiter"026E30F$nhttp://stacks.iop.org/0264-9381/28/i=14/a=145026?key=crossref.5263dd4e003e1401ba89a12c437121b9.

[135] C. Wetterich, "Cosmologies with variable Newton's 'constant'," *Nucl.Phys.* **B302** (1988) 645.

[136] C. Wetterich, "The Cosmon model for an asymptotically vanishing time dependent cosmological 'constant'," *Astron.Astrophys.* **301** (1995) 321–328, arXiv:hep-th/9408025 [hep-th].

[137] C. Wetterich, "Inflation, quintessence, and the origin of mass," arXiv:1408.0156. http://arxiv.org/abs/1408.0156.

[138] C. Wetterich, "Variable gravity Universe," *arXiv.org* **astro-ph.C** (2013) . http://arxiv.org/abs/1308.1019v1papers2://publication/uuid/785A0355-7777-418D-98F5-438A59B8B814.

[139] C. Wetterich, "Eternal Universe," *Physical Review D* **90** no. 4, (2014) 043520, arXiv:1404.0535. http://link.aps.org/doi/10.1103/PhysRevD.90.043520.

[140] C. Wetterich, "Hot big bang or slow freeze?," *Physics Letters, Section B: Nuclear, Elementary Particle and High-Energy Physics* **736** (2014) 506–514, arXiv:1401.5313.

[141] C. Wetterich, "Universe without expansion," *Physics of the Dark Universe* **2** no. 4, (2013) 184–187, arXiv:1303.6878.

[142] C. Wetterich, "Modified gravity and coupled quintessence," *Lecture Notes in Physics* **892** (2015) 57–95, arXiv:1402.5031.

[143] C. Garrod, "Dilatation symmetry of classical electrodynamics with charged particles of finite mass," *Phys. Rev. D* **1** (Mar, 1970) 1524–1526.

[144] C. Wetterich, "The Cosmological constant and higher dimensional dilatation symmetry," *Phys.Rev.* **D81** (2010) 103507, arXiv:0911.1063 [hep-th].

[145] J. Overduin and P. Wesson, "Kaluza-Klein gravity," *Phys.Rept.* **283** (1997) 303–380, arXiv:gr-qc/9805018 [gr-qc].

[146] Y. Pirogov, "Unimodular bimode gravity and the coherent scalar-graviton field as galaxy dark matter," arXiv:1111.1437 [gr-qc].

[147] H. Lu, Z. Huang, W. Fang, and K. Zhang, "Dark energy and dilaton cosmology," arXiv:hep-th/0409309 [hep-th].

[148] D. Blas, M. Shaposhnikov, and D. Zenhausern, "Scale-invariant alternatives to general relativity," *Phys.Rev.* **D84** (2011) 044001, arXiv:1104.1392 [hep-th].

[149] Y. Fujii, "Mass of the dilaton and the cosmological constant," *Prog.Theor.Phys.* **110** (2003) 433–439, arXiv:gr-qc/0212030 [gr-qc].

[150] C. Wetterich, "Cosmology and the fate of dilatation symmetry," *Nuclear Physics B* **302** no. 4, (1988) 668 – 696.

[151] C. Wetterich, "Dilatation symmetry in higher dimensions and the vanishing of the cosmological constant," *Phys.Rev.Lett.* **102** (2009) 141303, arXiv:0806.0741 [hep-th].

[152] A. R. Liddle, "An introduction to cosmological inflation," *Proceedings of ICTP summer school in highenergy physics 1998* **9901124** (1999) 36, arXiv:9901124 [astro-ph]. http://arxiv.org/abs/astro-ph/9901124.

[153] S. Clesse, "An introduction to inflation after Planck: from theory to observations," arXiv:1501.0046.

[154] M. Bartelmann, *Cosmology*. Heidelberg.

[155] B. Ratra, "Inflation in an exponential-potential scalar field model," *Phys. Rev. D* **45** no. 6, (Mar, 1992) 1913–1952. http://link.aps.org/doi/10.1103/PhysRevD.45.1913.

[156] M. Susperregi and A. Mazumdar, "Extended Inflation with an Exponential Potential," arXiv:9804081 [gr-qc]. http://arxiv.org/abs/gr-qc/9804081http://dx.doi.org/10.1103/PhysRevD.58.083512.

[157] P. Jain and G. Kashyap, "Relating the cosmological constant and slow roll to conformal symmetry breaking," arXiv:1405.7775. http://arxiv.org/abs/1405.7775.

[158] P. Jain, G. Kashyap, and S. Mitra, "The fine tuning of the cosmological constant in a conformal model," arXiv:1408.2620.

[159] D. Benedetti and F. Guarnieri, "Brans-Dicke theory in the local potential approximation," *New Journal of Physics* **16** (Nov, 2014) 34, arXiv:1311.1081. http://arxiv.org/abs/1311.1081.

[160] E. Alvarez, M. Herrero-Valea, and C. P. Martín, "Conformal and non conformal dilaton gravity," *Journal of High Energy Physics* **2014** no. 10, (2014) , arXiv:1404.0806.

[161] M. Serino, "Conformal Anomaly Actions and Dilaton Interactions," *arXiv* (2014) 0–154, arXiv:1407.7113. http://arxiv.org/abs/1407.7113.

[162] L. Faddeev and V. Popov, "Feynman diagrams for the Yang-Mills field," *Physics Letters B* **25** no. 1, (1967) 29 – 30.

[163] M. Faizal, "Perturbative Quantum Gravity and Yang-Mills Theories in de Sitter Spacetime," arXiv:1105.3112 [gr-qc].

[164] L. F. Abbott, "Introduction to the Background Field Method," *Acta Physica Polonica B* **13** no. 1, (1982) 1–18.

[165] D. F. Litim and J. M. Pawlowski, "On gauge invariance and ward identities for the Wilsonian renormalisation group," *Nuclear Physics B - Proceedings Supplements* **74** no. 1-3, (1999) 325–328, arXiv:9809020 [hep-th]. http://arxiv.org/abs/hep-th/9809020.

[166] J. Braun, H. Gies, and J. M. Pawlowski, "Quark confinement from colour confinement," *Physics Letters, Section B: Nuclear, Elementary Particle and High-Energy Physics* **684** no. 4-5, (2010) 262–267, arXiv:0708.2413.

[167] J. M. Pawlowski, "Wilsonian Flows in Non-Abelian Gauge Theories," *Thphys.Uni-Heidelberg.De* .

[168] J. M. Pawlowski, "On wilsonian flows in gauge theories," *International Journal of Modern Physics A* **16** no. 11, (2001) 2105–2110.

[169] D. F. Litim and J. M. Pawlowski, "Renormalisation group flows for gauge theories in axial gauges," *Journal of High Energy Physics* **2002** no. 09, (2002) 049–049, arXiv:0203005 [hep-th]. http://arxiv.org/abs/hep-th/0203005.

[170] D. F. Litim and J. M. Pawlowski, "Wilsonian flows and background fields," *Physics Letters, Section B: Nuclear, Elementary Particle and High-Energy Physics* **546** no. 3-4, (2002) 279–286, arXiv:0208216 [hep-th].

[171] J. A. Dietz and T. R. Morris, "Background independent exact renormalization group for conformally reduced gravity," *Journal of High Energy Physics* **2015** no. 4, (2015) , arXiv:1502.07396v1.

[172] J. Braun, H. Gies, and J. M. Pawlowski, "Quark Confinement from Color Confinement," *Phys.Lett.* **B684** (2010) 262–267, arXiv:0708.2413 [hep-th].

[173] J. M. Pawlowski, D. F. Litim, S. Nedelko, and L. von Smekal, "Infrared behavior and fixed points in Landau gauge QCD," *Phys.Rev.Lett.* **93** (2004) 152002, arXiv:hep-th/0312324 [hep-th].

[174] S. Folkerts, D. F. Litim, and J. M. Pawlowski, "Asymptotic freedom of Yang-Mills theory with gravity," *Phys.Lett.* **B709** (2012) 234–241, arXiv:1101.5552 [hep-th].

[175] S. Folkerts, "Asymptotic Safety for Gravity coupled to Yang-Mills Theory: an RG Study," Diploma Thesis, University of Heidelberg, 2009.

[176] I. M. Singer, "Some remarks on the Gribov ambiguity," *Comm. Math. Phys.* **60** no. 1, (1978) 7–12. http://projecteuclid.org/getRecord?id=euclid.cmp/1103904019.

[177] D. F. Litim and J. M. Pawlowski, "On General Axial Gauges for QCD," *Nuclear Physics B - Proceedings Supplements* **74** no. 1-3, (1999) 329–332, arXiv:9809023v1 [arXiv:hep-th]. http://linkinghub.elsevier.com/retrieve/pii/S0920563299001887.

[178] V. Branchina, K. A. Meissner, and G. Veneziano, "The Price of an exact, gauge invariant RG flow equation," *Phys.Lett.* **B574** (2003) 319–324, arXiv:hep-th/0309234 [hep-th].

[179] J. M. Pawlowski, "Geometrical effective action and Wilsonian flows," arXiv:hep-th/0310018 [hep-th].

[180] I. Donkin and J. M. Pawlowski, "The phase diagram of quantum gravity from diffeomorphism-invariant RG-flows," arXiv:1203.4207 [hep-th].

[181] H. Kawai, Y. Kitazawa, and M. Ninomiya, "Scaling exponents in quantum gravity near two dimensions," *Nuclear Physics, Section B* **393** no. 1-2, (1993) 280–300, arXiv:9206081 [hep-th].

[182] C. S. Fischer and J. M. Pawlowski, "Uniqueness of infrared asymptotics in Landau gauge Yang-Mills theory. II.," *Physical Review D - Particles, Fields, Gravitation and Cosmology* **80** no. 2, (2009) 1–12, arXiv:0609009 [hep-th].

[183] J. W. York, Jr., "Covariant decompositions of symmetric tensors in the theory of gravitation," *Annales de L'Institut Henri Poincare Section Physique Theorique* **21** (Dec., 1974) 319–332.

[184] J. James W. York, "Conformally invariant orthogonal decomposition of symmetric tensors on riemannian manifolds and the initial-value problem of general relativity," *Journal of Mathematical Physics* **14** no. 4, (1973) 456–464.

[185] R. Kuhfuss and J. Nitsch, "Propagating modes in gauge field theories of gravity," *General Relativity and Gravitation* **18** (1986) 1207–1227. http://dx.doi.org/10.1007/BF00763447. 10.1007/BF00763447.

[186] D. F. Litim, "Optimisation of the exact renormalisation group," *Physics Letters, Section B: Nuclear, Elementary Particle and High-Energy Physics* **486** no. 1-2, (2000) 92–99, arXiv:0005245 [hep-th]. http://www.sciencedirect.com/science/article/pii/S0370269300007486papers2://publication/doi/10.1016/S0370-2693(00)00748-6.

[187] D. F. Litim, "Optimized renormalization group flows," *Physical Review D* **64** no. 10, (2001) 105007, arXiv:0103195 [hep-th]. http://link.aps.org/doi/10.1103/PhysRevD.64.105007.

[188] M. Reichert, *Asymptotic safety of gravity coupled to matter*. Master's thesis, Heidelberg University.

[189] L. Dixon, L. Magnea, and G. Sterman, "Universal structure of subleading infrared poles in gauge theory amplitudes," *Journal of High Energy Physics* **2008** no. 08, (2008) 022, arXiv:0805.3515. http://arxiv.org/abs/0805.3515.

[190] J. Borchardt and B. Knorr, "Global solutions of functional fixed point equations via pseudo-spectral methods," arXiv:1502.07511. http://arxiv.org/abs/1502.07511$\delimiter"026E30F$nhttp://dx.doi.org/10.1103/PhysRevD.91.105011.

[191] M. J. Duff, "Twenty years of the Weyl anomaly," *Class. Quantum Gray.* **11** no. March 1993, (1993) 1387–1403, arXiv:9308075 [hep-th]. http://blogs.umass.edu/grqft/files/2014/11/Duff-anomaly-reminisces.pdf.

[192] N. Christiansen, *Towards Ultraviolet Stability in Quantum Gravity*. Diplom thesis, 2011.

[193] C. Rovelli, "Notes for a brief history of quantum gravity," *Proc. 9th Marcel Grossmann Meeting* no. July 2000, (2001) 32, arXiv:0006061 [gr-qc]. http://arxiv.org/abs/gr-qc/0006061.

[194] J. M. Martín-García, R. Portugal, and L. R. U. Manssur, "The Invar tensor package," *Computer Physics Communications* **177** no. 8, (2007) 640–648, arXiv:0704.1756.

[195] M. Q. Huber and J. Braun, "Algorithmic derivation of functional renormalization group equations and Dyson-Schwinger equations," *Computer Physics Communications* **183** no. 6, (2012) 1290–1320, arXiv:1102.5307.

[196] J. A. M. Vermaseren, "New features of FORM," arXiv:0010025 [math-ph]. http://arxiv.org/abs/math-ph/0010025.

[197] C. G. Callan, "Broken Scale Invariance in Scalar Field Theory," *Phys. Rev. D* **2** no. 8, (Oct, 1970) 1541–1547. http://link.aps.org/doi/10.1103/PhysRevD.2.1541.

[198] J. Alexandre and J. Polonyi, "Functional Callan-Symanzik equation," arXiv:0010128 [hep-th]. http://arxiv.org/abs/hep-th/0010128http://dx.doi.org/10.1006/aphy.2000.6109.

[199] P. B. Gilkey, "The spectral geometry of a Riemannian manifold.," *J. Differ. Geom.* **10** (1975) 601–618.

[200] P. B. Gilkey, *Invariance theory, the heat equation, and the Atiyah-Singer index theorem*. No. 11 in Mathematics lecture series ; 11 ; Mathematics lecture series. Publish or Perish, Wilmington, Del., 1984. Literaturverz. S. [339] - 345.

[201] D. Vassilevich, "Heat kernel expansion: user's manual," *Physics Reports* **388** no. 5–6, (2003) 279 – 360.

[202] A. Codello, R. Percacci, and C. Rahmede, "Investigating the Ultraviolet Properties of Gravity with a Wilsonian Renormalization Group Equation," *Annals Phys.* **324** (2009) 414–469, arXiv:0805.2909 [hep-th].

[203] O. Lauscher and M. Reuter, "Ultraviolet fixed point and generalized flow equation of quantum gravity," *Phys. Rev. D* **65** (Dec, 2001) 025013.

[204] R. T. Seeley, "Complex powers of an elliptic operator," in *Singular Integrals (Proc. Sympos. Pure Math., Chicago, Ill., 1966)*, pp. 288–307. Amer. Math. Soc., Providence, R.I., 1967.

[205] D. Fursaev and D. Vassilevich, *Operators, geometry and quanta.* Theoretical and mathematical physics. Springer Science+Business, Dordrecht, 2011.

[206] J. Meibohm, *Chiral fermions in asymptotically safe quantum gravity.* Master's thesis.

[207] R. M. Wald, *General relativity.* Univ. of Chicago Pr., Chicago, 1984.

[208] M. Kaku, *Strings, conformal fields, and M-theory.* Graduate texts in contemporary physics. Springer, New York ; Berlin ; Heidelberg ; Barcelona ; Hong Kong ; London ; Milan ; Paris ; Songapore ; Tokyo, 2. ed. ed., 2000.

[209] M. Schottenloher, *A mathematical introduction to conformal field theory.* No. 759 in Lecture notes in physics ; 759 ; Lecture notes in physics. Springer, Berlin ; Heidelberg, 2. ed. ed., 2008.

[210] S. Coleman, *Aspects of symmetry.* Cambridge Univ. Pr., Cambridge, 1. paperback ed. ed., 1988.

[211] R. Percacci, "Renormalization group flow of weyl invariant dilaton gravity," *New Journal of Physics* **13** no. 12, (2011) 125013. http://stacks.iop.org/1367-2630/13/i=12/a=125013.

[212] J. D. Bekenstein and A. Meisels, "Conformal invariance, microscopic physics, and the nature of gravitation," *Phys. Rev. D* **22** (Sep, 1980) 1313–1324.

Acknowledgements

First and foremost, I would like to express my gratitude towards my supervisor Jan for his outstanding support and encouragement, supplemented by the freedom needed when working on this thesis and the final pull when moving towards the finishing line.
Moreover, we would not have picked up this research topic without the vision of Christof, who believed in the physical appeal of the theory even when technical difficulties clouded my own eyesight.
Furthermore, I would like to thank Andreas for collaborating with me throughout portions of this work, and for sharing his knowledge on the subject and the technical aspects, as well as the asymptotic safety community in Heidelberg, most prominently Nic, Jan, Manuel and Kevin for advice, colleagueship and insightful discussions.
The everyday life at the institute was largely shaped by my office mates Jan, Manuel and Aaron, being available for conversations and discussions at all times, as well as the community of functional renormalization group researchers holding up a remarkable group spirit. Outside the institute, there are many people at many different places and from various backgrounds that shaped my life in the last years, and I am grateful to all of them for their very special contributions.
I would like to thank Andreas for proofreading large parts of this thesis and thereby improving its quality considerably - as well as Felicitas, Friederike and Philipp for doing me the honors of enjoying the sunrise over the Tower Bridge together with me after final intense hours completing this work!